BLANK PAGES
IN THIS
DOCUMENT
WERE NOT
FILMED

Bulletin No. 33

SHOCK, VIBRATION and ASSOCIATED ENVIRONMENTS

PART III

MARCH 1964

435514

Office of
The Director of Defense
Research and Engineering

Washington, D.C.

Bulletin No. 33

SHOCK, VIBRATION and ASSOCIATED ENVIRONMENTS

PART III

MARCH 1964

Office of
The Director of Defense
Research and Engineering

The 33rd Symposium on Shock, Vibration and Associated Environments was held in Washington, D. C. on 3-5 December 1963. The Navy was host.

Washington, D.C.

DISTRIBUTION

Aberdeen Proving Ground, Md.
- Att: Ballistic Research Lab. 1
- Att: Development & Proof Services 1
- Att: Physical Test Lab. 1

Advisory Group on Electron Tubes
- Att: Secretary 1

Aeronautical Standards Group, DC 1

Aeronautical Systems Division, WPAFB
- Att: FDFE, C. A. Golueke 1
- Att: FDD, H. A. Magrath 1
- Att: ASNDSV, R. F. Wilkus 1
- Att: ASTEVS, C. W. Gerhardt 1
- Att: AFML(MAMD), J. R. Henderson 1

Air Defense Command, Ent AFB
- Att: Deputy for Civil Engineering 1
- Att: ADIRP 1

Air Proving Ground Center, Elgin AFB
- Att: PGTRI, Technical Library 1

Air Force Flight Test Center, Edwards AFB
- Att: FTRLC, A. J. Davies 1

Air Force Headquarters, DC
- Att: AFCIN-3K2 1
- Att: AFDRD-GW 1
- Att: Opers. Analysis Off., Off VCOS, Library 2

Air Force Logistics Command, WPAFB
- Att: MCTEP, G. P. Civille 1

Air Force Missile Development Center, Holloman AFB
- Att: MDSGL-2, Mr. H. Dunbar 3

Air Force Missile Test Center, Patrick AFB
- Att: Chief, Tech. Systems Lab. 2

Air Force Office of Scientific Research, DC
- Att: Library 1

Air Force Regional Civil Engineer
- Att: North Atlantic Region, AFRCE-NA-A 1
- Att: South Atlantic Region, AFRCE-SA-E 1

Air Force Systems Command, Andrews AFB
- Att: Technical Library 2

Air Force Weapons Lab., Kirtland AFB
- Att: Development Test Division 1
- Att: WLRS, Dr. W. E. Fisher 1
- Att: SWOI 631-276 1

Army Air Defense Center, Ft. Bliss
- Att: Technical Library 1

Army Chemical Center, Md.
- Att: Library 1

Army Electronics R&D Lab., Ft. Monmouth
- Att: SELRA/SL-ADT 1
- Att: SELRA/SL-PEE 1
- Att: SELRA/SL-PRT 1
- Att: SELRA/SL-G 1
- Att: SELRA/SL-GTF 1
- Att: J. J. Oliveri 1

Army Engineer District, NY
- Att: NANGD 1

Army Engineer R&D Labs., Ft. Belvoir
- Att: Director of Research 1
- Att: Package Development Br. 1
- Att: Mr. A. Carolla 1
- Att: Chief, Spec. Proj. Branch 4

Army Engineer Waterways Exp. Sta., Vicksburg
- Att: Mr. J. M. Strange 1

Army Erie Ordnance Depot, Ohio
- Att: Chief Materiel Testing Div. 1

Army Materiel Command, DC
- Att: AMCRD-RS-CM 1

Army Materiel Command, Redstone Arsenal
- Att: Technical Library 4

Army Missile Command, Redstone Arsenal
- Att: AMSMI-RB 1
- Att: AMSMI-RG 1
- Att: AMSMI-RL 1
- Att: AMSMI-RS 1
- Att: AMSMI-RT 1
- Att: AMSMI-RTR, J. M. Taylor 1

Army Mobility Command, Centerline
- Att: Otto Renius 1

Army, Office Chief of Engineers, DC
- Att: ENGMC-EM 2

Army, Office Quartermaster General, DC
- Att: Military Planning Division 1

Army, Office Chief of Res. & Dev., Arlington
- Att: A. L. Tarr 1

Army, Office Chief Signal Officer, DC
- Att: R&D Division 1

Army, Office Chief of Transportation
- Att: Dir of Transportation Engrg. 1

Army Ordnance Ammunition Command, Joliet
- Att: ORDLY-T 1
- Att: NNSC/A 1

Army Ordnance Arsenal, Detroit, Mich.
Att: Tech. Library 2
Att: Engrg. Standards Unit 1
Att: Engrg. Design Div. ORDMX-N 1

Army Security Agency, Md. 1

Army Transportation Engrg. Agency, Ft. Eustis
Att: Library 1
Att: L. J. Pursifull 1

Arnold Engineering Dev. Ctr., Tenn.
Att: AEOIM 1

Atomic Energy Commission, Oak Ridge 6

Atomic Energy Commission, DC
Att: Library 1
Att: Div. of Reactor Development, Tech. Evaluation Branch (Army Reactors) 1

Aviation Supply Office, Phila.
Att: TEP-1 1

Ballistic Systems Div., AFSC, Norton AFB
Att: Technical Data Division 3

Boston Naval Shipyard
Att: Library 1

Bureau of Medicine & Surgery, DC
Att: Research Division 1

Bureau of Naval Weapons, DC
Att: DLI-3 2
Att: FWAA, C. H. Barr 1
Att: PREN-5 5
Att: RRMA 1
Att: RAAE-2 1
Att: RM-3 2
Att: RM-2 1
Att: RSSH 2
Att: FWAE 1
Att: RREN-8 1

Bureau of Naval Weapons Rep., E. Hartford 2

Bureau of Naval Weapons Rep., Pomona
Att: Chief Engineer 1
Att: Metrology Dept., Code 60 1

Bureau of Naval Weapons Rep., Sunnyvale 1

Bureau of Ships, DC
Att: Code 423 20

Bureau of Supplies & Accounts, DC
Att: Library 1

Bureau of Yards & Docks, DC
Att: Code D-440 1
Att: Code D-220 1
Att: Code D-220 (Unclassified Parts) 6

Coast Guard Headquarters, DC 1

David Taylor Model Basin, Portsmouth
Att: Code 281A 1

David Taylor Model Basin, DC
Att: Library 3
Att: Harry Rich 1
Att: Contract Research Administrator, 513 1
Att: J. A. Luistra, Code 591L 1

Dayton Air Force Depot, Gentile AFB
Att: MDMG 1

Defense Atomic Support Agency, DC
Att: Technical Director 1
Att: Weapons Development Div. 1
Att: John G. Lewis 1

Defense Atomic Support Agency, Livermore
Att: Administrative Officer 1

Defense Documentation Center, Alexandria 20

District Public Works Office, 14th ND 1

Electronic Systems Div., L. G. Hanscom Field
Att: Library 1

Electronics Supply Office, Great Lakes 1

Federal Aviation Agency, DC
Att. Emergency Readiness Division Off. of Plans & Requirements 2

Frankfort Arsenal, Phila.
Att: Library Branch, CC 0270/40 1
Att: David Askin, CC 1730-230 1

Harry Diamond Laboratories, DC
Att: B. M. Horton 1
Att: Chief, Lab. 700 1
Att: Branch 320, Miss Johnson 1
Att: Chief, Branch 850 1
Att: Ben Reznek 1

Inspector of Naval Material, San Francisco 1

Library of Congress, DC
Att: Exchange & Gift Div (Unclassified Only) 1

Long Beach Naval Shipyard, Calif.
Att: Code 240 1

Los Angeles Air Procurement District, Calif.
Att: Quality Control Division 1

Los Angeles Ordnance District, USA, Calif.
Att: ORDEV 1

Mare Island Naval Shipyard, Calif.
Att: Library 1

Marine Corps Equipment Board, Quantico 2

Marine Corps Headquarters, DC
Att: Res & Dev Section 1
Att: Code A04E 1

Maxwell Air Force Base, Ala.
Att: Air University Library 1

Mobile Air Materiel Area, Brookley AFB
Att: MONRPPR 1
Att: MONE 1

NASA, Ames Research Ctr., Moffett Field
Att: S. J. DeFrance, Dir. 1

NASA, High Speed Flight Sta., Edwards AFB 1

NASA, Goddard Space Flight Ctr., Greenbelt
Att: J. C. New, Code 320 1
Att: G. Hinshelwood, Code 623.3 1
Att: Elias Klein 1
Att: K. M. Carr, Code 321.2 1
Att: F. Lindner, Code 321.2 1

NASA, Langley Research Ctr., Va.
Att: Library 2
Att: S. A. Clevenson, Dynamic Loads Div. 1

NASA, Lewis Flight Propulsion Lab., Cleveland
Att: Library 1

NASA, Manned Spacecraft Center, Houston
Att: G. A. Watts 1

NASA, Marshall Space Flight Center, Huntsville
Att: Mr. R. M. Hunt, M-P&VE-S 1
Att: Mr. James Farrow, M-P&VE-ST 1
Att: AMSMI-RBLD 1

NASA, Scientific & Tech. Info. Facility, Bethesda
Att: S-AK/DL 1

National Bureau of Standards, DC
Att: B. L. Wilson 1
Att: S. Edelman, Mech. Div. 1

National Security Agency, DC
Att: Engineering 1

Naval Air Development Center, Johnsville
Att: E. R. Mullen 1
Att: Aeronautical Instruments Lab. 1
Att: NADC Library 2

Naval Air Engineering Center, Phila.
Att: Library 1

Naval Air Station, Patuxent River
Att: Weapons Systems Test (E. B. Hamblett) 2

Naval Air Test Center, Patuxent River
Att: Electronics Test Div. 1
Att: VTOL/STOL Br. 1

Naval Ammunition Depot, Crane
Att: Code 3540 1
Att: Code 3400 1

Naval Ammunition Depot, Earle
Att: Chief Engr., Materials Handling Lab. 1

Naval Ammunition Depot, Oahu
Att: Weapons Tech. Library 1

Naval Applied Science Laboratory, Brooklyn
Att: Library 1

Naval Attache, Navy 100
Att: Logistics Division 1

Naval Civil Engineering Lab., Pt. Hueneme
Att: Library 2

Naval Construction Battalion Ctr., Pt. Hueneme
Att: OIC, USN School, Civil Engineer Corps Officers 1

Naval Medical Field Research Lab., Camp Lejeune
Att: Commanding Officer 1

Naval Mine Engrg. Facility, Yorktown
Att: Library 1

Naval Missile Center, Pt. Mugu
Att: Library, N-03022 1
Att: Environment Div., N314 2

Naval Operations, Office Chief of, DC
Att: Op 31 1
Att: Op 34 1
Att: Op 75 1
Att: Op 07T6, T. Soo-Hoo 1
Att: Op 725 1

Naval Ordnance Lab., Corona
Att: Quality Eval. Lab 1
Att: Code 56, Sys. Eval. Div. 1

Naval Ordnance Lab., White Oak
Att: Technical Director 1
Att: Library 3
Att: Environmental Simulation Div. 6
Att: G. Stathopoulos 1

Naval Ordnance Test Sta., China Lake
Att: Technical Library 1
Att: Code 3023 1
Att: Code 3073 1
Att: Code 4062 1

Naval Ordnance Test Sta., Pasadena
Att: P8087 3
Att: P8092 1
Att: P8073 1
Att: P80962 1

Naval Postgraduate School, Monterey
Att: Library 1

Naval Propellant Plant, Indian Head
Att: Library 1

Naval Radiological Def. Lab., San Fran.
Att: Library 1

Naval Research Laboratory, DC
Att: Code 6250 1
Att: Code 6260 1
Att: Code 6201 1
Att: Code 4021 2

Naval Security Engrg. Facility, DC
Att: R&D Branch 1

Naval Supply R&D Facility, Bayonne
Att: Library 1

Naval Torpedo Station, Keyport
Att: QEL, Technical Library 1

Naval Training Device Ctr., NY
Att: Library Branch 1
Att: Code 4211 1

Naval Underwater Ord. Sta., Newport
Att: Tech. Documents Library 1

Naval Weapons Evaluation Facility, Albuquerque
Att: Library, Code 42 1

Naval Weapons Laboratory, Dahlgren
Att: Technical Library 1

Navy Central Torpedo Office, Newport
Att: Quality Evaluation Lab. 1

Navy Electronics Lab., San Diego
Att: Library 1

Navy Marine Engineering Lab., Annapolis
Att: Code 705 1

Navy Mine Defense Lab., Panama City
Att: Library 1

Navy ROTC & Admin. Unit, MIT, Cambridge 1

Navy Underwater Sound Lab., New London
Att: Technical Director 1
Att: J. G. Powell, Engrg & Eval. Div. 1

Navy Underwater Sound Ref. Lab., Orlando
Att: J. M. Taylor, Code 120 1

Norfolk Naval Shipyard, Va.
Att: Design Superintendent 1

Norton AFB, Calif.
Att: AFIMS-2-A 1

Off. Director of Defense R&E, DC
Att: Technical Library 3
Att: Mr. Melvin Bell 1
Att: Mr. Walter M. Carlson 1

Off. of Naval Material, DC 1

Off. Naval Research, DC
Att: Code 439 6
Att: Code 104 1

Off. Naval Research Branch Office, Boston 1

Off. Naval Research Branch Office, Pasadena 1

Off. Naval Research Branch Office, San Fran. 1

Ogden Air Materiel Area, Hill AFB
Att: Service Engr. Dept., OCNEW 1

Oklahoma City Air Materiel Area
Att: Engineering Division 1

Pearl Harbor Naval Shipyard
Att: Code 264 1

Philadelphia Naval Shipyard
Att: Ship Design Section 1
Att: Naval Boiler & Turbine Lab. 1

Picatinny Arsenal, Dover
Att: Library SMUPA-VA6 1
Att: SMUPA-VP7, R. G. Leonardi 1
Att: SMUPA-T, R. J. Klem 1
Att: SMUPA-D, E. Newstead 1
Att: SMUPA-VP3, A. H. Landrock 1

Portsmouth Naval Shipyard
Att: Code 246 1
Att: E. C. Taylor 1

Puget Sound Naval Shipyard
Att: Code 251 1
Att: Material Labs. 1
Att: K. G. Johnson, Code 242 1

Quartermaster Food & Container Inst., Chicago
Att: Dir., Container Lab. 1
Att: Technical Library 1

Quartermaster R&E Airborne Test Activity, Yuma
Att: QMATA 1

Quartermaster Res. & Engrg. Ctr., Natick
Att: Technical Library 2
Att: Dr. W. B. Brierly 1

Randolph AFB, Texas
Att: USAF School of Aviation Medicine 1

Rome Air Development Center, NY
Att: Dana Benson, RASSM 1

Rossford Ordnance Depot, Ohio
Att: Ordnance Packaging Agency 1

San Francisco Naval Shipyard
Att: Design Division 1

Savanna Ordnance Depot, Illinois
Att: OASMS 1

Sheppard AFB, Texas
Att: 3750th Tech. School (TC) 1

6511 Test Group (Parachute), El Centro
Att: E. C. Myers, Tech. Dir. 1

6570 Aerospace Med. Res. Labs., WPAFB
Att: MRMAE 1

Special Projects, USN, DC
Att: SP Tech. Library 1

Springfield Armory, Mass.
Att: Library 2

Strategic Air Command, Offutt AFB
Att: Operations Analysis Office 1

Supervisor of Shipbuilding, USN, Camden, NJ
Att: Code 299 2

Watertown Arsenal, Mass.
Att: R. Beeuwkes, Jr., Ord. Matls, Res. Off. 2
Att: Technical Information Sec. 1
Att: ORDBE-LE 1

Watervliet Arsenal, NY
Att: ORDBF-RR 2

White Sands Missile Range, NM
Att: Electro-Mechanical Div. 1
Att: ORDBS-TS-TIB 3

CONTENTS

PART III

Vibration Testing

Combined Temperature-Vibration Tests

Vibration Test Specification

Standardization of Vibration Tests

Application of Data to Design

Section 1
INSTRUMENTATION

EFFECT OF MOUNTING-VARIABLES ON ACCELEROMETER PERFORMANCE

B. Mangolds
Radio Corporation of America
Princeton, New Jersey

This paper describes a controlled program to investigate different mounting techniques for accelerometers. Recommended techniques are discussed.

The published basic characteristics of an accelerometer do not sufficiently define the device, and the good instrumentation engineer realizes that he must have more information than this in order to obtain accurate vibration data at any measurement point. Such "subtle" problem areas, which generally are not brought up in data sheets or sales talks (except possibly in reference to "Brand X") and should be taken into consideration are:

Interface (surface) condition,
Cross motion over full frequency range,
Polarity,
Torque sensitivity,
Acoustic sensitivity,
Stability of high cross-motion levels over full frequency range,
Dynamic linearity, and
Capacity temperature dependence.

By careful selection of suitable hardware, the engineer can feel satisfied that these problems are non-existent or are of known magnitude. Even with all of the above factors taken into account, the engineer often comes to the intuitive conclusion that additional unknown effects are influencing the data obtained. The practical significance of such effects depends on the application of this information; it can lead to misinterpretation of the test hardware response (if it is used as test data), or it can result in the generation of environmental conditions differing from those specified (if it is used as a control signal).

In order to use an accelerometer, one has to mount it. The Environmental Simulation Group at the RCA Space Center felt that these additional factors affecting accelerometer response arise largely because the transducer is seldom mounted in the manner envisioned by the manufacturer when it is designed. The need to clear vibration data of the influence of mounting variables was considered to be of such importance that a study of the matter (restricted, however, directly to the problems of importance to the RCA Environmental Simulation Group) was conducted.

The following selected list of mounting methods and associated factors related to the testing experience of this RCA Group defined the scope of the study:

MOUNTING METHODS

1. With Screws (Fixtures)
   - Direct mounting
   - Blocks (adaptation)
   - Blocks (insulation)
   - Studs (insulation)
2. Without Screws (Test Hardware)
   - Magnetic fastening (repositioning)
   - Pressure sensitive adhesion (repositioning and insulation)
     - Tapes (backing)
     - Films (transfer)

Chemical adhesion (insulation)
- Blocks
- Washers
- Paper

ASSOCIATED FACTORS

1. Temperature Ramps
2. Cable Routing
3. Magnetic Fields

Also investigated were the compatibility of various accelerometers in use and the techniques of handling these devices. As a result of the study, some models were immediately removed from circulation; the use of others was restricted; and accelerometer-housekeeping rules were tightened.

Specific personnel were assigned to the selection of accelerometers for future use in the Environmental Simulation Group, and closer supervision of personnel handling the accelerometers was instituted.

An example of the results of careless handling on an accelerometer is shown by the frequency-response curves of Fig. 1. Each curve represents the response degradation caused by fingerprint deposits, of varying degree, across the accelerometer cable receptacle.

Determination of the changes in the frequency-linearity of a given transducer was the main target of the study. Most of the work was performed using an Unholtz-Dickie Model 300 calibration system, Fig. 2. With the shaker kept at a constant g level (5-g peak for most work) this system swept up to 10 kc and plotted the frequency response of the specimen accelerometer as a percent deviation from the control transducer response at a normalized frequency (200 cps was used in this work).

Although vibration tests often stop at 2 kc, the frequency sweep, in this investigation, was extended to 10 kc because acceleration waveforms charted in actual tests often show a large harmonic content. The interaction of the Fourier components with the resonances caused by a poor mounting situation can lead to gross waveform distortion by selective amplification and attenuation.

All practically possible precautions were taken to vary only one factor at a time in these investigations. Tests were rerun as many as six times to prove the consistency of results before a conclusion was accepted.

A compression-type accelerometer representing the "work-horse" at the RCA Space Center was stud-mounted directly to the shaker

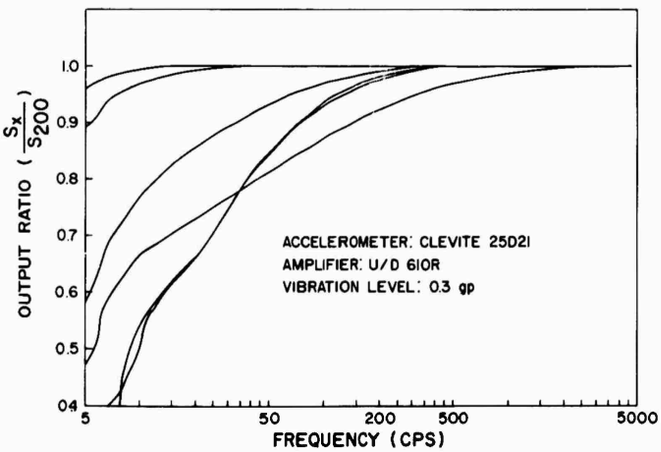

Fig. 1 - Degradation of accelerometer frequency response caused by shunt impedance (fingerprints) on cable receptacles

Fig. 2 - Accelerometer calibration setup, Unholtz-Dickie Model 300 System

and a comparison was made, at three different torques, between the frequency response with dry contact surfaces, and response with a light oil film bonding the interface. This comparison was repeated with shear models, previously found to be even less torque-sensitive.

The results generally agreed. The same frequency response is produced at less torque with an oil-film as with highly torqued dry surfaces; and a significant buildup in the high-frequency response (+25 percent at 10 kc) can be reduced to 5 percent when using oil with dry-surface mounting. The finding is of value particularly in shock tests.

Surfaces of odd shapes necessitate the use of adapters between the accelerometer and the test point. Also, to measure vibration along a cross-axis, an auxiliary block often is required to fulfill the need for three mutually perpendicular planes. One must then consider the addition of this new spring-mass element in series with the accelerometer and its effect on the accelerometer response curve as a function of block material and geometry. Block size was dictated by the accelerometer base area. Cubes of identical size were made from five common materials: aluminum, cold-rolled steel, brass, lucite, and fiberglas, and tests were made for each. The resulting response curves are shown in Fig. 3. Additional tests were made with lucite; and more response curves (shown in Fig. 4) were taken to determine the effect of adding cross-motion accelerometer to setup. Curve A is for the single in-line transducer; B and C show the result of adding, in turn, more accelerometers. The shift of resonance towards higher frequencies were explained by a stiffening effect on the sides of the block as accelerometers were added. This effect was verified when instead, small steel plates were cemented one at a time. Because of their low resonant frequency, Lucite blocks were removed from further consideration. For a while, Fiberglas (G-11) was used as block material, but later, as the insulated-wafer technique developed, this material was replaced by aluminum.

Insulating materials were of particular interest, because isolating an accelerometer electrically from ground is a well-known means of decreasing the influence of ground loops. Insulated triaxial accelerometers are available commercially, but they are economically impractical. Recently a new series of shear-mode accelerometers was investigated; their electrical circuitry is off ground and is inherently insulated, while the case can be grounded safely and all other electrical characteristics are of

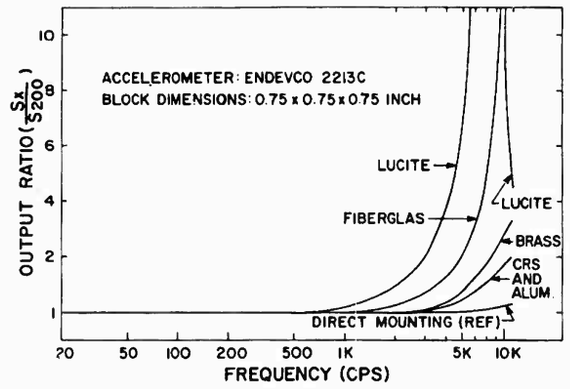

Fig. 3 - Effect of mounting-blocks on accelerometer response

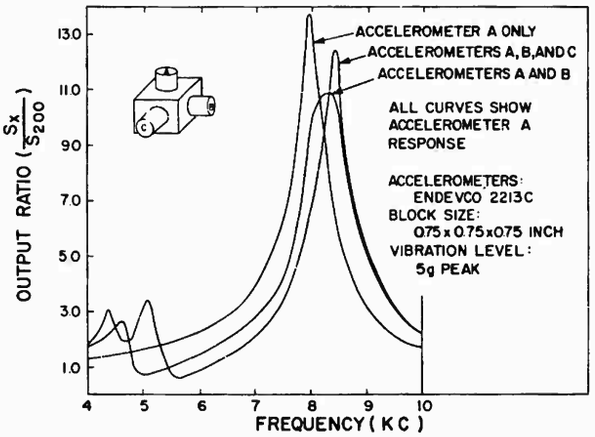

Fig. 4 - Effect on response of one accelerometer of adding additional accelerometers to mounting block

acceptable quality without apparent compromise. However, since presently-stocked accelerometers still have to be used for some time, the investigation included the effect of insulated mountings on these.

Where threaded holes can be tolerated, commercially-available insulated studs would be of prime interest. A comparison of the effect of four studs of this type (one having ceramic insulation) was made; the results are shown in the curves of Fig. 5. The same accelerometer and the same torque was used in all of these tests, with an oil-film on all interfaces. A reference performance-curve for the accelerometer mounted directly to the shaker also is given in Fig. 5. Although the difference of results among the studs used is not great, one stud having hexagonal flanges provided a decided advantage. High torque applied across the insulating layer affects its interface bond; this might not be readily apparent unless a comparative calibration run is made. The hex-flange construction, however, permits application of torque to the accelerometer side and the fixture side separately, without introducing a shear torque across the insulating medium. Better reliability and longer stud life can be expected from this design.

The use of these devices is restricted to systems where a threaded mounting-hole can be

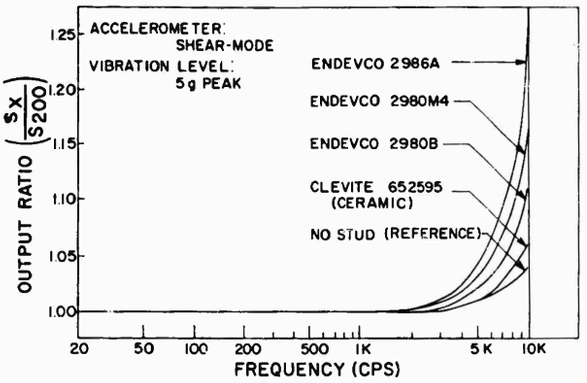

Fig. 5 - Effect of insulated mounting studs on accelerometer response

tolerated. Such an arrangement cannot be used on test hardware such as vidicon tubes, cameras, solar cells, and the like. Other methods such as cementing, vacuum, and magnetic-mounting techniques must be considered, and this makes the initial requirement for electrical insulation alone even more complex.

Vacuum mounting was ruled out as impractical for our particular conditions. Magnetic clamping is obviously usable only under special conditions; it was tried nevertheless, because of its simplicity and relocation. An accelerometer was mounted directly on a General Radio magnetic clamp Model 1560-P35 (Fig. 6); the resulting curve (Fig. 7) shows a fundamental resonance around 4 kc which limits this method even further. No attempt has been made to insulate the accelerometer from the clamp. Also, because of the relatively large contact surface of the magnet-to-fixture interface, small variations in the physical condition of the surface (which is difficult to control) had substantial effects on the curve shape. Because most structures are nonmagnetic, this technique is of limited interest.

Cementing an accelerometer in place with insulating material in-between is the most popular and practical mounting method for the majority of applications at the RCA Space Center. Considerable effort was spent in investigating materials, techniques, and frequency-affecting variables, and in the establishment and enforcement of everyday handling routines for AED technicians. Material search established melamine-impregnated Fiberglas (G-11) as the most practical insulating material for this purpose.

Fig. 6 - Accelerometer mounted by means of a permanent-magnet clamp

The performance of a number of blocks made of various insulation materials has already been shown (Figs. 3 and 4) in the discussion of adaptation of odd surfaces. Where odd surface shape was not a factor, there was no real need for the original high block, and consequently, the material was cut down to a disc.

In mounting a typical accelerometer having a hexagonal base, with a circular boss, the question arose whether there would be a variation in performance between mounting it on an insulating disc having the diameter of the boss, and mounting it on one having the diameter of

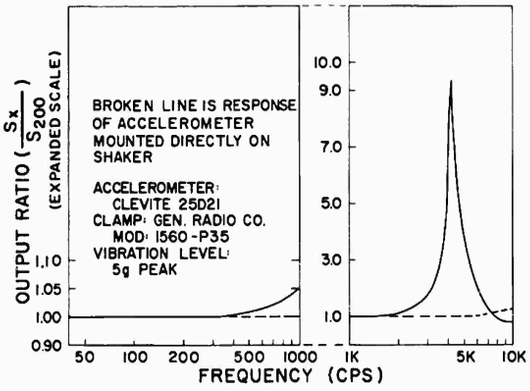

Fig. 7 - Response of accelerometer mounted by means of a permanent-magnet clamp

the hex extremes (with a cement filler surrounding the boss).

G-11 Fiberglas discs of two diameters were cut, in several thicknesses. The various responses obtained are shown, compared with the response of the accelerometer mounted solid, in Fig. 8. From these curves, it may be seen that a thinner disc of large contact area produces a curve closer to the reference curve. It should be kept in mind that this result represents a specific situation; that is, an accelerometer of a specific construction, mode of operation, weight, and interface area; and a specific disc material. Accelerometers which are sensitive to base deformation, cross-motion, or other special conditions at the interface (such as was found with some subminiature compression types) will respond differently.

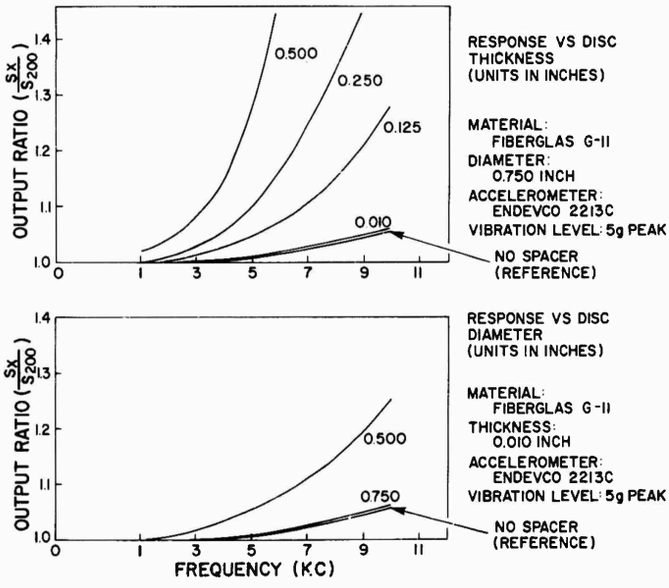

Fig. 8 - Effect of insulating-spacer geometry on accelerometer response

Of the cements tried (e.g., epoxies, dental cements), the best compromise was found in Eastman 910, but extreme care had to be exercised to establish a reliable adhesion. The use of cement brought a host of new problems hinging mainly on the practical, everyday enforcement of specified cementing routines, such as preparation and cleaning of surfaces, quality and quantity of cement, and hardware. Enforcement of gentle removal techniques also proved to be quite an administrative problem, and deviations from specified after-test cleaning methods of accelerometers still cause occasional thunder. Only chemical cleaning is permitted, and short of hot water, the only practical solvent so far known is dimethyl formamide, sold under trade names such as Gage Stripper. The precautions required in handling this chemical and the unpleasant odor involved, however, make it somewhat less than satisfactory for the purpose at hand.

Cemented accelerometers with hexagonal bases are removed readily by means of a suitable wrench that grips the base tightly, but with toroidal units, removal can become a problem unless the insulating disc is made with flats. Another difficulty with cemented assemblies of this form is their deceptively sturdy appearance. After a multitude of mounting and frequency-surveys under seemingly identical conditions (same bottle of cement, same operator and ambient conditions, same disc material and geometry, and identical accelerometer), it was found that the strength of a cemented mounting cannot necessarily be judged by hand pressure. The curves shown in Fig. 9 were made with such "sturdy" assemblies; the distortions were traced in every case to deficiencies in interface bond uniformity, such as incomplete area coverage caused by air bubbles in the cement layer. Since most of the time after the assembly is cemented in place a calibration by vibration cannot be done, the actual quality of the mounting cannot be verified. Its adequacy must be ensured by careful mounting techniques.

There are now three separate layers of dissimilar materials between test surface and accelerometer (cement-disc-cement), each with its own mechanical properties (mass and spring constant) and each able to distort the vibration environment to be transmitted to the accelerometer. Any decrease in the number of layers would mean an improvement all by itself. Since all that a disc does is to act as a spacer for electrical separation, and Eastman 910 cement is a good insulator when cured, then the disc could be omitted entirely, were it not for the uncertainty of the degree of separation. A strong

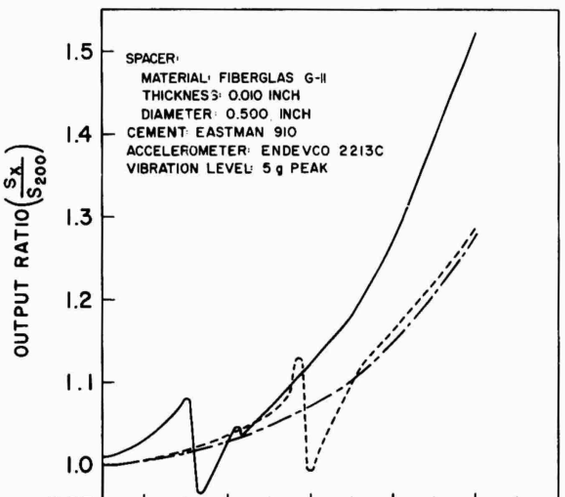

Fig. 9 - Effect of "Rocking" due to faulty cement bond on accelerometer response

person could apply more pressure during mounting and cut through the cement layer. The minimum amount of spacing material, just enough to prevent short circuits, should suffice. With this in mind, very porous (tissue) paper was fully impregnated with cement and used as a spacer. The resulting accelerometer response was that shown in the curves taken with ceramic-stud mounting in Fig. 6. A word of caution: It is not sufficient to apply cement to the paper on one side alone because the paper, acting as a mechanical filter, separates some components of the cement, and the result is a poor bond.

Using proper care, one may obtain excellent mechanical coupling and electrical insulation by this method. The disadvantage is mainly in the difficulty of removing the spacing material after a test.

In general, disadvantages of cementing are reliance on an individual's quality of workmanship, dependence on Standards-Laboratory calibration, and the required freedom from transverse waves over the area of contact. Flexing of the mounting surface can break the bond readily because of lower strength in shear. Therefore, cementing of control (servo) accelerometers is not permitted at the RCA Space Center. There are numerous applications, however, where it is the only method that can be used.

To provide easy removal or relocation of accelerometers, which is a simultaneous but opposite requirement to strength or mounting, the application of pressure-sensitive tapes and films (so-called transfer types) without backings was considered (such as Permacel Types P94, 6399, and ED4551, and "3M" Types 466, Y-400, and 666). Some results of tape mounting are shown in Fig. 10. For a while the use of prefabricated tacky discs, dispensed from rolls of backing material, was envisioned. But then the dependence of these discs on application pressure (sponge factor), temperature, and surface adaptability, as well as low shear strength, cold flow, and other disadvantages were established, and while in certain isolated and controlled cases tapes could be tolerated, the need for close continuous surveillance ruled them out as a general method.

If we enlarge the meaning of "mounting method" to include choice of location (where such a choice exists), the output of an accelerometer can be greatly affected by some specific conditions present at one mounting location and not at another.

The previously described insulating electrical barrier often doubles as a thermal barrier by delaying sufficiently an unavoidable rise in surface temperature to permit completion of the test. There is also, however, a different type of temperature sensitivity associated with some particular models; this causes new problems and is not as well known. Some accelerometers have been found to exhibit a rather pronounced high sensitivity of rate-of-change of

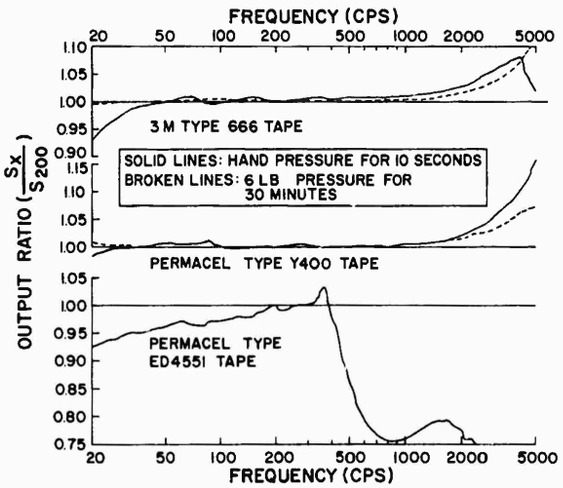

Fig. 10 - Effect of double-faced adhesive tape mounting on accelerometer response

temperature, or pyroelectric effect, which is not to be confused with ordinary ambient temperature effect. If during a test, an accelerometer is suddenly cooled due to the flow of liquid nitrogen in a nearby control line, or if it is suddenly heated by the blast of hot air from a rocket-engine firing, or even if the draft from an opened door sweeps over the accelerometer, a rather violent reaction may occur in the response. In some models, dc-shifts of high magnitude occur; these seem to be a function of the rate-of-change of temperature and the time constant (leakage resistance) of the particular instrumentation channel. The dc-shifts may over-drive the associated amplifier and, if part of the instrumentation involves work with filters (as double-integration of acceleration signals to obtain displacement data), the results can be disastrous. What happens when an accelerometer vibrating at 0.3 g at 235 cps was exposed to an illuminated 60-watt lamp passing over it at a distance of 4 feet is shown in Fig. 11. Trace (a) shows the acceleration signal, (b) the same once integrated, and (c) the same integrated twice by an Unholtz-Dickie Dial-a Gain amplifier Model 610RM3.

At low frequencies, with associated higher amplitudes, accelerometer cable-termination and routing can become important for some accelerometer models. While it is difficult to specify a uniform method, terminations such as those shown in Fig. 12 are not permitted at the RCA Space Center, regardless of model; a rule of thumb is to let the cable take its own natural straight-line position, as long as its weight does not become excessive. Some results with one case-sensitive accelerometer with different cable routing are shown in Fig. 13. The effect of cable routing on shear-type accelerometer was less pronounced than it was on the other types tested.

A condition not related to cable routing, but which can degrade a response curve, is shown by accelerometer "E". The contact-surface gap (exaggerated in the photo) is caused by foreign material in the mounting hole, inside the accelerometer preventing proper seating of the stud.

Jerking of the cable, or other application of sudden stress, creates substantial spurious signals in some cables. The output response of an accelerometer which was swept for magnitude comparison at 1 g is shown in Fig. 14. Point "1" on the curve shows the effect of hitting the floor with a 4-foot length of cable, folded four times. A 1-foot length, slightly and slowly stressed and then suddenly released, produced the spike at point "2". A 1-foot length was jerked to produce the spike at point "3". A wide difference in sensitivity to such shocks was found among different cable models.

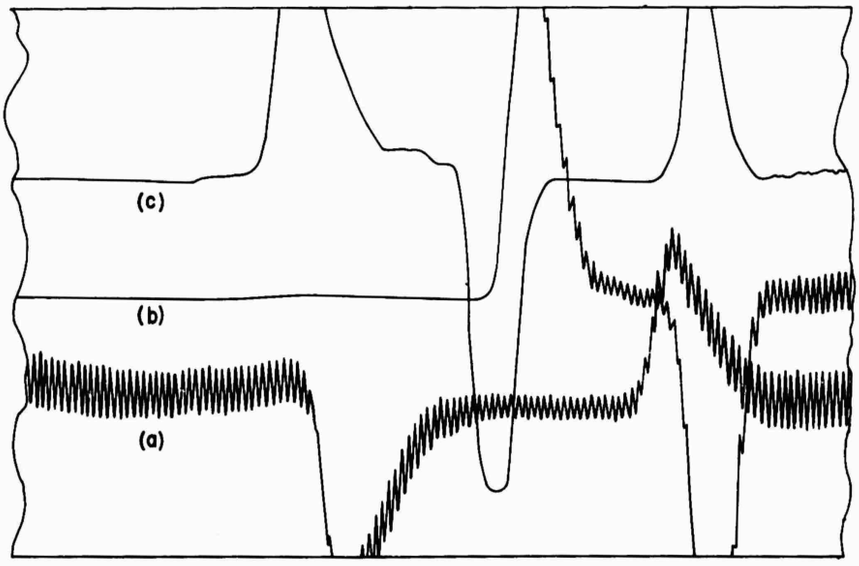

Fig. 11 - Chart recordings showing pyroelectric effect on accelerometer caused by sudden proximity of a 60-watt lamp

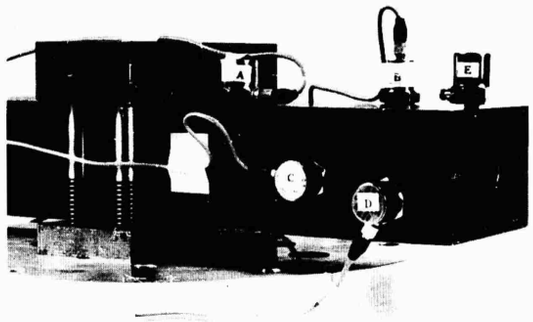

Fig. 12 - Unacceptable cable routings from accelerometer

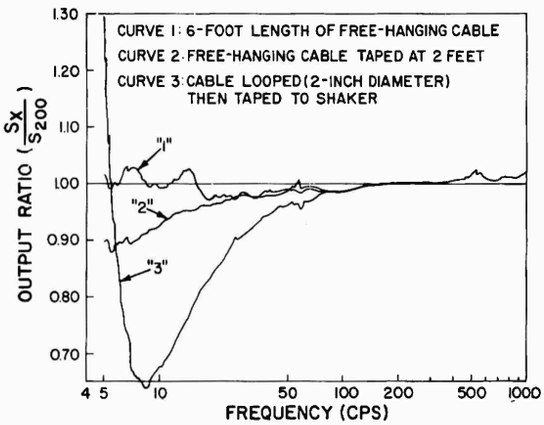

Fig. 13 - Effect of cable routing on accelerometer response

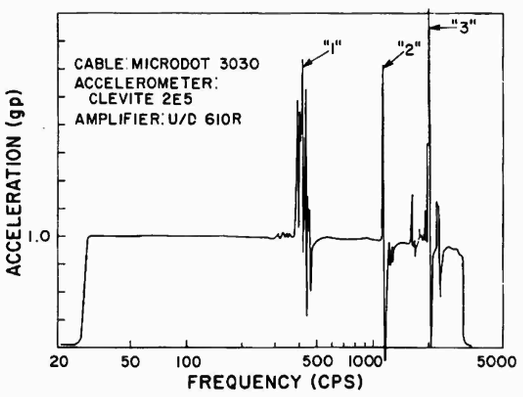

Fig. 14 - Accelerometer-response transients caused by sudden stressing of connecting cable (superimposed on a 1-g peak sweep)

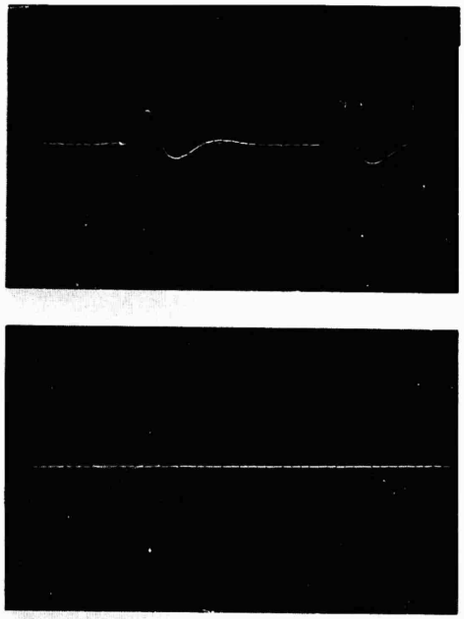

Fig. 15 - Influence of magnetic field (from shaker) on original (paramagnetic) model and modified (non-magnetic) model of an accelerometer

Finally, there are instances where accelerometers have to work in strong magnetic fields; for example, an input accelerometer near the junction of shaker armature and slip-plate might be exposed to a very strong magnetic environment created by the shaker field supply. Obviously, if this accelerometer is used for control, insensitivity to magnetic interference is of utmost importance. This interference might develop at two points; one, the accelerometer itself and the other, the accelerometer cable.

The center conductor of most cables is paramagnetic. Auxiliary cable vibrations, which has interfered, in some instances, with case-sensitive accelerometers was caused by ac magnetic fields.

Certain accelerometers used by the RCA Space Center were found to be paramagnetic; the manufacturers concerned are replacing these with great enthusiasm as it is brought to their attention. The difference between a particular model and its improved version, under identical conditions is shown in Fig. 15. The accelerometers were free-hanging without vibration near the mounting surface of a C10 shaker with the field supply turned on and then shut off. A field strength of 25 gauss at that point was measured in line with the sensitive axis of the accelerometer. Clearly, the cure here is to use the right transducer model.

It is felt that some gains have been made by this investigation. It has emphasized even more the engineer's need to know his accelerometer; it also has clearly shown that the user can make serious mistakes by unknowingly adding variables of his own.

Mr. Krause (Jennings Radio): Did you use just one brand of cable or did you try other brands?

Mr. Mangolds: We tried several brands.

Mr. Fry (U. S. Army Waterways Experiment Station): Have you any information relative to three accelerometers mounted in a box rather than on a block? In other words, one on the bottom, one on the side, and one on an end.

Mr. Mangolds: No.

Mr. Buist (Autonetics): We use Eastman 910 quite a bit, and many of the accelerometers are damaged in trying to get this cement off. You mentioned something about a solvent - - -.

Mr. Mangolds: Yes, the chemical name is N,N-dimethylformamide, but the same thing is available commercially under several trade names. One of them is Gage Stripper. We found this in connection with using the same type of cement on a strain gage.

* * *

SURFACE FINISH EFFECTS ON VIBRATION TRANSDUCER RESPONSE

R. W. Miller
U. S. Navy Marine Engineering Laboratory

An investigation is described to determine the effects of applied torque, surface finish, and surface flatness of transducers and mounting bases on vibration transducer sensitivity.

In recent years, the requirements for making structure-borne noise measurements in the higher frequency range have been increasing. As a result of these increased requirements we have had to take a closer look at some of the parameters affecting vibration measurements in the higher frequency range. One of our recent investigations was concerned with the effects of "surface finish" on the vibration transducer response. During the course of the investigation we were also able to observe the effect of surface flatness as well as the torque applied in attaching the transducer.

In order to determine the changes in transducer sensitivities that could exist under various mounting conditions and to reduce the experimental error of the investigation, the interferometer method of vibration calibration was selected for this study. The overall error of this calibration method is estimated to be between 2 and 3 percent. The investigation covered the frequency range from 200 to 15,000 cps. All calibrations were performed on Massa, Type 198 accelerometers attached to a National Bureau of Standards type high frequency vibration shaker, Fig. 1. Vibration displacement measurements were determined by the fringe disappearance method in conjunction with a Fizeau-type interferometer.

Since the vibration shaker used for this investigation is equipped with a removable head that can be replaced by similar heads, it provided a convenient means for making studies of surface finish and surface flatness. Figure 2 shows how the head is fitted to the shaker by the use of spanner wrenches.

To determine the effect of surface finish on the transducer sensitivity, five shaker heads were manufactured, each having a different surface finish as measured in micro-inches rms. The surface finishes for the five heads ranged from 9 to 230 microinches as shown by the numbers at the top of Fig. 3. The flatness (crown height) of the five heads ranged from 78 to 177 microinches as shown by the numbers at the bottom of Fig. 3. Figure 4 shows the Massa accelerometer, Type 198, ready to be torqued to the shaker head.

The base of the accelerometer used in conjunction with the surface finish study was found to have a surface finish of 9 microinches rms and a crown height of 57 microinches rms. A torque wrench was used as shown to measure the amount of torque applied in attaching the accelerometer. The same Massa accelerometer was attached, in turn, to each of the five shaker heads and calibrated over a frequency range of 200 to 15,000 cps. The mounting conditions (10 and 30 lb-in. torque, with and without silicone grease) allowed us to study the effect of torque and grease in conjunction with the various surface finishes.

To provide an ideal mounting surface to serve as a standard condition or criterion, an additional shaker head was lapped to a "perfect finish," Fig. 5. This surface was found to be flat, within one interference fringe, as determined by an optical flat and monochromatic light. For use with this "perfect surface" another Massa accelerometer, Type 198, was lapped so that it could be "wrung" to the shaker head and held in place only by the molecular attraction of the Johannson surfaces while being calibrated.

All results of the investigation were presented in the form of transducer calibration

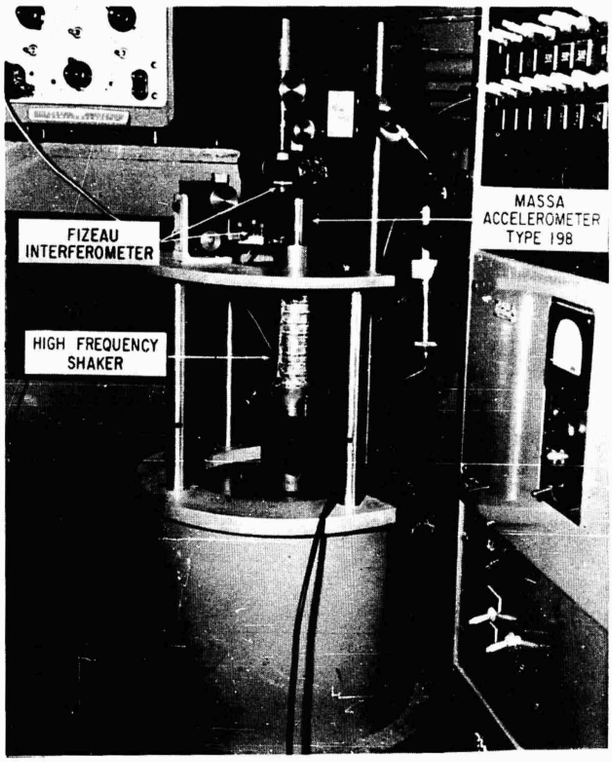

Fig. 1 - Massa accelerometer type 198 attached to an NBS-type high-frequency vibration shaker

curves, Fig. 6, which were presented in terms of acceleration versus frequency. This is a typical curve showing the sensitivity of the pickup under three different mounting conditions, when no grease is used between the pickup and the mounting surface. Curve 1 represents the transducer response under the ideal mounting condition, that is, when attached to the surface having the "perfect" finish. Curve 2 represents the transducer response when attached to a surface having a 150-microinch finish. Curve 3 represents the response of the transducer when attached to a surface having a 9-microinch finish.

Notice that the position of the curves 2 and 3 appear to be reversed. Normally, we would expect the response of the transducer, when mounted on a 9-microinch finish, to more closely approximate the ideal condition (curve 1) than when it is mounted on the coarser 150-microinch finish. This inconsistency as shown by curves 2 and 3 suggests that another variable is exerting considerable influence on the transducer response. The inconsistencies shown in the calibration curves, Fig. 6, are best demonstrated in Table 1 which gives the transducer sensitivity at 8000 cps under the various mounting conditions. The sensitivities obtained with the various surface finishes may be compared to the sensitivity produced by the ideal or standard surface shown at the bottom of Table 1.

By using the results from the "perfect surface finish" as a criterion, it can be seen that the surface finishes that produce the best results assume the following arrangement: 150, 63, 35, 9, and 230 microinches. The answer to this inconsistency is found in the column to the extreme right. Flatness measurements disclosed that the five shaker heads were convex at the center. The crown height, given in microinches rms, ranged from 78 to 177. Note that the surfaces having the 63-microinch finish and the 150-microinch finish produced the lowest sensitivity or the sensitivity most closely approximating the standard sensitivity given at the bottom of Table 1.

Fig. 2 - Removable head being fitted to the shaker by the use of spanner wrenches

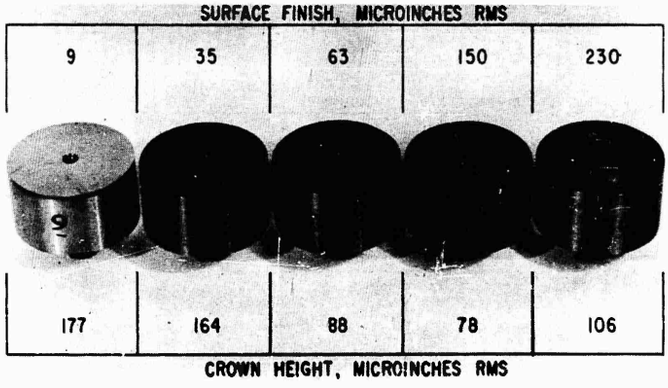

Fig. 3 - Shaker heads of varying surface finishes and crown heights

Looking at the crown height of these two surfaces, as shown in the column to the extreme right, we find that these two shaker heads have crown heights of 88 and 78 microinches, respectively, or the flattest surfaces of the group. These measurements indicate that crown heights as little as 78 microinches rms are more significant than the 150-microinch surface irregularities.

Further verification of the relationship of crown height to the calibration sensitivity is found in the numbers shown at the top of Table 1. When mounted on a relatively smooth surface having a 9-microinch finish, the sensitivity of the transducer rises to 114.5×10^{-6}. This error of approximately 30 percent in the calibration sensitivity is attributed to the extreme crown height of this particular mounting surface

TABLE 1
Transducer Response (Without Grease)

Torque (lb-in.)	Finish Microinches (rms)	Sensitivity of Accelerometer at 8000 cps (volts rms/cm peak/sec^2)	Crown Height (Microinches rms)
10	9	114.5×10^{-6}	177
	35	105.5×10^{-6}	164
	63	97×10^{-6}	88
	150	97×10^{-6}	78
	230	118×10^{-6}	106
30	9	105.5×10^{-6}	177
	35	96×10^{-6}	164
	63	89×10^{-6}	88
	150	86×10^{-6}	78
	230	95×10^{-6}	106
Standard Surface 85×10^{-6}			

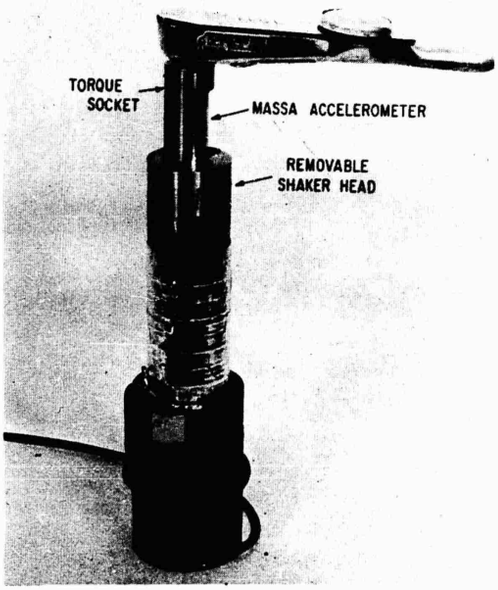

Fig. 4 - Massa accelerometer type 198 ready to be torqued to shaker head

which is 177 microinches rms, as shown in the column to the right.

At the bottom of Table 1, one may observe a change in the transducer sensitivity due to increased torque. Increasing the torque to 30 lb-in. had the effect of flattening the crown, thereby producing a more intimate contact between the transducer and the calibrator head. The sensitivities obtained under the 30-lb-in. torque condition are considerably lower in value and are approaching the sensitivity obtained under the ideal mounting condition.

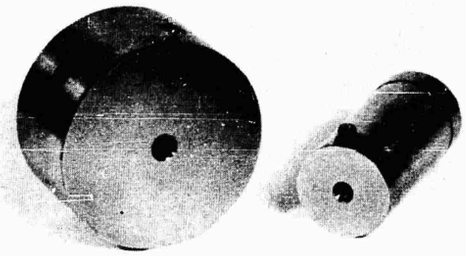

Fig. 5 - Shaker head with "perfect finish surface" and Massa accelerometer type 198

In addition to the study of the effects of surface finish, surface flatness, and applied torque, the effect of a silicone grease bond between the pickup and the mounting surface was also studied. Table 2 shows the transducer response at the 8000-cycle point when grease is used between the base of the accelerometer and the mounting surface. Notice that surface finish, crown height, and torque have no noticeable effect on the transducer calibration sensitivity when grease is used between the accelerometer base and the calibrator head.

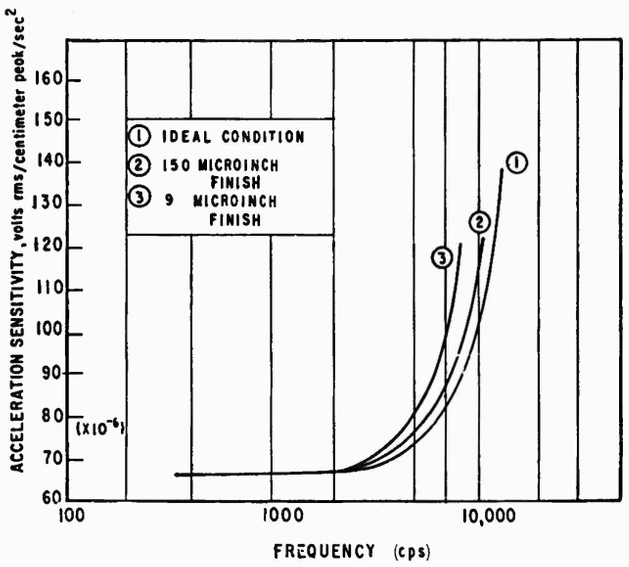

Fig. 6 - Transducer response at 10 lb-in. torque with no grease

TABLE 2
Transducer Response (With Grease)

Torque (lb-in.)	Finish Microinches (rms)	Crown Height (microinches rms)	Sensitivity of Accelerometer at 8000 cps (volts rms/cm peak/sec^2)
10	9	177	83×10^{-6}
	35	164	81×10^{-6}
	63	88	83×10^{-6}
	150	78	86×10^{-6}
	230	106	86×10^{-6}
30	9	177	85×10^{-6}
	35	164	84×10^{-6}
	63	88	83×10^{-6}
	150	78	84×10^{-6}
	230	106	86×10^{-6}
Standard Surface 85×10^{-6}			

In summary, vibration measurements performed on surfaces other than perfect and without grease are affected by surface finish, surface flatness, and torque. As a result of this study we are recommending that transducer mounting surfaces be kept within the limits of 230 microinches rms surface finish and 177 microinches rms surface flatness and that a lubricant be used between the transducer and the mounting surface regardless of the high degree of surface finish. This is not to infer that a perfect mounting surface and the use of a lubricant will solve all of the problems involved in high frequency vibration measurements. Controlling the surface mounting conditions as demonstrated, however, will result in more valid and more repeatable data.

DISCUSSION

Mr. Ramboz (Bureau of Naval Weapons): Can these tests be applied to all piezo-electric accelerometers in general, or only to the Massa accelerometers?

Mr. Miller: That would be a little hard to say. We only tried the Massa accelerometer Type 198. As you know this has a lower resonance than some accelerometers.

Mr. Ramboz: What material was the shaker head made of? Was this an aluminum head?

Mr. Miller: The calibrator head was made of steel.

* * *

CALIBRATION OF WATER COOLED HIGH TEMPERATURE ACCELEROMETERS

W. R. Taylor and C. D. Robbins
LTV Military Electronics Division
Dallas, Texas

This paper presents a specific method for calibrating a water-cooled high-temperature accelerometer. Topics discussed include heating device, fixture design, cooling requirements, instrumentation, and results obtained.

INTRODUCTION

In conducting environmental vibration tests combined with temperatures to 3600°F, it was required to use water-cooled accelerometers to monitor and control the acceleration on surfaces whose temperature exceeded the limits of ordinary accelerometers. Preceeding the test, calibrations were made on each accelerometer at temperatures ranging from ambient to 1850°F. This paper presents the methods and results of the calibration for Endevco Model 2206 accelerometers.

FIXTURE DESIGN

A special fixture was required to provide a back-to-back calibration, allow heating of the accelerometers being calibrated, and maintain approximate laboratory ambient temperatures at the standard accelerometer location and on the vibration exciter. A cross sectional view of the fixture setup is shown in Fig. 1. The fixture was fabricated from 300-series stainless steel because of its magnetic, electrical, and thermal conductivity characteristics. The 3.5-inch diameter by 6-inch high column, shown in Fig. 1 in the center of a 2 x 13.5 x 13.5-inch base plate, was welded in place at the base and drilled and tapped on the top for two model 2206 accelerometers to be calibrated. A 2-inch diameter cavity was created in the center of the base plate to allow additional welding of the center column and to provide a cooling cavity for the standard accelerometer. The pipe through the cavity was threaded into the column. A slug was welded in the pipe near the column base to mount the standard accelerometer. A washer type cap was placed over the pipe and welded on the inside to the pipe and on the outside to the fixture base to make a watertight seal. A groove was cut along the base of the fixture for the standard accelerometer cable. To protect the vibration exciter and standard accelerometer from excessive heat, water was circulated through four holes drilled through the fixture base. Two of the four holes opened into the center cavity of the fixture. Two surfaces of the fixture were machined to a flat, smooth surface for mounting of the fixture to the vibration exciter and for mounting of the 2206 accelerometers.

INDUCTION HEATER DESIGN

To heat the fixture, an induction coil was fabricated and placed around the fixture. The coil was designed to the basic requirements for induction heating at 3000 cps with current-carrying capabilities as the prime objective. Since power amplifiers were available for 3000-cps frequency operation with a surplus of power available, coil design was not critical. The coil was shaped on a wooden form so that the clearance between the coil and fixture was approximately 0.25 inch. Twelve turns of 1/4-inch copper tubing provided sufficient induced current in the fixture to generate the desired heating.

INDUCTION SYSTEM

With the exception of the induction heater coil, all components necessary to formulate an electrical induction heating system were

available in the Test Laboratories.[1] A schematic of the electrical system is shown in Fig. 2. In order to match the heater coil impedance more closely with the power amplifier output impedance, a multi-tapped auto-transformer was used. Several heavy duty 3-kc capacitors were connected parallel to the heater coil to tune the circuit for resonance. The impedance of the heater coil was extremely low; therefore, it was necessary to parallel two pairs of 2/0 cables between the coil and auto-transformer to reduce the I^2R losses in the cables.

SYSTEM COOLING

A schematic of the complete water-cooling system is shown in Fig. 3. The heating coil was fabricated from copper tubing to allow water cooling. Water was circulated through the coil from a commercial pressure source with flow controlled by a needle valve. Water connections to the coil were made with approximately 10 feet of rubber hose on each side of the coil to isolate the plumbing ground from the electrical power source. Figure 2 shows the points where the electrical connections were made to the coil. The electrical resistance of the water through the rubber hose to ground was high compared to the impedance of the coil. The shunt resistance across the coil established by the water in the hose was negligible.

In addition to the coil, water-cooling was provided for the matching auto-transformer and tuning capacitors. Since these items were commercially designed for high power operation, they included built-in cooling systems.

A special independent cooling system was assembled to maintain constant water pressure and flow in the 2206 accelerometers being calibrated. The system consisted of a constant-speed electric pump, a water reservoir, gages, filter, needle valves, flex lines, tubing, and fittings. The reservoir eliminated commercial

[1] C. D. Robbins, "Combining Induction Heaters with Existing Environmental Facilities to Conduct Tests at Re-entry Temperatures," Shock, Vibration and Associated Environments Bulletin No. 33 Pt. III (Dec. 1963) p. 141.

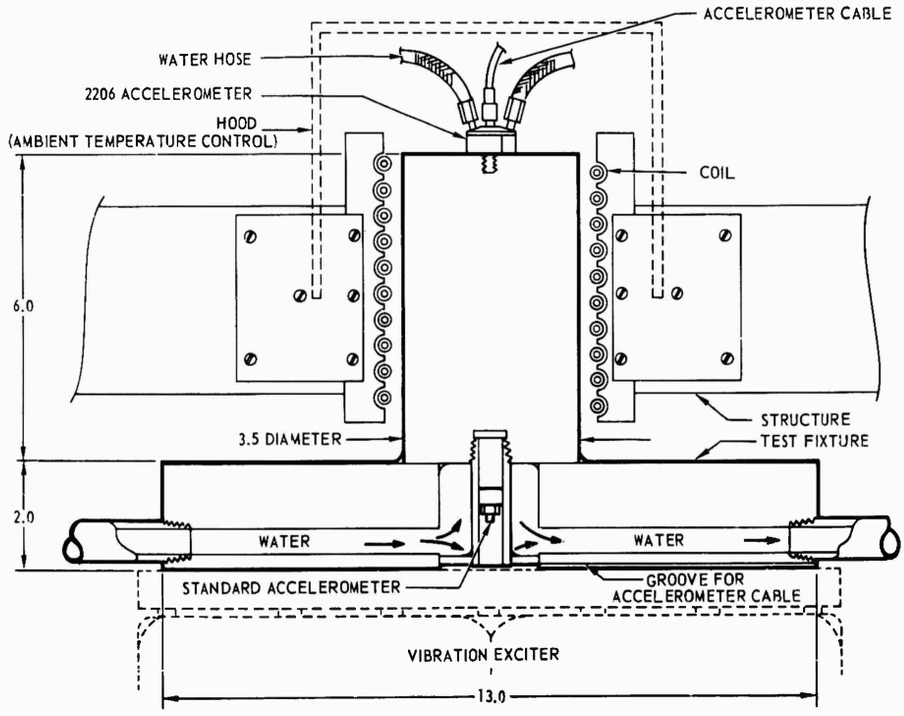

Fig. 1 - Vibration fixture

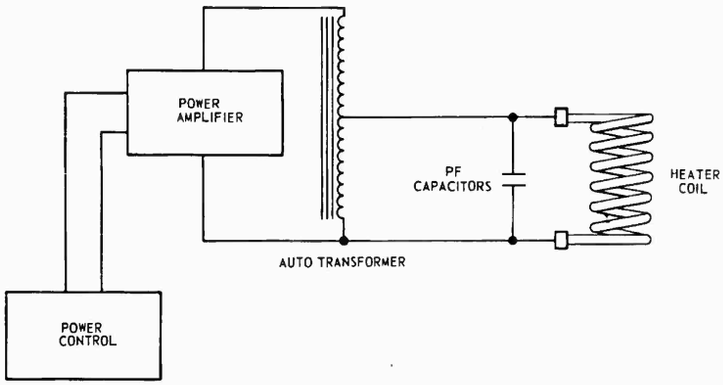

Fig. 2 - Electrical power system

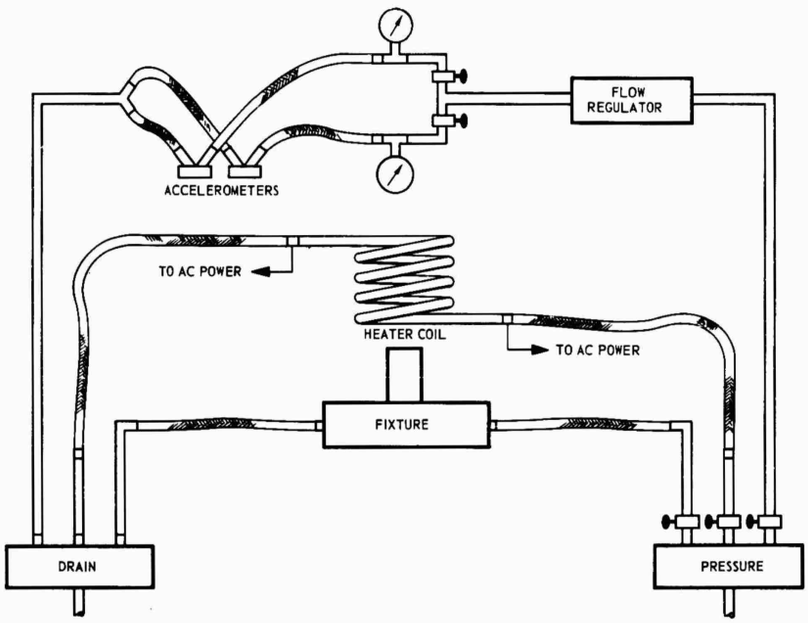

Fig. 3 - Water-cooling system

water-line pressure surges and acted as a heat exchanger. The system provided up to 1000 cc per minute waterflow at 60- to 90-psi pressure for each accelerometer. Water connections were made to each accelerometer through two -3 steel flex lines.

TEST TECHNIQUE

Prior to actual accelerometer calibration, all systems were setup to simulate actual test conditions. The fixture was heated to establish temperature conditions and rise time. Waterflows

were adjusted to give maximum cooling. Flow versus pressure was determined for each 2206 accelerometer. The electrical system was adjusted to give as little reflected power as possible to provide maximum heating efficiency.

After preliminary checkouts were complete, two 2206 accelerometers were installed on the fixture. Whytekote 505 lubricant was used to prevent thread galling during accelerometer removal. The standard accelerometer, Endevco Model 2226, and each 2206 accelerometer had laboratory ambient calibration certification traceable to the National Bureau of Standards. The standard accelerometer was installed on the slug in the bottom of the fixture and the cable brought out through the groove provided. A hood was located over the 2206 accelerometers to control the ambient temperature. The fixture was then excited on a C-25 shaker powered with a Ling Model PP20/20 amplifier. A pictorial view of the calibration setup is shown in Figs. 4 and 5. Vibration was applied at 2, 5, and 10 g under servo control with the standard accelerometer as control feedback. The output of each of the three accelerometers was recorded on adjacent channels of a Sanborn oscillograph recorder. The temperature of the fixture at the base of the 2206 accelerometer was increased from laboratory ambient to 1850°F in increments of approximately 250°F. At each temperature increment, vibration was applied at 2, 5, and 10 g with the frequency swept from 50 to 2000 cps in approximately 2 minutes. The induction heater coil was de-energized during vibration because the stray field from the coil was picked up by the accelerometer cables. Had it been necessary to maintain a constant temperature during vibration, a shield could have been built to isolate the cables from the coil field. At the lower temperature, the rate of temperature drop was only a few degrees in 2 minutes. At the higher temperatures, the rate was approximately 100°F in 2 minutes.

With full power applied and no interruptions, it took approximately 25 minutes to heat the fixture column from laboratory ambient to 1850°F. With the coil de-energized, it took approximately 1 hour for the fixture column temperature to decrease from 1850°F to 250°F. System cooling water was on at all times but, due to low thermal conductivity of the fixture, heat loss through the cooling water was small. High temperature calibration was accomplished on four 2206 accelerometers, two at a time.

TEMPERATURE MONITOR

Chromel-alumel thermocouples were mounted on the fixture near the accelerometer

Fig. 4 - Overall setup of vibration and instrumentation equipment

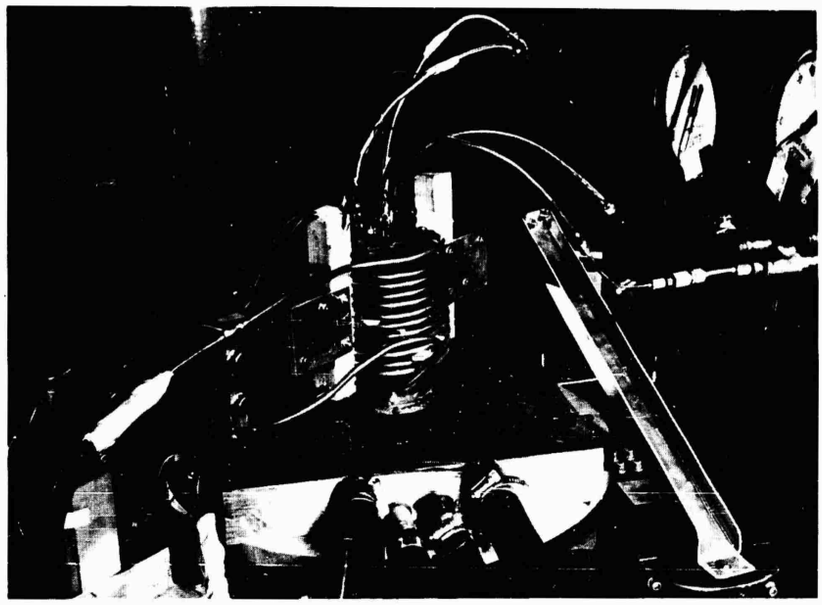

Fig. 5 - Coil-fixture-accelerometer setup (Power cables to the heater are not connected. Coil structure is stationary to vibration exciter frame. Cooling water is connected to coil and fixture base through rubber hoses. The 2206 accelerometers are mounted on fixture column. Thermocouples on inlet and outlet water lines and fixture.)

locations and on all inlet and outlet water lines. Temperature during the calibration was monitored and recorded on a Brown multi-point recorder calibrated for 0° to 2000°F ± 1 percent.

DATA REDUCTION

Temperature versus time was plotted from the Brown recorder and correlated with the power applied to the heater during the heating cycle and with the accelerometer output recordings during vibration. The output of each 2206 accelerometer at the different temperature increments was compared to the standard. Only one of the accelerometers indicated any appreciable difference between the output at ambient conditions and the output at elevated temperatures. Two accelerometer outputs are shown in comparison with the standard accelerometer in Figs. 6 and 7, at a vibration level of 10 g for three temperature conditions, ambient, 750°F, and 1850°F. The other 2206 accelerometers calibrated were similar to accelerometer number 36. Accelerometer number 36, shown in Fig. 6, had little or no change due to temperature variation, whereas accelerometer number 37, shown in Fig. 7, has considerable amplitude change in output due to temperature variation. The sensitivity of accelerometer number 36 changed less than 1 percent over the temperature range, whereas sensitivity of accelerometer number 37 changed approximately 10 percent. No interpretation of data outside the frequency band from 100 to 500 cps was attempted. Any consideration above 500 cps would have been difficult due to system resonances. It is interesting to note, however, that the resonances shifted downward in amplitude and frequency as the temperature was increased to where the fixture became "red hot."

CONCLUSION

After close evaluation of all significant data, it was concluded that three of the accelerometers could be used in high temperature application without consideration of changes in sensitivity due to temperature variations at the mounting base. The fourth accelerometer could be used if allowances were made for its variation in sensitivity over the temperature range. It was felt that a successful high temperature calibration had been obtained. Nevertheless there still remains the ever increasing requirement for more accurate calibrations.

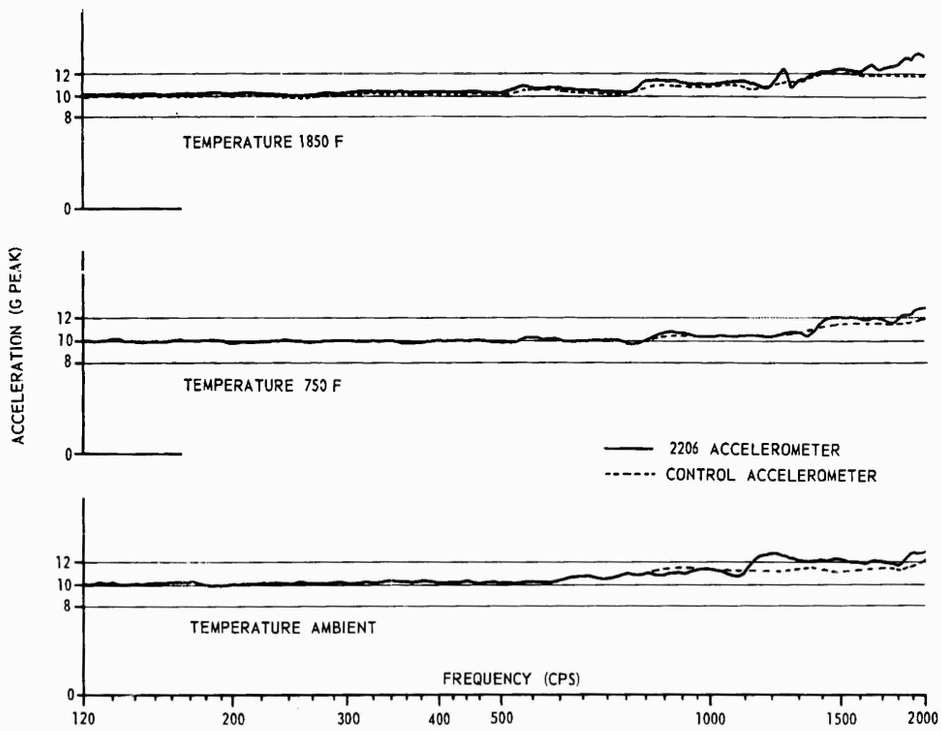

Fig. 6 - Amplitude vs frequency accelerometer No. 36

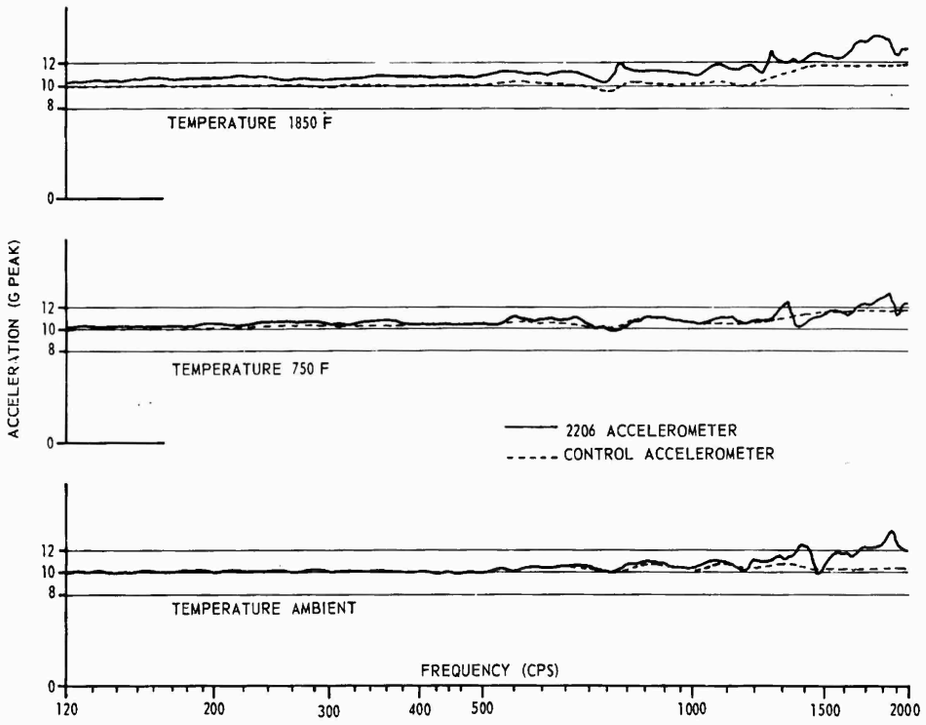

Fig. 7 - Amplitude vs frequency accelerometer No. 37

DISCUSSION

Mr. Wigle (Martin Company): What signal conditioning did you use to get from the accelerometer into the Sanborn Recorders?

Mr. Taylor: We used Endevco amplifiers which fed into Sanborn log-audio preamplifiers. Recordings were produced with the series 150 Sanborn recorder.

* * *

A METHOD OF EMBEDDING ACCELEROMETERS IN SOLID PROPELLANT ROCKET MOTORS*

R. L. Allen and L. R. Flippin
Thiokol Chemical Corporation
Wasatch Division
Brigham City, Utah

The MINUTEMAN Transportation and Handling Test Program involves vibration testing of full-scale motors. A major problem in the vibration testing of large solid propellant motors is developing a method of embedding accelerometers in the viscoelastic propellant. The accelerometers are needed to determine experimentally the dynamic response of the propellant during the environmental tests, and to verify the motor dynamic analysis.

The engineering analyses and experimental tests employed by Thiokol Chemical Corporation to develop the accelerometer installation method is the subject of this paper. The results of the instrumentation, and the degree to which the desired results were achieved are discussed.

Extensive engineering studies were made to determine the minimum number, location, and type of accelerometers required to describe the dynamic response of the propellant. A technique was developed for controlling the position and orientation of the accelerometers when embedded in the motor propellant. A laboratory research program was conducted to develop reliable bond joints.

The configuration finally selected utilizes 24 triaxial accelerometers, of which 14 are embedded in the propellant and ten are mounted on the propellant surface. The accelerometer and cable assemblies are precast in propellant wedges which are bonded in the case prior to casting the motor. Piezoelectric accelerometers were selected in order to meet the dynamic response, safety, density, and temperature specifications.

As a final verification of the design concept and to check out special manufacturing techniques and tooling, a subscale motor was successfully cast with accelerometers embedded in the propellant. This was accomplished prior to casting a full-scale motor. Both the subscale and full-scale motors were used in the vibration testing program.

Thiokol Chemical Corporation utilized a new vibration facility for performing these vibration tests. This facility is equipped with electrodynamic and electrohydraulic exciter systems which have combined capabilities of sinusoidal force outputs from 0 to 200,000 vector force pounds, and frequency capabilities from dc to 2000 cps.

With the design concept developed for internally instrumenting solid propellant rocket motors, it is technically feasible, as final confirmation of the motor integrity, to static fire these motors after the vibration tests are completed. This capability was a secondary program objective.

*This paper was not presented at the Symposium

INTRODUCTION

In the initial stage of the MINUTEMAN development program, the capability of the Stage I MINUTEMAN motor to withstand a prolonged transportation and handling environment was unknown. The chance that transportation and handling problems might occur as a result of vibration, shock, structural discontinuities, and localized loading required that the effect on reliability be investigated. In simple beams, these problems normally lend themselves to analytical study and analysis.

The Stage I motor, however, is a highly complex structure, comprised of a thin-steel outer shell approximately 5 feet in diameter and 20 feet long, with a thick bonding liner. Key areas inside the case are insulated with a rigid insulating material bonded to the shell. The case is filled with a large mass of viscoelastic propellant having a star-shaped core chamber through the center. With such a composite structure, the mechanical properties of which are either unknown or vary from specimen-to-specimen, classical beam analysis becomes inadequate in describing the response of the motor to a dynamic input.

Because of the specialized nature of this problem, a consulting service in Applied Mechanics performed an analysis and predicted the dynamic response of the Stage I motor when subjected to transportation and handling environments.

To verify this analysis by tests, Thiokol Chemical Corporation conducted road, air shipment, and obstacle course tests to determine how well the motor would withstand actual field conditions. Although a great amount of useful information was obtained from these tests, no satisfactory means was found to control the test environment over the entire frequency range and at the acceleration levels required to check the analytical predictions or to determine the dynamic response of the motor. The frequency excitation levels were so low in value that the motors tested by these methods responded essentially as a rigid body. No fundamental frequencies or mode shapes were measurably excited.

To determine the fundamental frequencies, mode shapes, propellant response, and to check the analytical predictions, Thiokol designed and constructed a vibration test facility at the Wasatch Division with the capability of testing the full-scale Stage I MINUTEMAN motor.

To fully describe the behavior of the motor, the propellant response was required as well as the case response. Engineering studies were conducted to establish the minimum number and location of accelerometers required to determine the dynamic response of the propellant during the vibration tests. A method of embedding these accelerometers was developed which enables the accelerometers to be fixed in prescribed locations during propellant casting. No adverse dynamic effects occurred on the motor or propellant from the embedded accelerometers and cable assemblies.

DISCUSSION

One of the major problems associated with this program was trying to determine the number and corresponding locations of accelerometers required to describe the dynamic behavior of the propellant during vibration tests.

Joint studies by Space Technology Laboratories, Dyna/Structures, Inc., and Thiokol indicated that the dynamic response of the Stage I propellant grain could best be determined by embedding three rows of accelerometers in the propellant at each of six linear cross-sectional stations within the motor (Fig. 1).

TRANSDUCER SELECTION

After the number and location of the accelerometers were determined, an accelerometer had to be selected which would meet the specifications for dynamic response, temperature, density, and safety. The general specifications for the accelerometers were:

1. Performance. The accelerometers had to contain three sensing elements in a single mounting case, with three mutually perpendicular axes of sensitivity. The sensing elements had to be capable of measuring minimum and maximum sinusoidal accelerations of 0.1- and 50-g peaks, respectively, applied in the direction of the particular axis or axes of sensitivity. The linearity of the response of the sensing elements had to be within ± 1 percent at any frequency between 2 and 2000 cps. The accuracy of the sensing elements at any frequency between 2 and 2000 cps, within the specified acceleration range, had to be within ± 5 percent. The phase shift between the applied stimulus and the electrical output of the sensing elements could not exceed 1 degree at any frequency or acceleration level within the specified ranges.

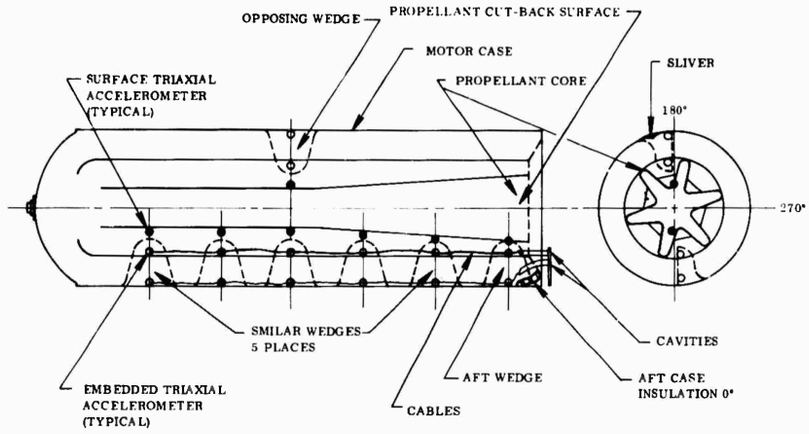

Fig. 1 - Internal instrumentation design concept

The distortion of the output waveform of the sensing elements could not exceed 5 percent of the fundamental signal of an applied stimulus. Cable connectors for the three axes of sensitivity for each accelerometer had to be located on a common side.

2. Safety. Piezoelectric self-generating accelerometers, suitable for embedding in live propellant, were used. The nature and low level of the electrical signal generated by this type of accelerometer eliminates the danger of inadvertently igniting the live propellant.

3. Density. The density of the accelerometer had to be the same as the live propellant, 1.7 grams ± 0.1 gram per cubic centimenter. The accelerometer center-of-gravity had to be located at the geometric center.

4. Temperature. An accelerometer operating temperature range between -20° and + 200°F was required.

The output response of the sensing elements at temperatures other than 70°F had to be within ± 5 percent of the reference output response at 70 degrees. (The response output of the elements was measured with a 2000 ± 200 picofarad cable). The accelerometer had to withstand temperature cycles up to 300°F without detrimental effects or impairments.

A Gulton triaxial piezoelectric accelerometer, part number TA 320106, was selected to meet the requirements and specifications within a designated time limit. Laboratory tests indicated that these accelerometers could be bonded in the propellant by priming the aluminum outer jacket of the accelerometer with Epon 812 (Epoxy, bond conditioner).

TRANSDUCER CABLE SELECTION

An interconnecting electrical cable, compatible with the piezoelectric accelerometer, was selected. Cable requirements were:

1. The cable outer covering or insulation had to be fabricated from a material which could be readily bonded to the live propellant.

2. The overall diameter of the cable had to be kept to a minimum to prevent overstressing the surrounding propellant.

3. The electrical capacitance of the cable could not exceed 40 picofarads per foot of cable.

4. The noise level could not exceed 1 millivolt peak-to-peak. The noise level was measured by vibrating a 10-foot section, with an initial 3-1/2 inch sag at the center, at 25 cps with a 1-inch double amplitude. During these tests, one end of the cable was connected to the exciter and the other end terminated at 100-megohm impedance source.

After electrically testing cables from several manufacturers, polyvinyl chloride, silicon rubber, and wrapped Teflon jacket materials were selected. An extensive laboratory testing program was conducted to aid in selecting the more suitable cable covering for bonding to live propellant, other factors being equal. A Gulton cable with a silicon rubber jacket, primed with UF 3170 (Silicon Primer), proved to be most compatible.

ACCELEROMETER AND CABLE ASSEMBLY VERIFICATION TESTS

The following problems associated with the use of the accelerometer and cable as an assembly had to be resolved:

1. What effect did the dielectric properties of live propellant have upon the characteristics of the accelerometer and cable?

2. What type of cable-to-accelerometer connection configuration was best (connector or integral connection)?

3. What effects would propellant shrinkage have on the accelerometer and cable assemblies during the cure cycle?

4. What would be the dynamic transmissibility of the accelerometer and cable assemblies when they were embedded in live propellant?

Verification Tests

In order to resolve these problems, accelerometer and cable assemblies were embedded in 10-inch propellant cubes for dynamic testing. For one type of specimen, the cable assemblies were routed directly out of the propellant. In a second type of specimen, the cables were coiled prior to routing out of the propellant to determine the effects on accelerometer output when loads were introduced into the cables. The test specimens were bonded to an aluminum plate which also served to attach the fixture to the exciter table. Each of the specimens underwent resonance search tests from 10 to 500 cps at a 1.0-g acceleration level. The samples were also vibrated at 500 cps and 3.0 g for 20 minutes. Side loads were applied to the cable assemblies to evaluate methods of connecting the cable assemblies to the accelerometers.

The test specimens exhibited a resonant condition starting at 490 cps and extending above 500 cps. The maximum frequency at which meaningful data were obtained was 500 cps, due to the frequency limitations of the exciter table. The "Q" at resonance was approximately 8.4. No changes occurred in accelerometer response when side loads were applied to the cable assemblies for either type of specimen. Direct routing of the cables from the specimen was selected as the simpler method of the two. After the verification tests were completed, the specimens were sectioned and inspected for bond separations. The bonds were good in all cases. The dielectric properties of the propellant had no effect on the accelerometer and cable assemblies. Thermal contraction of the propellant during cool down from the curing temperature did not affect the bond joints or the performance of the accelerometer and cable assemblies.

Safety Tests

After final selection of accelerometer and cable assemblies, safety tests were conducted to make sure that the live propellant could not be ignited by connecting the embedded accelerometer cable leads to electrical power supplies. Two types of specimens were prepared for these tests. The first type consisted of small samples of live propellant in which shorted accelerometer cables were embedded. In some of the specimens, the inner conductors were shorted; in others, the shield conductors were shorted, while still others had the inner conductor shorted to the shield conductor.

The second type of specimen was a small sample of live propellant with accelerometer and cable assemblies embedded. After the propellant had cured, the specimens were brought to an ambient temperature of about 80° F prior to testing.

The tests consisted of connecting the cables directly to 115-volt ac, 220-volt ac, and 440-volt ac power sources. The propellant did not ignite, indicating that no hazardous condition exists from the electrical power sources available in the vibration facility.

EMBEDMENT TECHNIQUE

In developing a method of installing a line of three accelerometers at six cross sections along the motor, these criteria were observed:

1. The accelerometer installation and cable routing could not change the dynamic characteristics of the propellant.

2. The accelerometer axes of sensitivity must be oriented within ± 1/4 inch and ± 2-1/2 degrees of each other and must be supported by propellant only.

3. The propellant must be cut back without cutting the accelerometer cables.

4. As a secondary objective, the motor would be static test fired after completing the dynamic tests.

Two of the three accelerometers and cable assemblies in each cross section were precast in propellant wedges, which were bonded into the case at each of the linear motor stations prior to casting the propellant. The position and orientation of the accelerometers in the propellant wedges were controlled during the wedge fabrication and were in the same relative position for each wedge (Fig. 2).

stations were installed on the propellant surface prior to attaching the aft closure. The accelerometer orientation was controlled by the mounting blocks used to install them. The mounting blocks, fabricated of balsa wood, were used to orient the accelerometers. The accelerometer and cable assemblies were easily removed after the dynamic tests were completed by shearing the mounting blocks close to the propellant surface.

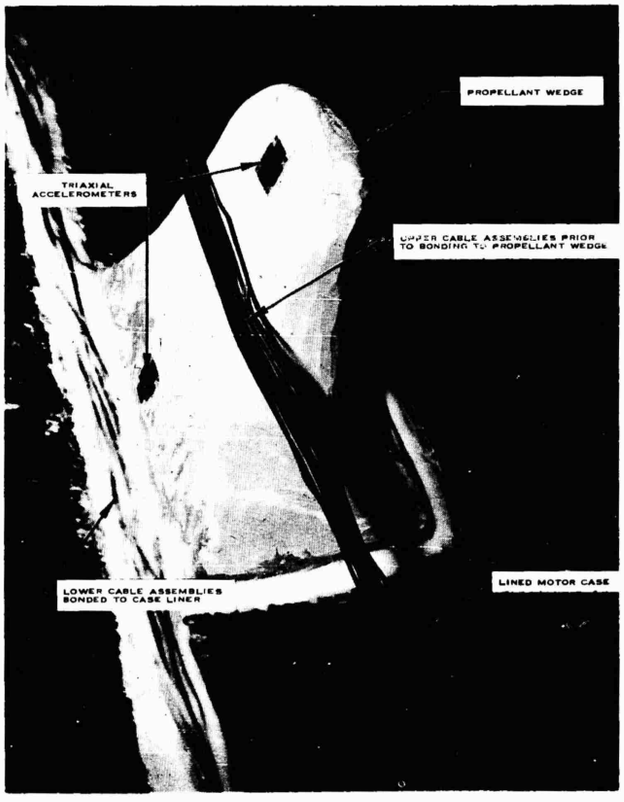

Fig. 2 - Typical propellant wedge installation

The wedges were installed so that a common edge of each accelerometer was located on the flat surface of the wedge. The wedges are located linearly in the case by measuring from a common reference point on the motor case. The flat surfaces of the wedges are angularly aligned in the case prior to bonding them in place.

The third accelerometer and cable assemblies required at each of the linear motor

The cable assemblies from the wedge located at the midpoint of the motor, 180 degrees from the continuous row of wedges along the 0-degree target side of the case, were routed circumferentially around the inside of the case. These cables intersected with the cables from the lower accelerometers, which were embedded in the continuous row or wedges. From this point, the cables were bundled together and were routed to the aft end of the motor.

The cable assemblies from the upper accelerometers, which were embedded approximately 11.5 inches inboard from the case, were routed parallel to the motor longitudinal centerline. The cables were spanned, telegraph style, between wedges and were bonded to the flat face of each wedge.

The cable assemblies from the lower accelerometers, which were embedded approximately 3 inches inboard from the case, were routed along the lined case to the aft end and were bonded to the case liner. All of the cables were tightly bundled before being bonded in position.

By utilizing the vacuum casting process, no voids occurred around the cable bundles during the propellant casting and curing processes. By routing the cables in the manner described, the feasibility of static firing the motor was enhanced, because the flame front would reach the cables in each cable bundle at the same time, and no radial path was provided for a burnthrough or increased burning area (Fig. 1).

The propellant is machined to a specified configuration to provide a plenum chamber (Fig. 1). This is called a cutback operation. The propellant cutback operation was performed successfully by providing cavities into which the cable assemblies could be placed during this operation. After the cutback operation was completed, the cable assemblies were routed out the aft end of the motor and the cavities around the cable assemblies were filled with propellant (Fig. 1).

BOND JOINT TESTS

Laboratory tests were conducted to evaluate the bond joint between cured propellant wedges and uncured propellant. By priming the cured propellant with Epon 812 prior to the casting operation, the bond joint between cured and uncured propellant was as strong or stronger than the parent propellant. Detailed studies were also conducted to make sure that the properties of the propellant did not change when exposed to three temperature curing cycles of 135°F of 96 hours duration each. These temperature cycles were required to cure the propellant wedges, the case propellant, and the propellant used to fill the accelerometer cable cavities. Laboratory tests proved that the propellant could withstand these temperature cycles with no physical property changes.

Laboratory tests were also conducted to determine a reliable bond joint between the propellant wedges and the case liner. A UF-2123, ambient-cured liner, was developed and evaluated for bonding cured TP-H1011 propellant on UF-2121 liner. The pot life of UF-2123 liner after de-aeration is 4 hours at 75° ± 5°F. Cure times are 96 hours at 75°F, 9 hours at 135°F, and 5 hours at 170°F.

Testing of UF-2123 liner was programed to include all phases of bonding cured propellant wedges in lined motor cases, including preheat prior to casting, vacuum casting conditions, and extended cure at 135°F. Tensile, shear, and fatigue tests were conducted on sample bond joints, using the de-aerated UF-2123 liner. In all cases, the bond joint had greater strength than the propellant. Other test samples were prepared using the same systems, curing, and testing conditions, with the exception that UF-2123 liner was not de-aerated prior to application. When these samples were tested, they gave lower values and swelled during the vacuum phase of testing. In all cases where the UF-2123 liner was not de-aerated and tested under vacuum, failure occurred in the UF-2123 liner.

These tests, using the de-aerated UF-2123 liner, established the minimum allowable tensile stress of the bond joint at 26 psi and the minimum allowable shear stress at 53 psi. From these test values, structural engineers finalized the wedge design. The bonding surface of the final wedge design was equal to approximately 135 square inches, which gave the bond joint a tensile safety margin of 8.32 and a shear safety margin of 65.42.

Additional test specimens were fabricated to simulate the bond joint between the propellant wedges and case liner. Various loads were applied to these test specimens when exposed to motor processing environment, and in all cases the bond joint was good.

The test data verified that the UF-2123 liner was an adequate adhesive for bonding cured TP-H1011 propellant to cured UF-2121 liner. These bond joints were satisfactory for either bayonet type casting or vacuum casting; however, when they are used with vacuum casting, the UF-2123 liner must be de-aerated prior to using.

SPECIAL EQUIPMENT REQUIREMENTS

Propellant Wedge Molds

The propellant wedges were designed to support two accelerometer and cable assembles in a specific orientation and location during

casting operations. The final wedges weighed approximately 45 pounds and were approximately 14 x 11 x 15 inches.

The fiberglass molds were designed and built to fabricate these propellant wedges. Three different mold configurations were built to meet all the requirements for instrumenting a motor. The first configuration was for the case wedges, the second was for the aft case wedge, and the third was for the opposing case wedge.

The first configuration excluded the case slivers at that location. The slivers were deleted because the close installation tolerance between wedges could be controlled more easily without them. The deletion of this one sliver will not appreciably affect the dynamic response of the propellant or motor (Figs. 1 and 3).

The second configuration is designed to fit over the aft case insulation and contains the cable cavity connections (Figs. 1 and 4).

The third configuration fits over the silver on the opposite side of the motor. Because only one wedge was installed on this side of the motor, the silver did not interfere with installation tolerances (Figs. 1 and 3).

The exact position and orientation of the accelerometers in the propellant wedges were accomplished with holding fixtures specifically located on the wedge mold. The accelerometer and cable assemblies were held in position by these fixtures while the propellant was being cast around them (Figs. 5 and 6).

The major problem associated with the wedge mold design was developing a technique to remove the propellant wedges from the

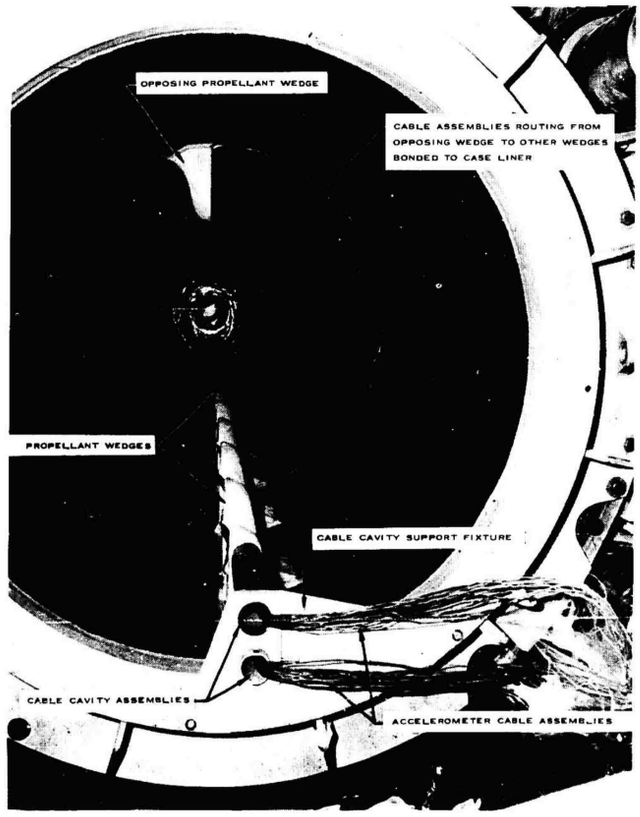

Fig. 3 - Propellant wedges installed in lined motor case

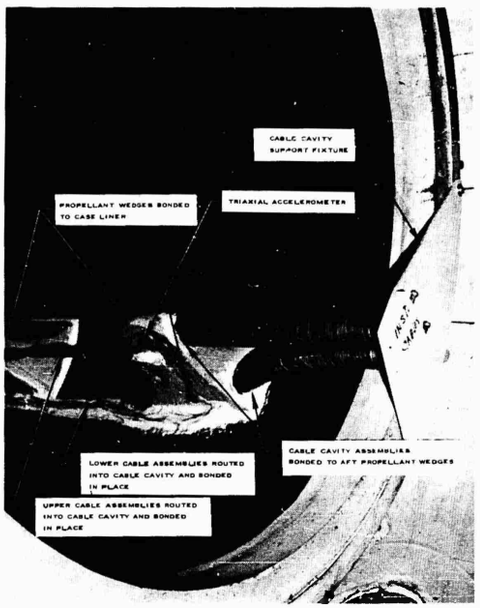

Fig. 4 - Aft propellant wedge installation

molds after they had cured. Laboratory tests indicated that a conventional rubber type parting compound would contaminate the propellant wedge and would prevent a good bond joint between the cured and uncured propellant. Attempts to remove the wedges from the mold with air ports in the molds and suction cup pulling devices proved to be unsatisfactory. The purpose of the air ports was to provide a means of breaking the bond between the wedge and the mold. This technique proved unsatisfactory because the air would escape out of a very narrow path and would not cause separation of the wedge and mold over a sufficiently large area. The suction cups were satisfactory, but no separation occurred between the wedge and mold. This removal problem was overcome by lining the molds with Teflon tape prior to casting the wedges. When used in conjunction with the air ports, the Teflon tape acted as a good parting material, and the wedges could easily be removed from the molds. No contamination problems occurred when Teflon tape was used.

Cavity Assemblies and Support Brackets

In order to perform the cutback operation, a cavity was provided in which the accelerometer

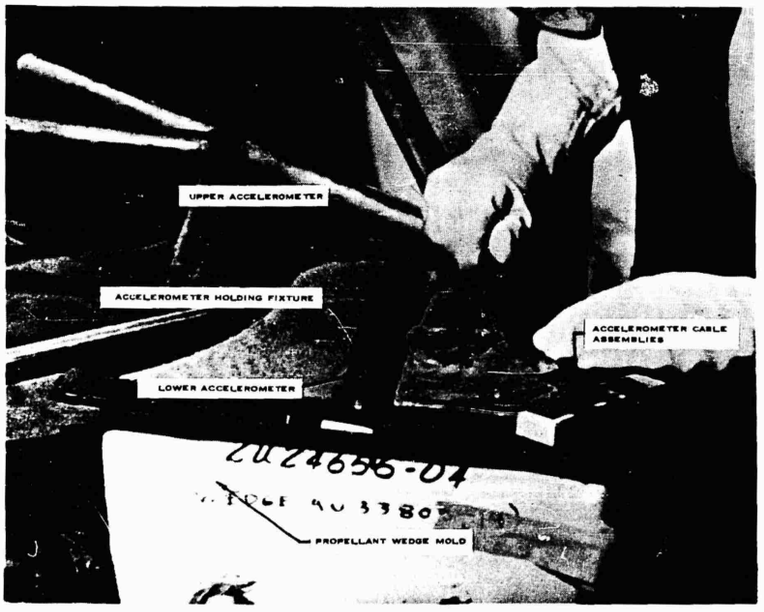

Fig. 5 - Technician finishing propellant wedge prior to curing propellant

Fig. 6 - Propellant wedge and casting mold

cable assemblies could be safely placed. After performing calculations and experimental tests on different methods of coiling the accelerometer cables, a cavity approximately 15 inches long by 2-1/2 inches in diameter was found to be satisfactory. These cavities were formed by casting the propellant around cavity assemblies (aluminum tubes). After the wedges had been installed in the case, the accelerometer cable assemblies were routed from the last wedge into the cavity assemblies, and the joint between the cavity assemblies and the wedge were sealed (Figs. 7 and 8).

The cavity assemblies were wrapped with Teflon tape to simplify removal after the propellant had cured. A support bracket was designed and fabricated to hold the cavity assemblies in position during propellant casting. This support bracket restrained any axial loading of the cavity fixtures due to buoyancy when the fixtures were submerged in uncured propellant (Fig. 4).

MANUFACTURING AND PROCESSING DETAILS

Preparation of Accelerometers and Cable Assemblies

The accelerometers were all calibrated electrically, and the calibration results for each axis of sensitivity were recorded. Prior to embedding the accelerometers in propellant, they

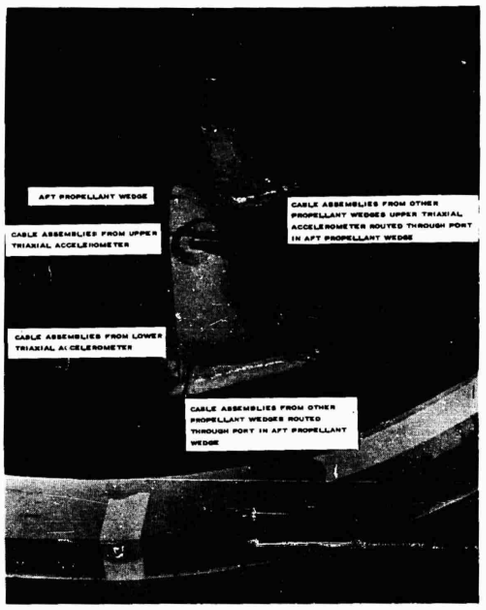

Fig. 7 - Cable routing at aft propellant wedge

were primed with Epon 812 Liquid Epoxy Resin to ensure a good bond with the propellant. Cable assemblies for each accelerometer axis of sensitivity were fabricated and identified with a coding number. The coding numbers were required to identify the embedded accelerometers and corresponding axis of sensitivity after completing the casting operations. The cable assemblies were connected and safety wired to the accelerometer. The cable assemblies were primed with UF-3170 sealant to insure a good bond when the assemblies were embedded in the propellant.

Installation and Electrical Tests of Accelerometers and Cable Assemblies

The accelerometer and cable assemblies were installed in the wedge and were checked electrically prior to casting the wedges. These electrical tests insured that the accelerometers or cables were not shorted or broken prior to embedding them in the propellant wedge. If any defect had existed, repairs or replacements at this stage of the process could have easily been made (Fig. 9).

The unique feature about the accelerometer cable used was that it had nearly zero series

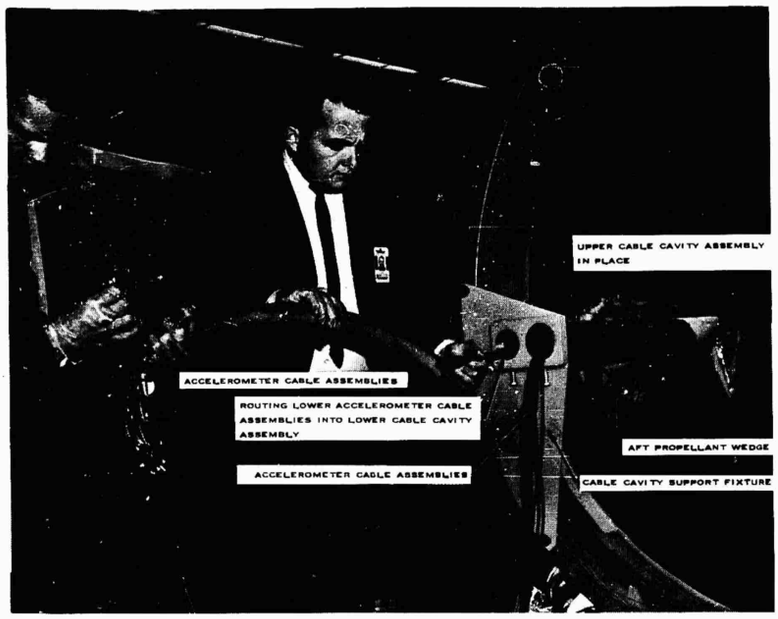

Fig. 8 - Installation of accelerometer cables in cavity assemblies

Fig. 9 - Accelerometer and cable electrical tests

resistance and a distributed capacitance of 33.6 picofarads per foot of cable. With this capacitance characteristic, the amount of capacitance a cable of a given length will have is known. By adding the capacitance of the accelerometer, the total capacitance of any accelerometer cable combination is known. One of the electrical tests utilized was to measure the capacitance of the accelerometer cable combinations. If the cable or accelerometer circuit is broken, it is easily detected and the specific location of the break is known within inches (Fig. 9).

An additional electrical check was required because the cable or accelerometers could have had a high resistance short which was not detected by the capacitance test. Any existing shorts were detected by putting a 50-volt dc input into the accelerometer cable combinations and measuring the resistance between the inner conductor and outer shield (Fig. 9).

Propellant Wedge Processing

After completing the electrical checks and lining the wedge molds with Teflon tape, the wedges were cast with propellant. Two small individual propellant batches were used to cast the propellant wedges. The propellant wedges were bayonet cast instead of vacuum cast to permit manual control of the cable routing and the flat surface of the wedge. After the wedges were cast, they underwent a cure cycle of 135°F for 96 hours.

After curing, the propellant wedges with the embedded accelerometer and cable assemblies were removed from the casting molds. The propellant wedges were individually X-rayed to verify that no voids or air pockets existed.

Installation of Propellant Wedges and Cable Assemblies

The propellant wedges initially were installed dry, positioned, and aligned. With the wedges in the proper position, the case liner was masked off so that the wedges could be quickly installed in the correct location after the bonding compound was applied. Because of the confined work area, only one wedge was handled at a time and always the extreme aft wedge. Therefore, after the locations were masked off, all the wedges were removed prior to permanently installing them with bonding compound (Figs. 10 and 11).

As each wedge was installed with bonding compound, its alignment was checked visually. After the opposing wedge on the 180-degree axis of the case was installed and aligned, the UF-2123 bonding compound was allowed to cure for 96 hours at ambient temperature (75°F). After the bonding compound on this wedge had cured, the motor was rotated 180 degrees and the remaining wedges were installed in the same manner. When the bonding compound on these wedges had cured, the cable assemblies from the opposing wedge were routed circumferentially around to the other wedges and were bonded to the case liner with UF-2123 liner. The motor was rotated as required during this operation. The cable assemblies from this wedge and the bottom cable assemblies from all the other wedges were routed along the case and into the lower cavity assembly (Fig. 1).

An electrical check was made before bonding the cables to the case liner to insure that the cables had not been damaged during the processing, X-ray, and installation operations. Any damaged cable assemblies were repaired prior to bonding them in place.

The lower cable assemblies were bonded in place, and the point between the lower cable cavity assembly and the aft wedge was sealed with UF-2123 liner (Figs. 4 and 12).

After the lower cable assemblies were bonded in place, the motor was rotated 90 degrees. The upper cable assemblies were bundled and routed along the wedge and into the upper cavity assembly. Rotating the case made it easier to bond the cable assemblies to the propellant wedges (Fig. 13).

An electrical check was again conducted before bonding these cables to the propellant wedges.

The upper cable assemblies were then bonded in place, and the joint between the upper cable cavity assembly and the aft wedge was sealed with UF-2123 liner (Fig. 4).

All of the installed propellant wedges were primed with Epon 812 to ensure a good bond between the cured propellant wedges and the remainder of the motor propellant.

Wedge Installation Tests

Before casting a full-scale motor with internal instrumentation, verification tests were performed utilizing an aft subassembly. The bond joint was checked by applying weights of 27, 18, and 10 pounds to the propellant wedges installed in the aft subassembly. The 27-pound weight, the most severe condition, reduced the safety factor from 8.32 to 2.83 (Figs. 14 and 15).

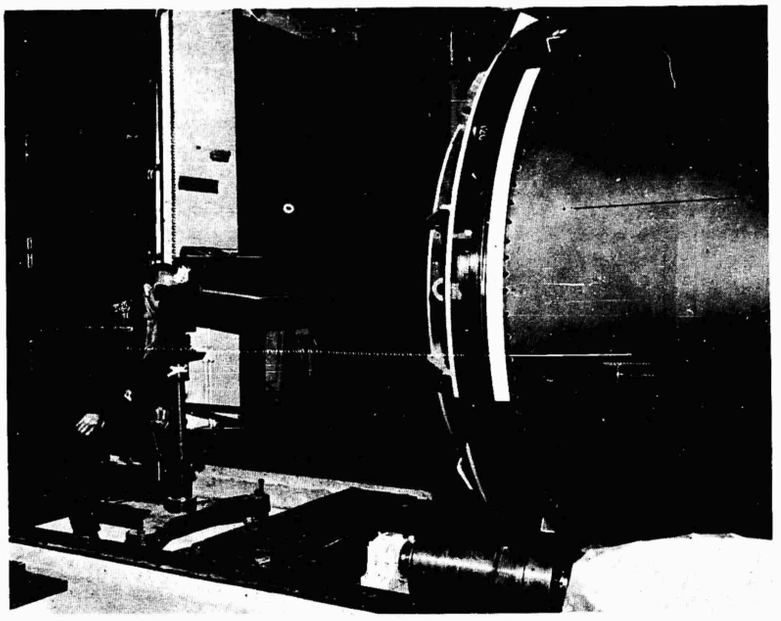

Fig. 10 - Propellant wedge alignment operation

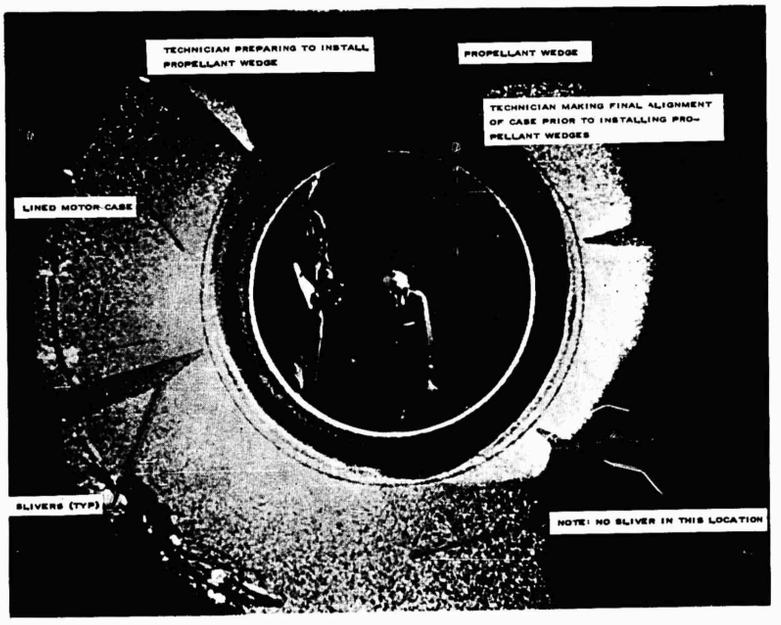

Fig. 11 - Propellant wedge installation

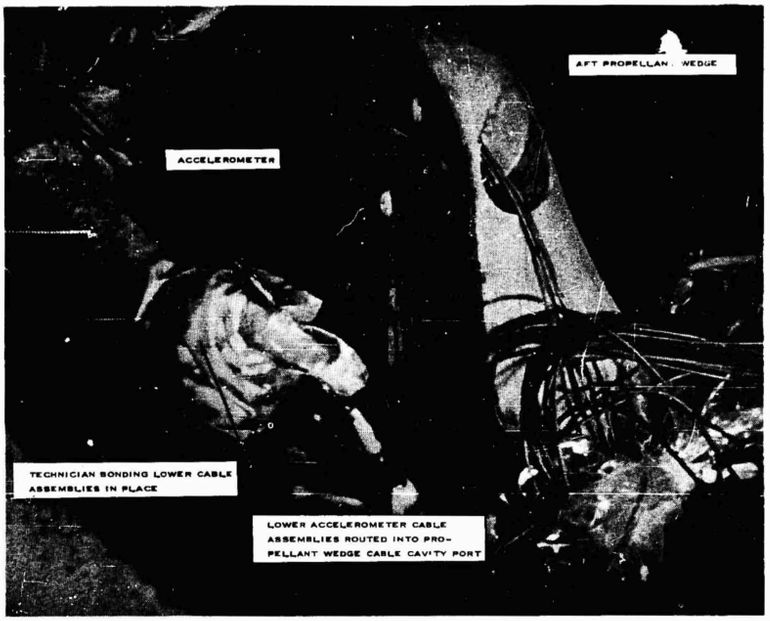

Fig. 12 - Bonding lower accelerometer cables

Fig. 13 - Positioning upper accelerometer cables prior to bonding

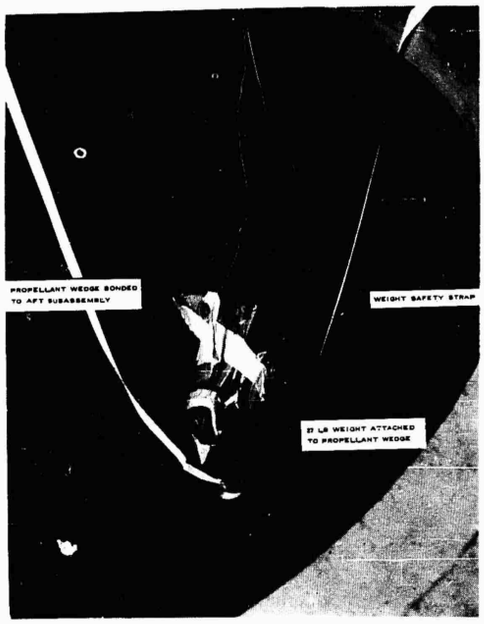

Fig. 14 - Weight installation on propellant wedge

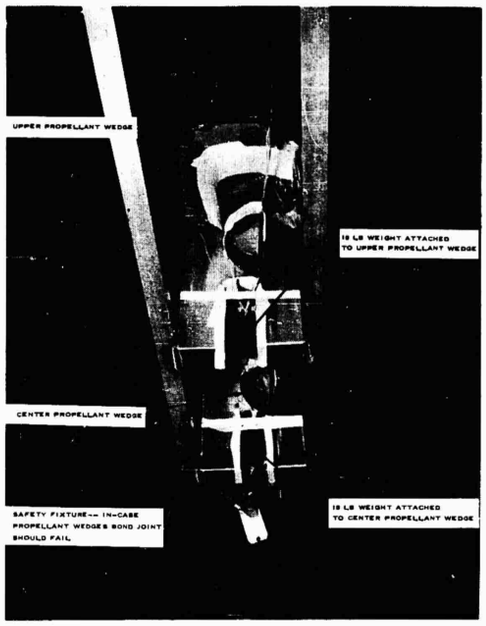

Fig. 15 - Weight installation on propellant wedges

The weighted wedges were exposed to temperature and vacuum conditions similar to those encountered during full-scale motor casting. No failures occurred during this temperature-vacuum cycle; therefore, the weights were removed and the subassembly was cast with propellant as a final confirmation of the design concept. The X-ray and visual inspections of this specimen after the propellant had cured proved conclusively that the concept was technically sound.

Casting and Curing Motor

After successfully completing the wedge installation tests in the aft subassembly, the full-scale motor was prepared for processing. The wedges were installed in the lined case and the motor was prepared for casting according to normal operating procedures. The casting core, the vacuum casting bell, and other miscellaneous equipment were installed (Figs. 16 and 17).

The motor casting and curing operations were accomplished with no problems or unusual occurrences. After curing, the cable cavity assemblies were removed, and the accelerometer cables were coiled and placed in the cavities below the cutback depth. The motor was cut back in accordance with normal processing procedures.

The accelerometer cable assemblies then were uncoiled and routed directly out of the cavities. The cavities were primed with Epon 812 Liquid Epoxy Resin prior to filling them with TP-H1064 propellant. This propellant is identical to TP-H1011 except that it has spherical aluminum particles instead of coarse ground aluminum particles. This propellant is less viscous in the uncured state than TP-H1011 and does not develop as many voids when filling small cavities. After filling these cavities, the motor was recycled at 135°F for 96 hours to cure the propellant.

Inspection and Final Processing

The motor was given a complete X-ray and ultrasonic inspection prior to installing the aft closure and nozzle assemblies. No voids or cracks were revealed in the propellant or around the wedges or cable assemblies.

Final electrical checks showed that all the accelerometer and cable assemblies were completely functional.

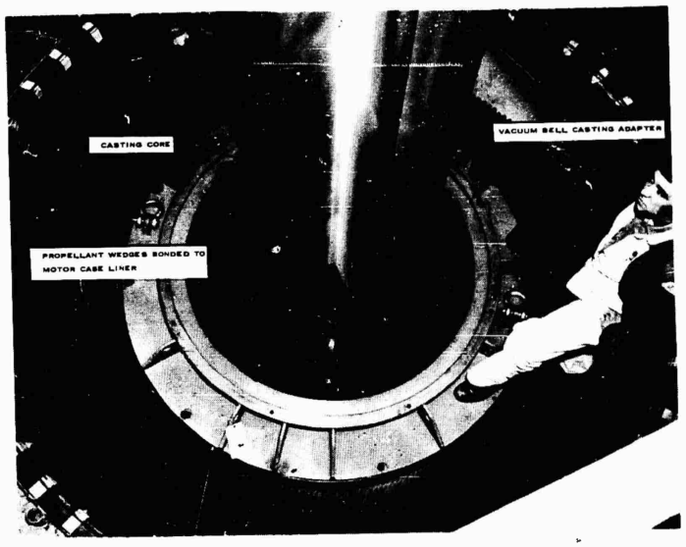

Fig. 16 - Casting core installation

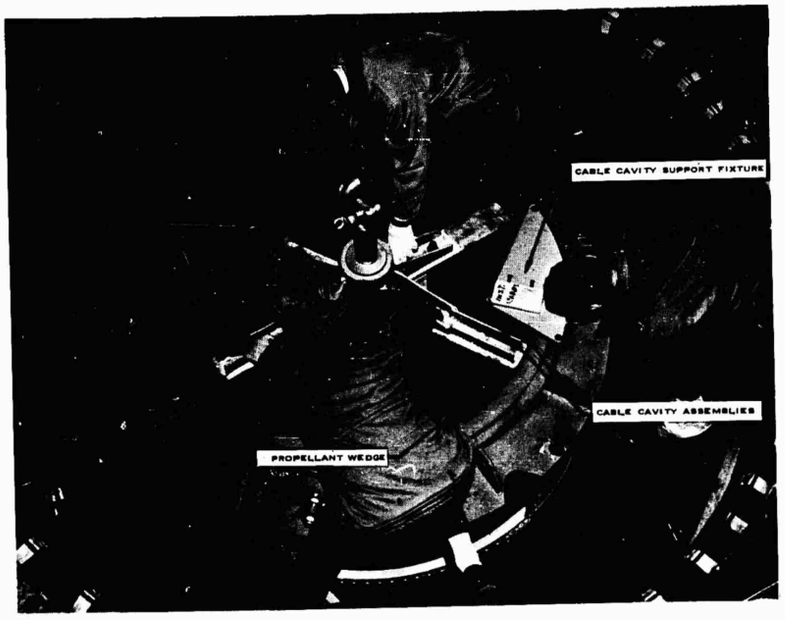

Fig. 17 - Casting core installation complete

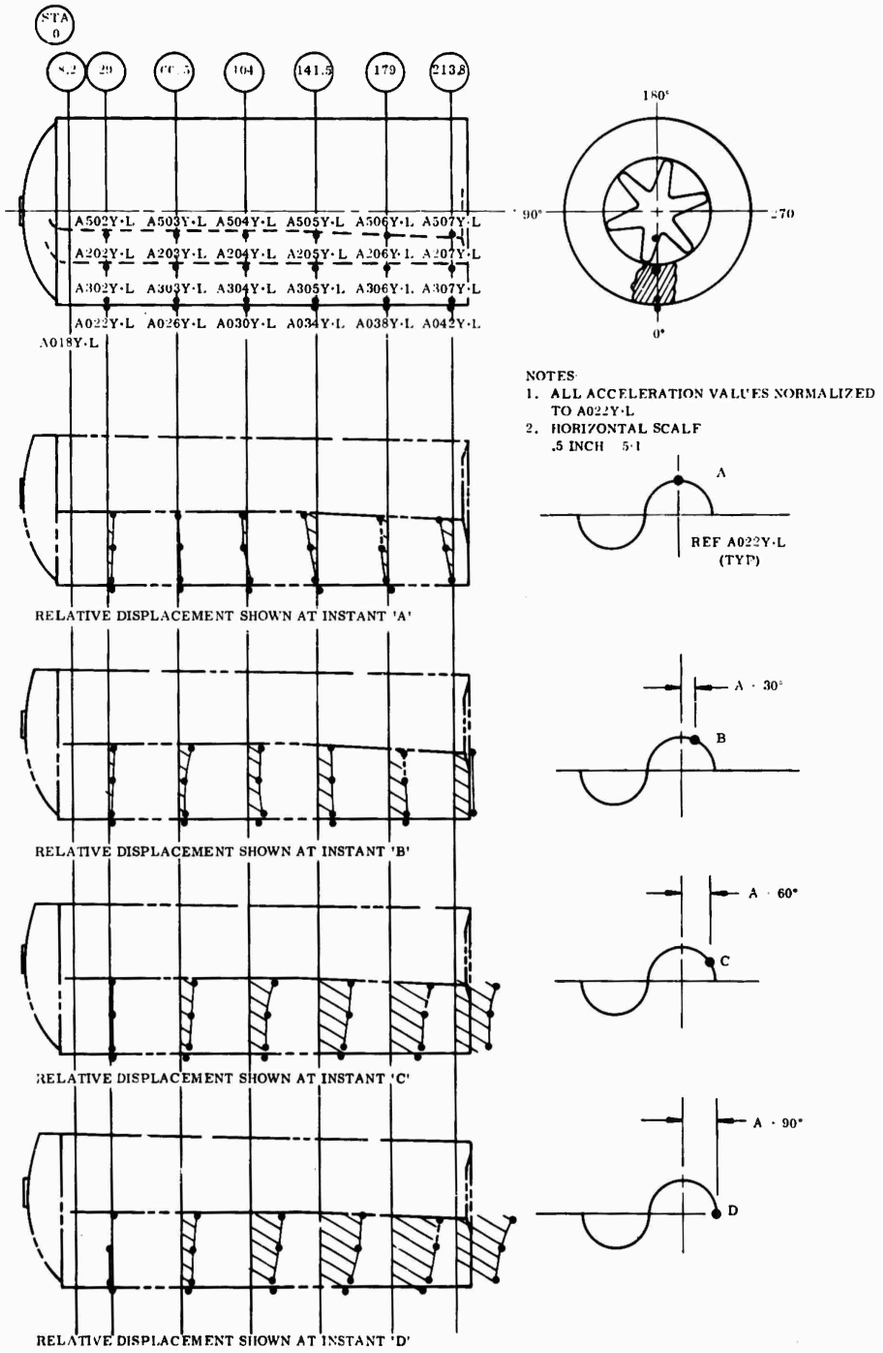

Fig. 18 - Longitudinal response of motor case and propellant, Test No. 1 TU-122-1834.1062, 47 cps

EXAMPLE OF RESULTS

Longitudinal Mode of Vibration

A typical example of the longitudinal wave propagation measured at the motor cross sections during resonance is shown in Fig. 18. The displacement is shown for a reference transducer at maximum response (A), 30 degrees later (B), 60 degrees later (C), and at zero (D). This covers the motion during one quarter of a sine wave. The relative motion of the motor case and different levels of the propellant can easily be seen by use of this type of plot. The mode shape of the motor cross sections are also defined. Similar information is obtained for tests in the transverse plane. This presentation, however, was not intended to present the technical results of vibration tests. This typical example is used only as an illustration of what may be accomplished with this method of instrumentation.

ACKNOWLEDGMENTS

The authors would like to acknowledge the valuable contributions and efforts of B. D. Bryner, J. O. Campbell, E. E. Meeker, R. E. Meyer, R. J. Porter, and T. Sedgwick in the successful development of this instrumentation technique.

* * *

CALIBRATORS FOR ACCEPTANCE AND QUALIFICATION TESTING OF VIBRATION MEASURING INSTRUMENTS

R. R. Bouche and L. C. Ensor
Endevco Corporation

Three calibrators are described in detail. The descriptions include block diagrams as well as a discussion of the consideration made in arriving at each calibrator design. An analysis of the errors present in the calibrators is included.

INTRODUCTION

Purchasers of vibration measuring instruments frequently require that acceptance and qualification tests be performed by the instrument manufacturer. These tests specify the calibrations to be performed on accelerometers and associated instruments to insure satisfactory performance. In addition, many users of vibration instruments perform their own acceptance tests or periodic recalibrations. This paper describes the design details of calibrators suitable for these measurements which are in regular use by one manufacturer. An error analysis indicates the accuracy obtained when using these calibrators. The descriptions in this paper are intended to aid in the design and use of similar calibrators in other laboratories. This will result in more uniformity in calibration procedures throughout the industry and will provide better understanding of the significance of the calibration data obtained.

The calibrators described in this paper are used for calibrating accelerometers in the range from 5 to 10,000 cps, 0 to 100 g, and from -300° to +750°F. Although used primarily for piezoelectric accelerometers, they can also be employed to calibrate other vibration transducers weighing up to 2 oz. The amplitude linearity and temperature response calibrators are designed differently than the sensitivity and frequency response measuring systems; sensitivity and frequency response calibrations are performed at a single acceleration level at various frequencies, while amplitude linearity and temperature response calibrations are usually performed at a single frequency. Although combined temperature and frequency response calibrations are possible over limited ranges, it is usually preferable to perform the calibrations separately and combine the results analytically.

Detailed error analyses for sensitivity and frequency response calibrations are included which indicate that at low frequencies the errors in calibration are comparable to those attained at the National Bureau of Standards. This occurs because the standards used are calibrated by the absolute reciprocity method at 50 cps. At higher frequencies the errors are slightly greater than the NBS errors since at these higher frequencies the standards are calibrated by the comparison method (using reference standards previously calibrated at NBS).

SENSITIVITY AND FREQUENCY RESPONSE

Three calibrators used for sensitivity and frequency response calibrations are illustrated in Figs. 1, 2, and 3. The shaker in Fig. 1 is equipped with both an electrodynamic velocity coil standard and a piezoelectric standard. The second calibrator (Fig. 2) is equipped with a piezoelectric standard using voltage amplifiers, and the third (Fig. 3) uses a piezoelectric standard with charge amplifiers. All standards are calibrated by the reciprocity method at 50 cps. In addition, the piezoelectric standards are calibrated by comparison to accelerometers previously calibrated at NBS.

The shakers are mounted on seismic blocks having resonance frequencies of 4 cps or less. The seismic block eliminates transmission of

building vibration to the shaker and prevents shaker induced vibration from being transmitted to the electronic components in the calibrator.

Velocity Coil-Accelerometer Calibrator

The block diagram for the first calibrator, equipped with both velocity coil and accelerometer standards is shown in Fig. 1. The oscilloscope is used to monitor the wave form and assure that no significant distortion is present. Locating the velocity coil in the shaker itself provides a calibration capability which is identical to that available at NBS. The accelerometer standard, also calibrated by the reciprocity method, has the advantage that it can be used over a wide frequency range. The errors of the accelerometer standards are nearly the same as that of the velocity coil standard, as will be shown. The accelerometer standard and a test accelerometer are attached back-to-back in a fixture designed to be used at frequencies up to at least 4000 cps. The shaker is suitable for routine calibrations from 20 cps to 4000 cps. The velocity coil standard is used only at 50 cps, the frequency at which its reciprocity calibration is performed.

The audio oscillator is set at the desired operating frequency and the acceleration adjusted to approximately 5 g which is well within the operating range of the shaker. Switch #1 is set to select either the accelerometer or velocity coil standard. The decade capacity is set at the value for which it is desired to measure the voltage sensitivity of the test accelerometer being calibrated. Use of a gain attenuator and two amplifiers permits the calibration of test accelerometers having voltage sensitivities between 0.5 mv/g and 14 volts/g. The amplifiers and the gain attenuator are set so that the output for the test accelerometer at switch #2 is somewhat less than the sensitivity of the coil and accelerometer standard. Both the accelerometer standard in combination with the third amplifier and the coil standard provide a calibrated sensitivity of exactly 100 mv (rms)/g (pk). (Note: this sensitivity is applicable to the velocity coil at 50 cps only.) The use of a frequency standard is unnecessary and is omitted when using the accelerometer standard. The voltage divider is then adjusted until the readings on the VTVM are identical with switch #2 in either position.

To obtain the test accelerometer sensitivity in mv (rms)/g (pk), multiply the voltage divider

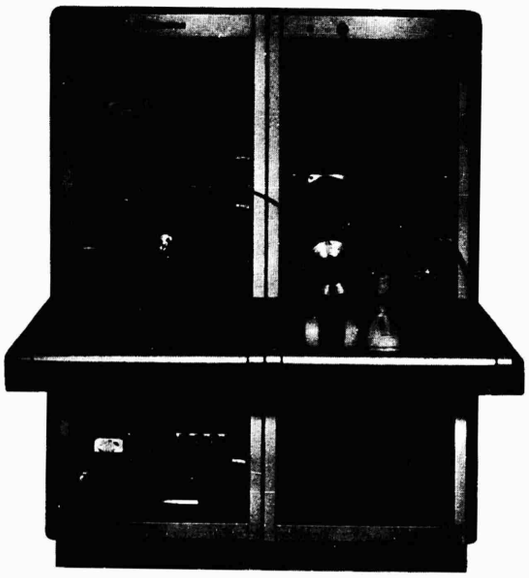

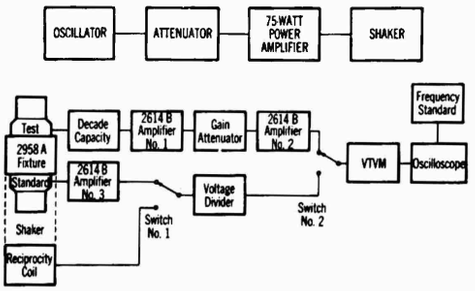

Fig. 1 - Sensitivity and frequency response calibrator equipped with velocity-coil and piezoelectric accelerometer-voltage amplifier standards and block diagram

reading by 100 times the first amplifier gain, times the second amplifier gain, and the gain attenuation. This procedure is repeated at each frequency at which a calibration is desired. The calibration obtained is the combined voltage sensitivity and frequency response of the test accelerometer.

Accelerometer-Voltage Amplifier Calibrator

The accelerometer-voltage amplifier calibrator is illustrated by the block diagram in Fig. 2. A reciprocity calibrated piezoelectric accelerometer is the only standard used. This calibrator is equipped with two vibration exciters in order to cover the entire frequency range from 5 to 10,000 cps. One shaker is used from 5 to 4000 cps and is rated at 50-lb force. The other, used from 4000 to 10,000 cps, is rated at 0.5-lb force. The large shaker is operated at accelerations up to 10 g, except where limited by a double displacement amplitude of 0.25 in. The small shaker although capable of operating at accelerations up to 1 g, is usually used at 0.5 g to avoid overheating the driving coil at frequencies near 10,000 cps.

Effective eddy currents may be induced in accelerometer cable by a combination of stray magnetic field and low accelerations. This effect can result in ground loop problems which can be eliminated by battery operating one of the voltage amplifiers when using the small shaker.

The standard accelerometer-voltage amplifier combination has been previously adjusted to a calibrated sensitivity of exactly 100 mv/g. When using the large shaker, the test and standard accelerometers are attached to a back-to-back fixture. Switch #1 positions the voltage divider in the circuit with the accelerometer having the highest sensitivity. Switch #2 is then alternated between the test and standard accelerometers while adjusting the voltage divider until both outputs are identical. The sensitivity of the test accelerometer is 100 times the test accelerometer output divided by the standard accelerometer output. This sensitivity calibration is repeated at each desired frequency in the range from 5 to 4000 cps.

Since the small shaker has a piezoelectric standard accelerometer built in, it is not necessary to use the back-to-back fixture. The test accelerometer is attached directly to the shaker and the ratio of the test to the built-in accelerometer output is measured using the same method employed with the large shaker. To verify that the sensitivity of the built-in accelerometer remains unchanged, the reciprocity calibrated accelerometer standard is attached to the small shaker and recalibrated at each frequency at which the test accelerometer is calibrated.

Although the procedure of changing a test accelerometer from shaker to shaker might appear quite cumbersome, it is possible to obtain calibration data throughout the range from 5 to 10,000 cps on a single accelerometer in approximately 1 hour.

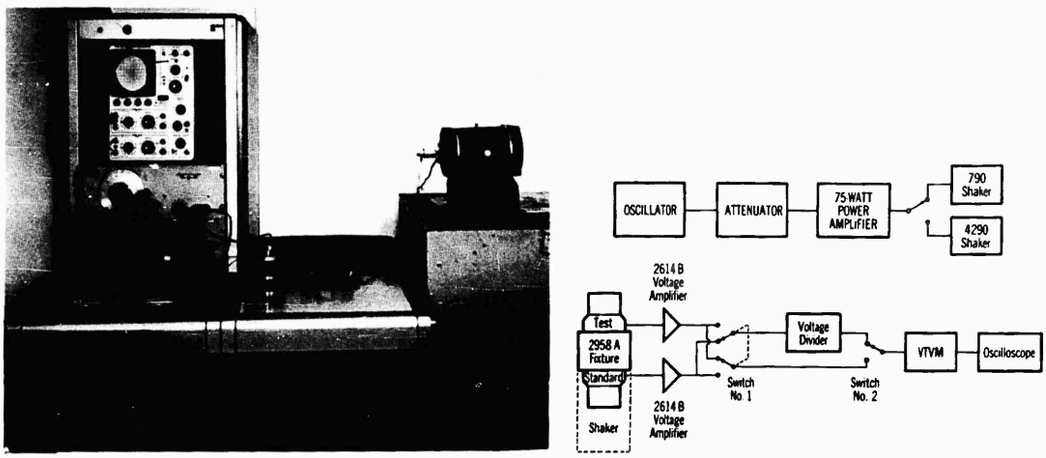

Fig. 2 - Wide frequency range sensitivity calibrator equipped with piezoelectric accelerometer-voltage amplifier standard and block diagram

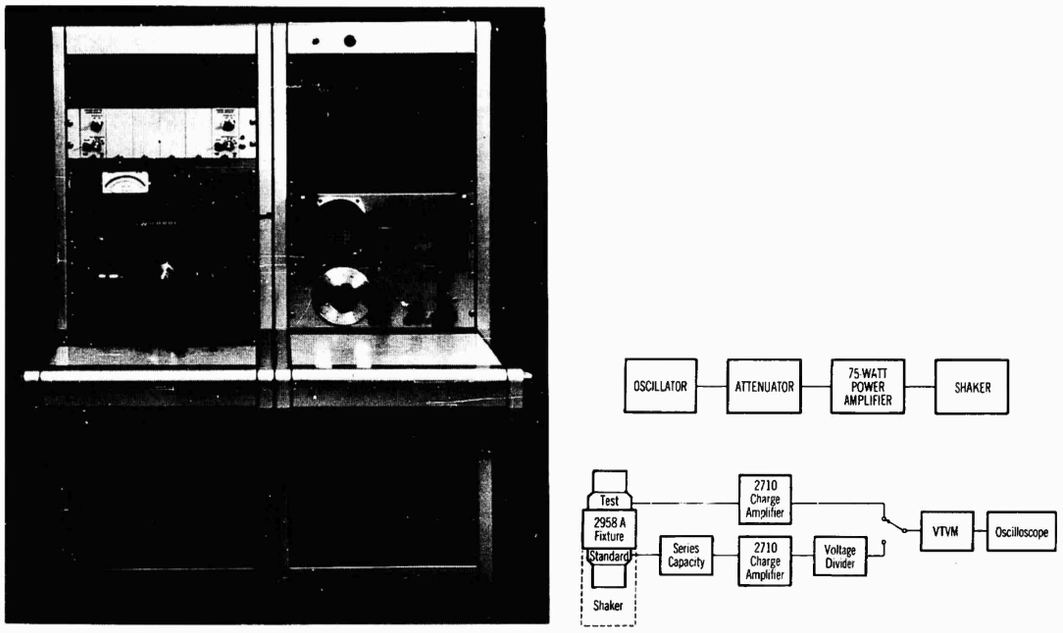

Fig. 3 - Sensitivity and frequency response calibrator equipped with piezoelectric accelerometer-charge amplifier standard and block diagram

Accelerometer-Charge Amplifier Calibrator

The block diagram of the calibrator using charge amplifiers is illustrated in Fig. 3. This calibrator is noteworthy for its simplicity of design. The gain adjust required to calibrate all piezoelectric accelerometers presently available is included in the charge amplifier. The reciprocity calibrated standard is adjusted so that its sensitivity is exactly 10 pcmb/g. This adjustment is made by inserting the proper value of series capacitor between the accelerometer and its associated charge amplifier. The sensitivity calibration is performed by vibrating the shaker at the desired frequency at approximately 5 g. The gain ranges on the two charge amplifiers are adjusted until the output of the test accelerometer is somewhat smaller than that of the standard accelerometer. The switch is alternated between its two positions and the voltage divider is adjusted until the outputs from the test and standard accelerometers are identical. The sensitivity of the test accelerometer is equal to 10 times the voltage divider setting times the ratio of the gains used in the two charge amplifiers. This procedure is repeated at each frequency at which a calibration is desired.

The simplicity of this calibrator is achieved primarily through the wide gain ranges provided in the charge amplifier. This feature permits calibration of any piezoelectric accelerometer having charge sensitivity from 0.5 to 3000 pcmb/g. These amplifiers provide a much higher output signal than that available in the two calibrators previously described. In addition, the complicated switching and attenuation circuits are eliminated. The accelerometer-charge amplifier calibrator is designed for use with piezoelectric accelerometers. It does not have the flexibility of the other two calibrators which can be used readily with other types of vibration pickups, e.g., electrodynamic velocity pickups and variable reluctance and differential transformer accelerometers. The shaker used in this calibrator is most useful in the frequency range from 20 to 4000 cps.

Shaker Characteristics

The shaker which is used in all three calibrators is suitable for any single axis vibration pickup weighing up to 2 oz. It may be used to calibrate heavier vibration pickups only over limited frequency ranges, since as the weight of the vibration pickup increases, the maximum

operating frequency decreases. This is not usually a problem because most of the heavier vibration pickups are designed to be used in lower frequency ranges. The one exception to this is the calibration of triaxial accelerometers in all three axes. Although the shaker used in these calibrators is suitable for the Z direction (directly perpendicular to the base of the accelerometer), it is not suitable for calibrating X and Y directions. This sensitivity measurement of X and Y axes requires a shaker whose moving element is specifically designed for mounting triaxial accelerometers in all three directions. It is expected, however, that the improved calibration shakers which have recently become available will be suitable for calibrating triaxial accelerometers.

The small shaker used for calibration to 10,000 cps may also be used for resonance frequency measurement.[1,2] This shaker has the advantage that the lowest elastic body resonance of the moving element is at 55,000 cps. As a result it is suitable for performing calibrations at frequencies to at least 10,000 cps. At frequencies near 10,000 cps the use of fixtures between the shaker and test accelerometer should be avoided. This requires that the shaker moving element be provided with several mounting holes in order to accommodate the variety of mounting studs used with accelerometers.

For calibration purposes, it is good practice to use a shaker only at frequencies above its rigid body resonance and below its elastic body resonance. Rigid body resonance is the resonance frequency determined by the stiffness of its flexure system and the weight of the moving element. The elastic body resonance is the resonance frequency determined by the distributed spring-mass characteristic of the moving element alone.

Excessive distortion may be present below the rigid body resonance. Under certain circumstances this distortion produces calibration errors which are not easily explained. To avoid these errors, shakers selected for calibration purposes should have their rigid body resonance below the operating frequency range.

A shaker may be used near or above its elastic body resonance if care is taken to assure that there is no relative motion between the test and standard accelerometers and that the apparent weight, as seen by each accelerometer, is sufficiently large. Considerable experience is required in using a particular shaker near the elastic body resonance to assure that these two requirements are met. True resonance frequency of an accelerometer is obtained only when the structure apparent weight is large compared to the mass element in the accelerometer. If the shaker apparent weight is not sufficiently large, the resonance frequency of the accelerometer will increase with a corresponding improvement in frequency response. This effect should not be confused with the effect of the accelerometer apparent weight on the structure motion as discussed by Schloss.[3] The apparent weight of any mounting fixtures must also be large enough to insure that lowest accelerometer resonance frequency is determined. Consequently, the deviations from flat frequency response will always be equal to or less than the deviations measured during calibration.

It is also important when using shakers for calibration purposes, to avoid frequencies where excessive transverse motion is present. The shaker employed in two of the calibrators exhibits transverse motion peaks near 900, 2400, and 3200 cps similar to those shown in Ref. 4. It can, however, be used as long as these few frequencies are avoided. Shakers which show considerably improved transverse motion characteristics have recently become available. There is still need, however, for a reasonably priced small calibration shaker with both good transverse motion characteristics and high frequency capability which is suitable for calibrating all accelerometers.

Error Analyses

Table 1 lists the various errors which occur in reciprocity calibration of a standard at 50 cps. They are comparable to the errors experienced at NBS when calibrating standards.[5] Errors are minimized because a shaker is selected in which the phase shift is exactly 0 or 90 degrees between the driver coil and velocity

[1] R. R. Bouche, "Characteristics of Piezoelectric Accelerometers," Test Engineering (Oct. 1962), pp. 16-18, 22, 24, and 38.

[2] R. R. Bouche, "Instruments for Shock and Vibration Measurements," Experimental Techniques in Shock and Vibration, ASME (1962), pp. 71-80.

[3] F. Schloss, "Inherent Limitations of Accelerometers for High-Frequency Vibration Measurements," J. Acoust. Soc. Am., 33, 4 (1961), p. 539.

[4] R. R. Bouche, "Improved Standard for the Calibration of Vibration Pickups," Experimental Mechanics, 1, 4, (1961), pp. 116-121.

[5] S. Levy and R. R. Bouche, "Calibration of Vibration Pickups by the Reciprocity Method," Journal of Research, National Bureau of Standards, 57, 4, (1956), pp. 227-242.

TABLE 1
Analysis of Sensitivity Errors for Reciprocity Primary Standards Calibrated at 50 cps

Measurement	Error (%)	
	Electrodynamic Velocity Coil	Piezoelectric Accelerometer
Mass	0.05	0.05
Transfer admittance intercept	0.2[a]	0.2[b]
Distortion	0.1	0.1
Voltage ratio	0.2[b]	0.2[a]
Frequency	0.05	0.05
Amplitude Linearity	0.0	0.0
Environmental effects (temperature, acoustic, etc.)	0.0	0.2
Estimated error[c]	0.3	0.4

[a]Assumes 90-degree phase shift.
[b]Assumes zero-degree phase shift.
[c]Determined from the root-mean-square of the individual errors listed in this table.

coil or piezoelectric accelerometer output. The estimated error for these calibrations is determined from the square root of the sum of the squares of the individual measurement errors. Experience indicates that the repeatability of the reciprocity calibration is comparable to this estimated error.

After the piezoelectric accelerometer is reciprocity calibrated at 50 cps, it is calibrated from 10 to 10,000 cps by direct comparison to an accelerometer that has been previously calibrated at NBS. The velocity coil is also calibrated with reference to the NBS calibrated standard, but only at 50 cps, the frequency at which it is used. The error analysis in Table 2 includes the error of 1 and 2 percent achieved by NBS. The voltage ratio error is larger above 4000 cps because the test and standard accelerometers must be mounted consecutively on the small shaker. Below 4000 cps a larger shaker is used which permits use of the back-to-back fixture and simultaneous readings of two standard accelerometers.

Table 3 is the error analysis of test accelerometer sensitivity obtained when using the standards described above. In addition to reciprocity and comparison calibrations of the standard, the piezoelectric accelerometer standards are calibrated by the optical method at 5 cps. The error for this calibration is 0.9 percent as listed in Table 3. The estimated errors applicable to the test accelerometer sensitivity at various frequencies are listed in the last five lines of the table. These errors are determined by taking the root mean square of the individual errors listed in Table 3 which correspond to applicable frequencies. The estimated error in the sensitivity at 50 cps does not exceed 1 percent, which is comparable to the error estimated on calibration performed at NBS. The error at the other frequencies are up to 0.7 percent larger than the error at NBS.

Instead of referring to the detailed errors in the Tables, the following simplified statement of errors is used. The estimated error of the test accelerometer sensitivity does not exceed 1.5 percent at frequencies up to 900 cps, 2.5 percent up to 4000 cps, and 3 percent up to 10,000 cps. These errors are obtained by grouping the root-mean-square values in Tables 2 and 3 and rounding off to the next higher 0.5 percent.

AMPLITUDE LINEARITY CALIBRATOR

The amplitude linearity calibrator is shown in Fig. 4. High accelerations are achieved with a resonance beam attached to a 10-lb-force-rated shaker. The moving element of the shaker is sufficiently small so that the beam resonates at its fundamental free-free mode. The beam is specially designed with a clamping fixture to minimize stress concentrations on the beam and avoid excessive fatigue failure. The design of the beam with this particular shaker results in

TABLE 2
Analysis of Frequency Response Errors for Primary Accelerometer Standards Calibrated from 10 to 10,000 cps

Measurement (cps)	Error (%)
NBS calibratcd standard (10-900)	1.0
NBS calibrated standard (900-10,000)	2.0
Relative motion (900-4000)	0.5
Relative motion (4000-10,000)	1.0
Voltage ratio (10-4000)	0.2
Voltage ratio (4000-10,000)	0.4
Estimated error (10-900)	1.0[a]
Estimated error (900-4000)	2.1[a]
Estimated error (4000-10,000)	2.3[a]

[a]Determined from the root-mean-square of the individual errors.

TABLE 3
Estimated Error of Sensitivity and Frequency Response Calibrators

Measurement (cps)	Error (%)		
	Velocity Coil Standard[a]	Accelerometer-Voltage Amplifier Standard	Accelerometer Charge Amplifier Standard
Standard Sensitivity:			
(50)	0.3	0.4	0.4
(5)	-	0.9	-
(10-900)	-	1.0	1.0
(900-4000)	-	2.1	2.1
(4000-10,000)	-	2.3	-
Voltage Ratio:			
(5-4000)	0.2	0.2	0.2
(4000-10,000)	-	0.4	-
Relative Motion:			
(900-4000)	-	0.5	0.5
(4000-10,000)	-	1.0	-
External capacity	0.5	0.5	0.25
Amplifier gain	0.2	0.2	0.7
Amplifier freq. response	-	0.5	0.5
Frequency	0.1	-	-
Environmental effects (temp., acoustic, etc.)	0.5	0.5	0.5
Estimated error:			
(50)	0.8[b]	0.9[b]	1.0[b]
(5)	-	1.3[b]	-
(10-900)	-	1.5[b]	1.5[b,c]
(900-4000)	-	2.3[b]	2.4[b,c]
(4000-10,000)	-	2.7[b]	-

[a]Used at 50 cps only.
[b]Determined from the root-mean-square of the applicable individual errors.
[c]Calibrator normally used from 20-4000 cps.
[d]Amplifier specially calibrated and adjusted.

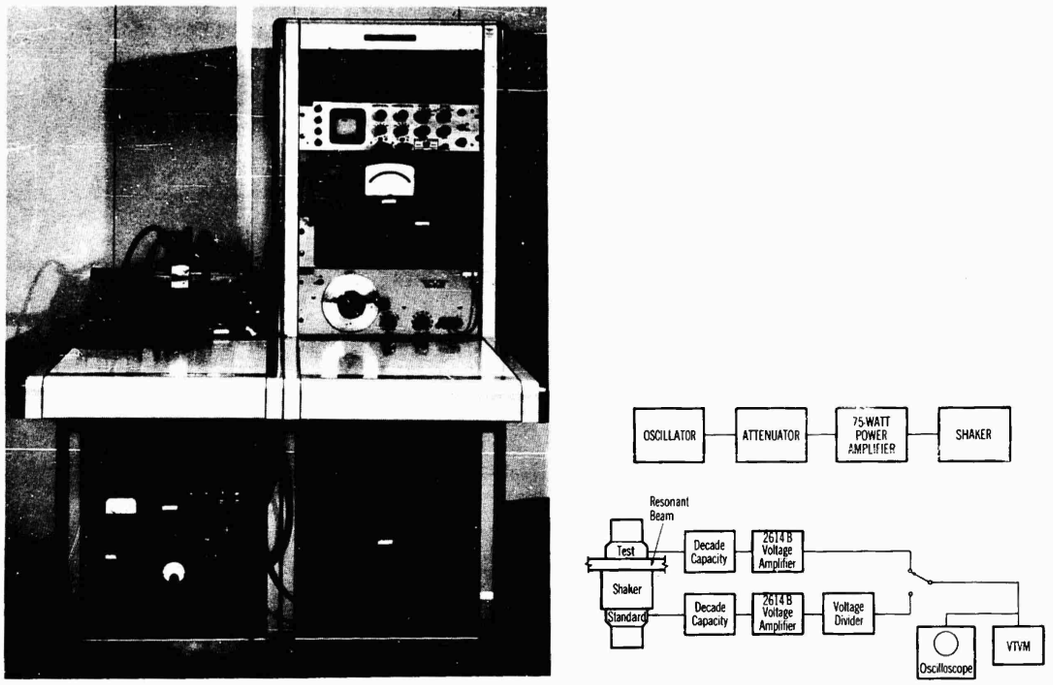

Fig. 4 - Amplitude linearity calibrator and block diagram

a resonance frequency of approximately 220 cps. With this beam, many hours of operation at 100 g can be obtained before fatigue failure of the beam occurs. Operation at up to 200 g can also be performed with somewhat lesser beam life. This design is particularly advantageous in that there is no relative motion between the test and standard accelerometers. The standard accelerometer is mounted at the opposite end of the shaker moving element from the beam. If desired, a back-to-back fixture may be used. Both the test and standard accelerometers are then mounted on the fixture and the fixture may be attached either on the beam or on the opposite end of the moving element.

Figure 4 also shows a block diagram of the 100-g calibrator. The decade capacities and the voltage divider are adjusted until the outputs from the test and standard accelerometers are equal at 10 g, as indicated by the VTVM. The applied acceleration is then increased to the desired level while the frequency is adjusted to the beam resonance. Amplitude linearity deviation is determined from the change in voltage reading obtained by switching the voltmeter from the standard accelerometer output to the test accelerometer output.

The estimated error in measuring amplitude linearity deviation on this calibrator does not exceed 1 percent. The standard accelerometer is previously calibrated by one of the absolute calibration methods. The optical method may be used at accelerations near 100 g. In addition, the amplitude linearity of the standard accelerometer may be verified by calibrating at higher accelerations on a shock calibrator. One such device; described in Ref. 6, is suitable for calibration up to 10,000 g.

TEMPERATURE RESPONSE CALIBRATOR

The temperature response calibrator shown in Fig. 5 is used for calibrations from -300° to +750°F. These calibrations are usually performed

[6] R. R. Bouche, "The Absolute Calibration of Pickups on a Drop-Ball Shock Machine of the Ballistic Type," Proc. IES (1961), pp. 115-121.

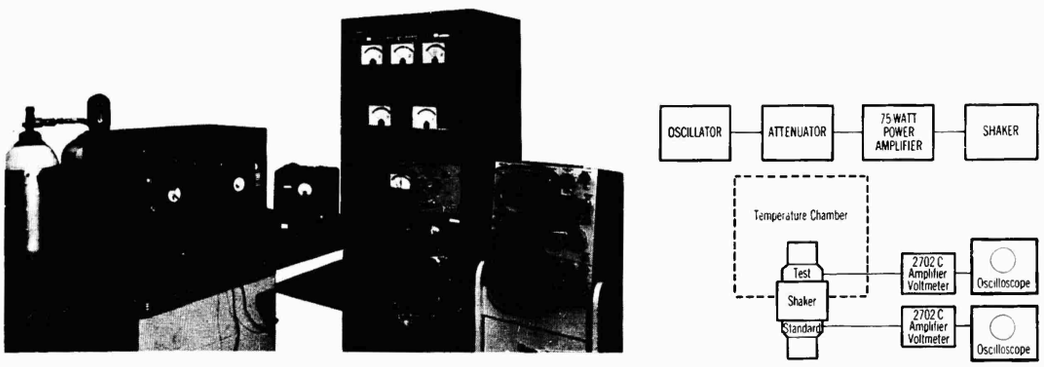

Fig. 5 - Temperature response calibrator and block diagram

at a single frequency. A comparison method is used in which the standard accelerometer is kept at room temperature outside the temperature chamber. The operation of the calibrator is similar to that of the amplitude linearity calibrator. The standard accelerometer is mounted to the shaker moving element at the end opposite from the test accelerometer. The shaker is operated in the vertical direction. A ceramic rod is attached to the top of the moving element and passes through the wall of the chamber. A steel fixture with thermocouple inserted is attached to the top of the ceramic rod and the test accelerometer is mounted on the fixture. Chamber temperature is automatically controlled by the output of the thermocouple.

The block diagram of the calibrator is also shown in Fig. 5. The shaker is vibrated at approximately 3 g. In practice up to four accelerometers may be calibrated simultaneously by using a larger mounting fixture and additional amplifier-voltmeters for each accelerometer. The standard accelerometer is monitored to insure that the acceleration level remains unchanged during the calibration procedure. Since the standard accelerometer is at the bottom of the shaker, it remains at room temperature. The sensitivity deviation at each temperature is indicated by the changes in voltmeter readings for each test accelerometer.

Three sources of error are present in performing this calibration. First, the error in maintaining constant acceleration which throughout the calibration is approximately 0.5 percent. Second, the scale reading of the voltmeter for the test accelerometer may be in error up to ±2 percent if readings at all temperatures are made on the same range. The third source of error is the combined effect of the temperature response of the particular accelerometer being calibrated and the accuracy of the temperature measurement. More specifically it is determined by the rate of change of the test accelerometer output with respect to temperature. The temperature is measured by the thermocouple output on a potentiometer to within the accuracy of the thermocouple. For most accelerometers, the estimated total calibration error is less than 5 percent.

This calibrator is designed primarily for use in the frequency range from 50 to 200 cps. The frequency range is extended down to 5 cps by inserting a dc bias voltage[7] on the driving coil of the shaker to support the weight of the moving element and accelerometer and by removing the stiff flexure plates normally used on the shaker. The frequency range may be extended to 4000 cps by using a back-to-back calibration fixture inside the chamber. Extreme care must be used here. The standard accelerometer must have small output deviations over the temperature range of intended calibration. In addition frequencies where transverse motion is present must be avoided.

COMBINED ENVIRONMENTAL CALIBRATIONS

The state of the calibration art is not yet sufficiently developed to permit combined calibrations of temperature response and amplitude linearity over the entire frequency range of

[7]B. Reznek, "Elimination of Static Shaker Deflections by D. C. Armature Biasing," Proc. IES (1963), pp. 425-432.

operation of all vibration pickups. Fortunately, accurate calibrations can be achieved by performing the amplitude linearity and temperature response calibrations at a single frequency as described above and then combining the results analytically with sensitivity and frequency response calibration data. This procedure is recommended for vibration pickups with small internal damping which are not used near their resonance frequency. It is particularly suitable for piezoelectric accelerometers which have almost zero damping and are normally used at frequencies below 1/5 of their resonance frequency. Although very small changes in internal damping and resonance frequency probably occur at temperature extremes, these changes have no effect on response below 1/5 the accelerometer resonance frequency.

Other vibration pickups which are normally used near their resonance frequency require combined amplitude linearity and temperature response calibrations. (See Fig. 15.23 in Ref. 8.) Fortunately, the transducer types which require combined environmental calibration are normally used only at frequencies up to a few hundred cps, and the special back-to-back fixture need not be employed. If combined temperature and frequency response calibration is attempted at frequencies above several hundred cps, the calibration results are frequently a measure of calibration error and not of accelerometer performance.

Since the internal resistance of piezoelectric accelerometers decreases at elevated temperatures, this may affect the response of the associated amplifier at frequencies below 50 cps. For this reason, it is sometimes desirable to verify the response at temperature of the accelerometer-amplifier system at frequencies as low as 5 cps. The combined temperature-low frequency calibration may be omitted if the resistance of the accelerometer is measured at the maximum operating temperature and the low frequency characteristics of the amplifier are known.

[8] R. R. Bouche, "Inductive-Type Pickups," Shock and Vibration Handbook (McGraw Hill Book Company, Inc., New York, N. Y., 1961), Vol. 1, Chap. 15, pp. 15-16.

CONCLUSIONS

The calibrators described in this paper are suitable for verifying the characteristics of vibration pickups for use in most vibration measuring applications. The three calibrators described for sensitivity and frequency response measurements are representative of the progress made in these calibrations over the past several years. The calibrator equipped with the velocity coil and reciprocity calibrated accelerometer is capable of performing calibrations comparable to those available at the National Bureau of Standards. The calibrator equipped with piezoelectric accelerometer and charge amplifiers is the simplest to operate yet maintains accuracies similar to the other sensitivity calibrators described.

The amplitude linearity and temperature response calibrators are used at frequencies up to several hundred cps. The amplitude linearity, temperature response, sensitivity, and frequency response calibration results can be combined analytically without sacrificing overall accuracy. It is not normally necessary to perform these calibrations simultaneously.

DISCUSSION

Mr. Mangolds (RCA): If you calibrate up to 50,000 cycles, how do you mount two accelerometers together back-to-back?

Dr. Bouche: The calibrations we performed up to 50,000 cycles were done on the little calibrator that I mentioned. We measured the resonance frequency of the accelerometer for the particular type of mounting for which the accelerometer was to be used. If a steel stud, or cementing technique was to be used, we measured the resonance frequency under those conditions. When using insulated studs, for example, the resonance frequency would be lower, and that is the resonance frequency that would be applicable for that particular situation. So, as indicated in your paper, the response does go up when using insulated studs. It goes up to frequencies near 5 or 10 kc, and that is an indication that if you are interested in using an accelerometer in this frequency range, you should select one which has a higher resonance frequency, and therefore, would have the response that you wanted, 5 or 10 kc.

Mr. Schloss (David Taylor Model Basin): Have you performed high frequency calibrations on different calibrators and obtained consistent results?

Dr. Bouche: In general, results obtained on different calibrators are consistent. This was demonstrated both by shock motion and sinusoidal motion calibrations. Resonance frequency measurements on a 2225 accelerometer using the mechanical excitation of a half-sine pulse applied to a steel anvil, indicated a resonance frequency of 80 kc. The same value was obtained when using a magnesium anvil. Similar results were obtained on other model accelerometers having lower resonance frequencies, e.g., the 2224 accelerometer with a 25-kc resonance frequency. These experimental results do not follow the theory presented in your paper, Ref. 3 above, which indicates that lower resonance frequencies should have been obtained.

Sinusoidal calibration results are similar to those obtained with shock motion excitation. High frequency sinusoidal calibrations are performed on a variety of shakers using steel and aluminum mounting surfaces. As an example, the response of a 2231 accelerometer was within 4 percent at 10 kc on two different calibrators using comparison and interferometric techniques. This agreed closely with the theoretical response corresponding to the 50-kc resonance frequency of the accelerometer. Accurate high frequency sinusoidal calibrations are obtained by meeting two requirements. The first requirement is that there be no relative motion between the standard and test accelerometers. Secondly, it is necessary for the mechanical impedance, as seen by the accelerometers, to be large compared to the mechanical impedance of the mass element in the accelerometer. These two requirements are achieved readily by using a high frequency shaker where the point and transfer mechanical impedances of the moving element are constant throughout the range of calibration frequencies.

Mr. Schwartz (USN Marine Engineering Lab.): My question has to do with your high temperature calibration. You mentioned that your first accelerometer was mounted on one end of a ceramic rod and the standard on the other. How do you take into account the compression wave effects in this rod?

Dr. Bouche: We perform the calibration only at frequencies below 200 cps. In the few cases where we do attempt high-frequency, high-temperature calibrations we use a back-to-back fixture inside the oven with a standard accelerometer of known temperature characteristics.

* * *

A PEAK SHOCK VELOCITY RECORDER FOR STUDYING TRANSPORTATION HAZARDS

M. Gertel
MITRON Research and Development Corp.

This paper describes a self-contained shock recorder package capable of recording 10,000 impact shocks or operating for 30 days unattended, whichever occurs first. This and similar packages will be shipped varying distances by several routine methods to obtain data for a statistical study of shipping and handling shock conditions.

INTRODUCTION

It has long been recognized that transportation environments should be defined on a statistical basis. Conceptually, this would make it possible to establish an optimum degree of protective packaging for shipping delicate precision equipment and other fragile items. In concept, the optimum would be based on trade-off considerations between the cost of damage versus the cost of protective packaging.

The effective execution of a statistically based transportation hazards study has been hampered till now, as may be inferred from Refs. 1 to 4, by the following:

1. Indecision as to appropriate shock parameters to measure

2. Lack of reliable, compact, self-contained and accurate shock instrumentation and recorders capable of long unattended operation.

Simple but effective solutions to both of these problems have now been determined as part of a continuing Army study involving the determination of criteria to be used in shipping container design and testing applications. The detailed analyses and results of the initial phases of this program are presented in Ref. 5. The results which are pertinent to a statistical study of transportation shocks are presented here.

The peak velocity, i.e., the time integral of a shock acceleration-time history, has been determined in Ref. 5 to be the most important parameter to monitor during studies of shipping shock conditions. Accordingly, a self-contained shock velocity recorder package has been developed for the U. S. Army Natick (Mass.) Laboratories, a field agency of the Army Material Command. This and similar packages will be shipped varying distances by a variety of routine methods to obtain data for a statistical study of peak impact velocity shock conditions prevalent during shipping and handling. The system has a recording capability of 10,000 impact shocks or 1 year of unattended operation, whichever occurs first. The results of a trial 500 mile shipment are presented here.

CONSIDERATIONS PERTINENT TO MEASURING SHOCK VELOCITY IN SHIPPING STUDIES

The major hazard anticipated during shipping is that of dropping the shipped item

[1] D. A. Fermage, "Transportation Shock and Vibration Studies," Final Report on Contract No. DA-44-009 eng 460 Engineer Research and Development Laboratories, Fort Belvoir, Virginia (1950).

[2] D. R. Craig and H. S. Youngs, "Design Objectives for Package Shock Recording Instrumentation," Shock and Vibration Bull. No. 20 (1953), pp. 160-171.

[3] K. W. Bull and C. F. Kossack, "Measuring Field Handling and Transportation Conditions," WADD Technical Report 60-4 (Feb. 1960).

[4] R. W. Saxton, "Evaluation of Commercially Available Portable Impact Recorders," Northrop Corporation Report NOR 62-70 on Contract No. NOw 61-0689-c (May 1962).

[5] M. Gertel and D. Franklin, "Determination of Container Design Criteria - Summary Report No. I," MITRON Research & Development Corporation Report 601-5 on Quartermaster Research & Engineering Command Contract No. DA 19-129-QM 2082 (OI 6150) (Aug. 1963).

during handling operations. The analysis of such drop shock conditions as applied to the design of protective cushioning provides a technical basis for specifying shock velocity as the key input design parameter. The protection problem is normally analyzed by considering that the impact kinetic energy ($1/2\ mv^2$) of the item is transformed into stored or potential energy in the cushioning material after ground impact. This simplified and practical analytical approach, in effect, creates a single degree-of-freedom problem which presumes that the shock impact duration of the outer container is very short relative to the natural period of the cushioning and hence will have no effect on the cushioning shock deflection. This simplification can be readily introduced because the vast majority of drop shock conditions involve hard impact surfaces with resulting shock (velocity change) durations on the order of 1 millisecond. In some instances durations up to as high as 10 milliseconds may be observed.

In the aforementioned shock cushioning design analysis, the impact kinetic energy (which is proportional to the square of the impact velocity) represents the "input" condition while the cushioning deflection represents the "response". Once the input velocity has been identified or specified, it is a relatively simple design problem to select an appropriate cushioning stiffness to limit the forces transmitted to the item. Accordingly, any study of transportation hazards must strive to quantitatively define impact velocity in order to initiate the cushioning design problem. Preferably, the impact velocity should be defined on a statistical basis to permit trade-off considerations between costs for protection against damage versus the cost of possible damage.

SHOCK VELOCITY TRANSDUCER

Figure 1 shows a four coordinate nomograph with shock spectrum (peak) responses plotted for five different half-sine acceleration pulses embodying the same velocity change but with different durations. The velocity change of each of the pulses depicted in Fig. 1 is 215 ips, which corresponds to the impact velocity of a 5-foot free fall. Each of the five curves is asymptotic to the 215-ips velocity line at extremely low frequencies. The frequency at which each "pulse" curve becomes asymptotic to 215 ips is interpreted as the highest permissible natural frequency which a transducer could have and still accurately measure the velocity change embodied in that particular acceleration pulse. It will be further noted in Fig. 1 that as the transducer natural frequency increases, the instrument response for the different durations departs from the constant velocity line and eventually oscillates slightly

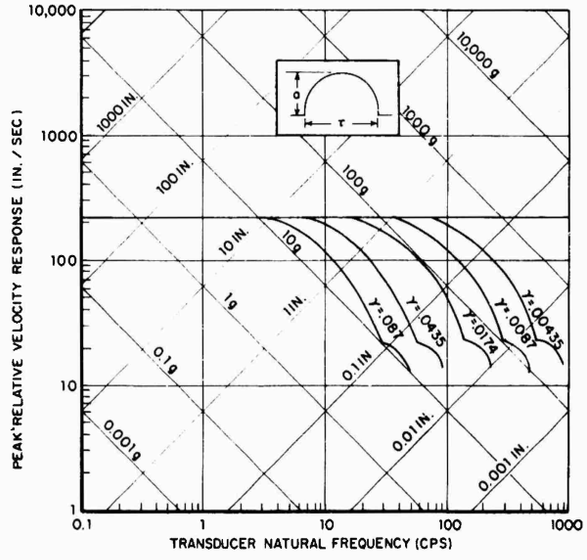

Fig. 1 - Response of velocity shock recorder to half-sine pulses of various durations

about a line representing constant acceleration. In this region, which is representative of transducers with high natural frequency, the deflection response of the instrument is proportional to acceleration.

Figure 2 shows a self-generating electrodynamic (coil and magnet) velocity transducer which was made for the study of transportation shock hazards described in Ref. 5. The transducer magnet slides over the coil and is spring mounted with a natural frequency of 10 cps. The length of the coil allows for magnet shock displacements of ±3.5 inches. This transducer has a capability of accurately recording the shock velocity of half-sine acceleration pulses with durations as long as 0.040 seconds approximately (refer to Fig. 1). Based on experience noted earlier, this magnitude of shock duration far exceeds the probable short shock pulse durations likely to be encountered in shipping.

SHOCK RECORDER

The shock recorder system is comprised of three mutually perpendicular self-generating velocity transducers whose signal outputs are recorded on three channels of a four channel magnetic tape recorder. The fourth channel is used for a time code signal. The shock recorder tape drive system is battery powered, and is designed to record shock pulses only when the impact velocity exceeds a preset level corresponding to a 2-inch free drop. The maximum capability is a 5-foot free drop. Figure 3 shows the system assembled in an aluminum framework in preparation for a shipping test. Figure 4 shows a closeup view of the tape recorder portion of the system. The prototype recorder is 6 x 6 x 4 inches. Smaller units have now been built.

The recorder steps the tape approximately 0.1 inch for each shock input. Thus, the record is not a time history but rather the waveform is condensed into a simple "spike" from which the peak can be readily determined electronically or by playback into an oscillograph. Based upon 0.1 inch of tape required for each shock, a 100 foot reel of magnetic tape will have a recording capability of well in excess of 10,000 impacts. Inasmuch as the battery drives the tape stepping motor on an intermittant basis, the battery power drain is very low. Accordingly, the recorder life in a remote shipping and storage operation is very nearly the same as the shelf life of the battery.

TRIAL SHIPMENT

To provide evidence of the reliability of operation of the velocity shock recorder system under actual field conditions, the prototype system (shown in Fig. 3) was shipped on approximately a 500-mile round trip. The framework (shown in Fig. 4) was placed in a 3/4-inch

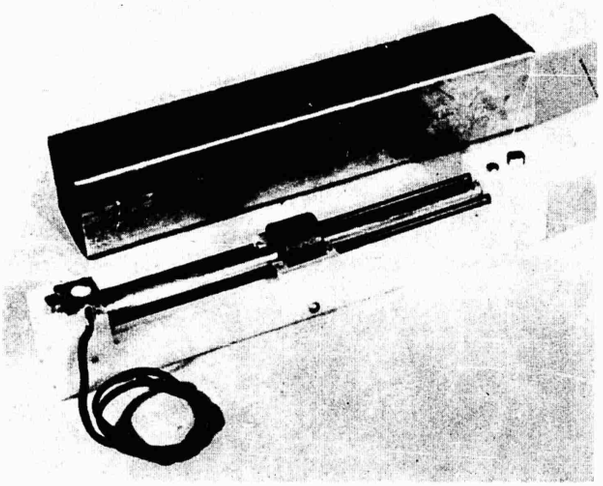

Fig. 2 - Operational prototype shock velocity transducer

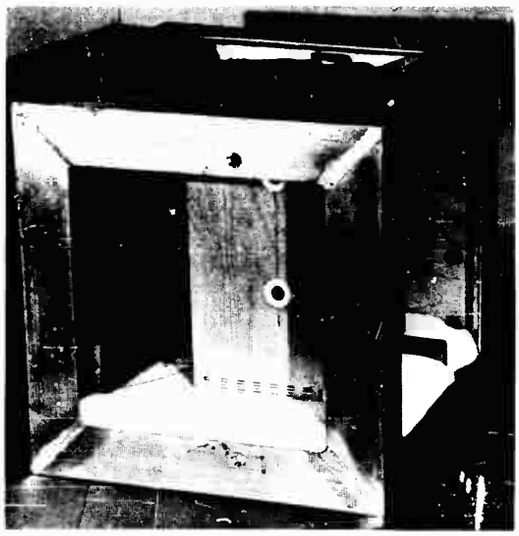

Fig. 3 - Aluminum frame with transducers and tape recorder box

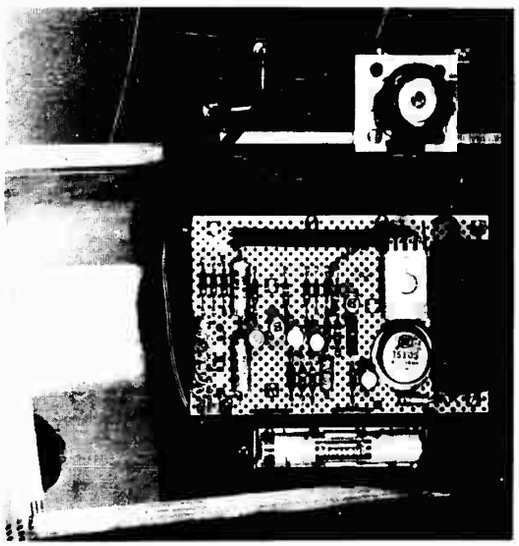

Fig. 4 - Operational prototype magnetic tape recorder

Fig. 5 - Shipping container

thick plywood box and then packaged in corrugated fiberboard. The complete package weighed 51 pounds and was a 14-in. cube in size. Figure 5 shows the package after the shipping test.

The trial shipment lasted approximately 3 weeks due to a mix-up which resulted in the box being accidently stored in a warehouse for 2 weeks before being returned to the sender. Immediately upon return, calibration drop tests were repeated to verify that the system was still operative. The system responded perfectly with no indicated change in calibration. For convenience, the system calibration was obtained as a plot of the velocity transducer output in millivolts as a function of drop height. The calibration of each transducer is adjusted to be the same and is shown in Fig. 6.

Figure 7 shows an oscillographic playback of the shocks recorded during the trial shipment. It is of interest to note that both positive (right side up) and negative (upside down) shocks, as well as sidewise and forward shocks were recorded.

The results of the trial shipping data of Fig. 7 are presented as a histogram plot of number of occurrences versus drop height in Fig. 8. The present sample size is too limited to perform any quantitative analysis. In a qualitative sense, however, it seems significant that approximately 25 percent of the impacts were directed along the "up" axis of the package. Moreover, the maximum "up" shock was greater than the maximum "down" shock. The histogram also has the barest skeleton indication suggesting a normal or Gaussian distribution with a near zero mean drop height.

CONCLUSIONS

It is deemed inappropriate to perform any more detailed analysis of the present trial data due to the limited sample size. It is only safe

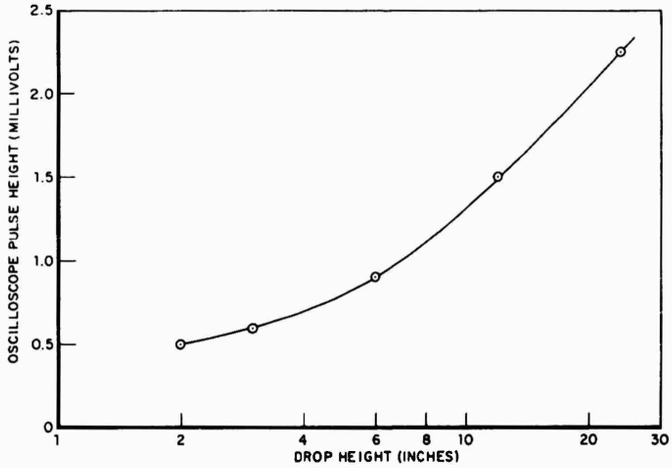

Fig. 6 - Calibration of drop height vs millivolts output

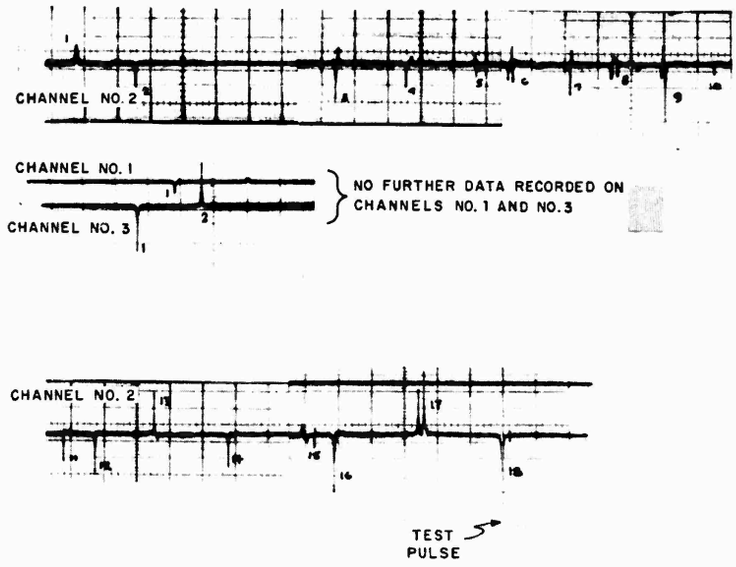

Fig. 7 - Oscilloscope pictures of results from shipping test

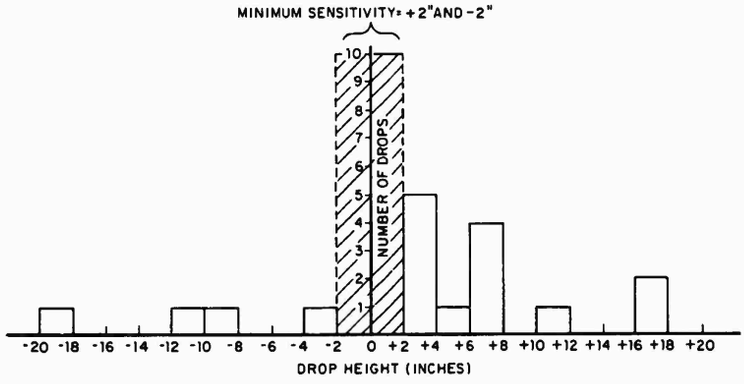

Fig. 8 - Histogram of drop height vs frequency of occurrence

to conclude that the shock velocity recorder described herein has performed successfully in a field trial and will be a useful instrument for obtaining valid statistical data on transportation and handling conditions. Further projected applications for the velocity shock recorder are as a tell-tale monitor to record shocks experienced by critical equipment items during shipment.

* * *

THE USE OF STRAIN GAGES TO DETERMINE TRANSIENT LOADS ON A MULTI-DEGREE-OF-FREEDOM ELASTIC STRUCTURES*

F. R. Mason
Lockheed Missiles and Space Co.
Sunnyvale, California

The procedure which will be outlined was first formulated in connection with attempts to arrive at an optimum design for a recovery pole used on aircraft as a part of a rig to effect the aerial recovery of parachute-borne re-entry capsules.

INTRODUCTION

The procedure which will be outlined was first formulated in connection with attempts to arrive at an optimum design for a recovery pole used on aircraft as part of a rig to effect the aerial recovery of parachute-borne re-entry capsules, but it is considered practical to extend this technique to the experimental determination of distributed transient loadings on other types of elastic structures, such as missiles or aircraft, or plate structures.

Two poles inclined downwards and outwards are cantilevered from the rear of the aircraft to support the rigging and the technique of recovery is for the pilot to make a pass over the parachute and snag it in the rigging (see Fig. 1). In many cases, the 'chute collides with one of the poles and bends or breaks it resulting, on occasion, in the loss of the payload.

In order to carry out a theoretical analysis to determine the response of the pole to parachute impact, a knowledge of the nature of the time and position varying load which the 'chute applies to the pole during the contact period is necessary.

THEORY

The state of affairs after impact when the 'chute is sliding down the pole is shown in Fig. 2; and Fig. 3 shows the mathematical model which is used to describe the system. The position of the load on the pole at any time may be obtained either from high speed movie coverage, as was done in this case, or by assuming that the 'chute is travelling along the pole at a uniform speed equal to its velocity component along the pole prior to impact.

1. Obtain time histories of the bending moments at several points along the pole by the use of strain gages.

2. Pole deflection at any point X at any time t is given by:

$$y(x,r) = \sum \phi_j(r) \times X_j(x) , \qquad (1)$$

where ϕ_j is some unknown function of time describing the generalized coordinate in the j^{th} normal mode, and X_j describes the j^{th} normal mode shape.

3. Bending moment at time t (and point X) is given by

$$M(x,r) = \sum \phi_j(r) \times Ml_j(x) , \qquad (2)$$

where Ml_j is the unit moment at the point x in the j^{th} mode.

4. Thus, for any given time, Eq. (2) gives the bending moment at any point. If, for example, the bending moment is measured at four points we may write down four equations with four unknowns, namely, ϕ_1, ϕ_2, ϕ_3, and φ_4.

*This paper was not presented at the Symposium.

Fig. 1 - Recovery aircraft and rigging

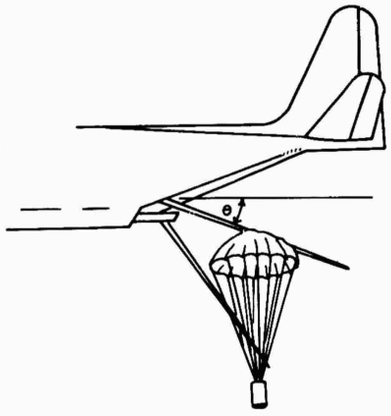

Fig. 2 - Chute-pole contact

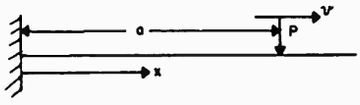

Fig. 3 - Mathematical model

5. Repeating the above process for a large number of times yields a plot of ϕ_j vs time from which a plot of $\ddot{\phi}_j$ vs time for each mode may be deduced.

6. By use of the following equation, the value of P at any desired time may be determined:

$$\ddot{\phi}_j + \omega_j^2 \phi_j = \frac{P}{R_j} (X_j)_a , \qquad (3)$$

where R_j is the generalized mass in the j^{th} mode and $(X_j)_a$ is the modal displacement in the j^{th} mode at the load point a.

It will be observed that in the case of a point load, which is presently being considered, the parameters for any one value of j are all that is required to find a complete time history of the load P. Thus, a good check on the accuracy of the results may be obtained by solving Eq. (4) using parameters for several values of j.

An alternative method for deducing the load-time history is to use the following equation:

$$M(x,r) = \sum \ddot{\phi}_j(r) \times \frac{Ml_j(x)}{\omega_j^2} + P(a-x) , \qquad (4)$$

where Ml_j is the unit moment at the point x in the j^{th} mode, ω_j is the natural frequency in the j^{th} mode, a is the position of the load at time t, and P is the unknown point load. This equation is merely a statement of the fact that the bending moment at any point is equal to the sum of the moments of the inertia forces plus

the moment of the applied loading about that point. This equation has the advantage that the terms within the summation sign generally converge more rapidly than do those within the summation sign of Eq. (2), and it also disposes of the necessity of deducing $\ddot{\phi}_j$ graphically from a plot of ϕ_j vs time. In fact, of course, P may be calculated directly from the set of simultaneous equations which Eq. (3) yields without the necessity of solving for $\ddot{\phi}_j$.

On the other hand, in the case of a point load, we are increasing the number of unknowns by one over Eq. (2), and hence reducing the number of modes which may be included in the computation by one which, in turn, leads to a degradation in accuracy. For example if we have strain gage measurements at four points, Eq. (2) enables us to find ϕ_1, ϕ_2, ϕ_3, and ϕ_4 whereas Eq. (3) only enables us to include the first three values of $\ddot{\phi}_j$ in the computation of load P.

For more than one load the number of modes which may be used is further reduced.

PRACTICAL APPLICATION TO THE RECOVERY POLE

Three strain gages were used and located as shown in Fig. 4. Values of natural frequencies and unit moments for the first two bending modes of the pole were deduced using a digital "lump-spring" program and are shown for the three relevant stations — 123, 245, and 338 inches from the tip — in Table 1. The relevant portion of the oscillograph trace showing the

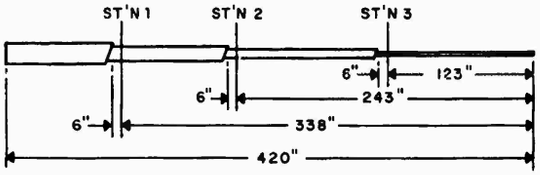

Fig. 4 - Strain gage locations

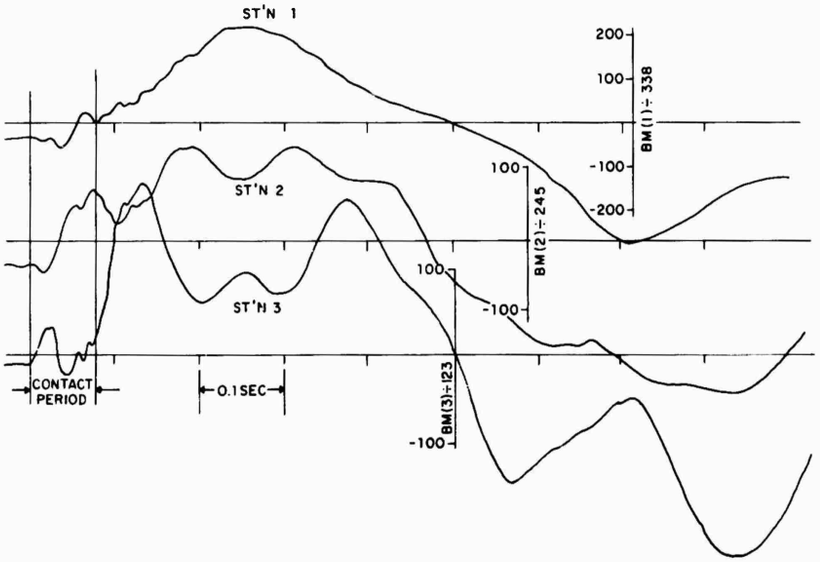

Fig. 5 - Oscillograph traces showing bending moments at three strain gage positions

bending moments at the three stations is shown in Fig. 5. High-speed movie coverage indicated that the initial point of contact of the 'chute on the pole was at 147 inches from the tip and that the total contact time between the 'chute and pole was 0.088 seconds. Assuming that the 'chute had a uniform velocity down the pole, the values of 'chute position for various times shown in Table 2 may be deduced. The values of bending moment are found directly from the oscillograph records by using the appropriate calibration factors.

TABLE 1

Station	Ml_1	Ml_2	Ml_1/ω_1^2	Ml_2/ω_2^2
123	97.4	925	3.36	2.32
245	278	670	9.6	1.68
338	472	-1,495	16.3	-3.75

TABLE 2

Time from Impact (sec)	Values of B.M. (lb - in.)			Load Position	Distance between Load and Station		
	123	245	338		123	245	338
0.015	4800	-1225	0	125	-	120	203
0.030	4920	2940	-2028	100	23	145	228
0.044	-1300	17150	-2400	75	48	70	263
0.060	1550	19600	21900	50	73	193	288
0.088	9850	14600	20300	0	123	245	338

The three equations for the first time interval are as follows:

$$4800 = 3.36\,\ddot{\phi}_1 + 2.32\,\ddot{\phi}_2,$$

$$-1225 = 9.6\,\ddot{\phi}_1 + 1.68\,\ddot{\phi}_2 + 120\,P,$$

and

$$0 = 16.3\,\ddot{\phi}_1 - 3.75\,\ddot{\phi}_2 + 203\,P.$$

Solving sets of equations such as the above for each time interval yields the plot of P vs time shown in Fig. 6. The curve shown ignores several negative "wild" points at times other than those in Table 2 which are probably a result of utilizing only two modes in the calculation, as are the negative loads (a practical impossibility for this problem) indicated at low times.

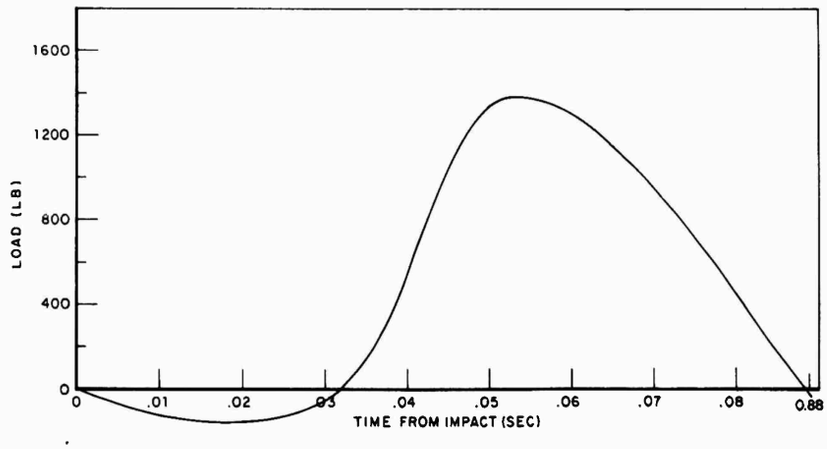

Fig. 6 - Computed load vs time

ASSESSMENT OF THE EFFECT OF NUMBER OF MODES INCLUDED

Table 3 shows the results of an analytical evaluation of a recovery pole of slightly different design to the one tested. With initial impact 210 inches from the tip. Values of load at 0.0395, 0.0791, and 0.1187 sec after impact are shown together with the load position. Bending moment components for three positions, one-quarter, one-half, and three-quarters of the pole length are shown due to (1) inertia in the first five modes, i.e., $\ddot{\phi}_j \, Ml_j/\omega_j^2$, and (2) applied loading P. The bending moment at any position is the sum of the six tabulated components. The relative contribution of each mode to the total bending moment is also apparent from Table 3.

Solving these and similar sets for the other two times yields the following values of load at the three respective times, 236, 1350, and 980 lb. These are considerably in error from the true values of 108.8, 783, and 640 lb.

It must be concluded, therefore, that more than two modes must be used for this problem to avoid serious degradation of accuracy. The larger the number of modes included the greater the accuracy and, it would appear to be reasonable to state that in the evaluation of transient loading on any structure by this method, sufficient instrumentation to facilitate the use of at least the first three modes is mandatory and the inclusion of more than three modes is highly desirable. If some prior knowledge of the approximate nature of the applied transient loading, which it is desired to find, is available, the correct decision regarding the relative importance of each mode is, of course, easier to make.

TABLE 3

Distance from Tip	Applied Load Moment	$\phi_1 Ml_1/\omega_1^2$	$\phi_2 Ml_2/\omega_2^2$	$\phi_3 Ml_3/\omega_3^2$	$\phi_4 Ml_4/\omega_4^2$	$\phi_5 Ml_5/\omega_5^2$	M
t = 0.0395 sec P = 108.8 lb - 40 in. from Tip							
110	0	-3,200	+1,700	-1,030	+214	+23.2	-2,300
210	7,600	-8,900	+2,750	-74	-281	-28.4	-1,167
310	18,500	-16,650	+336	+1,129	+233	+3	3,550
t = 0.0791 sec P = 783 lb - 70 in. from Tip							
110	31,300	-34,000	-16,960	-9,500	-3,250	+370	-23,600
210	110,000	-94,000	-24,200	-67	+1,750	+234	-6,300
310	188,000	-77,000	-2,940	+1,015	-1,450	-26.7	9,700
t = 0.1187 sec P = 640 lb at Tip							
110	70,500	-36,400	-1,700	-9,500	3,240	-320	25,820
210	135,000	-101,000	-2,770	-690	-4,250	-450	25,840
310	198,000	-190,000	-3,360	1,040	3,500	51.2	9,180

By using the first two modes only, for which the appropriate values of Ml_j/ω_j^2 are as shown in Table 4, and the value of total bending moment shown in Table 3, the following set of simultaneous equations may be set up for time 0.0395 seconds.

$$3550 = 14.6 \, \ddot{\phi}_1 + 0.42 \, \ddot{\phi}_2 + 170 \, P,$$

$$1167 = 7.8 \, \ddot{\phi}_1 + 3.46 \, \ddot{\phi}_2 + 70 \, P,$$

and

$$-2300 = 2.8 \, \ddot{\phi}_1 + 2.12 \, \ddot{\phi}_2.$$

TABLE 4

Station	Ml_1/ω_1^2	Ml_2/ω_2^2
110	14.6	0.42
210	7.8	3.46
310	2.8	2.12

POSSIBLE EXTENSIONS OF THE METHOD

The basic concept applied to a point load and a cantilever beam has just been described, but it is considered practical to extend this technique to the experimental determination of transient loadings, either discrete or distributed, on other types of elastic structure.

Consider, for instance, the lateral gust loading on a missile. This will be a function of position and time. Hence assume

$$\frac{p}{r} = \sum a_n(r) \times X_n(x), \qquad (5)$$

where p is the load per unit length, r is the local mass per unit length, a_n is some function of time associated with the n^{th} bending mode, and x is the n^{th} bending mode shape.

Assume, further, that the bending displacement at any point is:

$$y = \sum \phi_n(r) \times X_n(x),$$

where ϕ_n is the generalized coordinate in the n^{th} mode.

During a virtual displacement in the j^{th} mode of $\delta y = X_j \, \delta\phi_j$, the virtual work of the applied loading p is

$$\delta w_p = \int_0^L X_j \times r \sum a_n(r) \times X_n(x) \times \delta\phi_j .$$

From orthogonality considerations

$$\int_0^L r_1 X_n \times X_m \times dx ,$$

where $n \neq m$ is zero. Thus

$$\delta w_p = \delta\phi_j \, a_j \int_0^L r X_j^2 \, dx$$

$$= \delta\phi_j \, a_j R_j ,$$

where R_j = the generalized mass in the j mode. It may be readily verified from any dynamics text that the virtual work of the inertia and elastic forces in the j^{th} mode is

$$\delta w_{IE} = -R_j(\delta\phi_j) \, \ddot{\phi}_j - \omega_j^2 \phi_j(\delta\phi_j) R_j .$$

Hence, equating the total virtual work to zero we get

$$\ddot{\phi}_j + \omega_j^2 \times \phi_j = a_j . \qquad (6)$$

As described previously, if bending moments at n points on the missile are known then plots of ϕ_j and $\ddot{\phi}_j$ vs time for the first n modes may be deduced using the modal unit moments. Hence plots of the value of a_j vs time may be made from Eq. (6), and an evaluation of the transverse gust loading follows from Eq. (5).

Since the gust could come from any azimuthal direction it would be necessary to carry duplicate instrumentation at two positions 90 degrees apart and evaluate the load component in the two directions in order to arrive at the total load.

It may be readily appreciated that, by using a similar approach, a means of evaluating transient loads on other types of structure, such as aircraft lifting surfaces, and the like, may be readily devised.

* * *

AUTOMATIC ACCELEROMETER CHECK-OUT EQUIPMENT

G. M. Hieber and B. Mangolds
Radio Corporation of America
Princeton, New Jersey

This paper describes a system for reducing instances of lost or erroneous accelerometer data. The system allows a relatively rapid means of checking 59 channels for faulty equipment or faulty setup. In this method, a charge amplifier is cycled through each input circuit to sense for changes of capacity. When no changes are sensed, a programmed calibration signal is then applied to all channels, by transformer coupling, in series with the shield of each accelerometer co-axial cable.

Frequent calibration of instrumentation is necessary to prevent misinterpretation or loss of data. In a complex series of tests, it is desirable to have a quick and thorough means available to check an instrumentation setup. Thus, an automated system which calibrates from the transducer through the data reduction process is desired. The particular equipment to be discussed is an approach to this goal.

Vibration measurements are made almost exclusively by piezoelectric accelerometers at the Astro-Electronics Division of RCA (AED), because of their small size, broad frequency response, and high output. The only positive method of calibrating most transducers is to subject them directly to the phenomena to which they are sensitive. Thus, for an accelerometer, it is necessary to vibrate the transducer over both its full frequency range and dynamic range. Although this can be done before and after a test program, there are occasions where it is not feasible, e.g., between test runs, when accelerometers are mounted on or inside equipment, or where the sensitive axis of an accelerometer is arranged to sense acceleration in other than the excitation axis (to obtain information such as cross-motion). In such cases, it is necessary to have a substitute method of accelerometer check-out; one which does not involve vibration.

The following is a list of the causes of data loss and data misinformation:

Causes of Data Loss

Accelerometer opens or shorts
Accelerometer falls off
Cable opens or shorts
Electronic equipment fails
Human error occurs, e.g., forgetting to turn on power or neglecting to put in recording paper

Causes of Data Misinformation

Accelerometer change in sensitivity due to damage
Accelerometer unduly susceptible to factors such as cross-axis motion, temperature, mounting stresses, or magnetic fields
Undetected nonlinearities in the instrumentation system
Erroneous range settings or mixed channel connections of system
Misinterpretation of data

A good "quick look" system will minimize the difficulties of data loss, since problems can be detected when they occur during a test.

Undue susceptibility of accelerometers to environments other than vibration along the sensitive axis can be alleviated by a careful selection of transducers.

Human error can be reduced by providing careful and detailed test procedures, and insisting on strict adherence to them.

The above measures, however, will not insure presentation of valid data. It is necessary to have a check-out system or procedure preventing system nonlinearities or sensitivity changes which cause erroneous results. A good check-out system should also aid in reducing all other difficulties with the exception that it will not prevent an accelerometer from falling

off, nor will it reduce environmental susceptibility of the accelerometers. Through past experience, next to human error, the greatest sources of difficulty are opens and shorts in accelerometer cables.

Automatic check-out equipment now used at AED is shown in Fig. 1. It will determine whether there is a short or an open in the sensing circuit, which may be caused by either the accelerometer or the cable. In addition, the equipment will calibrate all channels, checking all electrical equipment settings. One approach which has been used to provide this same information is the self-calibrating accelerometer. In this method, a signal is applied to a force generator inside the accelerometer which drives the seismic mass; the resulting output signal from the accelerometer is checked to determine any deviation from its previously calibrated condition. This method is rather expensive for general laboratory usage. It also requires an extra cable for every accelerometer which can, as previously mentioned, be a source of trouble. The system utilizing signal insertion at the accelerometer also requires an extra cable. This system is advantageous since it supplies all the information desired and does not necessitate the extra cable. The only deviation this system will not reveal is loss of sensitivity caused by a cracked crystal which will change the capacitance of the accelerometer-cable system by less than 10 percent. This is such a rarity that it should not detract from the equipment.

A block diagram of the check-out equipment is shown in Fig. 2. Basically, a charge amplifier is cycled through each channel. When the total capacity of the channel remains unchanged, the charge amplifier in conjunction with a pulse circuit will generate a pulse, advancing the selector switch to the next channel. Should a short or open condition exist in the transducer system, a change in total capacitance results, thus the pulse will not be formed. Therefore, the equipment will stop at the malfunctioning channel. If the switch cycles through all channels successfully, it can then be assumed that no shorts or opens exist in the transducer section of the instrumentation. When the check-out sequence is completed, a signal is simultaneously applied to all channels. This signal is programmed to check the dynamic range and frequency response of each channel. The programmed signal is sent through the instrumentation system to the tape recorders where it is checked to insure that the entire system is within calibration. The main signal insertion and adjustment functions are performed by means of components packaged in

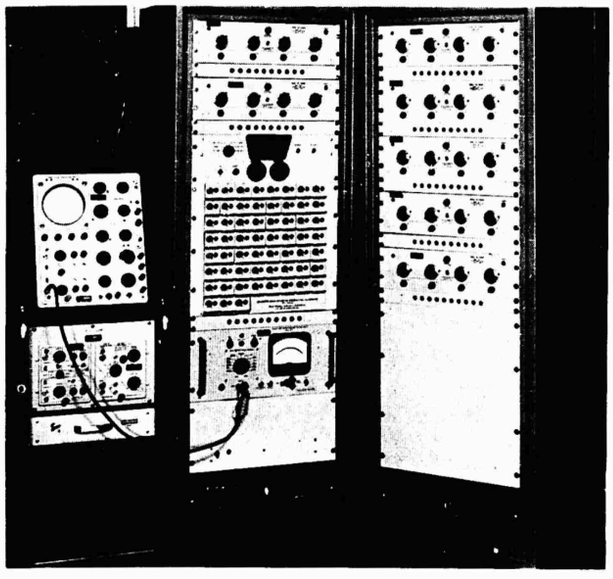

Fig. 1 - Automatic accelerometer check-out equipment

readily interchangeable modules (one of which is shown in Fig. 3) and designed to support channel integrity.

The calibration signal is transformer-coupled in series with the shield of the accelerometer coaxial cable, just ahead of the cathode follower. Transformer coupling is advantageous since there is no grounding problem, allowing more flexibility in connecting the calibration source. During signal insertion, the primary of the transformer is energized by a signal generator. The system is designed so that the inductances, capacitances, and impedances involved do not create a frequency or phase distortion in the desired range: crosstalk is better than 80 db.

Each channel has three adjustments. One adjusts the sensitivity of the charge amplifier to the particular capacitance range of the accelerometer and cable combination of that channel. The other two adjustments provide coarse and fine control of the calibration signal for that channel. A manual cycle is used for setting up the equipment.

The equipment can handle 59 accelerometer channels and can be set up in a few minutes since the adjustments are few and simple. By

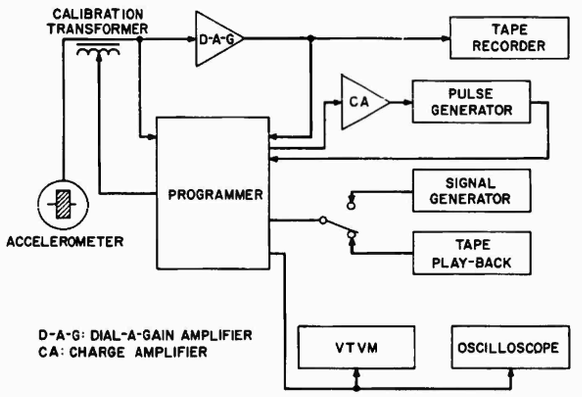

Fig. 2 - Automatic accelerometer check-out equipment, block diagram

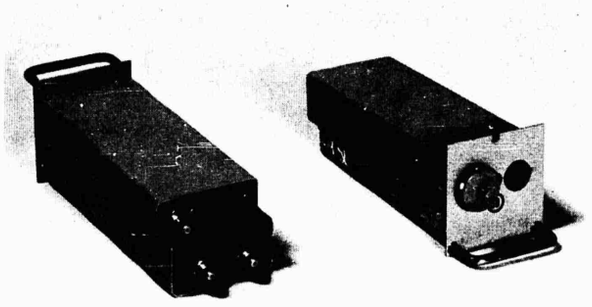

Fig. 3 - Calibration module, front and rear views

properly programming a calibration signal, not only can the recording equipment be checked out, but a complete check-out is available for data reduction equipment, since the calibration signal provides a means of checking either x-y records or oscillograph records at specific frequencies over the full dynamic range of the data acquisition system.

* * *

THE CONDENSER MICROPHONE FOR BOUNDARY LAYER NOISE MEASUREMENT*

W. T. Fiala and J. J. Van Houten
LTV Research Center, Western Division
Anaheim, California

INTRODUCTION

Programs to establish the magnitude, spectra, and spatial distribution of boundary layer pressure fluctuations are a paramount part of flight vehicle research. Microphone instrumentation which will perform in the combined environments of temperature, pressure, vibration, and shock are required to support these measurement programs. A microphone system which will achieve the broad performance characteristics required to meet this aerospace need is discussed in this paper.

ENVIRONMENTAL PERFORMANCE REQUIREMENTS

The most severe requirement on the instrumentation is the environmental extremes encountered during flight. These include temperatures covering the range from -65° to 600°F and altitudes to 150,000 feet. Severe vibration levels encountered during flight must not compromise system integrity nor drastically change system sensitivity. Additional environmental extremes include humidity, acoustic noise, shock, explosive hazard, and chemical contamination.

The system must have a frequency response which is flat from 20 cps to 20 kc. When wind tunnel model evaluation of boundary layer effects is to be investigated, this response must extend to as high as 100 kc. A dynamic range covering sound pressures from 100 to 170 db (re: 0.0002 dyne/cm^2) is required to support both the model studies involving low level acoustic noise and the problems at higher intensities associated with sonic fatigue of structure. Finally, the conflicting requirement of extremely small microphone size with a high sensitivity adds yet another constraint on system design.

Altitude and Temperature Stability

Measurement of boundary layer pressure fluctuations at high vehicle Mach numbers subjects the pressure transducer or microphone to a broad range of temperatures and ambient pressures. At supersonic speeds to Mach three, surface temperatures to 600°F may be encountered. A microphone system which is temperature and altitude insensitive is, of course, desired. A condenser microphone[1] has been designed with minimal change in sensitivity at temperatures to 600°F. At frequencies to 20kc, this condenser microphone design is essentially altitude insensitive, to reduced pressures equivalent to 150,000 feet. This is accomplished with a diaphragm stiffness which is high in comparison to the stiffness of the cavity behind the diaphragm.

Vibration Sensitivity

The boundary layer pressure fluctuations create vibrational acceleration of the vehicle surface. With a microphone flush mounted at the vehicle surface, these accelerations are sensed by the pressure transducer. Therefore, a microphone which is essentially insensitive to acceleration is required. The condenser microphone offers the best possibility for achieving a low vibration sensitivity over an extended frequency range. With the condenser microphone, a vibration sensitivity corresponding to 80-db sound pressure level for 1-g acceleration of the microphone may be achieved. Vibration

*This paper was not presented at the Symposium.

[1] B. R. Beavers, "High Temperature Condenser Microphone System (Abstract)," J. Acoust. Soc. Am., Vol. 35, No. 5 (1963), p. 781.

sensitivity of a condenser microphone[2] is readily established and directly proportional to the mass of the diaphragm.

Frequency Response and Sensitivity

The use of scale models to study boundary layer effects requires a transducer with flat frequency response to 100 kc. To achieve the dynamic range desired, the transduction sensitivity should be in the order of -70 db (re: 1 V/dyne/cm^2). With this sensitivity and the electrical noise thresholds associated with condenser microphone instrumentation, a dynamic range in the order of 100 db is possible.

CALIBRATION

An extensive calibration of the microphone is required to establish the characteristics of the transducer for boundary layer evaluation. This calibration must cover the envelope or environmental extremes establishing change in response with temperature and altitude as well as dynamic range.

With the condenser microphone, it is possible to use the electrostatic principle of calibration to establish change in sensitivity with temperature and reduced pressure. The diaphragm of the microphone is driven with an electrostatic force which simulates the sound pressures to be measured. The force generated on the diaphragm is independent of temperature and reduced pressures. With the complete microphone system placed in the environmental chamber, calibrations are performed over the complete frequency range to establish both change in sensitivity and response.

The absolute sensitivity of the microphone is established by use of the pistonphone.[3] The basic calibration at normal atmospheric conditions is accomplished by comparison with a laboratory standard microphone. This calibration is usually performed in a large anechoic chamber, using suitable electrodynamic and electrostatic transmitters as the source. A verification of the linearity of the microphone is accomplished by use of a standing wave tube.[4] The device now in use, Fig. 1, is designed to yield sound pressures as high as 180 db with a total harmonic distortion of less than 5 percent. The frequency response and sound pressure levels achieved by the standing wave tube used in our laboratory are shown in Fig. 2.

The pressure response of the microphone is necessary to interpret measurements made with the transducer flush mounted at a vehicle surface. The electrostatic method of calibration previously mentioned yields the pressure response directly at frequencies which are not too near the resonant frequency of the microphone. At frequencies near the microphone resonance, this method does not yield a true pressure response. The mechanical impedance associated with the diaphragm stiffness and the dynamics of the cavity between the microphone and electrostatic actuator create a situation which is difficult to define. Calibrations in this frequency range are justified by use of the free field microphone response and a calculation of the diffraction characteristics in this pressure range.[5]

The calibrations to establish pressure response in the frequency range from about 20 to 100 kc are the most difficult and least reliable. A summary of the calibrations required to establish the characteristics of a system for boundary layer measurement is given in Table 1. An estimate of the precision of these calibrations has also been included in this summary.

At higher frequencies the sensitive element of the microphone has a size comparable to the vortices existing within the boundary layer. It is necessary to provide a correction which accounts for the microphone size and its correlation with the boundary layer pressure fluctuations. A recent article by Corcos,[6] provides a means of establishing values for this correction factor, at the Mach numbers of interest.

SYSTEM CAPABLE OF MEETING THE PERFORMANCE REQUIRED

A miniature condenser microphone has been developed specifically to meet the aerospace

[2] E. Rule, et al., "Vibration Sensitivity of Condenser Microphones," J. Acoust. Soc. Am., Vol. 32, No. 7 (1960), p. 82.

[3] Glover and Baumzweiger, "Moving Coil Pistonphone for Measurement Sound Field Pressure," J. Acoust. Soc. Am., Vol. 10 (1939), p. 200.

[4] Beranek, Acoustic Measurements (John Wiley & Sons, Inc., New York, N.Y., 1949), p. 172.

[5] Rivin and Cherpak, "Method for Measuring & Calculating the Diffraction Coefficient of Microphones," Soviet Physics Acoustics, Vol. 5, No. 3 (Feb. 1960).

[6] G. M. Corcos, "Resolution of Pressure in Turbulence," J. Acoust. Soc. Am., Vol. 35, No. 2 (1963), p. 192.

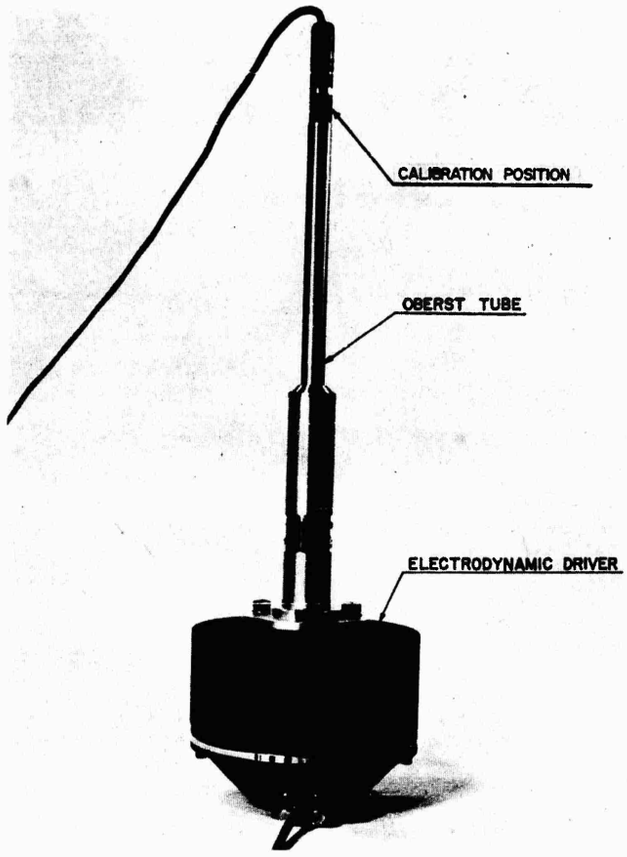

Fig. 1 - Standing Wave Tube; Sound pressures to 180 db are generated for microphone linearity calibrations

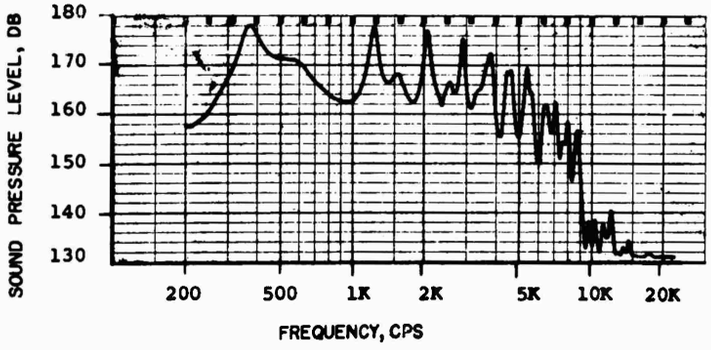

Fig. 2 - Standing Wave Tube Response; Less than 5-percent total harmonic distortion is experienced at the peaks in the response of this device.

TABLE 1
Microphone Calibrations Required for
Boundary Layer Noise Measurement

Calibration Required	Method of Calibration	Frequency Range	Accuracy of Measurement
Absolute sensitivity	Pistonphone	20 to 200 cps	± 1/4 db
Frequency response	Comparison with lab standard	100 cps to 10 kc 10 to 100 kc	± 1/2 db ± 2 db
Variation with temperature (0° to 525°F)	Electrostatic actuator	20 cps to 20 kc	± 1/2 db
Variation at reduced pressures to 100,000 ft.	Electrostatic actuator	20 cps to 20 kc	± 1/2 db
Linearity with sound level (80 to 180 db)	Standing wave tube (Oberst's tube)	400 cps	± 1/2 db

requirements previously discussed. It has the broadband response characteristics required and the stability compatible with the previously mentioned environmental extremes. This condenser microphone has been calibrated to establish its change in sensitivity with temperature and altitude variation.[7] Circuitry has also been developed to complement the use of this microphone for boundary layer noise measurement. This circuitry includes a miniature cathode follower capable of operation to 600°F and an airborne power supply for flight application.

Miniature Condenser Microphone

The condenser microphone being used for boundary layer measurement is of stainless steel construction with mating parts designed to yield minimal change in sensitivity with temperature. The active diameter of this microphone is 0.16 inch. It is designed for convenient flush mounting at an aerodynamic surface. An illustration of the microphone and a cathode follower capable of operation within the temperature range from 0° to 525°F is shown in Fig. 3; the basic response of this microphone is shown in Fig. 4; and Fig. 5 illustrates the frequency response at various reduced pressures. A summary of the characteristics of this microphone system is as follows:

PERFORMANCE

Sensitivity Measured at Cathode

Follower Output: -72 ± 1 db (re: 1 V/dyne/cm^2)
Linear Limit, SPL: 170 db (re: .0002 dynes/cm^2)
Frequency Response: ± 1 db 20 cps to 40kc
Resonance Frequency: 60,000 cps
System Noise: Equivalent to an SPL of 70db

ENVIRONMENTAL CHARACTERISTICS

Variation of Sensitivity with Temperature: ± 1 db (0°F to 525°F)
Variation of Sensitivity with Altitude: No variation below 5 kc
Vibration Sensitivity: 1-g Acceleration produces equivalent SPL of 79 db.

PHYSICAL

Active Diaphragm Diameter: 0.160 inch
Housing Diameter: 0.280 inch
Housing Length: 0.360 inch

GOALS FOR FUTURE DEVELOPMENT

Considerable emphasis is now being placed on calibration of transducers for boundary layer noise measurement. Particular interest is being given the frequency range from 20 to 100 kc. It

[7] N. J. Meyer and J. J. Van Houten, "Calibration of A Miniature Condenser Microphone at Elevated Temperature and Reduced Pressure," J. Acoust. Soc. Am., Vol. 35, No. 5 (1963), p. 781.

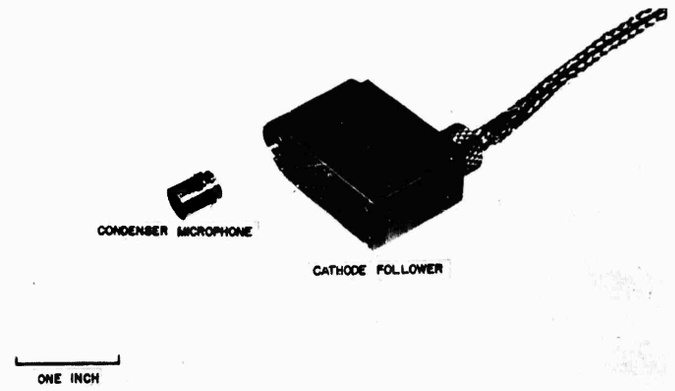

Fig. 3 - Condenser Microphone and Cathode Follower; Stable operation is achieved within the temperature range from 0° to 525°F.

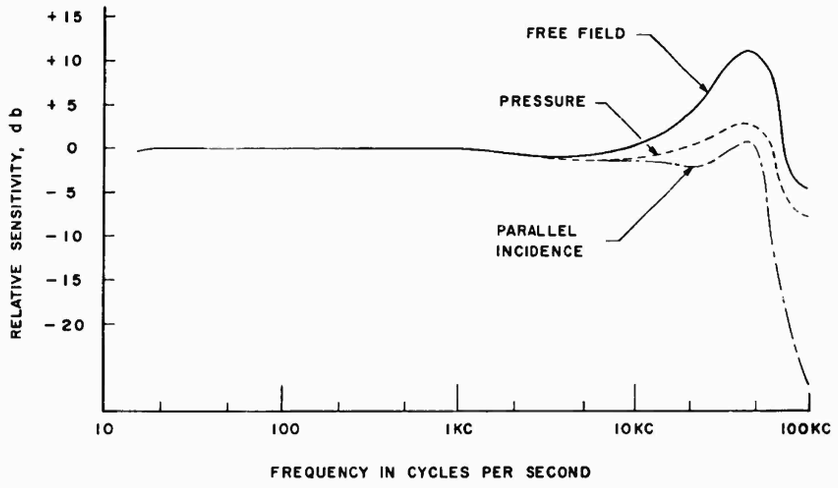

Fig. 4 - Relative Response; The pressure response of the microphone is utilized for boundary layer noise measurement

would be desirable and is the goal of our present research activities in this area to perform calibrations over the complete envelope of temperatures and altitudes, with sound pressures at intensities approximating the operational levels anticipated.

Studies are in progress which will lead to a microphone system capable of operation to 1000°F with the performance requirements necessary for boundary layer noise measurement. It will be possible to achieve systems capable of even higher temperatures for short time durations as a result of these studies.

The electroacoustic design problem posed by the aerospace measurement problem discussed in this paper is extremely difficult and challenging. As further research develops and innovations in solid-state devices become available, the performance of pressure transducers at environmental extremes will be greatly extended.

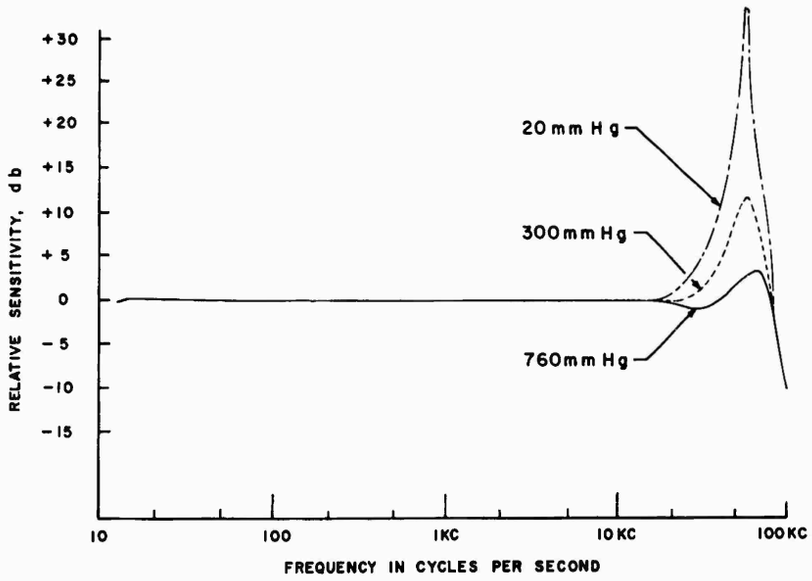

Fig. 5 - Sensitivity variation with altitude; the microphone response is shown for pressures equivalent to sea level, 25,000, and 80,000 feet altitude

* * *

A TEST VEHICLE PROTECTION CIRCUIT*

E. L. Gardner
Atomics International
Canoga Park, California

One of the problems facing the testing engineer in a vibration environment laboratory is the protection of expensive devices under test from damage due to inadvertent excessive loads. These loads can result from several causes as the following examples experienced in our laboratory will illustrate:

1. The test specimen was the first of its kind; its responses were unknown to the degree that it might have been damaged by what was assumed to be a safe input.

2. The console operator changed the setting of the vibration level range switch or level control knob in the wrong direction.

3. A tape recorder operator accidently cut off a tracking filter in the servo loop causing the shaker driver amplifier to develop full power.

In the event of such emergencies, the reaction time of the operator may be slow enough to permit severe damage to occur before he can reduce the drive signal. What is needed then is a circuit which can respond to an excessive signal in a few milliseconds. It would also be helpful if the device were easy to calibrate and had a reset means which does not override the cut-off circuit. It should have its own power supply and be independent of the driver signal servo system, except that it should patch into the signal circuit ahead of the master gain control. Such a circuit was developed in the SNAP Environmental Vibration and Shock Laboratory at Atomics International. It has been in constant use for more than a year. It has proven so useful that our most experienced operators prefer not to run tests without it.

Usually two or more of these circuits are used at one time. Several of the circuits can be supplied by the same battery, as power is drawn only after the cut-off action has been initiated. A neon annunciator lamp is provided to permit the testing engineer to determine which of several monitored points on the test specimen experienced the excessive response. The circuit was designed to be used with an Endevco Dynamonitor. The dynamonitor has sufficient output voltage and power to drive the safety circuit without further amplification. It consists of a diode pump, a potentiometer, a silicon controlled rectifier, a relay, and a battery. The schematic circuit diagram, Fig. 1, also shows the annunciator lamp and reset switch which are accessory to the safety circuit. The two-diode circuit was used to permit operation on excessive input voltages of either polarity. None of the circuit elements are critical, and most can be found among the spare parts in a vibration laboratory.

About the only unique thing in this circuit is the method of reset. When the reset switch is actuated, the conduction of the SCR is stopped by bypassing the relay current to ground. Since there is no signal from the test specimen at this time, the SCR is reset. But, the relay is still holding the driver input signal circuit open and will continue to until the reset switch is released. If the master gain control has not been set to a reduced level the safety action will recur immediately. By resetting in this manner the safety circuit cannot be overridden. Note also that the drive signal passes through the power on-off switch and will be interrupted if the safety circuit power is turned off.

The calibration of the safety circuit is accomplished in such a manner as to provide an operation check of the device. The accelerometer pickup is placed on a calibration shaker and driven to the specified g limit. The range switch and gain control of the dynamonitor are adjusted to provide at least 1 volt from its output. The 10-turn potentiometer of the safety circuit is adjusted until the cut-off action occurs. The potentiometer dial reading is noted. The dial is turned up scale about 10 points and

*This paper was not presented at the Symposium.

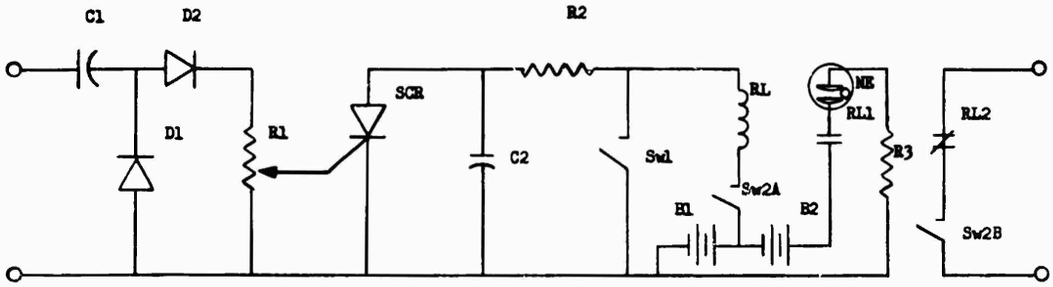

PARTS LIST

B1 & B2	45 Volt Battery
C1	20 uf Condenser
C2	.02 uf Condenser
D1 & D2	1N1695
R1	20k 10-Turn Potentiometer
R2	910 ½-Watt Resistor
R3	40k ½-Watt Resistor
RL	DPDT Relay
SCR	2N2325
Sw1	Reset Switch (Pushbutton)
Sw2	DPST Switch

Fig. 1 - Protection circuit schematic

the reset switch is pushed. When it is released the cut-off action will cease. The potentiometer is then set to two dial divisions from the actuation point. The accelerometer is then installed on the test specimen. The circuit is now ready to help protect the test specimen from prolonged overload and the testing engineer and console operator from embarrassment.

* * *

Section 2
SHOCK TESTING

THE DESIGN AND ADVANTAGES OF AN AIR-ACCELERATED IMPACT MECHANICAL SHOCK MACHINE

L. F. Thorne
The Bendix Corporation
Kansas City, Kansas

INTRODUCTION

Modifications were made to a standard 6-inch Hyge mechanical shock actuator, so that "reverse firing" could be accomplished. In this application, the Hyge is utilized as a velocity generator by accelerating a shaft-mounted specimen carriage into an impact material positioned between the carriage and the top of the Hyge machine, Fig. 1.

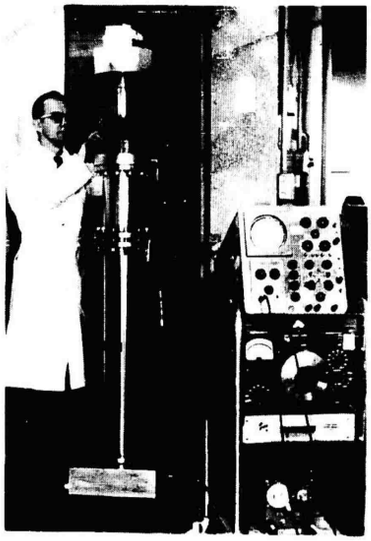

Figure 1

The reverse Hyge design, its operation, and its advantages over the original system are described. A curve showing theoretical energy of the machine at inches of displacement is presented. Measured pre-shock velocities are reflected in a graph showing actual energy, and in information on the percent of shock pulse velocity change attributed to the rebound of the impact material. Versatility of the machine can be seen in photographs which display its shock pulse capabilities. Other photographs show pre-shock and post-shock accelerations.

THE 6-INCH HYGE

The Hyge mechanical shock actuator can be assembled in a number of configurations to meet a variety of shock specifications. One unit configuration of the 6-inch Hyge, Fig. 2, is designed to achieve high levels of acceleration at relatively short pulse durations by rapidly shutting off the fluid flow through an orifice.

The system actuates when air introduced into the lower chamber (fire pressure) unseats the piston seal by exceeding a set pressure in the upper chamber by the ratio of areas exposed above and below the piston. The fire pressure acting over a now larger area exposed below the piston accelerates the piston, fluid, shaft, and specimen carriage until the metering pin enters the orifice, shutting off fluid flow. The resulting shock pulse is controlled by the shape and diameter of the metering pin.

The machine described above has many applications; however, certain disadvantages of

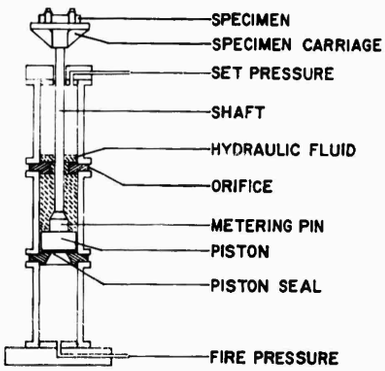

Figure 2

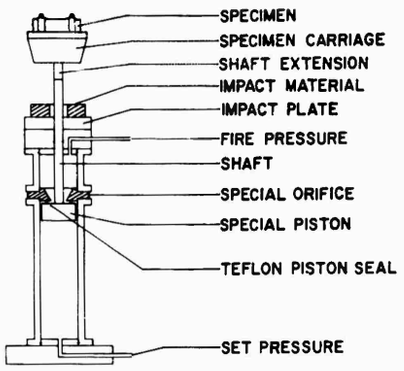

Figure 3

the system limit its versatility. During the shock pulse, the combined weight of the specimen, specimen carriage, and shaft is held by the threaded connection joining the shaft and piston. Specimen weights must be minimized at higher levels of shock to prevent separation of the shaft from the piston. The shaft behaves as a spring upon impact, the magnitude of its oscillations limiting minimum undistorted pulse capability. To change pulse duration any significant amount, the machine must be disassembled and fitted with a metering pin of different design.

THE MODIFIED 6-INCH HYGE

Standard components from a 6-inch Hyge actuator are utilized in the modified design, Fig. 3. The principle of operation is the same as for the normal Hyge machine, except the piston seal seats below the orifice. When the fire pressure in the upper chamber exceeds approximately five times the set pressure in the lower chamber, the system actuates, accelerating the specimen carriage into the impact material. The pulse characteristics, i.e., pulse shape, pulse duration, and maximum g-load, are controlled by the initial set pressure and the dynamic spring constant of the impact material.

During the shock pulse, the weight of the moving components is supported by the impact material; therefore, specimen-fixture weight is limited only by the velocity change of the shock pulse desired. Less weight (piston) extending the shaft upon impact decreases shaft resonance excitation, decreasing shock pulse distortion. The shock signature is changed by adjustments to the dimension or hardness of the impact material. Rebound properties of the material can contribute significantly to the overall velocity change capability of the machine.

CAPABILITIES OF THE MODIFIED DESIGN

Tests of the modified design were conducted using a 12-inch-long, 6-inch Hyge cylinder mounted on a 37-inch-long, 6-inch Hyge cylinder. The theoretical energy curve, Fig. 4, was calculated from expansion and compression ratios for a set pressure of 400 psi and a fire pressure of 2000 psi. Operating the machine at these pressures, the velocity of its moving components at inches of displacement was determined by graphical integration of pre-shock

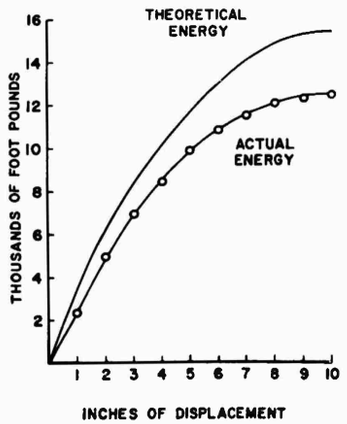

Figure 4

acceleration photographs. This information is reflected by the curve representing the machine's actual energy.

The accelerated weight consisted of a 7.5-lb piston, a 20-lb shaft with connections, and a 32.5-lb specimen carriage. A displacement of approximately 10 inches occurs before the force of expansion above the piston and the force of compression below the piston are equal. Therefore, at a stroke less than 10 inches (distance between the bottom of the carriage and the top of the impact material) the specimen carriage is held in contact with the impact material, minimizing post-shock accelerations. A 6- to 8-inch stroke is normally used for testing. At maximum pressures (400-psi set pressure and 2000-psi fire pressure), the velocity of the total accelerated weight of 60 lb reached 105 fps in 8 inches of stroke.

CONTROL OF THE SHOCK PULSE

Die rubber and molded polyurethane elastomers are being used as impact material for shock pulse control. Shock levels of 1000 g, Fig. 5, and 2000 and 3000 g, Fig. 6, were performed on 70 durometer die rubber. Pre-shock and post-shock acceleration of the 1000-g pulse is displayed. Figure 7 shows shock signatures of 3000 and 4000 g accomplished by using molded polyurethane elastomer pads as the impact medium. All testing was done on 21 square inches of material, 4 inches thick (two, 2-inch thicknesses). A rebound velocity of approximately 40 percent of the impact velocity was experienced from both materials. Shock history was monitored by Tektronix oscilloscope Model 535, Hughes memoscope Model 104, and Endevco accelerometer Model 2225. Filtering was at 10,000 cps.

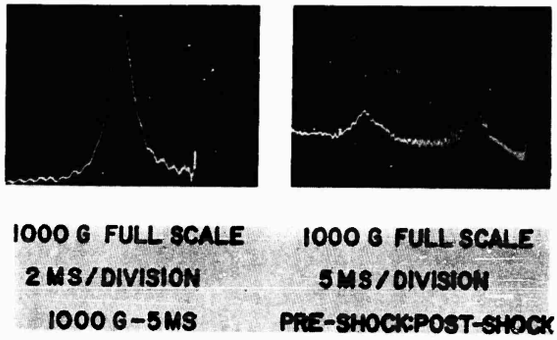

Figure 5

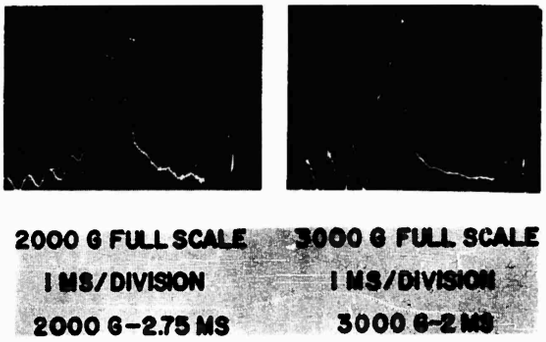

Figure 6

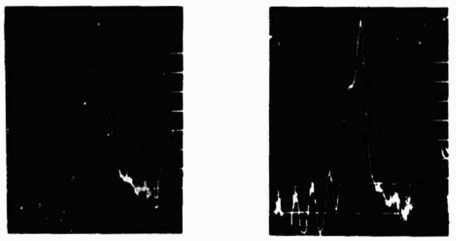

3000 G FULL SCALE
1 MS/DIVISION
3000 G – 2.5 MS

4000 G FULL SCALE
1 MS/DIVISION
4000 G–2 MS

Figure 7

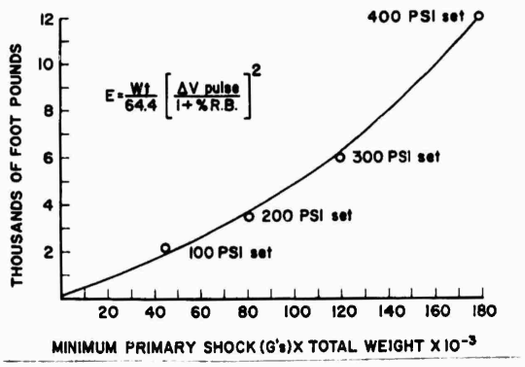

Figure 8

PRE-SHOCK AND POST-SHOCK ACCELERATIONS

In most instances pre-shock and post-shock acceleration (of the machine to the specimen) is limited to 20 percent of the primary shock. Post-shock acceleration of the "Reverse Hyge" is minimized by contact of the specimen carriage on the impact material. The primary shock pulse must be five times as great as the machine's pre-shock. At maximum operating pressures, the combined weight of the piston, shaft, and specimen carriage (60 pounds) reached a pre-shock acceleration of 600 g. Therefore, the minimum shock pulse for 60 pounds at maximum pressures would be 3000 g. Reference can be made to Fig. 8 to determine the minimum primary shock on the total accelerated weight that would be five times the machine's pre-shock acceleration.

THE MODIFICATIONS

The specimen carriage has a flat striking surface of area sufficient to support expansion of the impact material. An impact plate bolted on top of the Hyge cap plate also serves as expansion support. A shaft extension connecting the specimen-carriage to the Hyge shaft is used to maintain the desired stroke length by adjusting for differences in material height. The orifice plate opening and piston seal are sized for a fire pressure ratio of 5 to 1. The piston seal is fabricated from 1/8-inch teflon sheet, and bolts into the face of the piston. Reliefs machined on top and bottom surfaces of the teflon form the sealing surface.

CONCLUSION

Continued use of the Reverse Hyge has shown its shock repeatability to be better than ±10 percent of the desired level. Pulse distortion, as seen on photographs displaying shock capabilities, will be decreased by designing a lighter piston.

At maximum operating pressures, a triangular shock pulse of 4600 g at 2 milliseconds was recorded. Efforts to increase the machine's capability (high g, shorter pulse) will include the investigation of high impact strength plastic as a source of shock pulse control.

* * *

SIMULATING FLIGHT ENVIRONMENT SHOCK ON AN ELECTRODYNAMIC SHAKER

G. W. Painter and H. J. Parry
Lockheed-California Company
Burbank, California

A program to develop a method to produce oscillatory acceleration transients with adjustable shock spectra will be described. Using this method, a wide range of pulse conditions can be accommodated including an "average" or "data envelope" type pulse. The equipment used and some results of the experimental program to date will be discussed.

INTRODUCTION

Laboratory environmental shock testing generally involves subjecting equipment to a motion-time transient that approximates some well known classical pulse shape. Typical examples are the half-sine and saw-tooth acceleration pulses. These test pulses generally bear little resemblance to the complex transients that are experienced in the operating environment. Their amplitude and duration are generally so chosen as to produce a shock spectrum that is, at all frequencies, in excess of that associated with transients measured during operation. Since the pulse shape fixes the shape of the response spectrum, the test engineer must accept spectral magnitudes at some frequencies that are considerably in excess of operational levels. Furthermore, it is usually not possible to ameliorate the distortion introduced by the dynamic response of the test fixture.

Shock testing is usually accomplished by drop testing or by impacting the equipment with a moving mass. In recent years increased attention has been given to the use of electrodynamic shake tables for applying the desired test transient. These efforts have accompanied the production of large shakers and electronic amplifiers and have arisen not only from a desire to allow greater flexibility in controlling the magnitude and duration of the test pulse, but also from a consideration of the potential cost reduction that could be realized if the same machine could be used for both shock and vibration testing. For the most part, the use of electrodynamic shakers has been confined to the production of approximate classical time functions such as the half-sine.

Recently, Schwabe[1] described a method for generating arbitrary voltage transients and then producing corresponding acceleration-time transients on a shake table with minor distortion. Although the transients described were, at least in a practical sense, confined to the generation of relatively simple oscillatory acceleration-time patterns, the results were sufficiently encouraging to suggest further work. It was decided to explore other possibilities for shake table shock testing, placing particular emphasis upon the production of motion-time transients that would have arbitrarily defined shock spectra.

SHOCK AND FOURIER SPECTRA

Although a peak response (shock) spectrum can be derived from a given time function, the inverse operation of deriving a time function from the shock spectrum cannot be carried out. There does exist a unique relationship between the complex Fourier spectrum and its associated time function. Furthermore, a linear relationship exists between the undamped residual shock spectrum and the absolute Fourier spectrum. As a result of these considerations, initial attention was given to the problem of finding a

[1] H. Schwabe, "An Approach to Polaris Flight Shock Simulation by Electrodynamic Shaker," Shock, Vibration, and Associated Environments, Bull. No. 31, Part II (Mar. 1963), pp. 144-163.

time function whose absolute Fourier transform (and hence, whose undamped residual shock spectrum) would approximate a desired shape and magnitude. The absolute Fourier spectrum contains no phase angle information, and there are an infinite number of time functions associated with a given, absolute Fourier spectrum. Nevertheless, once the absolute Fourier spectrum has been specified, the phase angle variation cannot be arbitrarily selected. Indeed it can be shown that if the Laplace transform of the time function is "minimum-phase" (i.e., no zeros exist in the right-hand plane), the phase angle variation is entirely dependent upon the absolute Fourier spectrum. These matters fall within the field of circuit synthesis and although of considerable importance lie beyond the scope of this paper.

Although by analytical methods it would have been possible to derive any number of time functions that would satisfy a given absolute Fourier spectrum, it was of practical necessity to provide a method which would permit the test equipment operator to rely upon instrumentation alone for deriving and producing a required acceleration transient.

It will be shown that the method developed not only provides for the generation of time transients whose absolute Fourier transform approximates a desired value, but is also suited to the generation of complex transients that will yield a close approximation of desired damped shock spectra patterns.

TIME FUNCTION SYNTHESIS

If the complex Fourier transform $F(j\omega)$ is specified, its associated time function $f(t)$ is given by the relation:

$$f(t) = \frac{1}{2\pi} \int_{-\infty}^{+\infty} F(j\omega) \exp(j\omega t)\, d\omega. \qquad (1)$$

It can also be shown that when a system, whose transfer function is given by $F(j\omega)$ is subjected to a unit impulse, the resulting response transient will be $f(t)$. It is this relationship, which follows directly from Eq. 1, that forms the basis for the transient synthesis method that was devised.

The foregoing suggests that if an electrical network can be synthesized whose absolute transfer function, $F(\omega)$, adequately approximates a desired value, the corresponding voltage response transient (representing $f(t)$) can be generated by applying a voltage pulse of very short duration to the network imput. Such a procedure would be quite difficult if one were to attempt to construct electrical networks analogous to complex structures. In practice, however, the dynamic response characteristics of structures should be viewed as requiring a statistical description rather than an exact one. This observation becomes increasingly true at higher frequencies where the response characteristics are dominated by local resonances.

There are several simple Fourier spectrum contours that are of general interest. Three such forms that might be considered are exemplified by low-pass, high-pass, and band-pass filters. Voltage transients derived from a selection of band pass filters by applying a unit impulse to their input terminals are given in Fig. 1. Up to this point the discussion of time function synthesis rests upon a firm analytical base. The objective of the program, however, was to synthesize motion transients on a shake table whose shock spectra would approximate certain arbitrary patterns. The method devised,

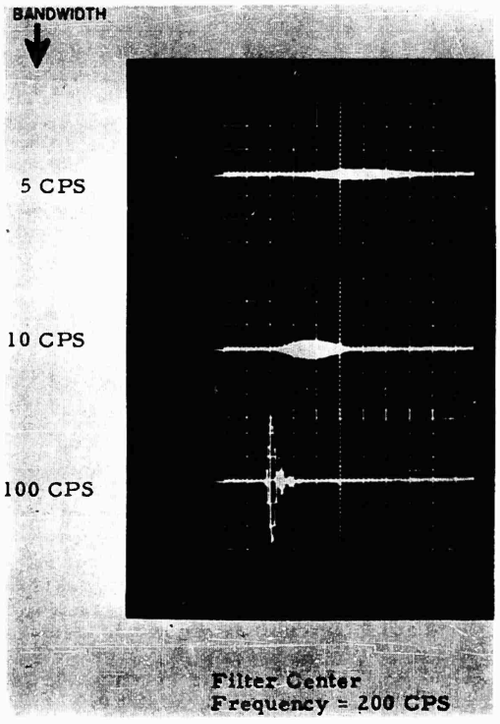

Fig. 1 - Transient responses of band-pass filters excited by a short voltage pulse

although suggested by the relation between the Fourier transform and its corresponding representation in the time domain, was actually derived empirically. It will be shown that the transient synthesis method developed is quite analogous to the procedures followed in shaping the power spectral density function associated with random vibration.

Most readers will be familiar with the upper schematic diagram given in Fig. 2 which shows the generating, compensating, shaping, and readout operations involved in random vibration testing. The "white" noise generator has a power spectral density which is essentially constant over the frequency range of interest. Undesirable variations in the total system transfer function are corrected by employing various compensation filters. Shaping of the power spectral density is accomplished by adjusting shaping filters while monitoring that portion of the mean square signal that passes through a narrow-band analyzer. A schematic representation of the shock transient synthesis method is given in the other schematic of Fig. 2. The "generating source" is a voltage pulse generator. The pulse produced is sufficiently short (100 microseconds) to have an associated Fourier transform which is virtually flat from zero to above 2000 cps. (It is useful to note that the spectral representations of the unit impulse and white noise are both constant over an infinite frequency range.) The voltage pulse is applied to a network of compensating and shaping filters, an operation which closely parallels the procedure followed in random vibration testing. The table motion transient is sensed by an accelerometer whose output signal is fed to a shock spectrum analyzer that was developed during the course of the program. This analyzer employs operational amplifiers and can be considered to be a special purpose analog computer. The Q of the analyzer is continuously adjustable in an interval of 5 to 50. Once selected, Q remains constant as the resonance of "sampling" frequency is adjusted. This frequency is continuously variable in an interval from 20 to 2000 cps. A study of Fig. 3 will show that the transfer function of the shock spectrum filter has a value of unity (zero db) at zero frequency. It follows, that although the filter output will be most sensitive to those spectral components of the input transient that fall in the vicinity of the sampling frequency, it will also be affected somewhat by all of the spectral components that lie below the sampling frequency. The damped shock spectrum analyzer is, therefore, seen to differ in this respect from the narrow-band

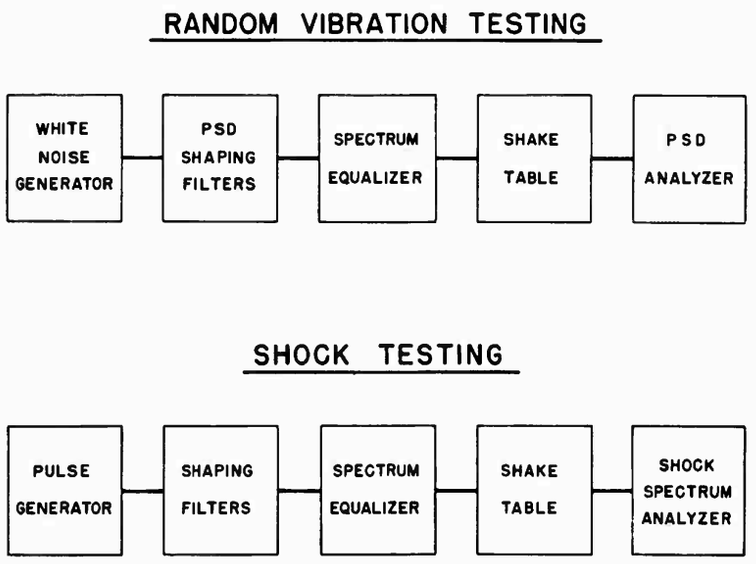

Fig. 2 - Power spectrum and shock spectrum synthesis

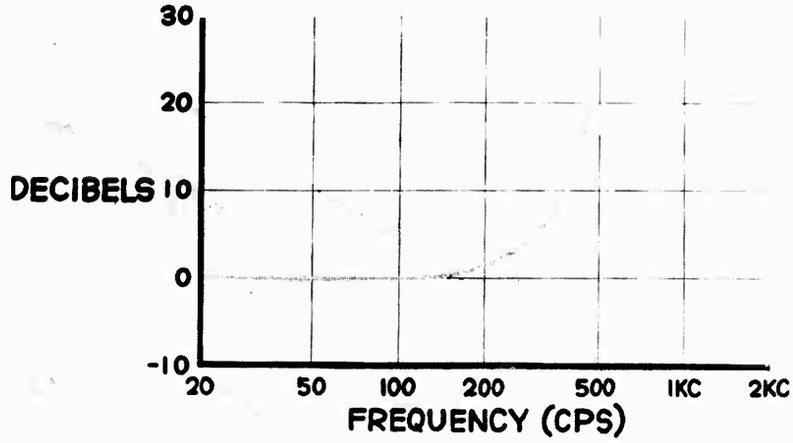

Fig. 3 - Constant "Q" analyzer forward transfer function, Q = 10

filter-analyzer employed in random vibration testing. In the latter case the energy passing through the filter is confined virtually only to those frequency components that lie in the immediate vicinity of the center frequency.

TRANSIENT SYNTHESIS PROCEDURE

Shock transients are produced with the present system by the following procedure:

The shaker system is first equalized by the familiar techniques used in random vibration testing. An array of 1/3-octave band shaping filters is then introduced into the system. The input terminals of all the 1/3-octave band filters are subjected simultaneously, at periodic intervals, to a voltage pulse from the pulse generator. The output transients from all of the filters are fed to a summing amplifier whose output is in-turn passed to the shock spectrum analyzer. Separate gain controls are provided for each of the 1/3-octave band shaping filters. As mentioned above, the output of the shock spectrum analyzer is affected by all frequencies that fall below the sampling frequency but very little by higher frequencies. For this reason transient synthesis involves a "building block" process. The lowest frequency components are introduced first, and high frequencies are added sequentially. Synthesis is accomplished by first reducing all filter gain controls, except for the one associated with the lowest band, to zero. With the frequency of the shock spectrum analyzer set at the center frequency of the first 1/3-octave band, the gain of the latter is adjusted until the peak response of the analyzer, as indicated on an oscilloscope, has the desired magnitude. The same procedure is followed as higher and higher 1/3-octave bands are introduced until the acceleration transient produces the required shock spectrum envelope over the entire frequency range of interest.

The choice of 1/3-octave band filters for shaping the table transient was an arbitrary one. The shock spectra envelopes which were to be duplicated were generally rather smooth, containing no sharp peaks or notches. The production of transients with jagged spectra would require shaping filters of narrower bandwidth. Sharp deviations in shock spectra which might arise from narrow peaks and notches tend to become increasingly subdued as the Q of the spectrum analyzer is decreased. In the majority of cases the Q of the analyzer was set at 10, a value that previously had been employed in deriving the shock spectra associated with transients measured in flight.

EVALUATION OF THE SHOCK TRANSIENT SYNTHESIS METHOD

The development of the transient synthesis method can be divided into three phases. In the first phase no shake table was involved, and the total system consisted of the pulse generator, 1/3-octave band shaping filters, summing amplifier, the shock spectrum analyzer, and an oscilloscope. The voltage transient produced at the output terminals of the summing amplifiers was considered to represent an acceleration

signal. The capability for shaping a voltage transient whose shock spectrum approximates a desired pattern is indicated in Figs. 4 and 5, where the desired spectra are based on transients recorded during Polaris operation. The agreement between the desired and produced spectra is seen to be very good. A photograph of the voltage transients associated with the spectra given by Fig. 4 is shown in Fig. 6. The absolute Fourier spectrum for the same transient is given in Fig. 7. During the next phase of the development, a small calibrating shaker with an accelerometer attached to the table was introduced, and the acceleration transient was shaped to yield the desired spectra. These efforts also were successful and we proceeded to evaluate the capability for producing desired transients in typical hardware mounted on a full scale electromagnetic shaker.

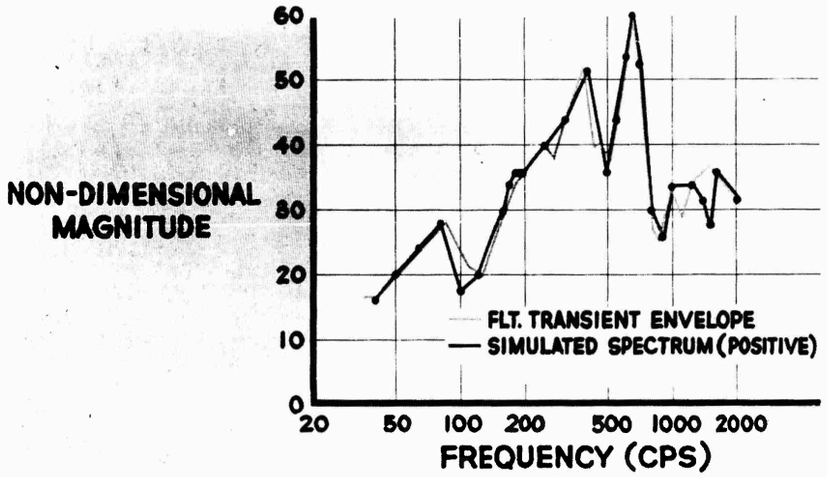

Fig. 4 - Simulated shock spectrum, positive

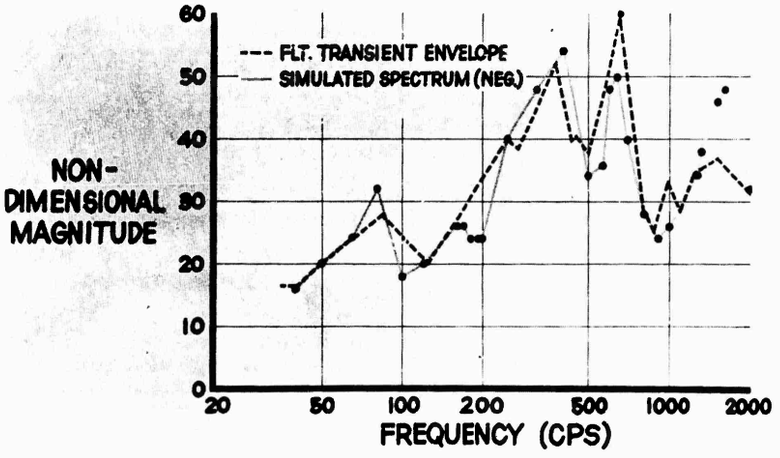

Fig. 5 - Simulated shock spectrum, negative

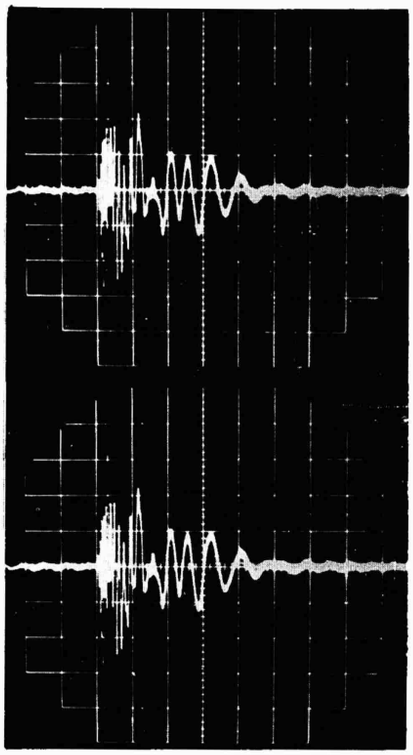

Fig. 6 - Simulated pulses

This final phase of the program was carried out using a table having an output vector force of 5000 pounds. The hardware attached to the table consisted of a test fixture weighing approximately 50 pounds whose configuration is shown in Fig. 8. An accelerometer was attached on the fixture near the end of the overhanging section, as shown in the photo. The response function indicated by the accelerometer involved a multitude of sharp resonances and anti-resonances. A comparison of the system transfer function before and after equilization is given by Figs. 9 and 10, respectively. The shock spectrum derived from the transient that was synthesized is shown in Fig. 11. This spectrum obtained is seen to be in close agreement with that required. An interesting fact associated with the synthesized pulses is that as the effective bandwidth of the shock transient increases, the ratio of the peak acceleration of the shock spectrum to the peak acceleration (magnification ratio) of the transient decreases. The transients that produced the shock spectra shown in Figs. 4 and 11 had rather broadband Fourier spectra and the associated pulse to spectrum magnification ratio, based on a Q of 10, was approximately 3. This compares with theoretical values of 1.6 and 1.9 for the half-sine pulse and unit step, respectively. The transient produced by ringing a single 1/3-octave-band filter with a unit impulse gives a magnification ratio of approximately 6. For the spectrum shape shown in Fig. 11 and total table equipment weight of 50 pounds, it was possible to produce transients whose peak acceleration spectrum was 300 g.

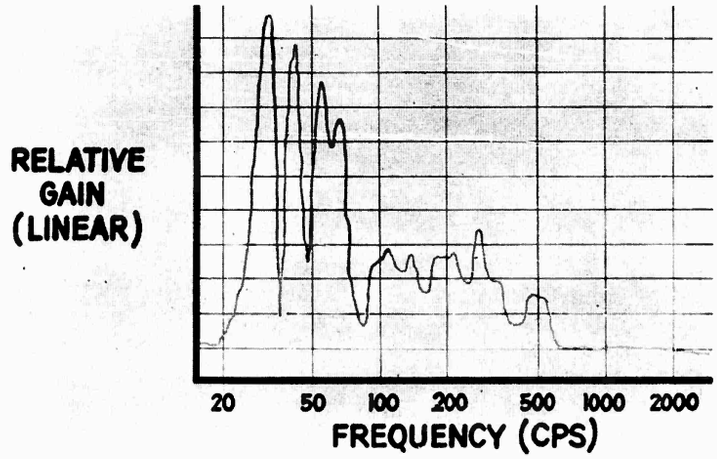

Fig. 7 - Absolute Fourier spectrum of transient shown in Fig. 5

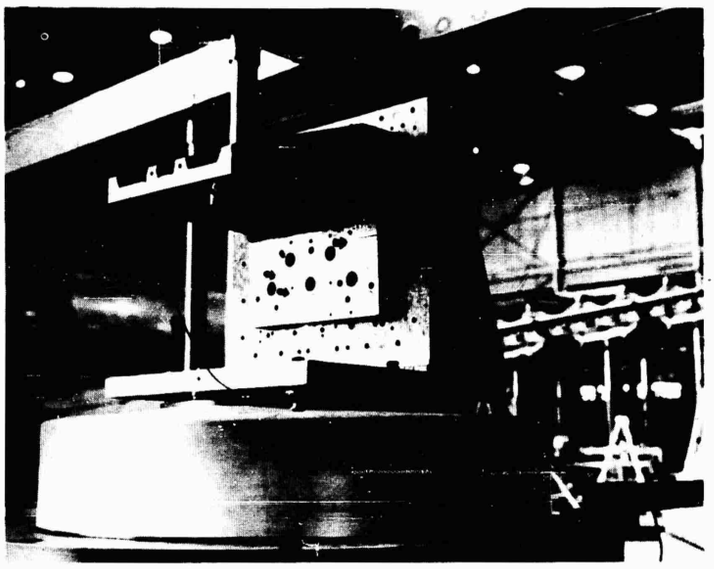

Fig. 8 - Cantilever beam fixture

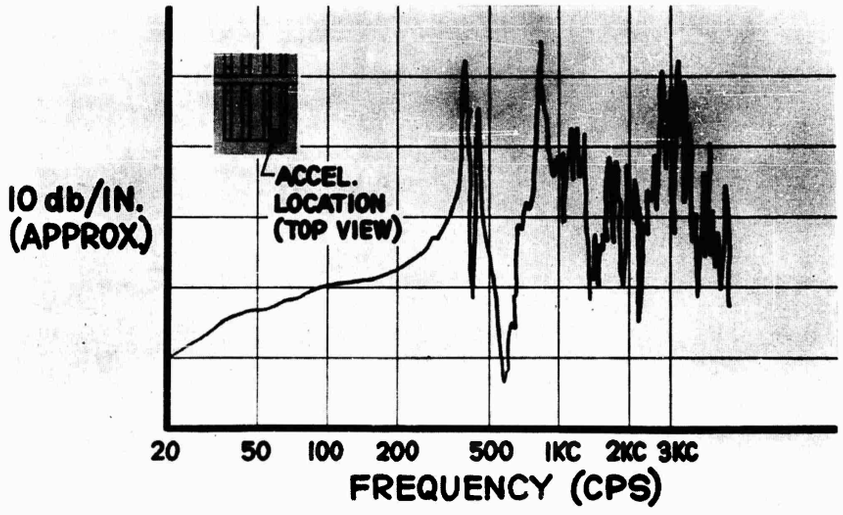

Fig. 9 - Fixture response, no equalization

These levels were achieved with a 5000 pound vector force table.

The peak table displacement is controlled largely by the spectrum level required at low frequencies. The displacement limitations were not remotely approached with the transients reported here, since the spectral pattern to be produced had negligible values below 40 cps.

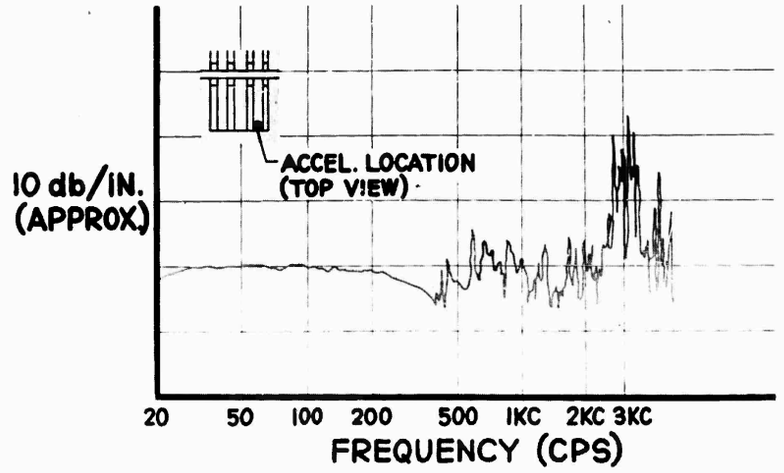

Fig. 10 - Fixture response, with equalization

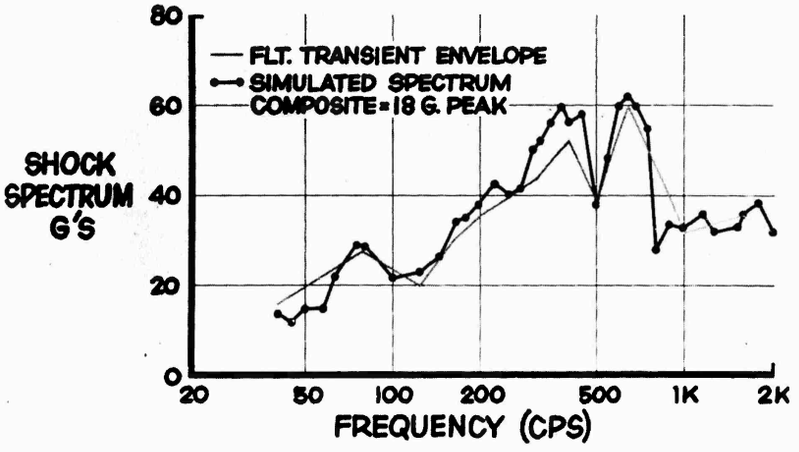

Fig. 11 - Shock spectrum obtained with cantilever beam fixture

NONLINEAR EFFECTS

From the standpoints of both time and economics, it is highly desirable to synthesize the shape of the shock transient at low acceleration levels, and then increase the gain to give the required acceleration level for the actual shock test. This procedure eliminates the need for employing a dummy table load during the transient shaping operation, since the levels involved during shaping could hopefully be low enough to avoid the possibility of prior damage to the hardware to be tested. The success of this plan requires that the system be reasonably linear.

In order to examine the effect of possible nonlinear response upon the shock spectrum, transients were synthesized at low peak acceleration and then increased to a much higher level while leaving the shaping filter settings unchanged. The results obtained are shown in Figs. 12 and 13. In the former case the equipment shown in Fig. 14 was attached to the table while in the latter case the cantilever beam

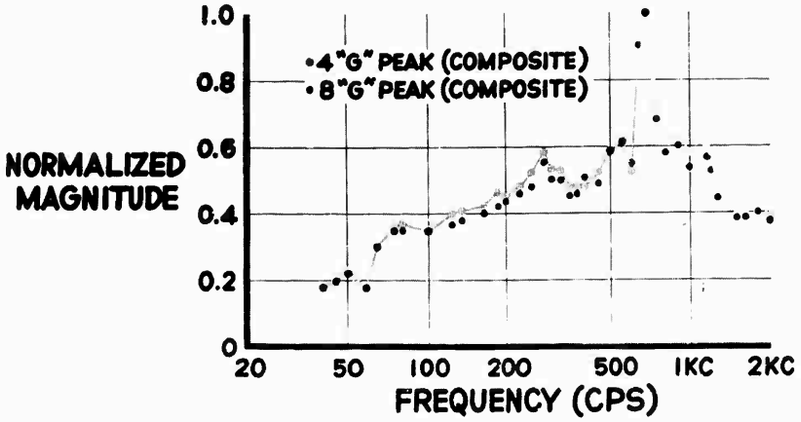

Fig. 12 - Normalized shock spectra at two different levels

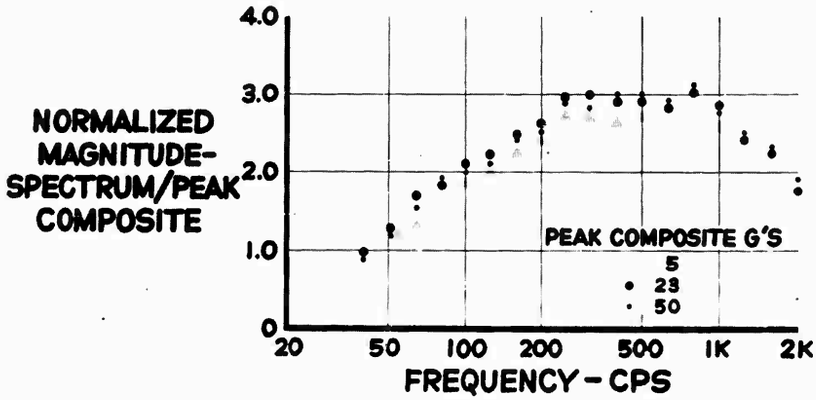

Fig. 13 - Measured data book spectra comparison

fixture, Fig. 8, was attached. In both cases the spectrum shape is seen to be virtually independent of the acceleration level of the transient. Since the equipments chosen to load the table are typical of most types that are encountered in environmental shock testing, it appears reasonable to expect that nonlinear response generally will present no problem.

CONCLUSION

At the time of this writing all development efforts have been confined to the generation of acceleration transients that will produce a specified damped acceleration shock spectrum envelope based on a Q of 10. The spectrum patterns involved have been relatively smooth since they were based on a large number of tests. The transient synthesis technique that has been described is by no means confined to spectral patterns of the type that have been described, however. Indeed, if an adequate supply of shaping filters were available, there appears to be virtually no limit to synthesis capabilities. It might be desired, under certain circumstances, for instance, to simulate transients that involve prolonged ringing at certain frequencies, so as to simulate the behavior of a lightly damped structure vibrating in its normal modes. These could be realized readily by employing narrow band peak-notch or second order filters as shaping devices.

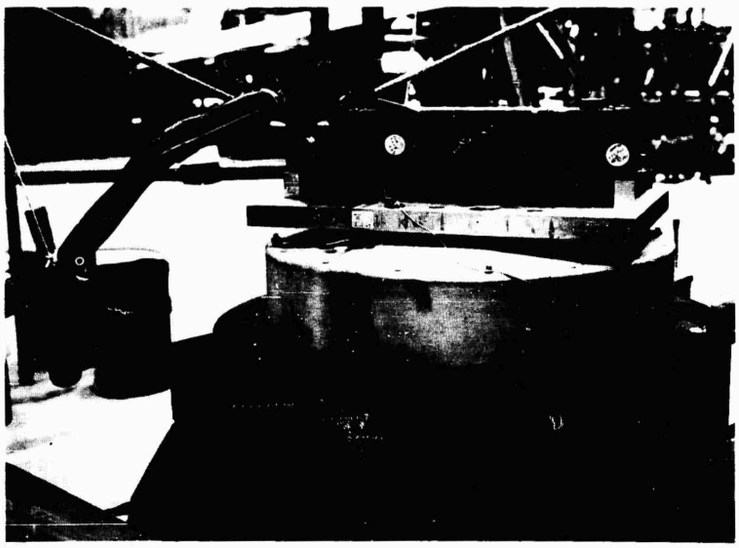

Fig. 14 - Interlocks I

Although the primary development effort has been directed at producing transients that will provide a specified shock spectrum, it should be remembered that the method is equally well suited to the simulation of the absolute Fourier spectra. Actually, in some cases, it may be more desirable to design the transient to yield a specified Fourier spectrum, since this spectrum provides a considerably better description of structural response than damped shock spectra.

The test method described has been found to be highly practical and entirely compatible with commercially available shake table systems. Its advantages, when compared to conventional methods, are as follows:

1. Shock tests can be conducted with the same test machine employed in vibration testing.

2. The transient can be shaped to provide a close approximation of the desired shock spectrum.

3. Non-representative oscillations peculiar to fixture design can, if desired, be practically eliminated.

4. The high velocity change, associated with drop testing, can often impose unrealistic loads upon components having a low natural frequency. The new method can eliminate this problem.

5. In tests that employ classical unidirectional pulses, the severity of the test specification derived is greatly dependent upon the Q value that is assumed for the hypothetical resonators in deriving shock spectra from flight transients. The choice of Q becomes less critical when oscillatory test transients are synthesized to yield damped spectra based on the same Q value used in determining the shock spectra of transients recorded in flight.

6. It appears that the method can be extended to simulate desired three-dimensional spectral envelopes.

7. Positive and negative spectra are virtually identical, eliminating the need for changing equipment orientation.

Further developmental work will be required to realize the full potential of the method.

ACKNOWLEDGMENT

The development that has been described is part of a BuWeps project assigned by the PMS Division of the Lockheed Missiles and Space Company. The authors gratefully acknowledge the support and encouragement provided by K. Kuoppamaki and J. E. Barkham of the Lockheed Missiles and Space Company.

Mr. Campbell: I'm sure there will be questions from those who are curious about what this does to the vibration machine after repeated shock.

Mr. Painter: I can only comment that we haven't broken ours yet. I might add that we get sort of a bonus here as far as the amount of shock spectrum that you get for a given peak amplitude. If one has a half-sine wave, the ratio of the maximum shock spectrum amplitude to the amplitude of the sine wave is about 1.8:1. For the spectrum I showed here, it is about 3:1. If one is simulating a very narrow band phenomenon it can approach 10:1, if you are using a Q of 10 for the spectral analysis. The fact that you do have more wiggles gives you a higher ratio of shock spectrum to the peak transient.

Mr. Bogdanoff (Midwest Applied Science): This was a very interesting paper, Mr. Painter. Have you considered the possibility of detecting nonlinearities in mechanical systems by this technique?

Mr. Painter: No, we have not. I would think that if one wanted to do that, he could do better with a sinusoidal excitation.

Mr. Mahaffey (Chance Vought Corp): You mentioned that you induced a pulse which you then shaped. What was the shape of the original pulse that you started with?

Mr. Painter: This pulse was essentially rectangular with a duration of about 100 microseconds. The important thing is that it have enough magnitude to make your signal-to-noise ratio as high as possible, and that it be short enough so that its Fourier transform doesn't fall off very much within the frequency range of interest. Now a hundred microseconds of pulse doesn't start falling off very much until you get above 2000 cps. This was the range we covered and if we wanted to go higher than that we would have used an even shorter pulse.

Dr. Vigness (NRL): This method will be particularly useful and suitable when you have an opportunity to get into your missile or whatever it might be and make measurements which you can analyze in terms of shock spectra with the equipment actually in place. Otherwise, there really isn't any advantage of having a nice detailed shock spectrum, because they vary so much from one point or condition to another. I would like to ask one question, though. This technique is used on an electro-dynamic shaker where the clearances are quite limited. Could you give some idea as to what problems you might run into there?

Mr. Painter: We have run into no problem at all of this sort in the case of the particular transient that we were producing because the spectrum requirements tapered off and at 40 cps they were quite low. We haven't had the problems that may result from trying to produce half-sine waves on shakers. There, of course, if you have a pulse of fairly long duration and high amplitude, a high velocity is developed that you have to get rid of, and this requires a very large displacement amplitude available on the shaker. But, if the spectrum requirements in the low frequency regions are not too great, it is not injurious to use this technique with conventional shakers. In this case, we didn't come close to approaching the limitations of the Ling shaker.

Mr. Stewart (Douglas): You mentioned duplicating absolute Fourier spectra so frequently that I think you gave the impression that it is reasonable to duplicate measured Fourier spectra. You didn't mean to do that, did you?

Mr. Painter: I didn't mean to imply that. I think, however, that if one could ever state with certainty that he has one and only one transient that he ever encounters in service, it would be very reasonable to do this. I do not think the fact that phase relationships are not necessarily the same would constitute a problem. It is interesting to note that there is a relationship between a residual shock spectrum and the absolute Fourier spectrum, and that relationship says nothing about phase. Apparently one can have a great number of phase relationships and still have the residual and absolute Fourier spectra directly related. But, of course, the phase would affect total shock spectra.

Dr. Curtis (Hughes Aircraft): It is customary to compute spectra with a Q somewhat higher than 10. Do you have any feel for the ability to reproduce and match a desired spectrum for Q's, lets say, up to a hundred?

Mr. Painter: We have tried this technique with a Q of 50. That is as high as our analyzer would go. I think we could probably increase it, but we haven't made the effort. With regard to what is conventional, some of you may recall a questionaire that was sent out by the SAE G-5.7 subcommittee on shock in which we asked what Q's were in use by different people. I don't

know how many of you read the summary, but it was published in some of the minutes. It turned out that more people, for some reason or other, seem to prefer a Q of 10 than any other Q. This is something on which I do not think there has been any standardization. Everybody has his own opinion as to what Q should be. The reason we used a Q of 10 here was because this was the value that was used in deriving the spectra from Polaris flights.

* * *

DYNAMIC MOORING TESTS OF ONE-QUARTER SCALE MODELS OF THE GEMINI AND AGENA SPACECRAFT

N. E. Stamm and L. A. Priem
McDonnell Aircraft Corporation

One phase of the NASA-Gemini space program is the rendezvous and mooring of the earth orbiting Gemini and Agena-D spacecraft. The McDonnell Structures Laboratory simulated the mooring portion of this program using 1/4-scale models of the spacecraft suspended from "zero spring rate" support systems.

Some of the problems which evolved from this test included the design and fabrication of dynamically scaled models, development of "zero-g" suspension systems, and control of the relative model attitudes and velocities at impact.

The 1/4-scale mooring test provided data which substantiated initial design concepts and established mooring parameters which must be maintained for a successful mooring of the two spacecraft.

INTRODUCTION

One phase of the NASA-Gemini space program is the rendezvous and mooring of the McDonnell built Gemini spacecraft and the Lockheed built Agena-D target vehicle equipped with a McDonnell mooring adapter. The mooring adapter on the Agena is basically a receiving cone mounted on shock absorbers which guide the rendezvous section of the Gemini spacecraft into the required position for latching the two vehicles together.

The McDonnell Structures Laboratory conducted a dynamic mooring test program using 1/4-dynamically-scaled test vehicles. The purpose of this program was to:

1. Determine the stability of the shock absorbing modes.

2. Determine the maximum impact loads in various structural components.

3. Determine the performance of the latching mechanism.

4. Determine the limiting relative velocities and alignments which insure proper "latch-up."

DESIGN AND CONSTRUCTION

Scale factors furnished by the McDonnell Structural Dynamics Department were applied to the models during their design to insure that the test was dynamically correct and the data obtained could be converted and applied to the full-scale spacecraft. The rigid body mass of each model was assigned to be 1/100 scale to facilitate testing, instead of 1/64 which would have been the scale factor if all the model components were 1/4 the size and constructed of the same material. This presented the problem of fabricating a structure strong enough to withstand the impact loads and still capable of meeting the weight requirements. Also, the calculated scale factor for the three axes mass moment of inertia was 1/1600 which meant the structural mass had to be concentrated fairly close to the center of gravity to obtain the proper inertia values. The Agena model, which had a very small value of roll inertia, had to be designed so that its weight could be changed considerably without an appreciable change in the roll inertia. The proper values of weight and inertia were obtained by thin-walled tubular construction with movable ballast. The inner mold lines of the mooring cone and outer mold lines of the Gemini rendezvous section were

geometrically scaled down from the full-size prototypes. The mold lines of the remainder of the models were not maintained. The surfaces of the Agena and the Gemini models which contacted one another during mooring were constructed of the same material used in the full-scale configurations.

At the base of the Agena mooring cone, three equally spaced spring-loaded latches drop into recesses in the rendezvous section of the Gemini when the Gemini bottoms on the cone stops. The latches and recesses are properly positioned for engagement by guiding an indexing bar on the Gemini nose with a roll slot in the mooring cone. The spring constants and geometry of these latches were scaled from the full-size prototypes.

One of the more interesting design problems in the construction of the models was the hydraulic shock absorbers (dampers) which attach the mooring cone to the Agena. Seven dampers dissipate energy associated with relative vehicle longitudinal, lateral, and rolling motion. In the full-scale prototype spacecraft, the dampers are attached with mono-ball type fittings which were impractical in the model design because of the size limitations. A ball and socket type fitting was used to secure the dampers on the model which established single point pivots and maintained small size. Four semiconductor strain gages were bonded to the damper end fitting shafts in order that damper loads could be recorded. A microscope was employed in the placement of the strain gages on the shafts since the shafts were only 1/8 inch in diameter. To insure that the mooring cone will always be in the extended position prior to impact with the Gemini spacecraft, four dampers contain preloaded compression springs. The orifice area varies with stroke on the dampers without springs and a constant orifice area is maintained on the dampers containing springs. To prevent the two spacecraft from rebounding due to the energy stored in the damper springs, very small return orifices are provided on these dampers. Since the compressed lengths of the model dampers ranged from 3 to 1-7/8 inches, it was difficult to design dampers which had the proper operating characteristics and still be geometrically scaled in length and stroke from the full-size dampers. For the dampers requiring smaller return orifices, a check ball was used to close off most of the compression orifice area. The variable orifice was obtained by a fixed tapered metering pin which fits into an orifice in the piston. Friction was the biggest problem involved in obtaining damper performance which matched scaled theoretical prototype curves, since the scale factor for frictional forces was 1/25. All contacting moving parts had to be highly polished to close tolerances. Each damper was calibrated individually and the orifice modified until the desired operating characteristics were obtained. Calibration was performed by impacting the damper with a specific mass at a known velocity and recording the damper load and stroke versus time.

Since this test was to simulate a maneuver which takes place between earth orbiting vehicles, it was desirable that the models be free to move linearly and angularly in any direction with minimum friction. This was accomplished by supporting each model with a 30-foot long cable which was connected to a spring suspension system that effectively provided a zero spring rate about the equilibrium position. The supporting cable was attached at the center of gravity of the model to an arrangement of gimbles which allowed rotational freedom. The spring suspension system design was based on information obtained from W. G. Molyneux.[1] The suspension system was basically a model support spring connected to two lateral rods each in compression from a tension spring. As the model's center of gravity moved up or down during mooring, the compressive forces in the rods canceled the change in the force exerted by the support spring thereby producing a zero spring rate about the equilibrium position. The friction in the system amounted to only about 0.06 pound.

TEST SETUP AND PROCEDURE

The models were properly positioned to give the desired relative impact attitudes, and each pulled back an equal distance from the impact point, based on pendulum geometry, and simultaneously released to obtain the desired relative impact velocities. (See Fig. 1.) The maximum relative impact velocity was only 1.58 feet per second and the small amount of centrifugal force caused by this velocity was counteracted by the frictional forces in the suspension system. The spring suspension systems were each positioned so the cable pivot point was directly over the model's center of gravity in the latched position. A surveyer's transit was used to check each model's attitude and relative position prior to release. A variety of combinations of relative velocities, attitudes, and cone impact points were tested to establish parameter envelopes which insure vehicle "latch-up."

---

[1] W. G. Molyneux, "Supports for Vibration Isolation," Royal Aircraft Establishment Technical Note No. Structures 211.

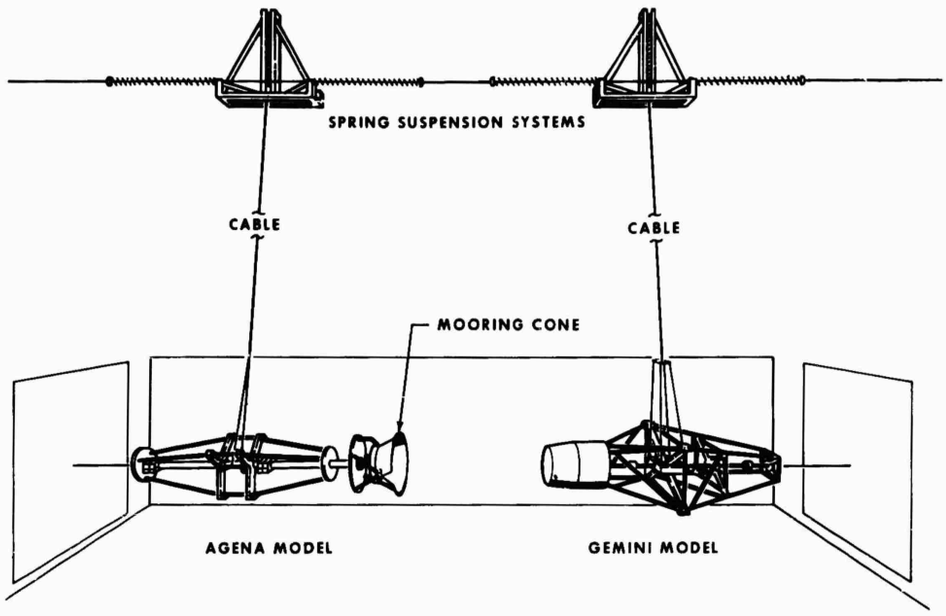

Fig. 1 - Gemini mooring test setup, 1/4-scale model

An interesting problem developed during the test because the models were very free to rotate in any direction about their centers of gravity. Small air currents within the building caused the models to move before they were released, which made it almost impossible to obtain the desired impact conditions. Even if someone would walk close to the models or large banks of movie lights were turned on, the air disturbance caused model movement. This problem was essentially eliminated by enclosing the area around the models with a clear plastic tent.

Each model was instrumentated with six linear accelerometers which were used to determine the linear and angular accelerations at the model's center of gravity during mooring. Axial loads were also recorded for selected dampers. Regular and high-speed movies were taken to study the motion of the dampers, latches, and mooring cone, and to give a visual history of the attitudes of each model.

RESULTS

The dynamic model mooring test effectively simulated the orbital mooring of the Gemini spacecraft and Agena booster. The orbital condition of the vehicles was realistically duplicated by the spring suspension systems. The tests confirmed the basic design of the full-scale mooring system since the mooring loads were within the design values, and no undesirable modes of damper collapse were found. Limiting envelopes of relative vehicle attitudes and velocities at impact were established that insure proper "latch-up." The 1/4-scale mooring test provided data which substantiated initial design concepts and established mooring parameters which must be maintained for a successful mooring of the Agena booster and Gemini spacecraft.

* * *

Section 3
VIBRATION TESTING

PROBLEMS AND CONSIDERATIONS IN COMBINING SINE AND RANDOM VIBRATION IN THE ENVIRONMENTAL TEST LABORATORY

A. R. Pelletier
Radio Corporation of America

Four basic conditions or requirements must be considered when sweeping sine and random signals are combined into one vibration test environment. Each of the four conditions will be discussed in detail as to problems, advantages and disadvantages, and the necessity and justifications to impose each requirement.

INTRODUCTION

With the advent of manned space systems and the associated high reliability requirements, the laboratory vibration test equipments, requirements, and techniques have evolved from the relatively crude sinusoidal testing methods of recent years, to the application of test equipments and procedures relating to complex random vibration. In fact, the test engineers and technicians have just begun to thoroughly familiarize themselves with the complexities and limitations associated with the relatively inf ntile random vibration systems and techniques, wherein the testing approach and philosophy are rapidly advancing to a high degree of sophistication.

In many instances, the sinusoidal and random tests which are ordinarily performed either singularly or sequentially, are no longer considered adequate to assure the degree of required reliability. A combination or weighted mixture of sine and random vibration into one environmental test stimulus is at least a desired, if not as yet a specified, requirement on space systems and subsystems. The ultimate goal of the sine-random combination is an increase in reliability, based upon a closer approximation of the actual vibration environment. In many instances, however, the intent can be partially or even totally defeated, and the application of the sine-random combination can produce unwarranted and deleterious effects on the test specimen.

As an example, a dangerous situation can develop if equipment malfunction is induced by overtesting. Although the cost and time involved in failures caused by overtests, which are incorrectly assumed to be legitimate failures, could be staggering, these do not constitute the greatest reliability danger; the ultimate in damage is the result of assuming the reliability of an item which successfully survives an undertest. These overtests and undertests can go entirely unnoticed, especially on complex multiple-degree-of-freedom systems, when new or relatively untried complex test techniques and equipment are applied indiscriminately, or without detail consideration of all aspects of the procedure.

Combining a sweeping sinusoidal signal and a shaped random signal for vibration test in the laboratory poses severe problems and require special considerations heretofore unnecessary, but which must now be recognized and dealt with. The interaction between the sine and the random in the areas of control, shaping, and especially shaker equalization procedures, should receive careful and detail consideration. In some instances, such as in tests performed on small components with relatively few degrees-of-freedom, the crosstalk or interaction phenomena between the sine and random

excitations is non-existent or negligible and can usually be discounted. There exists an extreme danger, however, of damaging interaction between the sine and random signals when applied on the subsystem and systems level because of the inherent multiple-degree-of-freedoms of the systems and the associated frequency coupling.

There are several methods and procedures used in the test industry to combine sine and random vibration into one environmental test stimulus. The method to be chosen, however, is often dictated by several relatively uncontrollable factors such as the availability of complex and costly test and control equipment, program schedule and available test time. A major consideration involves the shaker equalization procedures and associated equipment, and the specified test levels and spectrum of both the sine and random environments. The sine-random mixing procedures and equipments which are presently available for combining sine and random vibration, do not possess all the desired and optimum features and characteristics. The choice of procedure necessarily involves a compromise and tradeoff. Careful study and deliberate consideration of all aspects such as test objectives, type of test, levels and spectrum of the sine and random signals, test equipment availability, capability, and limitations, are all required to optimize the choice of test method.

Since no single method will meet all the desired features of equalization, shaping, mixing, and so on, the procedure which most closely approaches all the optimum conditions and features, as applicable to a specific test, must be determined and used.

There are four basic conditions, which although considered idealistic, must be considered when sine and random signals are combined into one vibration environment in the laboratory. The implication associated with the term "idealistic" is not that the satisfaction of these optimum features is impossible or that all vibration test problems can be resolved by meeting the four idealistic conditions, but that the total satisfaction of these optimum features would increase the testing reliability to a large degree. The four conditions are as follows:

1. performing sine and random equalization at test levels without fatigue to the test item,

2. instant equalization,

3. performing sine and random equalization independently, and

4. constant monitoring and visual indications of test specimen response to the vibration stimulus.

In the following paragraphs each of the four conditions will be discussed in detail as to the problems, advantages, disadvantages, and the necessity and justification to impose each requirement during a combined sine and random test. No detail effort is attempted to explain the various equalization procedures, the need for equalization, or shaker response characteristics. It is assumed that these subjects are familiar to the reader and therefore, only those equalization problems which could result in wrong or misleading assumptions from the test data or applicable to combining sine and random vibration into one environment, are emphasized.

SINE AND RANDOM EQUALIZATION PERFORMED AT TEST MAGNITUDES

Whenever possible, especially when the test levels are relatively high compared to the usual low level equalization magnitudes, equalization should be performed at the test levels.

Low level equalization may not excite the test specimen coupling modes which would possibly be excited by the higher test levels. In addition, low level equalization does not take into account the nonlinearities of the system. Therefore, a specimen response curve, equalized flat at low vibration levels, may exhibit several peaks and notches when large vibration test levels are generated. Indeed, it may be possible due to the test specimen nonlinearities, that the peaks and notches which exhibit themselves at low test levels, will shift downward in frequency with an associated reduction in transmissibility or Q. Under these specific conditions, the peaks and notches which have been eliminated by low level equalization, may show up to some extent at higher test levels. This phenomenon can occur when the resonant peaks and notches associated with the response curve, shift down in frequency at higher test levels, thereby causing the inverse peaks and notches, which had been inserted during low level equalization, to cease to be the exact inverse of the response curve.

The equalization peaks and notches which were inserted at low levels, could then exhibit

themselves in addition to, or in combination with, the peaks and notches associated with the higher test levels. This could result in an unequalized system with multiple or complex peaks (or both) and notches in the response curve, in a system assumed to be equalized.

While a considerable downward shift in resonant frequency due to specimen nonlinearities, requires an extreme increase in damping at the higher vibration levels,

$$fn = \frac{1}{2}\sqrt{\frac{k}{m}\left[1 - (c/c_c)^2\right]} ,$$

a proportionally larger reduction in Q value may be anticipated at the higher test levels where

$$Q = \frac{1}{2\,(c/c_c)} ,$$

when c/c_c is less than 0.1. This indicates for example, that a spectrum response curve (g/e versus f) possessing a notch having a Q of 20 which is evident at low acceleration levels and which has been eliminated during low level equalization by the insertion of a peak filter with a Q of 20, could evidence itself as a peak with a Q of 5 at the higher test levels. This would be the result of a Q reduction from the low level Q value of 20 to a Q of 15, as influenced by the increase in specimen damping at higher test levels.

It should also be emphasized that even a high level sine sweep equalization using peak-notch filters, is not entirely reliable for random equalization. This can be attributed to the fact that a specimen response to a flat random forcing function is different from specimen responses elicited by swept sinusoidal excitation. This is due to the "multiple resonance" phenomena exhibited by randomly excited physical configurations. This fact has been borne out in actual laboratory equalization tests performed on multiple-degree-of-freedom systems, with the equalization having been performed at various input levels.

INSTANT EQUALIZATION

The time spent in equalizing the test specimen should be such that the equalization procedure does not contribute to specimen fatigue or failure. This is the basic reason for the low level equalization procedure presently used in industry.

Obviously, the time spent in equalizing should be inversely proportional to the equalization levels; i.e., the higher the equalization levels, the faster the equalization must be accomplished.

Another fact to consider is the optimization of facility time, manpower, schedule, and expense. Long and tedious equalization procedures may not be justified if the system response can be predicted and can be taken into account in the final analysis of results.

In view of these facts, a system with instant equalization is the optimum and a fully automatic equalization system is called for.

INDEPENDENT SINE AND RANDOM EQUALIZATION

This is probably the area where the greatest precaution should be taken if the test results are to be correctly interpreted.

During automatic or semi-automatic equalization, the sine or random servos (or both) should be completely independent of one another; i.e., the sine servo should not be influenced by random signal levels and obviously the random servo should not respond to the sinusoidal sweep levels.

In most cases, whenever a combined sine-random environment is applied, a tracking filter of comparatively small bandwidth is required to track the sweeping sine signal which commands the sine servo. For optimum performance, the tracking filter should be 1 cps in bandwidth and should possess rectangular response (∞ slope) characteristics. In addition, the filter should not affect the servo response time.

Whenever the tracking filter is wider than 1 cps, it will be influenced to various extents (depending on the filter bandwidth) by signals other than the sine sweep frequency. During a combined sine sweep and random vibration test, deviations or changes in the random levels which occur due to specimen mechanical impedance changes (fatigue or failure), may take place in frequency bands which do not at a particular instant, comprise the sine sweep frequency. If these impedance changes in the random signal influence the sine servo, a large increase in the sine level as commanded by the sine servo could result. This occurrence could cause a catastrophic failure due to the "out of specification" sine input magnitude.

. The occurrence of this phenomenon is more probable when semiautomatic equalization is used; i.e., the sine servo is utilized for control of the sine sweep, but random equalization is performed manually by adjustment of several narrow band filters. Under semiautomatic conditions, the sine servo attempts to adjust all changes in level within the tracking filter band. In instances where no tracking filter is used, the sine servo receives its commands based on the rms sum of the wide band random level and the instantaneous sine sweep level.

The adverse effects and consequences of not using a tracking filter during combined sinusoidal and random tests, can be appreciated by the following example: let

PSD (power spectral density of random signal) = 0.05 g^2/cps,

sine level = 1 g rms (sine sweep),

BW (bandwidth of random and sine) = 2000 cps,

Random rms level = $\sqrt{(0.05)\ (2000)}$ = 10-g rms,

and

$$\text{Random rms + sine rms} = \sqrt{(10)^2 + (1)^2} = 10.05\text{-g rms}.$$

If mechanical impedance change causes rms random level to drop to 9.5-g rms, new random-sine total equals

$$\sqrt{(9.5)^2 + (1)^2} = 9.52\text{-g rms}.$$

Sine servo senses change from 10.05 to 9.52 g and adjusts overall level back to 10.05 g rms by raising the sine level to:

$$10.05 = \sqrt{(9.5)^2 + x^2}$$

$$x^2 = 3.3\text{-g rms}.$$

The sine level increased to 3.31-g rms or 331-percent overload.

Obviously, if the sine sweep is at a resonant frequency of a system component, the item may fail when subjected to the 331-percent overload.

The use of a narrow-band tracking filter will alleviate the adverse effect of the sine feedback system but the total adverse effect cannot be totally discounted even with a relatively narrow (20-cps) tracking filter.

Example: let

PSD = 0.15 g^2/cps,

BW of tracking filter = 20 cps,

sine level = 0.5-g rms,

Random rms level in filter band = $\sqrt{(0.15)(20)}$ = 1.73-g,

and

$$\text{Random rms level plus sine rms level} = \sqrt{(1.73)^2 + (0.5)^2} = 1.8\text{g}.$$

If random g level dropped to 1.5-g rms in the 20-cps filter bandwidth due to a change in the system mechanical impedance, the sine level would increase to 1-g rms or a 200-percent overload.

It can be deduced from the previous examples, that the feedback effect is a function of several parameters such as tracking filter bandwidth, ratio of random to sine level, magnitude of changes in mechanical impedance, change in random level, and the sine sweep frequency at the instance of mechanical impedance change. Each factor must be carefully considered in the final analysis of results.

When both, a sine servo and random servo (automatic equalization) are used without a tracking filter, for example, both the random and sine servos attempt to correct simultaneously for any changes in the overall response level. Level adjustment is then performed simultaneously or by the servo with the maximum response capability.

If conditions during a test were such that the signal magnitude in a high-level random band were to drop suddenly due to changes in the specimen mechanical impedance within the aforementioned band as shown in the previous example, and if this level change was detected and corrected for by the sine servo (crosstalk of tracking filter), catastrophic failure of the specimen could result. At the instant of mechanical change, the sine sweep frequency could possibly be outside the band of impedance change, but the sine servo would nevertheless issue the command to increase the sinusoidal level to make up for the drop in random level. The sinusoidal level could then be increased above the test specification and cause the specimen to fail. (See Fig. 1 for a further explanation

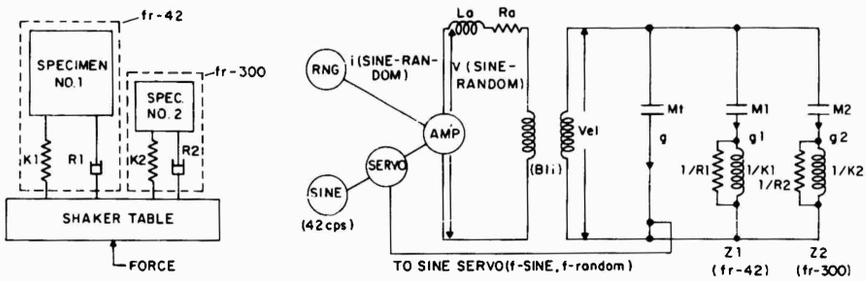

MECHANICAL SYSTEM

WITHOUT FEEDBACK
1. Vel decreases as Z1 and Z2 resonate
2. ∴ g1 and g2 increase to Q levels
3. g decreases

RESULT:
Specimen #1 may fail due to overtest
Specimen #2 may not fail due to undertest

ELECTRICAL MOBILITY ANALOG

WITH FEEDBACK
1. Servo commands Sine Oscillator to increase Vel until g increases to $\sqrt{(g\ Sine)^2 + (g\ random)^2}$
2. As Vel increases, g1 and g2 increases
3. Vel increase is due to Sine increase only, g1 increase out of proportion to g2
4. This makes g1 too high, g2 too low

Fig. 1 - Explanation of phenomena by means of electrical mobility analog

of phenomena by means of electrical mobility analog.) The reverse (below specification testing) can also be the case due to specimen nonlinearities at resonance. The higher order harmonics are excited and the servo applies correction for the rms sum of the fundamental frequency and the generated harmonics when actually the corrections should be applied totally at the fundamental. Therefore, the fundamental frequency is not servo controlled and maintained at the higher required levels.

CONSTANT MONITORING AND VISUAL INDICATION OF SPECIMEN RESPONSE

When random vibration is applied to a multiple-degree-of-freedom-system, using a fully automatic or semi-automatic equalization system as previously described, it is desirable that a constant visual indication of system response be made available during a test. If a vibration test is performed using automatic or semi-automatic equalization and no provisions for monitoring the system response are provided, catastrophic or unnecessary failure (or both) of the test specimen or portion thereof, may result.

This occurrence can be attributed to the fact that a sudden impedance change usually indicates a drastic change in specimen parameters and most probably a failure. In most cases, especially during development type tests, the test should be stopped immediately and the failure investigated.

If corrections in input levels are automatically administered by the servo (positive feedback loop) and if these corrections are influenced by the "failed" portion of the specimen, other cumulative failures could result which may have been prevented by system shutdown after the first failure.

DISCUSSION

Dr. Mains (GE): I feel compelled to raise the voice of the loyal opposition. It saddens me on two accounts to hear what I have just heard. Our speaker, I think, has striven hard and done a good job, but is trying to solve the wrong problem. Dr. Vigness presented a paper yesterday which showed a figure which demonstrated what happens if you force the full input

motion at an anti-resonance point. There is an inconsistency between that figure and what you are trying to do here which must be resolved, and I don't think it is resolved by instant equalization. The other thirg that saddens me is this mixing of donkeys and dogs — sinusoidal and random excitation. It comes about only because somewhere somebody once thought a random spectrum had to be flat. Why? I never saw one that was flat. Why do you have to impose a sinusoidal excitation on top of a random spectrum?

Mr. Pelletier: This work was undertaken because of firm test requirements which are imposed on us.

Dr. Mains: I repeat that you are to be commended for doing a good job — unfortunately of the wrong thing because you have been required to do the wrong thing. Let me plead with you, instead of working so hard to comply with an incorrect specification, to kick back a little bit and try to have the specification changed.

Mr. Pelletier: We have brought this up and have found it almost impossible to change them. For example, what I am referring to here is a NASA specification applied to Grumman on a lunar excursion module and passed down through RCA which we, in turn, will pass on to our subcontractors. We have found it extremely difficult to negotiate with Grumman on the changing of a specification, and I don't see how I can go to NASA on these things. These specifications are being imposed by NASA through Grumman, and Grumman is firm about them. They impose these requirements on all their suppliers and they are very adamant about it. There are probably good arguments on the affirmative side because I'm sure that the NASA and Grumman people know what they are doing.

Mr. Cohen (NOL): You seemed to be concerned during the equalization process at some level lower than the actual test level about getting fatigue failures. Have you actually encountered this in your laboratory?

Mr. Pelletier: I haven't, but Grumman assures us that they have. In my experience I have performed many tests in which I lacked confidence in the results. In some cases failure may have occurred prior to the actual test and gone unnoticed.

* * *

FLEXURE STABILIZATION OF A REACTION VIBRATION MACHINE

R. H. Chalmers, Jr.
U. S. Navy Electronics Laboratory
San Diego, California

This paper describes a method of restraining reaction vibration machines to planar simple harmonic motion even though test loads represent an appreciable percentage of the moving weight and exhibit severe resonances or isolation.

The Navy Electronics Laboratory has been engaged in shock and vibration testing of Navy electronics equipment for many years. We have often had occasion to perform vibration tests on large low density structures such as shipboard radar antennas. One antenna, a 14 by 16-foot flat array weighing 4800 pounds, converted the desired 20 milli-inch horizontal excursion into a massive rocking motion that resulted in a 325 milli-inch vertical excursion measured 4 feet from the center of rotation. The vibration machine being used was a 10,000-pound capacity reaction machine which is suspended to behave as a free body at frequencies of 5 cps and higher. Calculations showed that a similar rocking motion could be caused by a cyclic vertical force couple that reached peaks of 324,000 lb.-ft.

Planar simple harmonic motion is obtained on a reaction vibration machine by locating the center of gravity of the total moving mass at the point of force generation. This is accomplished, for horizontal motion, by adding weight above or below the point of force generation until the center of gravity is properly located. Unfortunately, such balancing is normally based on the location of the static center of gravity of the test load, and only for the theoretical perfectly rigid structures do the dynamic and static centers of gravity coincide. When any portion of a test load experiences an excursion greater or less than the excursion of the rest of the moving mass, that portion sees a different g-level and has a different apparent weight. The center of gravity must move to accommodate the change in apparent weight. At each discrete frequency and amplitude, a test load exhibits a unique response, and has a unique location for the center of gravity. Consequently, depending on amplitude and frequency, there can be an infinite number of locations for the center of gravity. Static measurements can determine only one of these locations.

Why not compute the locus of the center of gravity and balance the machine for frequencies of interest? If sufficient information existed to compute the locus, there would be no need to conduct the vibration test. Practical considerations, such as weight limitations of the suspension system, physical effort and time required to change counterweights make balancing for specific frequencies inadvisable.

How then is crosstalk, the undesired motion of the table caused by the vertical force couple, to be controlled?

It can be minimized by causing the test load to be only a very small percentage of the total moving mass. While this approach seems simple and promising, it is inefficient and impractical. To make the 4800-pound antenna 1 percent of the moving mass, the vibration machine and counterweight would have to weigh 475,000 pounds, and the vibration generators would have to produce sufficient force to drive all the added mass.

The method investigated at NEL for controlling the crosstalk is flexure stabilization of the vibration machine. Through the use of flexure beams, the machine has virtually no vertical compliance while the horizontal compliance remains essentially unchanged.

Four flexure beams were designed that have a vertical to horizontal stiffness ratio of

1000 to 1. The beams were attached to each of the four corners of the table at the top and to a massive concrete slab at the bottom. The flexure beams bypass the machine's normal suspension system and allow free movement in only one direction. Any vertical forces developed on the table are transmitted through the vertically stiff flexure beams to the concrete slab.

The flexure beams were machined from 8 x 8 inch S.A.E. 4340 steel (chrome-nickel-molybdenum). The semi-circular grooves near each end of the beams are of 4-inch radius and are centered so that the two weakened sections are 3/4-inch thick and 36 inches apart. In operation the beams undergo double cantilever bending. Generous radii, mirror polishing of the necked down sections, and limiting of the bending stress to less than 1/4 of the yield strength promote long life for the flexure beams. Holding the maximum tensile and compressive stresses to less than 3000 psi limits the flexure beam's vertical deflection.

The concrete slab weighs approximately 625,000 pounds. It is shaped to cause as great an amount of the surrounding earth as is possible to move as a unit with the slab. Because the slab was to resist rocking or torsional motions, it was shaped to present a high polar moment of inertia. An effective mass polar moment of inertia for the earth-slab system was calculated to be 7.5 million lb-ft-sec^2. The high polar moment of inertia and stress levels of less than 50 psi in the concrete hold motions at the point of flexure attachment to unnoticeable levels.

Preliminary tests of the flexure-stabilization system have just been conducted at the Laboratory. When a test load was placed on the vibration table and the machine adjusted for 10 milli-inches horizontal excursion, the load developed 230 milli-inches of vertical motion, as well as 140 milli-inches of horizontal motion. When the machine was stabilized by the flexures, the vertical motion was reduced to 20 milli-inches and the horizontal motion to 100 milli-inches. Although tests have not been completed, it appears that when the vibration machine has been set to provide the desired 10 milli-inch drive, vertical magnitude should not exceed 2 milli-inches, which approaches an acceptable level of cross-talk. Increasing the rigidity of the attachment of the flexures to the table is expected to bring crosstalk well within tolerable limits.

The flexure beams are peculiar to the stabilization of this type machine. Other types of machines have inherent cross axis stiffness that may or may not be sufficient to restrain the cross-talk, but the need for polar moment of inertia is universal. Any vibration test pad that is to handle loads similar in response to the ones described here must have similar polar moments of inertia if crosstalk is to be limited to acceptable levels.

After testing of the flexure stabilization system on a variety of test loads, it is intended to publish a formal Laboratory report that will cover in detail the theory, design, construction, and testing of the system. Those interested in making inquiry should address:

Commanding Officer and Director
U.S. Navy Electronics Laboratory
San Diego, California (92152)
(Attention: R. H. Chalmers, Code 3360)

DISCUSSION

Mr. Gunkel (Autonetics): Would you make any comment as to the approximate value for your polar moment of inertia?

Mr. Chalmers: The effective mass polar moment of inertia for the earth slab system was calculated at 7-1/2 million lb-ft-sec^2.

* * *

AN ALTERNATE METHOD OF EXCITER SYSTEM EQUALIZATION

D. Scholz
McDonnel Aircraft Corporation

A remote equalizer-analyzer system is adjusted to the inverse of the mechanical characteristics of the unequalized test setup by means of a prerecorded tape signal. A taped input containing the desired test spectrum is then played through the system. The output is the equalized spectrum.

INTRODUCTION

Prior to the acquisition of multi-channel equalizer-analyzers, equalization for random vibration testing at McDonnell Aircraft Corporation was accomplished with peak-notch and broad-band filters. The ever increasing number of random vibration tests has created such a demand for the equalizer-analyzer units that an analyzer unit isn't always available at the test site. Therefore, an alternate method of equalization was attempted to replace the time consuming method of using peak-notch and broad-band filters.

The equalization method chosen involves the use of a remote site equalizer-analyzer to adjust a recorded noise signal to a signal whose frequency spectrum is the inverse of the electro-mechanical characteristics of the unequalized shaker system. The recorded noise signal with the inverse spectrum could then be applied to the unequalized shaker system, and the resulting acceleration would then possess the desired test spectrum characteristics.

PROCEDURES AND RESULTS

The system used for this test was an exciter system and a horizontal oil table combination, with a 20-pound test fixture attached to the horizontal table. The fixture was non-resonant in the test frequency range—20 to 2000 cps. This system was chosen because it is one of the more difficult systems to equalize. A constant voltage plot of the response of this system was obtained by applying a constant voltage from an oscillator to the exciter system, varying the oscillator frequency through the test frequency range, and recording the output voltage from an accelerometer on an X-Y recorder. The accelerometer was located at the proposed input accelerometer location on the horizontal oil table. The plot obtained is presented in Fig. 1. The setup frequency and acceleration level for this plot were 100 cps and 1 g_{peak} respectively. The plot shows a high resonant condition at about 1100 cps and a large attenuation of acceleration above about 1300 cps. Both of these conditions are difficult to cope with when the peak-notch and broad-band filters are used.

The first step taken in this equalization method was to play an input magnetic tape recording containing the desired shaped random spectrum (shown in Fig. 2) into the exciter system and to record simultaneously the output voltage of the input accelerometer. A plot of the normalized power distribution obtained during this step is presented in Fig. 3. The overall acceleration level of the recorded signal was 13 g_{rms}. The power distribution of this recorded signal differs from the desired test spectrum because of the electro-mechanical characteristics of the unequalized exciter system.

The noise signal from the output voltage recording of the input accelerometer was then played into a remote-site multi-channel equalizer-analyzer, and the equalizing filters were adjusted to transform this unequalized power spectrum back to the desired power spectrum shape.

This adjustment of the multi-channel filters in essence equalized the exciter system for the

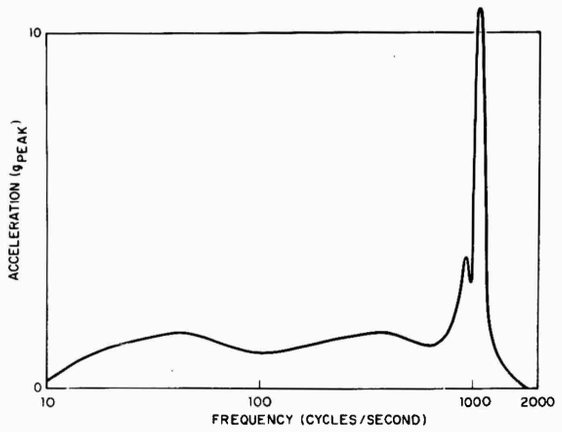

Fig. 1 - Constant voltage plot (Setup frequency and level—100 cps; 1 g)

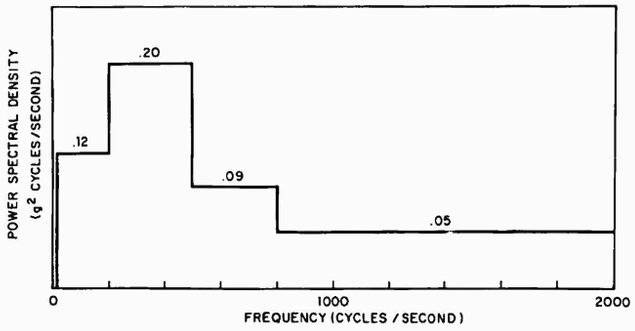

Fig. 2 - Desired vibration spectrum (Overall acceleration level—12.6 g_{rms})

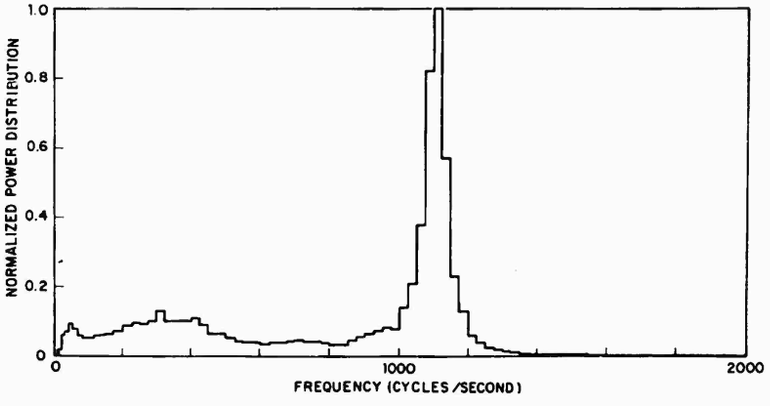

Fig. 3 - Power spectrum obtained through unequalized shaker system

frequency band and levels of the desired shaped random spectrum. This was accomplished, however, by bringing the electro-mechanical characteristics of the unequalized exciter system to the multi-channel equalizer-analyzer via magnetic tape.

With the equalizer filter settings unchanged, the original input tape was played into the equalizer and the output signal recorded on magnetic tape. A plot of the normalized power distribution of this recorded signal is presented in Fig. 4. This power distribution differs from the desired test spectrum by the inverse of the electro-mechanical characteristics of the exciter system.

The noise signal with the inverse power spectrum was then applied to the exciter system. A sample of the output voltage of the input accelerometer was recorded and analyzed. The overall acceleration level of the recorded signal was again 13 g_{rms}. A plot of the power distribution of this recorded signal is presented in Fig. 5. This power spectrum agrees quite well with the desired test spectrum. Fluctuations of the power level of adjacent filters as shown on this plot are well within allowable tolerances (+40-30 percent of Power Spectral Density) and may be attributed to human error in reading the fluctuating power level of each filter on the analyzer.

SYSTEM VARIATIONS

The slight ripple in power distribution between 900 and 1150 cps, as shown in Fig. 5, is

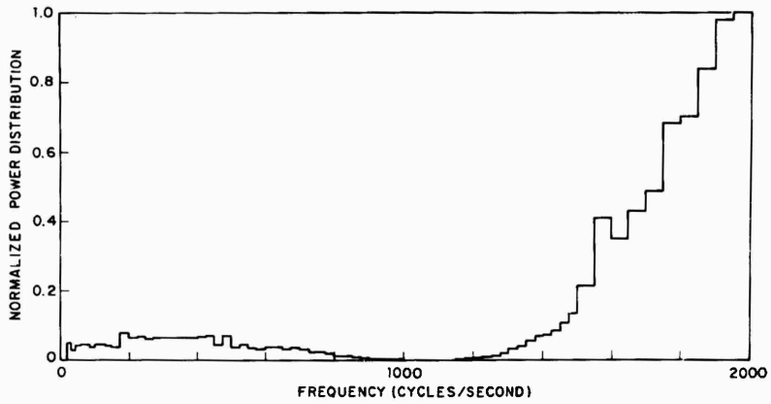

Fig. 4 - Inverse power spectrum

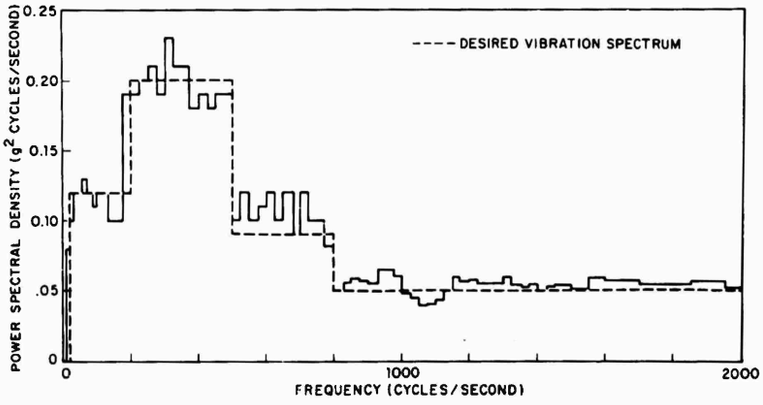

Fig. 5 - Spectral density analysis of input accelerometer (Overall acceleration level--13 g_{rms})

due to the shift in resonant frequency encountered when the acceleration level in the resonant frequency range changes. The actual acceleration level applied to the horizontal oil table in this frequency band for the first and last steps of this method was not determined, but it can be assumed that the level was different for each of these steps.

Although a non-resonant fixture was used for this test, a resonant fixture could have been used provided the mass of the test specimen was simulated and was a small percent of the total moving mass so the effect of specimen resonance was minimized. The response of the exciter system would become more complex, but no additional steps would be required to produce the desired spectrum.

For this test, two magnetic tape recorders were required because the original input signal was recorded. In the event that only one tape recorder would be available, the original input signal could be provided by a noise generator. Any noise source could be used provided the signal was stationary and had normal Gaussian distribution.

DISCUSSION

Mr. Spada (Raytheon): Do you find when you change your setup that this changes your response, especially in the horizontal axis?

Mr. Scholz: This was a study to see whether or not it was feasible to use the technique for a particular test. We made no changes in setup because this was done in about half a day. I would expect that the response would change if the setup changed. It would be necessary to get in each particular setup all of the peculiarities of each particular resonance, and it would be necessary to insure that your accelerometer location was at the exact same point. Of course all of this becomes very complicated if you use a resonant test fixture, or if the mass of your specimen is large with respect to the total moving mass of the exciter system and oil table combination.

Mr. Spada: At Raytheon we have tried this method and found that even changing the stiffness of the bolts or tightening the bolts changed the spectrum considerably.

Mr. Scholz: We have found that the data can be taken and analyzed so quickly that we would not have to change anything. In other words, we would tie the bolts down, make our setup, run our response, go out to our analyzer, adjust it all, come back, and we have the same setup. So we get around the problem that way.

* * *

CORRELATION OF DAMAGE POTENTIAL OF DWELL AND CYCLING SINUSOIDAL VIBRATION

E. Soboleski and J. N. Tait
U.S. Naval Air Development Center
Johnsville, Pennsylvania

This paper presents the results of a study conducted to determine whether present specifications which require sinusoidal resonance dwell testing could be replaced by increased-time sweep cycling. Fatigue failure is used as an equivalent damage criterion. Methods are presented by which test procedure parameters may be determined.

INTRODUCTION

WEPTASK No. RAV03J001/2021/R008-01-01, Problem No. 11 requested the U.S. Naval Air Development Center (NAVAIRDEVCEN) to study the problem of vibration testing of avionic equipment.

Tests were made on simple cantilever beam specimens to determine the correlation produced by sinusoidal dwell and sweep frequency vibrations. The specimens were made of square, bus bar, cold-drawn copper wire.

SUMMARY OF TEST RESULTS

The method of testing — subjecting a single cantilever beam specimen to a sinusoidal dwell and logarithmic sweep vibrations — proved satisfactory. By use of the failure data, a curve was developed by plotting the various values of stress against their corresponding values of the number of stress reversals. With this curve it was possible to predict specimen failures under any prescribed dwell or logarithmic cycling conditions. Although the fatigue curve was limited to the test specimen, it produced the possibility of predicting failures of many materials.

CONCLUSIONS

The fatigue damage summation data yielded results which showed that a correlation exists between dwell and logarithmic cycling. The vibration testing of avionics equipment can therefore be improved. The correlation made possible a sweep test that will permit equivalent fatigue to all parts of equipment over the entire frequency test band.

CHOICE OF SPECIMENS

Since the military specifications being considered are concerned with the testing of avionics equipment, the specimens chosen for this research program had to be representative of materials used in avionics equipment. After a careful search of the many component parts which are used in the construction of avionics equipment, bus bar wire was chosen as the most suitable. The wire was used as a simple cantilever beam, and it produced results that were easily evaluated. The thickness dimension tolerances were found to be within ± 0.001 inch. The bus bar wire had fewer nicks, scratches, bends, or other defects than most other electronic components. Changes to obtain a particular shape or size by machining or other processes which would alter the original physical characteristics of the metal were not necessary. The square type was chosen because preliminary tests revealed that nearly all of the round type exhibited various patterns of elliptical motions when sweeping through the vibration frequency band. This phenomenon produced results which were extremely difficult to evaluate.

PURPOSE

The present test procedure of MIL-T-5422E requires vibration test times to be

divided between the most severe detected resonances and cycling. Since the procedure provides for dwell vibration at only four of the most severe resonances in each axis, it is quite likely that not only are many resonances undetected and ignored, but also that the most severe ones are not selected for vibration. The remaining cycling vibration time may be inadequate for conducting reasonable tests and permitting failures to occur to the ignored and undetected resonances or other weaknesses of the equipment. Due to these many difficulties, tests cannot be performed adequately to produce failures which may represent the weakest link in the design of the equipment and be the cause of numerous failures which affect the reliability of the equipment.

This paper presents the results of an investigation to determine whether a practical sweep test, covering the entire frequency test band, could be devised which would produce failures equivalent to those of fixed frequency dwell.

CRITERIA FOR FAILURE

Several criteria for failure were considered, such as frequency shift, decrease in specimen output, and total separation (specimen broken in two parts). Total separation was selected as the criteria of failure. The selection was influenced by experience gained in the laboratory testing of the many complex electronic equipments. Test results indicated that most failures of the equipment's internal parts and components occurred because of total separation.

Although little difficulty was encountered in detecting the parameters when subjecting the cantilever beam specimens to dwell vibrations, this did not hold true for sweep cycling. Even by a close surveillance, the changes in end of beam displacement and the downward frequency shift of the beam were difficult to detect because of the constant change of input frequency and output as the specimen was vibrating through the resonant frequency band. Since an accurate failure time could not be obtained at the sweep frequency, a correlation with dwell could not be achieved by direct measurement.

The selection of total separation was further reinforced by preliminary vibration tests. A group of cantilever beam specimens were vibrated at resonance with a number of different vibration inputs. With the larger inputs, the frequency shift and the reduced output occurred so rapidly that they masked out or coincided with total separation.

FIXTURE, BRASS WEIGHTS, AND BLUR GAGES

A fixture was fabricated of heat-treated steel. Machined grooves held the specimen under test. Uniform specimen clamping was insured by the use of a torque wrench. Cylindrical brass weights were secured to the specimens by set screws. Precision blur gages were mounted to the faces of the weights for reading vibratory displacements. These items are shown in Fig. 1.

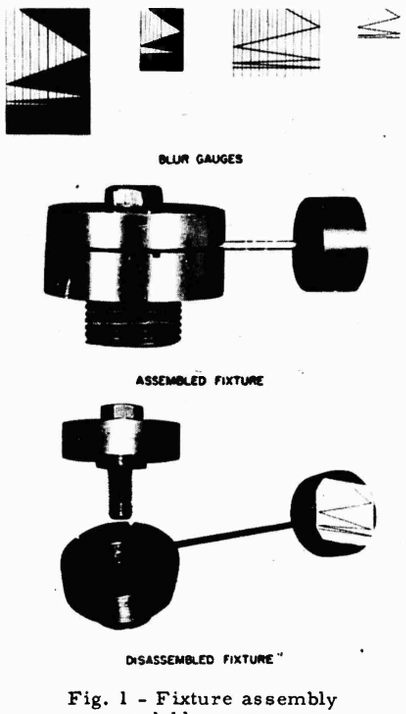

Fig. 1 - Fixture assembly and blur gages

TEST PROCEDURE (CYCLING THROUGH RESONANT BAND)

The test equipment was arranged as shown in Fig. 2. A new unstressed 2-inch length of specimen was secured in the fixture.

The oscillator sweep rate was selected and the microswitches were set to the upper and

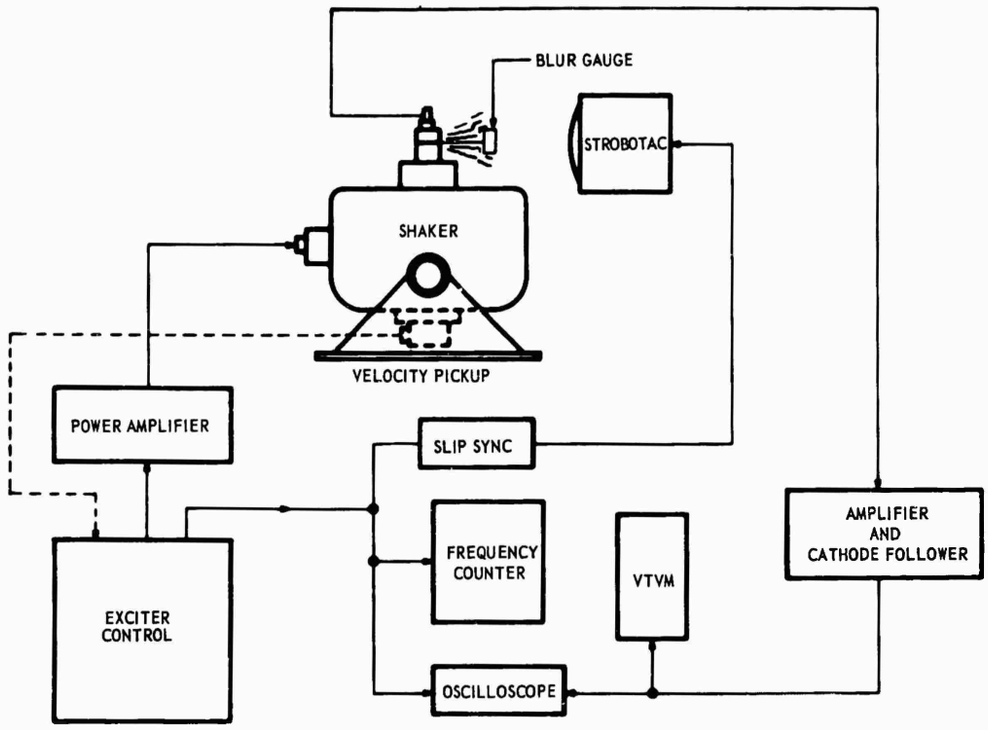

Fig. 2 - Test equipment arrangement

lower limits of the frequency band to be swept. The bandwidth for the input amplitude and the sweep rate of the oscillator that insures peak resonant amplitude were both determined by preliminary laboratory tests.

For initial table inputs which are lower than the endurance stress amplitude of the material, only that portion of the bandwidth which would fatigue the specimen was timed. The microswitch stops were set so that the frequency limits would permit vibration of the specimens at an amplitude slightly lower than the calculated endurance limit.

The power amplifier gain was increased to the vibration input level and the oscillator was engaged together with a stop watch to measure the failure time. Another stop watch was used to time the upward and downward portions of the swept band. For vibration table amplitudes equal to or above the stress endurance limit of the specimen, the total bandwidth between the upper frequency limit and lower frequency limit was timed because the vibrating specimen was accumulating fatigue at all times. Both procedures were repeated a number of times to obtain an average for one sweep.

While the specimen was being vibrated through the sweep frequency band, the mode of vibration of the cantilever beam was observed by means of a strobe light and slip sync. The output was read on the blur gage. The gage was also used to indicate whether the sample was vibrating in a pure vertical plane. The total output could be read at any part of the sweep frequency band. The resonant frequency was determined by observing the blur gage for maximum excursion.

The velocity pickup which generated the voltage used to determine table input was also connected to an oscilloscope to observe waveform. This was necessary to assure that the table was vibrating sinusoidally at all times.

While observing the output on the blur gage, a decrease in amplitude could be detected, and failure could be expected to occur in a short

time. This observance yielded the time of failure on a stop watch and aided in detecting accurately the portion of the band in which failure occurred. The data were recorded and the procedure was repeated for another test on a new specimen.

TEST PROCEDURE (FIXED FREQUENCY DWELL)

The same test setup as shown in Fig. 2 was used. The instruments used in all tests were calibrated in accordance with manufacturer's instructions. The fixture for the bus bar wire specimens under dwell testing was the same as for "cycling through the resonant band." The necessary vibration table inputs were determined for the tests. The average resonant frequency for each input was determined by preliminary laboratory tests, and was held constant during the dwell.

The oscillator for controlling the vibration table frequency was set to the average resonant frequency of the input selected for the test. The vibration table amplifier level was increased rapidly to give the desired input level. As soon as the input was reached a stop watch was engaged to measure the accumulated time to failure. The oscillator frequency was fine tuned while observing the blur gage for maximum output. The resonant frequency was thus determined. The specimen output and the frequency at which resonance occurred were recorded. The mode of vibration of the cantilever beam was observed by a strobe light and slip sync and recorded. The waveform of the vibrating table was observed on an oscilloscope to insure a sinusoidal motion. When failure occurred, the timing watch was stopped and the accumulated time recorded. The oscillator frequency was calibrated after each few samples to avoid frequency drift. This was important as a slight shift in frequency could result in yielding an erroneous number of stress reversals. A new selected beam sample was fixed to the vibration table and the test repeated.

LIST OF SYMBOLS

A Area under y_1A.M. versus N curve, above $(y_1\text{A.M.})_e$, measured between N_o and N_f (in.^{2})

A' 64.5A (in.-cycles)

A.M. Absolute magnification, instantaneous value, dimensionless

$$\text{A.M.} = \frac{r^2}{\sqrt{(1-r^2)^2 + 4b^2r^2}}$$

A.M._{max} Absolute magnification, maximum value, dimensionless

a Distance from weight center of gravity to end of beam (in.)

b Damping coefficient, dimensionless

C_1 Constant of integration, dimensionless

c Distance from neutral axis to beam outer fibers (in.)

d Diameter of weight (in.)

dy/dx Slope of elastic curve, dimensionless

E Modulus of elasticity of cold-drawn copper (psi)

e Base of natural or Naperian logarithms, dimensionless

f Applied frequency (cps)

f_1 Lower sweep frequency limits (cps)

f_2 Upper sweep frequency limit (cps)

f_D Frequency at which maximum y_2 occurs (cps)

f_n Natural or resonant frequency (cps)

g Length of weight (in.)

h Distance from weight center of gravity to beam root (in.)

I Moment of inertia of beam (in.^{4})

K Sweep rate constant, dimensionless

K' Time-rate-of-failure coefficient, dimensionless

ℓ Overall beam length (in.)

M_{st} Static beam moment (in.-lb)

m Number of logarithmic sweeps, dimensionless

N Number of stress reversals accumulated

N_f Stress reversals at upper frequency when $\sigma = \sigma_e$ (cps)

N_o Stress reversals at lower frequency when $\sigma = \sigma_e$ (cps)

N_{af} Average stress reversals at failure

N_{res} Stress reversals accumulated during one 1-1/6 octave sweep

N_{test} Stress reversals accumulated during one 6-2/3 octave sweep

N_{total} Total stress reversals accumulated during m sweeps

Q Maximum value of y_2/y_1, dimensionless

RT Relative transmissibility, instantaneous value, dimensionless

r Frequency ratio, f/f_n or f/f_D, dimensionless

t Time, instantaneous value (sec)

t_1 Time at f_1 (sec)

t_2 Time at f_2 (sec)

t_{af} Average time to failure (sec)

W Weight (lb)

x Distance along beam from origin (in.)

y_1 Vibration table displacement (in. double amplitude)

y_2 Vibratory displacement at end of beam (in. double amplitude)

y_a, y_b Components of y_{st} (in.)

y_{st} Static deflection at end of beam (in.)

y'_{st} Static beam deflection at center of weight (in.)

y_{rel} Relative vibratory displacement between end and root of beam (in. double amplitude)

y'_{rel} Relative vibratory displacement between center of weight and root of beam (in. double amplitude)

$\Delta(y_{rel})$ Mean value of y_{rel} in excess of $(y_{rel})_e$ during one sweep (in. double amplitude)

$(y_{rel})_e$ Value of y_{rel} at σ_e (in. double amplitude)

$(y_{rel})_{mean}$ Mean value of y_{rel} during one sweep (in. double amplitude)

$(y'_{rel})_{mean}$ Mean value of y'_{rel} during one sweep (in. double amplitude)

$(y'_{rel})_{Test\ 18}$ Value of y'_{rel} for Test 18

σ Stress (psi)

σ_e Endurance limit stress (psi)

σ_y Yield stress (psi)

σ_{st} Static stress (psi)

σ_{dyn} Dynamic stress (psi)

σ_{ult} Ultimate stress (psi)

σ_{total} Total stress (psi)

$(\sigma_{dyn})_{mean}$ Mean value of dynamic stress during one sweep or during one dwell history (psi)

$(\sigma_{total})_{mean}$ Mean value of total stress during one sweep or during one dwell history (psi)

θ Angle between the horizontal and a tangent to the beam at the point of concentrated load application (rad)

ANALYTICAL PROGRAM

Stress-Amplitude Relationship

The following analysis is required for both dwell and logarithmic cycling.

The loaded test specimen was treated as a massless cantilever beam in order to determine the static deflections. The effect of beam mass was determined to be negligible.

The deflection y_{st} consists of two parts, y_a and y_b. By using the classical expressions for a massless cantilever beam with concentrated load at its free end

$$y'_{st} = y_a = -\frac{Wh^3}{3EI},$$

$$y_b = -\frac{W_{ah}^2}{2EI},$$

$$y_{st} = y_a + y_b = -\frac{Wh^2}{EI}\left(\frac{a}{2} + \frac{h}{3}\right).$$

For the relatively small beam deflections encountered during the tests, it was assumed that stress varied linearly with beam deflection. Since peak-to-peak specimen displacements were observed, given displacements were divided by two in order to determine the corresponding stress levels. Thus,

$$\sigma_{dyn} = \sigma_{st}\left(\frac{y'_{rel}}{2y'_{st}}\right).$$

Since the quiescent point for vertical vibration occurs at a deflection of y'_{st},

$$\sigma_{total} = \sigma_{dyn} + \sigma_{st}.$$

The values of y'_{rel} were determined by the use of the classical expression for absolute magnification, A.M. On the blur gage at the free end of the beam

$$y_{rel} = y_1 A.M.$$

This was modified to yield y'_{rel} for the center of mass

$$y'_{rel} = \left(\frac{y'_{st}}{y_{st}}\right) y_{rel} = \frac{2hy_1 A.M.}{3a + 2h}.$$

REDUCTION OF DWELL DATA

If the dwell tests had been performed at f_n, and if there had been no shift in apparent resonant frequency at the values of y_1 used, the tests would have been true resonance dwell tests, with $r = 1$ and A.M. $= 1/2b$.

The tests were performed, however, at frequencies previously determined at low values of y_1. Therefore, the test frequency in each case was above f_D, with $f - f_D$ increasing as y_1 was increased. Since neither f_D nor b could be measured directly, it was necessary to use values based upon the logarithmic cycling data. Tabulated values of f_D and b were used to plot the curves of Fig. 3. Although Fig. 3 is based on weight No. 1, weights No. 1 and 2 were used for the dwell tests. It was recognized, however, that b is independent of specimen weight; experiments showed that the variation of f_D/f_n is also independent of specimen weight. The values of b were therefore read directly from Fig. 3 for all dwell tests. For the dwell tests using weight No. 1, the values of f_D were read directly from Fig. 3. For the dwell tests using weight No. 2, values of $f_d/f_n = f_D/64.0$ were tabulated. (See the f_D curve of Fig. 3.) These values were then multiplied by 53.4 to yield f_D values for weight No. 2. A summary of the calculation steps follow below.

In order to calculate A.M., it was first necessary to calculate the relative transmissibility, RT,

$$RT = \frac{y_2}{y_1} = \sqrt{\frac{1 + 4b^2r^2}{(1 - r^2)^2 + 4b^2r^2}}$$

$$= \left(\frac{\sqrt{1 + 4b^2r^2}}{r^2}\right) A.M.$$

$$A.M. = \left(\frac{r^2}{\sqrt{1 + 4b^2r^2}}\right) RT.$$

Using the linear stress-amplitude relationship, the initial stress values were then calculated.

Weight No.	b	f_n (cps)	f_D/f_n	f_D (cps)	f (cps)	r
1	Fig. 3	64.0	Not req.	Fig. 3	Meas.	f/f_D
2	Fig. 3	53.4	$\frac{f_D \text{ (Fig. 3)}}{64.0}$	$\left(\frac{f_D}{f_n}\right)$ 53.4	Meas.	f/f_D

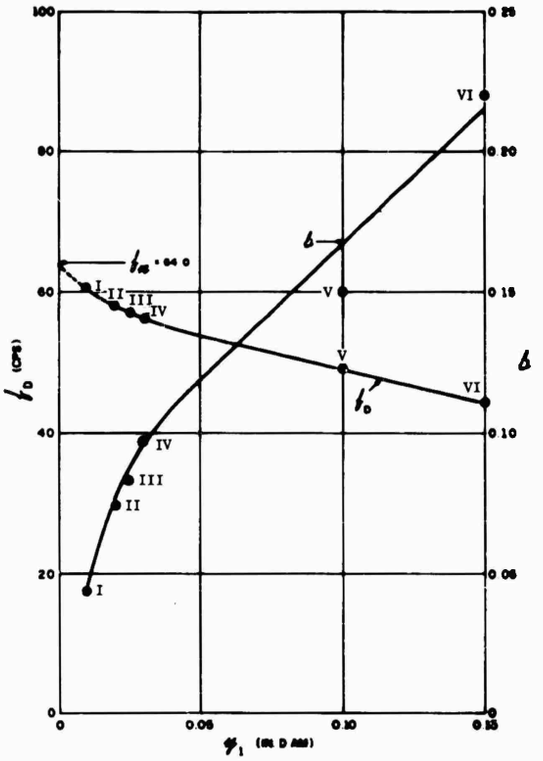

Fig. 3 - Variation of f_D and b with y_1

During dwell, the applied frequency was held constant. Due to progressive fatigue, y_2 suffered an almost immediate initial decay followed by a levelling out, and ending with an increase in the decay slope until failure occurred. Four time-rate-of-failure curves were drawn from these tests during which y_2 was continuously monitored. From these, a mean time-rate-of-failure curve was drawn. This is shown in Fig. 4. The idealized curve was derived by first noting that f_D was continuously decreasing during the four tests, even though y_1 was held constant at 0.03 in. Assuming that b was initially 1/2 Q = 0.0768 and remained constant, effective values of r, and thus y'_{rel}, were computed for various points on the mean y_2 versus t curve. By using a curve showing RT versus r for $1.0 \leqq r \leqq 2.5$, values of r were read corresponding to the values of $RT = y_2/0.03$ for each value of t. A.M. and y'_{rel} were computed using the expressions previously derived. The average value of f for the four tests was 53.2 cps. The average value of t_{af} was 198.25 sec. The average $N_{af} = 2ft_{af} = 2(53.2)(198.25) = 21{,}100$ stress reversals.

From tensile tests, $\sigma_y = 40.0\,K$ psi and $\sigma_{ult} = 55.0\,K$ psi. The idealized curve of Fig. 4 was modified, as σ_{total} was considered unlikely to exceed 40.0 K psi. Although y'_{rel} values were large, the specimen material began to yield early in its failure history. The linear stress-amplitude relationship no longer held true. The resultant curve is shown in Fig. 4. The mean value of σ_{total} was determined by measuring the area of the resultant curve from N = 0 to N = 21,000 stress reversals. Thus,

$$(\sigma_{total})_{mean} = \frac{\Sigma(\sigma_{total}\ \Delta N)}{N_{af}} = 31{,}700 \text{ psi.}$$

Since the weight and input amplitude were the same for the time-rate-of-failure tests and for dwell test No. 18, the ratio of $(\sigma_{dyn})_{mean}$ to the apparent value σ_{dyn} for dwell test No. 18 was determined. Thus,

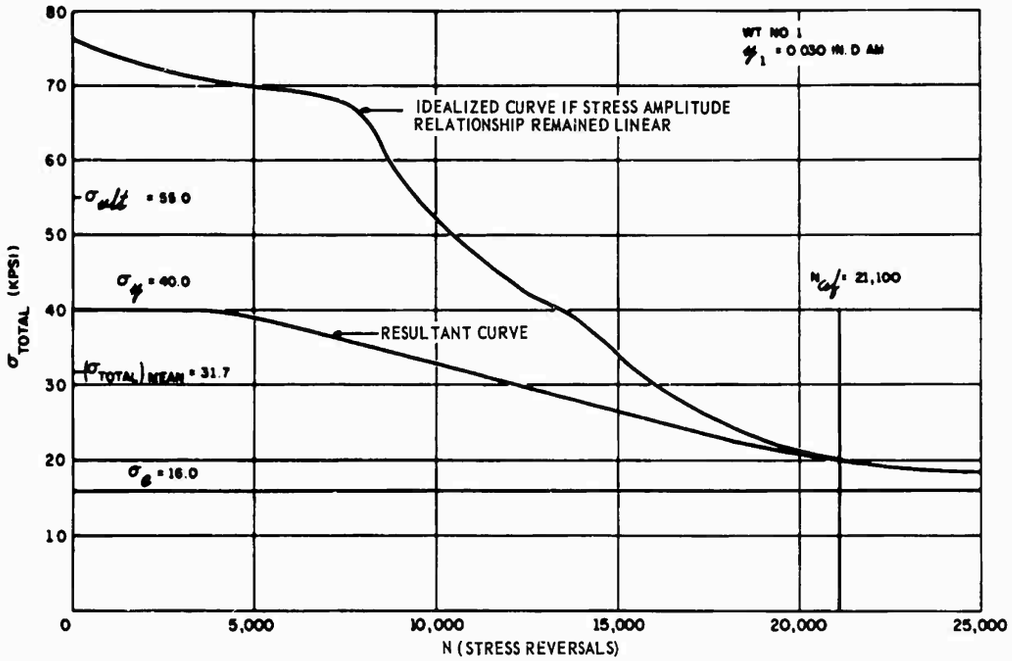

Fig. 4 - Mean time-rate-of-failure

$$K' = \frac{(\sigma_{total})_{mean} - \sigma_{st}}{492{,}000\ (y'_{rel})_{Test\ 18}} = 0.316.$$

The apparent values of σ_{total} for the 18 dwell tests were multiplied by 0.316 to yield the values of $(\sigma_{total})_{mean}$ plotted in Fig. 5.

The summation of N for each dwell test was 2 tf stress reversals.

Reduction of Logarithmic Cycling Data

Sweep Rate Calculations - For logarithmic cycling, the instantaneous applied frequency is of the form $f = f_1 e^{K(t-t_1)}$. For one octave, $e^{K(t-t_1)} = 2$; $K(t - t_1) = 0.692$.

Cycling parameters of the Bruel and Kjaer Vibration Exciter control were as follows:

Angular time rate of logarithmic frequency dial = 0.1931 deg/sec, this is equivalent to 5.178 sec/deg.

Angular spacing of frequency dial = 21.7 deg/octave.

For one octave, $(t - t_1) = 5.178(21.7) = 112.4$ sec/octave.

$K = 0.692/112.4 = 0.006159$; thus $f = f_1 e^{0.006159(t-t_1)}$.

This expression was used for Cycling Tests I through IV, during each of which at least one sweep was accomplished prior to failure. Cycling Tests V and VI each accomplished failure during the first sweep; the times-to-failure were measured, and from these the frequencies at failure were computed. The sweep rate data for the six tests are tabulated.

Stress and Stress Reversal Summation Calculations - A first approximation of a fatigue curve for cold-drawn copper indicated that $\sigma_e \approx 15{,}000$ psi.

Using the linear stress-amplitude relationship,

$$(y_{rel})_e = 2y_{st}\left(\frac{\sigma_e}{\sigma_{st}}\right) = 0.0332$$

(for weight No. 2, used in all cycling tests).

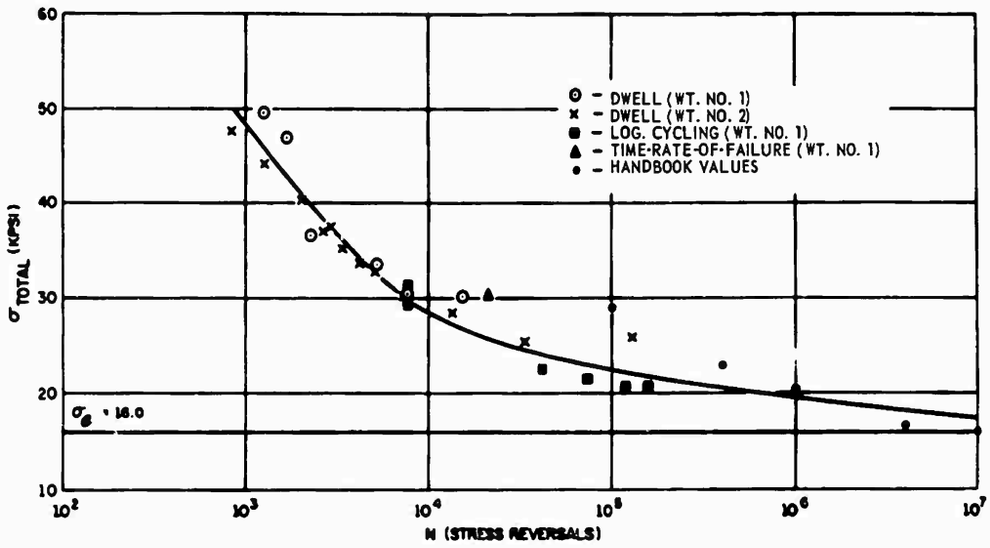

Fig. 5 - Fatigue curve for cold-drawn copper

Using the constant value of y_1 for each of the cycling tests, the values of y_{rel} were computed and tabulated for many values of r. For cases I through IV, values of b were determined using the maximum values of y_2 attained during the first sweep. Thus,

$$b = \frac{1}{2Q} = \frac{y_1}{2(y_2)_{max}} .$$

For cases V and VI, values of b were determined by comparing the buildup rate of y_2 with buildup rates for known values of b. The stress reversal summations were determined for each cycling test by using the following relationship:

$$\frac{N}{2} = \int_{t_1}^{t_2} f dt = \int_{t_1}^{t_2} f_1 e^{Kt} dt = \frac{f_1}{K} \left[e^{Kt_2} - e^{Kt_1} \right] .$$

In order to avoid negative values of N, a value of f_1 could have been selected in each case such that the corresponding value of y_{rel} would be less than $(y_{rel})_e$. Thus, both the "clock" and the "counter" would have been started before significant fatigue-producing stress levels were achieved. Values of t and N were computed and tabulated for each value of r. Six curves of y_{rel} versus N/2 were plotted. These are shown in Fig. 6. The $(y_{rel})_e$ line was drawn in at 0.0332 in. For tests V and VI, ordinates were drawn in at 5775 and 5015 cycles, the respective N/2 values corresponding to the failures which occurred on the first sweep of each. The areas thus formed with base line at 0.0332 in. were measured using a polar planimeter. The values of $(N_f - N_o)$ were multiplied by the number of sweeps to failure to obtain the total number of accumulated stress reversals. After applying the proper scale factor to the areas, they were divided by corresponding values of total $(N_f - N_o)$, thus yielding $\Delta(y_{rel})$ values. Then,

$$(y'_{rel})_{mean} = 0.768 \left[\Delta(y_{rel}) + 0.0332 \right] .$$

Dwell Cycling Correlation for Specimens

The various values of σ were plotted against their corresponding values of N, using both dwell and logarithmic cycling data. A high density of points resulted in the region between $N = 10^3$ and $N = 10^6$. Handbook data were used to fill in the region between $N = 10^6$ and $N = 10^7$. Values for round rotating beam specimen fatigue tests were used since data were not available for cantilever beam tests. The failure rates are different since the surface fibers in a round specimen are equally stressed in a rotating fatigue test and only a portion of the surface fibers are stressed in a square specimen during a cantilever fatigue test. A smooth curve was then plotted which included

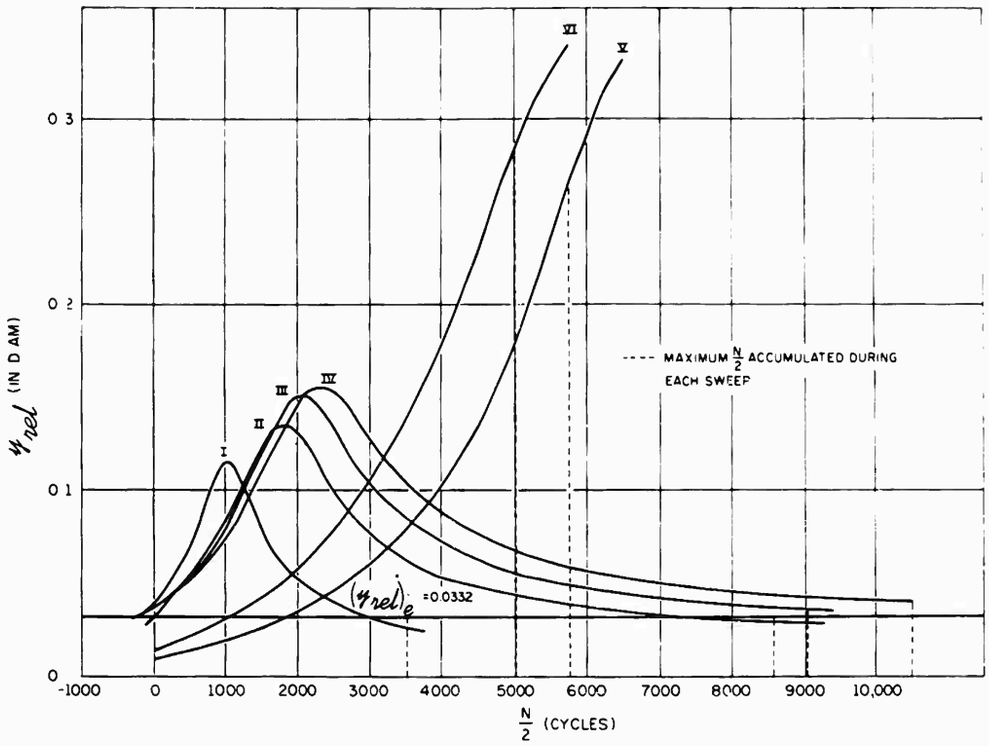

Fig. 6 - Variation of y_1 A.M. with N for logarithmic cycling

the results of all tests. This curve is shown in Fig. 5.

At this point it was possible to predict specimen failures under any prescribed dwell or logarithmic cycling test conditions. Although the curve was limited to the specimen material, it demonstrated that specimen failure can be predicted for other materials.

The program outlined in this paper has been thoroughly documented in Naval Air Development Center Report No. NADC-EL-6323, A Study Program to Modify the Vibration Requirements of Specification No. MIL-T-5422E(ASG), which will be published later.

DISCUSSION

Mr. Himelblau (Nortronics): You mentioned that this work was related to MIL-T-5422E. Will your results have any effect on that document?

Mr. Tait: We are working with Mr. E. L. Sanborn of the Bureau of Naval Weapons, Avionics Division. I would not like to comment but I feel that if Mr. Sanborn were here he might throw some light on this. It is a little bit too early to predict what effect this will have on specification changes. There are some other things we want to do. For example, we are starting to run some random tests on the same samples under the same physical test setup to see what we can learn. I don't want to venture a prediction, but I think that sooner or later there will be an effect, either from our efforts

or from the combined efforts of all who are working in this field. I do think that there will be some changes in the specification.

Mr. Himelblau: Didn't you say that the ultimate use is for the design of avionics equipment?

Mr. Tait: If I said that, I probably should have related it directly to MIL-T-5422E which is not a design specification. MIL-T-5400 is a design specification and the two are more or less related.

Mr. Himelblau: Why did you select simple cantilever specimens rather than complicated avionics gear?

Mr. Tait: That's a good question. The purpose of selecting simple cantilever specimens was that we wanted our initial investigation of this problem to be limited to something where all parameters could be measured readily and with great uniformity. There are, of course, cantilever responses in avionics equipment. There are all kinds of responses. We realize that our simple system is an idealized setup, but certainly representative of avionics equipment in principle if not in direct application. There were some thoughts advanced in the beginning of the program that perhaps we ought to work with a simulated box with various spring mass systems. However, we wanted to conduct so many tests to failure that this presented many difficulties in costs, procurement, and time, as well as getting uniformity among specimens. We found that we had such sufficient control of our simple specimens that we were able to get very consistent results with as few as five specimens for a particular test condition. This is after we got things under control. But I realize that there is much more to be done and I think that certainly some tests should be applied to selected avionics specimens.

Mr. Himelblau: Then I assume that before you decide to make any major changes in regard to avionics equipment you would include such equipment somewhere in your test program?

Mr. Tait: I think there should definitely be more investigation in this direction.

* * *

SIMULATION OF REVERBERANT ACOUSTIC TESTING BY A VIBRATION SHAKER

D. U. Noiseux
Bolt, Beranek, and Newman Inc.
Cambridge, Massachusetts

Random noise testing of structures having a linear response can be simulated by a mechanical shaker. One may do a low-level acoustic test while monitoring vibration at a few critical points, and then excite the structure with mechanical shakers at higher vibration levels to simulate proportionally higher acoustic levels. The need of a low-level sonic excitation may be removed by measuring the radiation impedance of the structure, its mode density, and monitoring the mechanical power applied to the structure by a shaker. Available estimates[1] of radiation impedance and mode density for simple geometries, can be used instead of direct measurements.

Experimental results, using the second approach, are presented. A closed box, with an internal panel is suspended in a reverberant room excited by bands of random noise. The pressure levels in the room are measured together with the vibration level of different points of the box. The same box is then excited by a mechanical shaker, through an impedance head connecting the box to the shaker armature. The electrical outputs of the impedance head are transformed electronically to give the average mechanical power applied to the box. The vibration levels of the box are monitored.

Comparison of the experimental results, for acoustical and mechanical excitation with calculations derived from available theory[1] show encouraging agreement. Extensions and limitations of this technique are discussed.

INTRODUCTION

High level acoustic tests can be simulated with vibration shakers under certain conditions. The basic theory has been presented elsewhere.[2,3] We present here experimental results, with emphasis on the conditions under which these results are valid.

Since the cost of high-level acoustic tests is often prohibitive, a less expensive test with smaller and much more efficient vibration shakers is attractive. In such applications the efficiency of shakers is a few orders of magnitude greater than the efficiency of equivalent sound sources. The shakers would be directly attached to the structure under test (an instrument package for example), while in the case of the acoustic test the prime power has to be converted first into acoustic power with an efficiency of only a few percent; then the power absorbed by the test object is only a small fraction of the total acoustic power available, the remaining power is absorbed by the walls of the test room.

[1] R. H. Lyon, "An Energy Method for Prediction of Noise and Vibration Transmission," Shock, Vibration, and Associated Environments Bulletin No. 33, Part II (1964), pp. 13-25.
[2] D. U. Noiseux, J. J. Coles, N. Doelling, and G. Maidanik, "Dynamic Response and Test Correlation of Electronic Equipment," ASD-TDR-62-614 (Aug. 1962).
[3] R. H. Lyon, G. Maidanik, E. Eichler, and J. J. Coles, "Random Vibration Studies of Coupled Structures in Electronic Equipments - Vol. I," ASD-TDR-63-205 (Apr. 1963).

REVIEW OF THE CONDITIONS TO BE SATISFIED FOR SIMULATION

In the following paragraphs we enumerate and briefly discuss the conditions which must be satisfied by the structure and its environment in order to enable acoustic tests to be replaced by mechanical ones.

1. The acoustic field to be simulated is a random noise with a continuous, but not necessarily uniform, spectrum. The field then is such that it contains most frequency components, and these components are uncorrelated. Moreover, in a given narrow frequency band, the components have approximately equal amplitudes.

2. The acoustic field to be simulated is a diffuse one, that is, in terms of room acoustics, it is a reverberant field. Thus if the structure has a directional preference in accepting acoustic energy from one or the other field components (modes), energy is available to it in that direction in an amount that is independent of this direction.

3. The test structure has many modes within each frequency band, and they are spatially uniformly and randomly distributed throughout the structure. This insures that all modes in the band are excited and that statistically they are excited to approximately equal levels, i.e., the mean response velocities of the modes are approximately equal.

Although these conditions may appear at first rather restrictive, they cover, to a good degree of approximation, many cases of considerable practical interest. For example, they cover cases where instrument packages inside a missile or a jet aircraft are placed in positions where they are subjected to rather random and complex sound fields, which resemble reverberant sound fields in rooms. On the other hand, the instrument package is usually made up of a complicated combination of panels and beams. Such structures would generally satisfy the third set of conditions.

When the conditions stated above are satisfied by the structure and the acoustic field the response of the structure to the acoustic field is proportional to this coupling factor:

$$\frac{\text{average acceleration of the structure (rms)}}{\text{average acoustic pressure (rms)}} \approx \left(\frac{R_{rad}}{R_{tot}}\right)^{1/2},$$

where the average refers to time and spatial averages.

The quantity R_{rad} is defined such that should the structure be set into vibrational motion corresponding to its response, the acoustic power which it will radiate, P_o, is given by:

$$P_o = \overline{v^2} R_{rad},$$

where v^2 is the mean square velocity averaged in time and space of the motion of the structure.

Similarly,

$$P = \overline{v^2} R_{tot}$$

is the total dissipation of power in the structure, that is, the mechanical and the radiation losses.

For well designed structures, R_{tot} should be as large as practical. This may be achieved by damping treatments. On the other hand, R_{rad} is set by the geometry of the structure. Typically, for ribbed panels and boxes made of ribbed panels R_{rad} is an increasing function of frequency until coincidence frequencies of the panels are reached, after which R_{rad} becomes essentially constant as shown in Fig. 1. For the cases where R_{tot} is almost constant, the acceleration response of the structure to constant acoustic pressure level is expected to increase with frequency until coincidence frequencies are reached, then to level off. In contrast, the acceleration response of the structure to acceleration excitation from a shaker should be roughly constant.

In the following sections we introduce different degrees of simulation and present experimental results.

DEGREE OF ACOUSTIC SIMULATION

The degree of acoustic simulation could be related to the use of acoustic sources involved in the simulation. In a low degree of simulation, only acoustic sources are used; in a higher degree of simulation only vibration shakers are involved.

It will also become apparent that for a higher degree of simulation, more information is required about the test structure. And, conversely, as the energy transmission from the acoustic field to the vibration field is better understood better simulation becomes possible.

We will discuss simulation of a high acoustic level by a low acoustic level, simulation of a high acoustic level by a low acoustic level source and vibration shakers, and simulation with vibration shakers only.

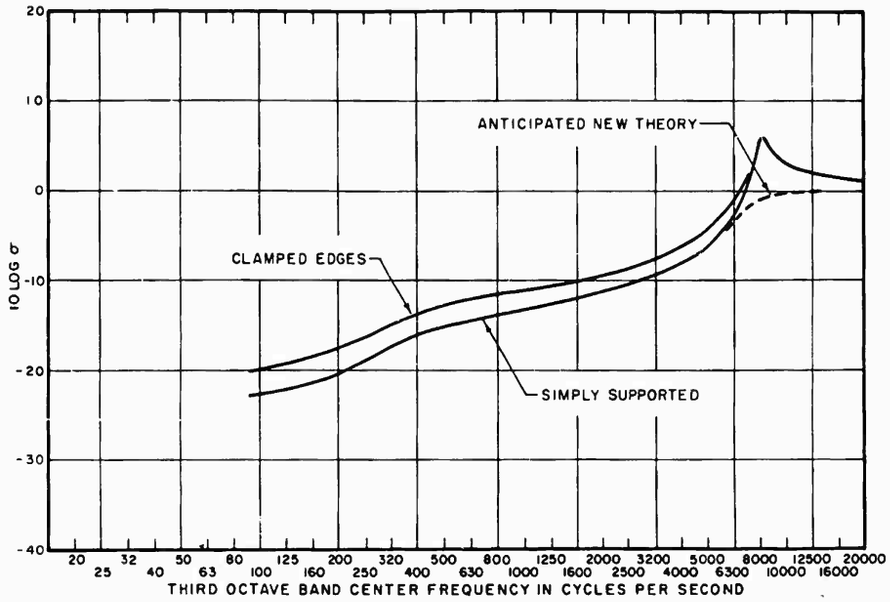

Fig. 1 - Calculated radiation efficiency σ of the box

SIMULATION OF A HIGH ACOUSTIC LEVEL BY A LOW ACOUSTIC LEVEL

This case, almost trivial, and yet most important, requires that the vibration response of the test object be essentially linear. It requires also, in order to draw conclusions from the test, that the failure vibration levels of the critical components be known.

By the expression essentially linear we mean that any actual nonlinearity should have a negligible reaction on the response of the structure. For example, the critical components may be diodes, relays, klystrons, and so forth; the malfunction of such components should not change appreciably the vibration response of the substructure on which they are located.

The simulation test consists of applying a lower acoustic level than the full test would require, with proper field distribution and spectrum. The vibration levels at the critical points are monitored with accelerometers. These measurements are then extrapolated proportionately to the desired high level. These extrapolated values are then compared with the vibration levels at which the critical components would fail.

We have mentioned only the vibration response of the critical components because of the inefficiency of the acoustic pressure around critical components to excite them. Rather the acoustic energy received by the primary structure and transmitted through it to the critical components is dominant. In fact, it is difficult to find a case where the acoustic pressure around the component itself is the cause of its malfunction, rather than the mechanical vibration of whatever the component is mounted on.

The required linearity of response is indeed restrictive. But in many cases, instrument packages which have been designed to provide mechanical strength to low frequency vibrations will almost necessarily have linearity of response at all frequencies when exposed to very high levels of acoustic excitation.

The following example[4] of tests performed on a missile guidance computer will illustrate this case.

This large computer, weighing approximately 200 pounds, had experienced malfunction caused by electrical failures of point contact diodes. The levels at which these diodes would

[4]D. U. Noiseux, C. W. Dietrich, E. Eichler, and R. H. Lyon, "Random Vibration Studies of Coupled Structures in Electronic Equipments - Vol. II," ASD-TDR-63 (submitted Oct. 1963).

fail were investigated separately by vibration tests on the diodes.

The whole computer was subjected to low-level acoustic tests in a reverberant room. Such diffuse field was considered a good approximation to actual environment. The acceleration responses of typical circuit boards were measured inside the computer. The computer was also subjected to direct mechanical excitation at the base of its vibration mounts; the acceleration responses of the same boards were measured. The laboratory results of circuit board vibrations were scaled up proportionately to the levels of excitation and spectrum of both the acoustic field and the vibration excitation of the vibration mounts, which were obtained from actual test firings of the missile.

These results are shown in Fig. 2. The sum (on a power basis) of the response to acoustic excitation and to the direct mechanical excitation is also shown. It is interesting to note that acoustic excitation dominates at high frequencies. Finally, these laboratory results are compared with actual measurements made on the computer during firing. Figure 3 shows this comparison. The agreement is quite encouraging. Shown in Fig. 3 is a range of frequency and vibration levels where diode failures were encountered.

These tests served to show that diode failures were possible under the environment of the computer, and that the acoustic environment at high frequency was the main cause of failure. An interesting point is that these results were obtained with a 20-pound-force shaker and a 50-watt loudspeaker. These sources were found adequate to give sufficient signal-to-noise ratios for all the measurements made.

SIMULATION OF A HIGH ACOUSTIC LEVEL BY A LOW ACOUSTIC LEVEL SOURCE AND VIBRATION SHAKERS

This technique consists of applying first the proper acoustic field at a low level and monitoring the acceleration response of a few points on the test package; then the acoustic field is turned off and small shakers are connected at the location of the monitored points on the test package. Power is applied to the shakers such that the vibration levels of the

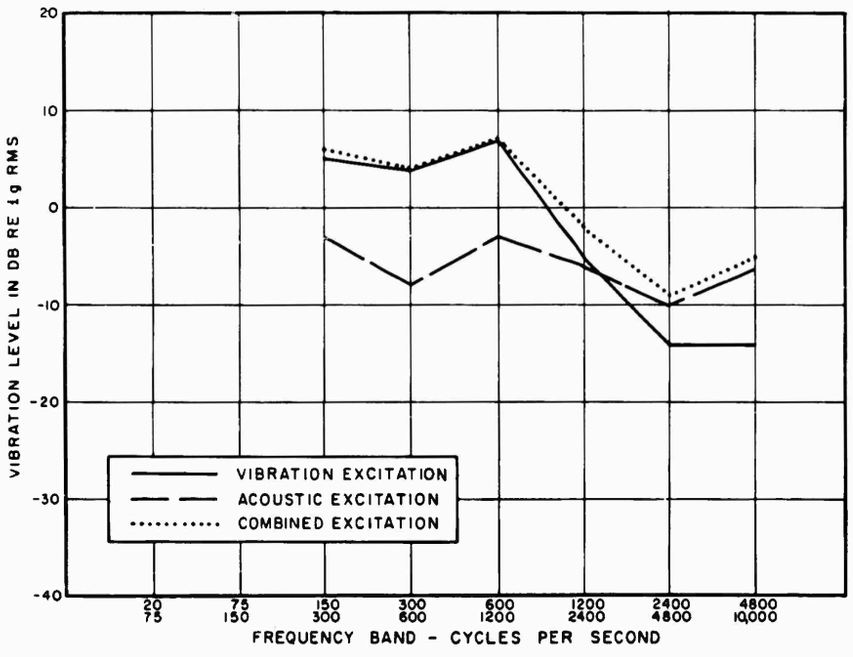

Fig. 2 - Predicted response of board Z219 for acoustic and vibration environment of 75F-9

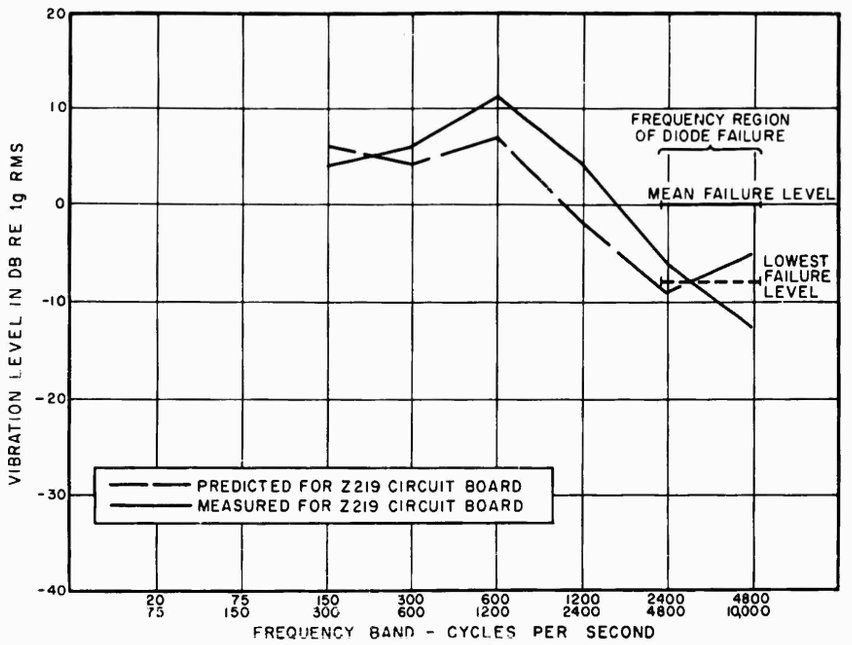

Fig. 3 - Comparison of predicted response of Z219 for 75F-9 and measured response of Z218 from 75F-9

monitored points are heightened proportionally and attain values that would correspond to the desired high-level acoustic field.

This technique assumes that the following conditions apply:

1. Linearity of response which permits scaling the levels of the monitored points proportionately to the desired level of simulation.

2. Complexity and close coupling of the main structure so that only a few small shakers are needed.

One does not need to know the sensitivities of critical components, as was required in the preceding case: the actual vibration levels which would result from the high level of acoustic excitation are obtained with the shakers.

The difficulties of this technique reside mainly in the judicious selection of the attachment points of the small shakers, the number of shakers required, and the spurious loading of the structure by the vibration shakers. It appears that when the structure is rather complex and tightly coupled, such that the vibration field of the test object is essentially a reverberant one, only one shaker would suffice and that its attachment point and the loading at that point are not critical.

SIMULATION WITH VIBRATION SHAKERS ONLY

We consider first a structure composed of an assembly of panels and beams all tightly coupled. We then consider the substructures attached to the primary structure.

Primary Structure

All the conditions listed in the second section now apply. In addition, we need to know the following information:

1. The mode density n_s (number of modes per radian per second) of the test structure.

2. The radiation resistance R_{rad} of the test structure.

The spectrum of the random noise excitation is assumed supplied by a knowledge of the environment.

The mode density n_s of the structure can be obtained by calculations when the structure is essentially composed of panels and beams. Otherwise, it may be obtained by direct measurement; the structure is excited by a small shaker and the acceleration responses of a few locations on the structure are monitored. The excitation is a pure tone which is very slowly swept through the spectrum. By recording the acceleration response on a graphic level recorder, one counts the number of peaks within each segment of the spectrum, e.g., third octave bands. The mode density as a function of the center frequency of these frequency bands may thus be obtained. The technique is rather straightforward. The mode density will be almost a constant since it is dominated by the panels of the structure.

The radiation resistance R_{rad} could either be calculated for simple assembly of panels and beams or measured by the reverberant room technique for measuring the power P_o radiated from a source. Since the power radiated P_o is:

$$P_o = \overline{v^2} R_{rad},$$

and $\overline{v^2}$ is the mean square velocity of the panels of the structure. We can solve for R_{rad} in each frequency band of excitation when P_o and $\overline{v^2}$ can be measured simultaneously. P_o is determined from the reverberant room constants and microphone measurements.

It is not necessary to determine the total loss resistance R_{tot}. This quantity is, however, required if one wishes to predict the acceleration response of the structure to reverberant sound fields. A convenient technique to obtain R_{tot} is to measure in each frequency band the decay rate or reverberation time of the response of the structure when random excitation in frequency bands applied by a shaker is suddenly turned off. The reverberation time T_S, which is the time required for the response to decay by 60 db, yields R_{tot},

$$R_{tot} = \frac{13.8\, M_S}{T_S},$$

where M_S is the total mass of the structure.

Having obtained this preliminary information, it can be shown that the mean square acceleration $\overline{a^2}$ of the structure excited by an acoustic field of mean square pressure $\overline{p^2}$ is given by

$$\overline{a^2} = \frac{n_s}{M_s} \times \frac{R_{rad}}{R_{tot}} \times \frac{2\pi^2 c}{\rho} \times \overline{p^2},$$

where ρ and c are the ambient density and speed of sound.

Since the power input P_{in}, supplied by the acoustic field to the structure, is equal to the power dissipated by the structure,

$$P_{in} = \overline{v^2} R_{tot} = \frac{\overline{a^2}}{\omega^2} R_{tot}.$$

We obtain from the equations above

$$P_{in} = \frac{n_s}{M_s} R_{rad} \frac{2\pi^2 c}{\rho\omega^2} \overline{p^2}.$$

In order to simulate the response of the test object caused by a random noise excitation in a reverberant field having a mean square pressure $\overline{p^2}$, one has to supply to the test object, by means of shakers, the mechanical power P_{in} given above. This is done by using an impedance head between the shaker and the test object. The electrical outputs of the impedance head are transformed to give signals proportional to velocity and force, then multiplied together and the result integrated to yield the average power P_{in}. Figure 4 shows the instrumentation used to obtain the average input power.

Substructure

The substructure could be for example an electronic circuit board.

Following the same pattern, the modal energy exchange between the main structure and a substructure is related by a coupling factor which is similar to the ratio R_{rad}/R_{tot} used in the case of acoustic excitation. Here, however, the source of excitation is the primary structure, the receiver is the substructure, and the coupling resistance replaces the radiation resistance. The coupling factor is more easily expressed as a ratio of loss factors η which are related to the reverberation time T by

$$\eta = \frac{2.1}{fT},$$

where f is the frequency. For simple connections between plates we obtain the expression

$$\frac{\overline{v_{ss}^2}}{\overline{v_s^2}} = \frac{n_{ss}}{n_s} \frac{M_s}{M_{ss}} \frac{\eta_c}{\eta_c + \eta_{ss}},$$

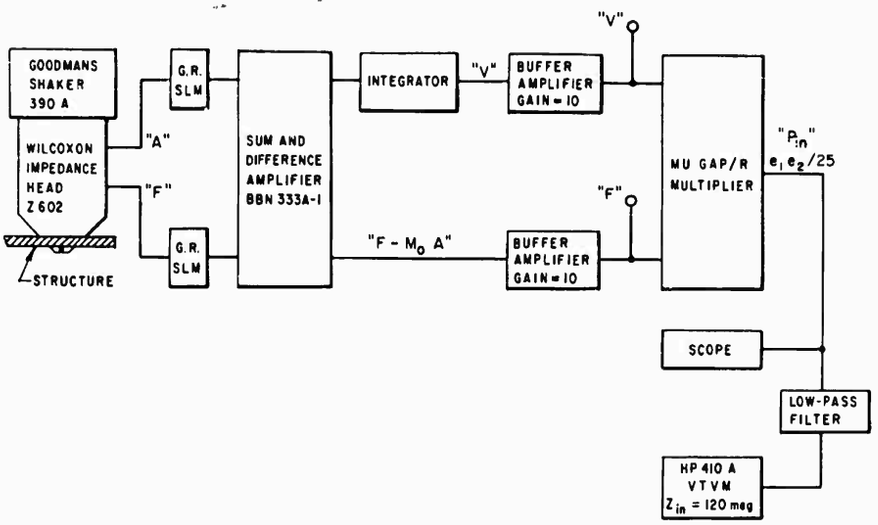

Fig. 4 - Multiplier circuit diagram

where subscript s referred to the main structure, subscript ss to the substructure, and subscript c to the coupling.

Example[4]

As a controlled experiment a closed metal box was fabricated, containing an inside panel tied by studs to two opposite sides of the box. The dimensions of the box were approximately $12 \times 16 \times 18$ inches.

The box was tested in the acoustic field of a reverberant room and its acceleration response was measured. The radiation resistance and mode density of the box were calculated. The reverberation time of the box was measured. The response of the box was then calculated as indicated above.

Figure 5 shows the reverberation time of the box. In Fig. 1 the radiation resistance is given as a radiation efficiency (ratio of radiation resistance to outside area of the box and the acoustic impedance ρc). Figure 6 compares the calculated and the measured acceleration response of the box to acoustic excitation. This result illustrates that the response of the box to acoustic field can be predicted, although the accuracy in this particular case is not very high.[5]

We proceed to simulate the response of the box to acoustic excitation by using only vibration shakers. Only one shaker is used because the box is a tightly coupled structure. The criterion consists of comparing the calculated and the measured value of mechanical power required to give the same acceleration response of the box. If these two values of power agree, then the simulation is successful. If the acceleration response used as a base is the one obtained by acoustic measurement as shown in Fig. 6, the degree simulation would be only partial, because an acoustic test would have been used. On the other hand, if the acceleration response used as a base is the calculated one of Fig. 6, then the simulation would be complete since no acoustic excitation would have been used. The first result of partial simulation is shown in Fig. 7. The mechanical power calculated from the predicted values of R_{rad} and the measured values of acceleration response of the box to sound pressure are compared with the measured mechanical power required to give the same acceleration response; the agreement is good illustrating that power is the true basis for equivalence.

The second result of complete simulation consists of using as a base the predicted acceleration response of Fig. 6 instead of the measured one. The result is very similar to that of Fig. 7 illustrating that, at least under the conditions stated, a fair simulation of acoustic testing with only vibration shakers is possible.

[5]The results of Fig. 6 were not as encouraging as other measurements on similar structures have previously shown. See for example, the results of Section II in Ref. 2.

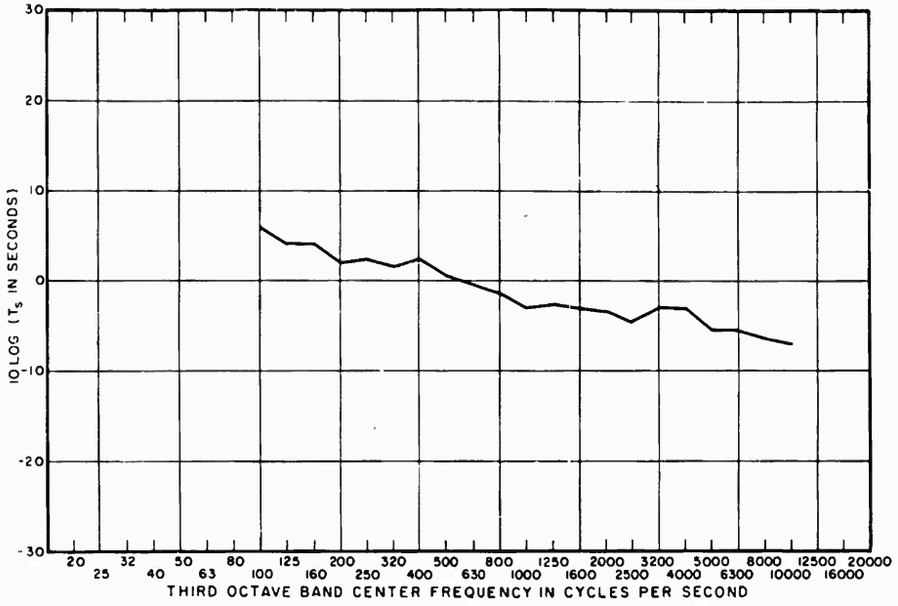

Fig. 5 - Reverberation time of the box

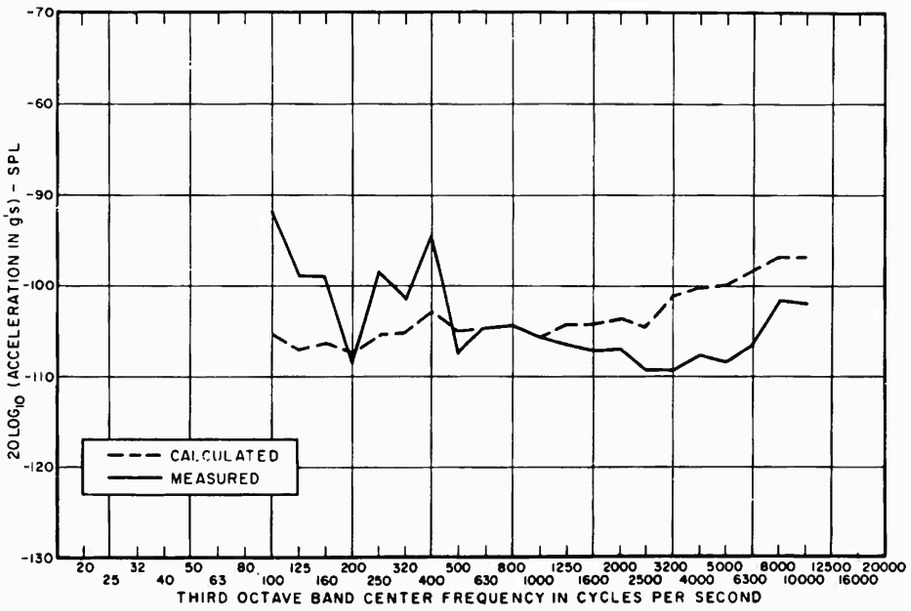

Fig. 6 - Acceleration response of the box to acoustic reverberant excitation

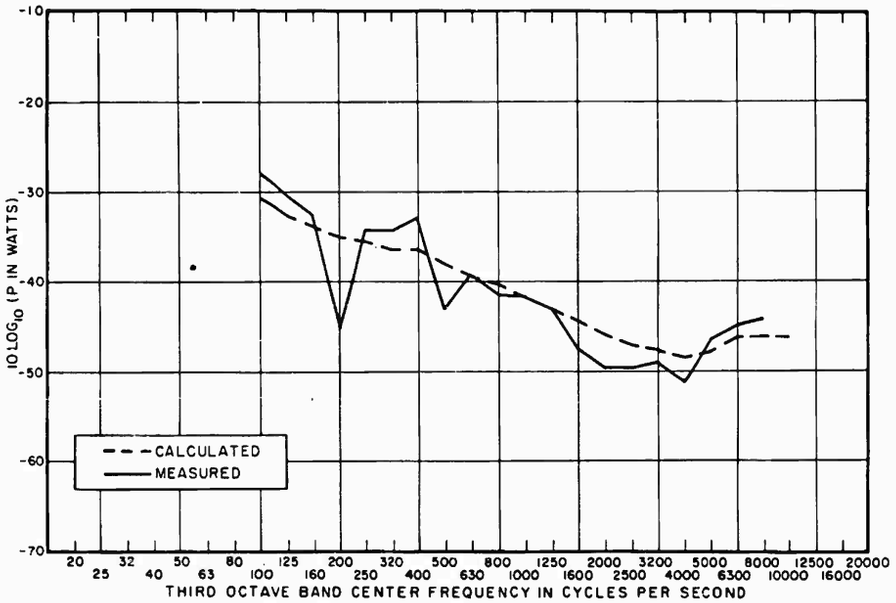

Fig. 7 - Mechanical power in 1/3 octave bands required to simulate 100 db SPL excitation

It is noted that the differences between the simulated test and the actual acoustic tests grow progressively larger at lower frequencies. This is obtained because the frequency bands of excitation used for these tests were of constant percentage bandwidth; since the mode density of the box structure is essentially constant, the lower frequency bands contained fewer modes per band leading to greater uncertainty. It follows also that the present theory does not completely predict the response of the structure at single selected modes. In particular, the level of response of the first mode alone, which is often of much importance because of the large displacements associated with it, is obtained only with considerable uncertainty. Analysis of the limits of these uncertainties form an important area of investigation.

Additional measurements on the same test box gave the ratios of the acceleration of the subpanel to that of the box for two different damping conditions for the subpanel. The predicted ratios were calculated from reverberation time measurements of the subpanel giving the loss factors as shown in Fig. 8. The calculated acceleration ratios are compared with those actually measured in Figs. 9 and 10. Again the agreement is encouraging.

CONCLUSIONS

Different cases of acoustic simulation have been discussed showing progressively higher degrees of simulation up to the case where no acoustic sources are used, but only vibration shakers. Each case has very practical applications.

The attraction of simulating high level acoustic tests with shakers is that the cost of the excitation is drastically reduced. More simulated acoustic tests are then possible. It is also a challenge in that simulation requires a better understanding of the interrelated acoustic and vibration phenomena.

Although the simulated tests now appear capable, in some practical cases, of replacing full scale acoustic tests, the acoustic tests would still be required as a final proof until more investigation provides the detailed knowledge required to make the present simulation techniques a reliable testing tool.

The present approach should also eventually provide guides for the design of complex packages to be exposed to intense sound and vibration excitation. These guides would attempt to

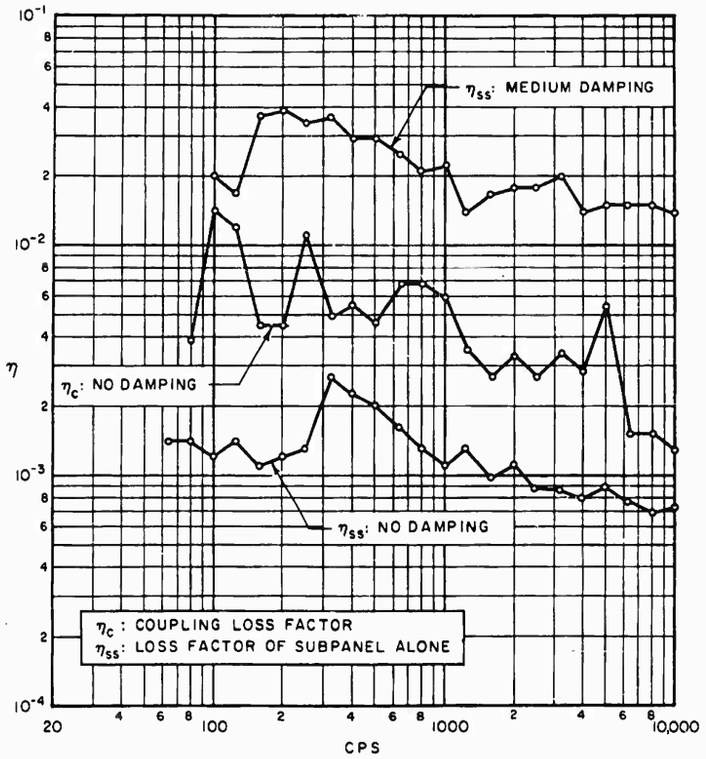

Fig. 8 - Loss factor η of subpanel in third octave bands

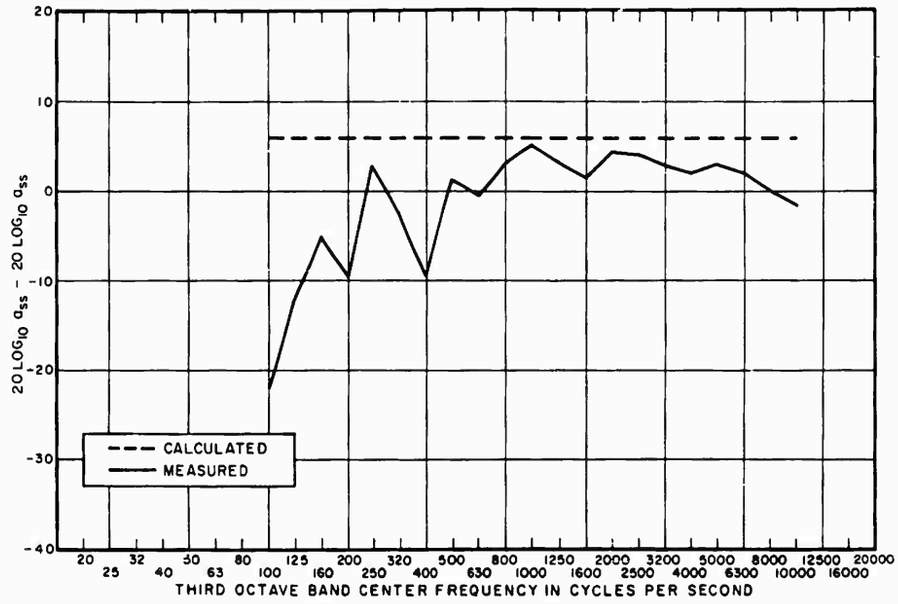

Fig. 9 - Ratio a_{ss}/a_s of accelerations of internal panel and box with negligible damping of the internal panel

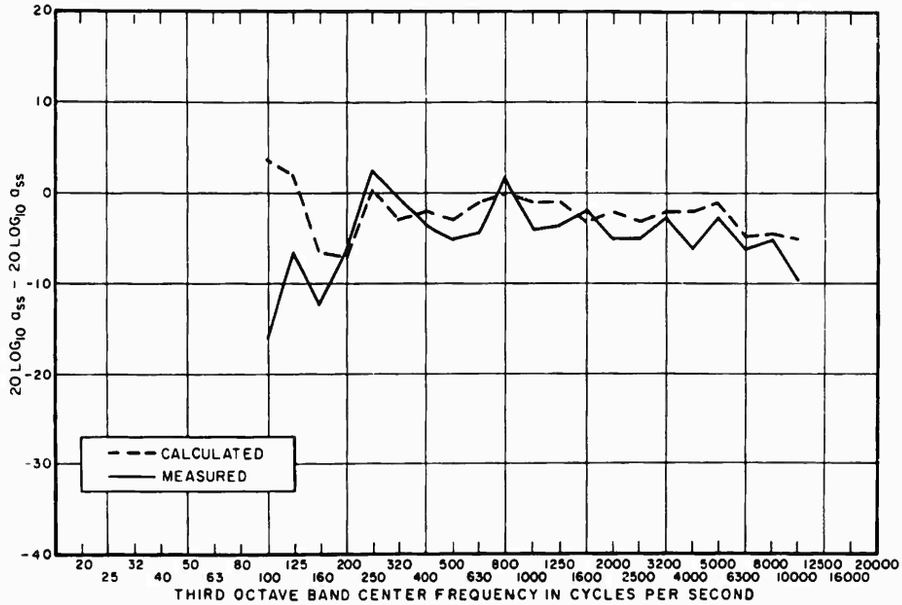

Fig. 10 - Ratio a_{ss}/a_s of accelerations of internal panel and box with medium damping of the internal panel

show how to minimize the coupling between acoustic field and vibration of the structure and between vibration of a substructure and its primary structure.

ACKNOWLEDGMENTS

The collaboration of Messrs. E. A. Starr and C. W. Dietrich in obtaining the measurements reported is gratefully acknowledged. This work was supported by the Aeronautical Systems Division, Air Force Systems Command, Wright-Patterson Air Force Base, Ohio.

DISCUSSION

Mr. Himelblau (Nortronics): I have a question about applicability of the power method. You are dealing here with an investigation of levels over fairly wide frequency bands — octave or third-octave bands. There are structures, however, consisting of electronic components that might be susceptible to certain frequencies within a wide band. How do you deal with the vibration simulation of the acoustical response in this case?

Dr. Noiseux: The technique used is a statistical one. It depends strongly on the average response of the test object over many modes and over many points. We find that the uncertainty of the prediction increases considerably as one wants to look at only one mode or only one point of the structure. Some attempts, with some success, have been made by variational analysis to obtain the limits of this uncertainty, and indeed we hope that more work will be done in this direction.

Mr. Himelblau: If you place your shaker at a particular point, there will be some modes that will be driven better than others. In fact there will be some modes that will not be driven at all. You said that you did not feel that the location of the shaker was critical. Is this on the basis of looking at several modes rather than looking at them individually?

Dr. Noiseux: Indeed, this is the essential basis of this approach. Even in the actual environment inside this missile, the distribution of the acoustic field is unknown. It is so complex as to be impossible of definition. This is why the process of approximating such a field is one which is perhaps even more complex, but complex in a uniform way. There are variations from one test object to another in production. There are variations indeed in the actual time history of the pressure from firing to firing. It seems appropriate to use a field which is a little more general, such as a reverberent field, rather than an actual specific field and its distribution, taken from a specific case of one actual firing. I think this is similar to the custom of using pure tone or sine waves to test a simple amplifier, although it would be used for speech. The test signal is of simpler nature, but is general enough to show the property of the object of interest.

* * *

Section 4
COMBINED TEMPERATURE-VIBRATION TESTS

COMBINED HIGH TEMPERATURE-VIBRATION TEST TECHNIQUES

H. S. Bieniecki and E. Kuhl
McDonnell Aircraft Corporation

The development of a high temperature-vibration test facility to accommodate specimens up to a weight of 200 pounds and to temperatures of about 4000°F will be described. Test procedures will be discussed, as well as the instrumentation and controls used to measure and regulate the vibration and temperature conditions.

INTRODUCTION

The re-entry environment imposes a number of interacting conditions on a blunt-nosed vehicle traveling at hypersonic speeds. Since complete simulation of the re-entry environment is not yet practical, it is important to simulate certain crucial interacting conditions. Dynamic loading at high temperature is one of the conditions that can be reasonably simulated.

The refractories used in re-entry structures are well known for their low mechanical and thermal shock capabilities. In common engineering materials failure begins with plastic flow, creep, or incipient cracking. This provides a certain amount of design latitude. With refractories, however, failure is nearly always catastrophic. Techniques have therefore been developed to confine or restrict refractory failures. One of the oldest techniques is the mosaic approach which limits the size of the structural units so as to avoid thermal gradients high enough to cause any unit to fracture. Some design techniques are also directed toward continued function of the overall structure in spite of the fracture of individual units. The use of composite layers of high to low elastic modulus refractories has had success in certain applications. This technique permits incipient cracking under thermal shock rather than total fracture. From the foregoing it is evident that the added complexity of design or fabrication methods for blunt-nosed re-entry structures makes it mandatory to test each design under a combined high temperature and vibration environment. This is the only present means of obtaining assurance of functional reliability under simultaneous conditions of high thermal and mechanical stress.

DESCRIPTION OF TEST FACILITY

A special test facility was constructed at McDonnell Aircraft to conduct combined high temperature-vibration tests on blunt-nosed re-entry structures. The facility can be arranged to accommodate specimens ranging in weight up to about 200 pounds. Temperature levels of 4000°F can be attained at the present time. The facility is relatively straight-forward in design. It is comprised of two distinct units: one for providing the high temperature environment and the other for providing the vibration environment. A side view of the test facility is shown in Fig. 1.

The high temperature unit had been designed initially for static tests on refractory specimens in general but was readily adapted for use in the combined facility. The unit is of the combustion type consisting simply of a cluster of six standard oxyacetylene heating torches mounted in a small circular pattern to produce a flame about 2 inches in diameter. The torches are housed

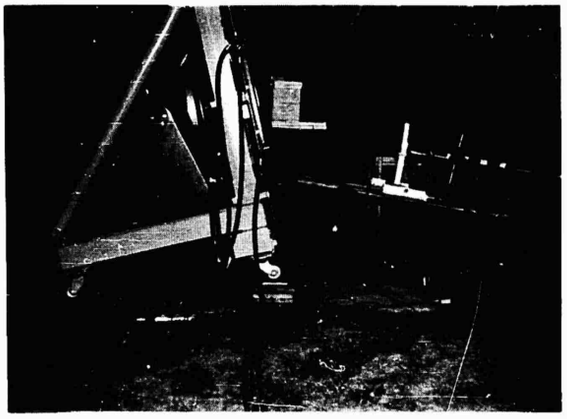

Fig. 1 Side view of the test facility

in a conically shaped, water-cooled, copper heat shield which protects the torches from radiant heating during operation. The flame can be adjusted to produce an oxidizing, neutral, or reducing atmosphere. The heat flux output of the unit is approximately 180 Btu/ft^2-sec as measured by a cold wall calorimeter. Heat flux on the specimen is regulated by varying the distance from the torch unit to the specimen. The torch assembly is therefore mounted on a dolly and rails. The torch assembly can also be arranged for the combustion gases to impinge on the specimen at the desired re-entry angle. Auxiliary equipment for the combustion unit includes manifolded gas supply systems with flowmeters and dual stage regulators capable of maintaining a constant temperature environment for about 6 hours. Electrical valves for instant shut-down of the unit are also provided. Figure 2 shows the combustion unit controls.

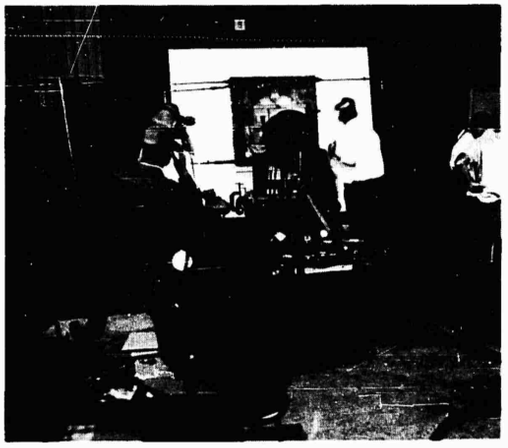

Fig. 2 - View of the facility showing combustion unit controls

The vibration unit in the combined facility is designed around a water-cooled electrodynamic exciter rated at 6000 pounds of force output. The exciter is mounted to a sturdy steel main frame with four leveling screws that permit the exciter to be accurately aligned with the specimen drive fixture. The drive fixture itself is mounted to the main frame on four laminated, beryllium-copper, roll flexures. These flexures permit motion in the horizontal direction but are extremely stiff in the vertical direction to eliminate an overhanging moment on the flexures of the exciter's armature. Figure 3 illustrates the drive fixture mounting.

The drive fixture was fabricated of 1/4-inch stainless steel plate and is basically a cylinder greatly stiffened internally with a spoke or spider type of construction. Brackets are included at the sides of the cylinder for attaching the roll flexures and a flange is located at the rear for mounting to the exciter. At the specimen end of the fixture a water-cooled chamber was provided primarily to keep the specimen mounting bolts cool enough to hold the specimen reliably and also to prevent any serious heat conduction back to the exciter. Blind access tubes, just large enough for a socket wrench, were provided through the cooling chamber to permit mounting the specimen. A large flat tube was also provided to bring out a group of specimen thermocouple leads and pressure tubes. The specimen mounting face on the fixture had to be carefully machined to receive the specimen. Subsequent tests require inspection

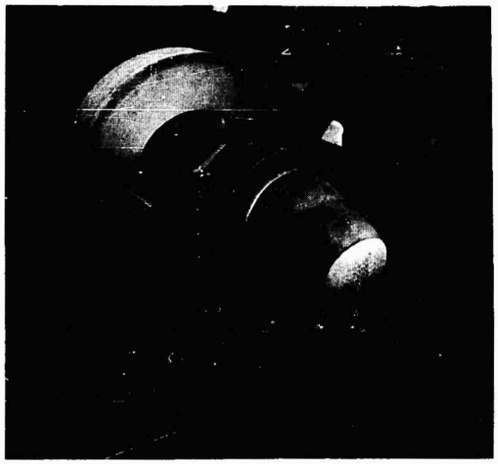

Fig. 3 - Drive fixture shown mounted to frame on beryllium-copper roll flexures

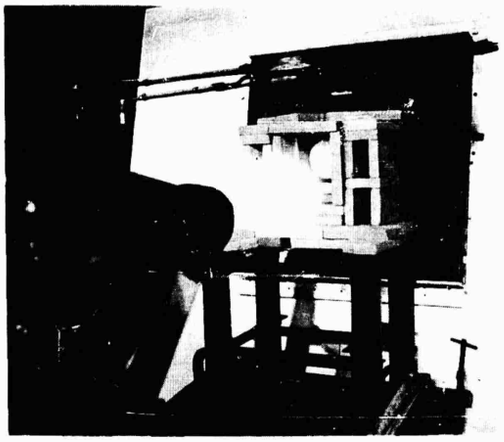

Fig. 4 - Circular primary heat shield mounted on the square secondary heat shield

and re-machining to avoid specimen chatter from the imposed vibration environments.

The exciter unit was protected generally from the combustion unit by a broad steel plate. The real problem, however, lay in absorbing and dissipating the entire heat output of the combustion unit within less than a foot of the torch nozzles. This was accomplished by employing a primary heat shield, or heat sink, contoured to the mold line of the test specimen. This shield, which receives the torch blow-by directly off the specimen, is a high capacity unit constructed of copper plate and tubes and is manifolded at top and bottom for symmetrical single pass flow. This primary shield is mounted to a larger secondary shield which is also water cooled and of copper plate and tube construction. The secondary shield is in turn mounted to the broad steel plate covering the entire frame. Figure 4 shows the heat shield arrangement. Insulation blankets and sheet insulation collars are used behind the secondary shield as additional protection and as seals around the drive fixture. The drive fixture, primary heat shield, and secondary heat shield each have their own cooling water supply in addition to that required for the exciter and for the combustion unit.

The electro-dynamic exciter is controlled by a water-cooled accelerometer mounted at the specimen end of the drive fixture and is backed up by another accelerometer in the exciter mounting head. An automatic programmer permits a continuous logarithmic sweep of five different levels of any combination of displacement and acceleration within the exciter capabilities. Random excitation can also be provided.

PROCEDURE

In the test procedure, a checkout of the vibration unit is first conducted with a dummy specimen. The drive fixture is then dismounted, the test specimen is installed, and the drive fixture is remounted with the test specimen. Specimen flight thermocouple leads are next connected to automatic recording oscillographs. (Pressure leads were neglected in this series of tests.) The vibration and combustion units are positioned to give the desired re-entry angle simulation. A refractory brick shroud is then constructed around the specimen to minimize heat losses and provide protection against air gusts. Figure 5 shows the shroud during a test at about 4000°F. Surface temperatures on the specimen are monitored by an optical pyrometer. Temperature levels and heating rates are controlled by manually varying the torch to specimen distance. When the required test temperatures are reached and stabilized, the specimen is subjected to the appropriate vibration spectrum. Pyrometer observations of the specimen surface temperature are periodically recorded and significant changes in the specimen are noted as they appear. The actual vibration environment applied, as seen by the forward accelerometer, is plotted automatically during the test. Figure 6 shows an overall view of the test facility in operation.

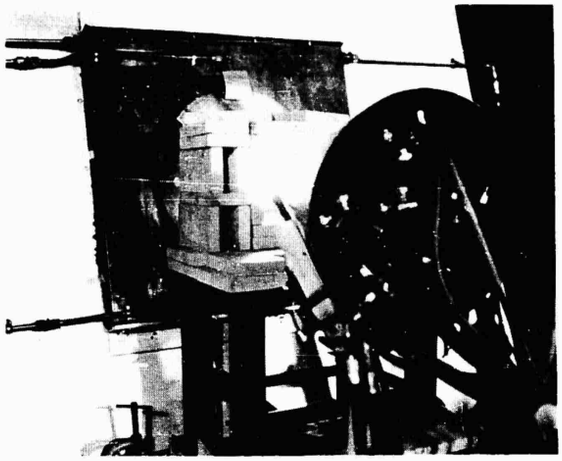

Fig. 5 - The refractory brick shroud minimizes heat losses in approaching higher temperatures

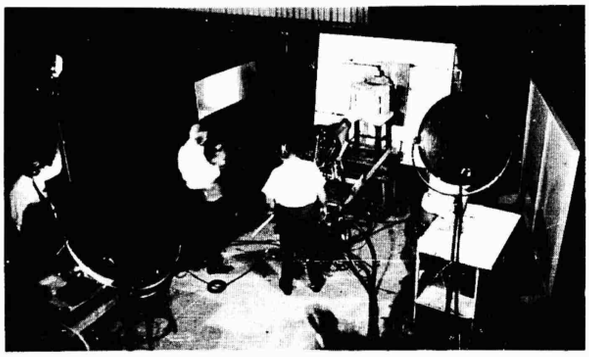

Fig. 6 - Overall view of the test facility in operation

CONCLUSIONS

There are certain areas of refinement that can be made in the technique and in the facility. It would be very desirable to have powered rather than manual control over the heat flux, and this refinement is in the design stage. This would permit much better simulation of the time-temperature profile. A new singular heat source capable of much higher test temperatures is already under construction. Better simulation of the vibration aspect of the re-entry environment of course has to wait on actual flight data for a given design. To reduce setup time mechanical refinements for simpler mounting and dismounting of the test specimens would be very desirable.

* * *

COMBINING INDUCTION HEATERS WITH EXISTING ENVIRONMENTAL FACILITIES TO CONDUCT TESTS AT RE-ENTRY TEMPERATURES

C. D. Robbins and E. L. Mulcahy
LTV Military Electronics Division
Dallas, Texas

Amplifiers designed to drive electrodynamic vibration exciters can be used to power induction heaters. This paper will present both history and theory of operation of the induction heater. Design parameters of efficiency, skin effect, hysteresis, temperature gradients, insulation, and safety will be briefly discussed. Details will be presented on susceptor technique, induction coil design, utilization of existing amplifiers to excite the coil, and illustrations of actual tests.

INTRODUCTION

During the course of high temperature materials development work at Ling-Temco-Vought, it became necessary to carry out environmental tests of various materials to verify their reliability under severe operating conditions for which they were designed to operate. Of particular interest was the combined vibration and temperature environment encountered during re-entry of a space vehicle. Heat shields and leading edges of such vehicles are exposed to severe vibration and temperatures in excess of 3000°F. Heretofore these two environmental conditions have been simulated separately with no attempt to combine them. The advantage of such a test facility is that conditions similar to those occurring during vehicle flight can be duplicated in the laboratory.

The initial effort to build such a facility was tailored to the requirements for testing a particular nose cone. An induction furnace was combined with an electrodynamic vibration exciter to provide the desired environment. Subsequent tests of the system have proved it to be adaptable to a wide range of transient re-entry temperature and vibration conditions. The work was accomplished by Military Electronics and Astronautics Divisions of Ling-Temco-Vought, Inc., Dallas, Texas.

DESIGN REQUIREMENTS

The furnace was designed to heat a 100-pound ceramic nose cone to a maximum temperature of 3600°F, create specified temperature gradients, and be located so that vibration could be applied in one axis only—perpendicular to the principle axis of the nose cone. The time-temperature and time-vibration level profiles are shown in Fig. 1. The temperature shown in Fig. 1 is for the stagnation area on the nose cone as shown in Fig. 2. The time-temperature profile for other locations noted in Fig. 2 are shown in Fig. 3.

These temperature and vibration profiles were established from analyses of the proposed flight for the nose cone during re-entry. It should be noted that the test conditions are transient and the time-temperature profiles for the nose cone show a cooling condition while undergoing vibration, i.e., the nose cone has passed the maximum temperature level before being subjected to vibration.

SELECTION OF HEATING METHOD

In the early design stages of the re-entry test facility the furnace types considered were resistance, gas, and induction. Previously, a

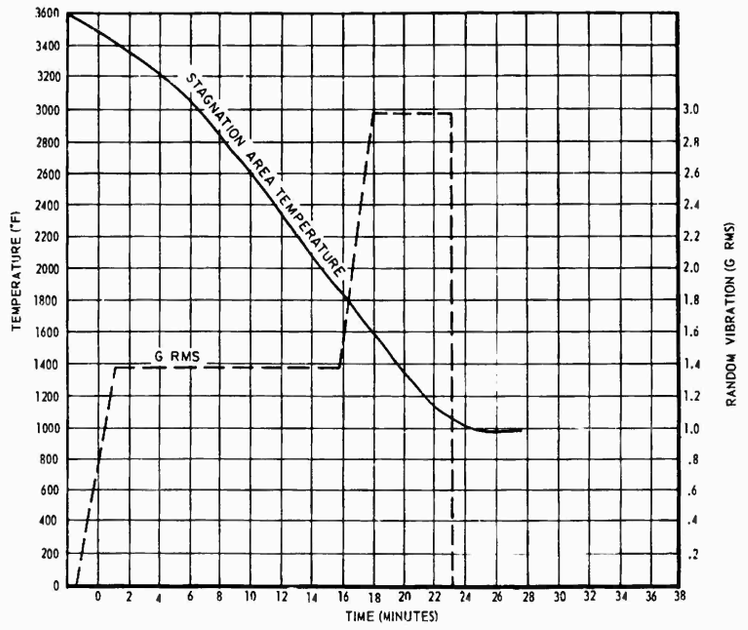

Fig. 1 - Test Condition

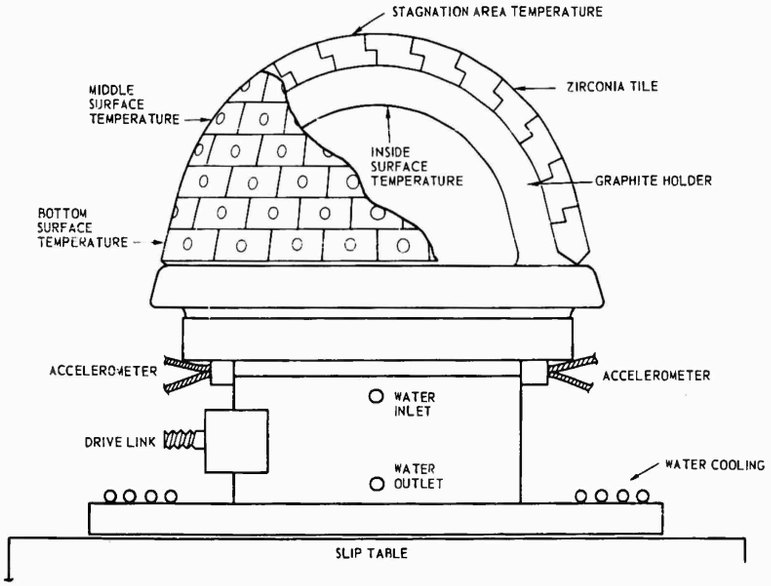

Fig. 2 - Nose Cone-Fixture Assembly. The outside cone surface is a layer of zirconia tile attached to a graphite inner shell by zirconia pins. The graphite holder is bolted to a molybdenum ring below which is bolted to the fixture. Water is circulated through center portion of fixture and tubing welded to base plate which also served as slip plate. Endevco 2206 water cooled accelerometers monitored vibration.

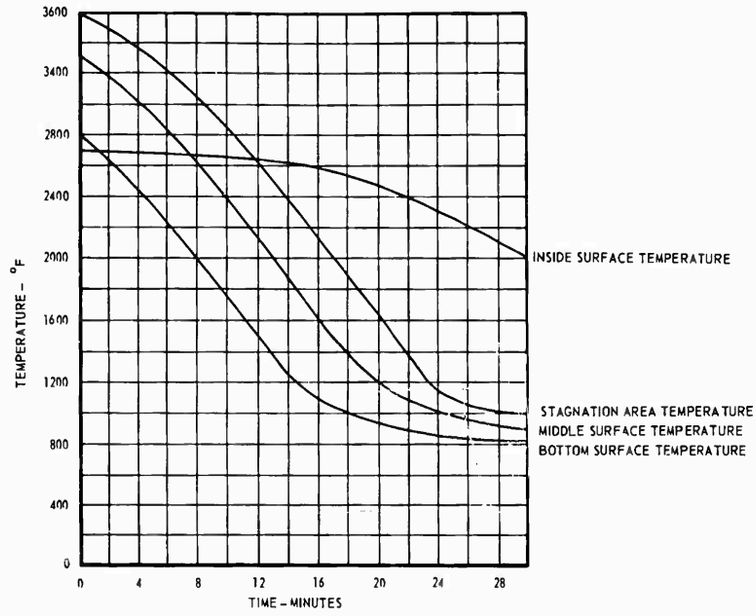

Fig. 3 - Temperature Profiles. Temperature versus time for the locations shown in Fig. 2.

propane furnace had been developed and successfully used for conducting re-entry tests on nose cones.[1] Primary limitations of this type furnace were the complex thermal shielding required to protect the vibration equipment, lack of precise temperature control, and difficulties in creating the required temperature gradients. Resistance furnaces were ruled out because of the oxidation problem of heating elements at temperatures in excess of 3000°F unless an inert atmosphere was maintained in the furnace. The induction heating technique was chosen because the required temperature of 3600°F could be obtained and suitable power supplies already existed in the Test Laboratories in the form of variable frequency power amplifiers designed to drive electrodynamic vibration exciters. Thus the cost for adding a high temperature furnace to the existing vibration equipment was that required to build the induction susceptor, coil and support structure and purchase relatively inexpensive electrical equipment to match the induction coil to an amplifier.

[1] C. F. Hanes, "A Technique for Performing Vibration Tests at High Temperatures in Excess of 3500°F," Shock, Vibration and Associated Environments Bulletin No. 33, Part III (March, 1964), p. 153.

INDUCTION HEATER DESIGN

Susceptor

To heat the ceramic nose cone a susceptor was required since the nose cone material, being electrically nonconductive, could not be heated directly. The susceptor technique allows a conducting material to be heated inductively while it in turn radiates energy to the test article. A large number of conducting materials may be heated inductively; the conditions of the test dictate which material will be most suitable. In this case the material was required to withstand an operating temperature of 3600°F in an oxidizing atmosphere. Graphite proved to be the best available material. It is relatively inexpensive and can be machined easily to the required shape. A cross sectional view of the susceptor and induction coil is shown in Fig. 4. It was positioned so that approximately 1 inch of clearance existed between the susceptor and nose cone. The contour of the inside surface of the susceptor was the same as the nose cone.

Oxidation resistance coatings are available which will protect graphite to approximately 3000°F. At a temperature of 3600°F oxidation is a problem; however, in this particular

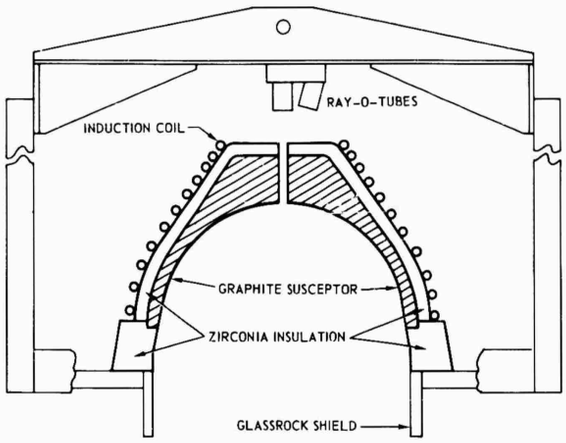

Fig. 4 - Furnace Assembly. Inside susceptor surface contour was that of the nose cone. Graphite thickness was greater at the top because a cylindrically shaped coil is more efficient than one conically shaped. The glassrock reduced the heat loss between furnace and fixture. Ray-o-tubes were aligned with susceptor holes for temperature monitor.

application the rate of oxidation was such that the operational life of the susceptor was greater than the time required to accomplish all calibrations and tests. Therefore, no coating was applied, however, the layer of zirconia insulating paste applied to the exterior surface provided some oxidation protection.

Frequency Selection

After choosing the susceptor material an operating frequency of 3000 cps was selected. This frequency readily lends itself to heating minimum wall thicknesses of approximately 1 inch. Operation at a lower frequency would have required thicker susceptor walls, thereby adding excessive mass to the system and causing a longer response time. In addition, this frequency was compatible with the capability of the Ling PP175/240 power amplifier which was available in the Testing Laboratories. Also, electrical equipment rated at 3000 cps was readily available for tuning the induction coil to the amplifier.

Coil Design

The coil consisted of 15 turns of 5/8-inch copper tubing which was shaped around the susceptor as shown in Fig. 4. The coil was held in place on the susceptor by clamps made of asbestos board to prevent coil movement when power was applied. The coil was water cooled.

Temperature Gradients

The induction coil was designed to create the temperature gradients on the nose cone specified in Fig. 2. The coil windings were concentrated in the areas where the higher temperatures were required so that greater power density was induced in that area. The surface temperature at any particular area on the nose cone was predominately influenced by the temperature of the corresponding area on the susceptor.

Tuning Circuit

It was necessary to tune the furnace coil to the power amplifier. First, the coil was tuned by adding capacitors in parallel so that the lagging power factor of the coil could be corrected. Then an auto-transformer was selected to provide the correct voltage and current required at the furnace.

Furnace Support Structure

In order to meet the required test conditions, controlled cooling of the nose cone after it was heated to the maximum temperature was provided by making the furnace movable in a vertical direction, i.e., it could be gradually raised, allowing the nose cone temperature to follow the required profile. The lower portion of the structure contained the capacitors and auto-transformer. To the lower structure was attached a frame-work which extended up and over the vibration slip table. The framework had vertical guide rails in which the furnace carriage could be moved by an overhead hoist.

Furnace Temperature Control

Temperature control of the furnace was accomplished manually by the standard master gain potentiometer on the power amplifier control console.

INSTRUMENTATION

The nose cone and susceptor were instrumented with high temperature thermocouples, where operating conditions made it possible. Optical temperature measuring devices, such as Ray-o-tubes and Shawmeters, were used elsewhere. Instruments were connected to strip chart recorders for continuous recording of temperature.

VIBRATION FIXTURE

In order to carry out vibration tests on the nose cone while it was being subjected to the re-entry time-temperature profile, a special water-cooled fixture was designed and built as shown in Fig. 2. The center portion, which was welded to the base, was in the form of a pipe with 1-inch wall thickness. Water was circulated through the fixture. The bottom of the $24 \times 24 \times 2$ inch base plate was finished for use directly on a slip table. Water was circulated through tubing welded to the base plate for additional cooling. The nose cone was bolted to the fixture. A drive link connected the vibration exciter to the center of gravity of the fixture and nose cone. High temperature, water cooled accelerometers were mounted on the fixture for vibration control and data acquisition. These accelerometers were calibrated to 1850°F preceding the test.[2]

TEST PROCEDURE

Since vibration was applied during the time the nose cone was cooling, only one amplifier was required. The procedure for testing the nose cap was to connect the induction heater to a Ling PP175/240 power amplifier and heat the nose cone to the conditions indicated at t = 0 on Fig. 3. This required 90 minutes with a peak power demand of approximately 70 kw. Then the amplifier was switched to a Ling L-200 vibration exciter and the vibration test was initiated. The nose cone temperature was controlled by gradually raising the furnace while the required vibration level was programmed to the nose cone fixture. Temperature and vibration data recorded throughout the test were analyzed later for verification that the test requirements had been satisfied.

REVIEW ON INDUCTION HEATING

Induction heating has been used widely as a production tool for many years but now is becoming a tool for satisfying some of the complex heating requirements associated with today's advanced materials research programs. Its main advantages include fast heating rates, high power densities, and accurate temperature control. Induction heating takes advantage of the phenomena called skin-effect and electromagnetic induction. Skin-effect is a term describing the current concentration near the surface of a conductor when a rapidly alternating current flows in the conductor. Electromagnetic induction, discovered by Michael Faraday, is an effect produced by varying a magnetic field in an electrical conductor (susceptor). This effect in turn produces a current in the conductor. The result is a method for heating an object by using the object as its own heat source. Furthermore, the method requires no physical contact or heat transfer by radiation, conduction, or convection between the object and the energy source.[3]

---

[2] W. R. Taylor and C. D. Robbins, "Calibration of Water Cooled High Temperature Accelerometers," Shock, Vibration and Associated Environments Bulletin No. 33, Part III (March, 1964), p. 19.

[3] P. G. Simpson, Induction Heating (McGraw-Hill Book Co., New York, 1960).

Power Supplies

Most induction heating applications require a power supply with a frequency between 60 and 450,000 cps. For low frequency the skin-effect is less pronounced and is used primarily for through heating of large objects such as billets. Frequencies near 450,000 cps generally have been used for surface heat treating of metals because the skin-effect is greatly pronounced, causing the heat to be generated near the surface. Frequencies from 1000 to 10,000 cps are widely used for induction furnaces. Frequency converters are used when a frequency other than the supply frequency is required. Motor-generators are the usual means of frequency conversion from 1000 to 10,000 cps while oscillator circuits are used for frequencies to 450,000 cps. The choice of frequency depends on available power supplies, susceptor size and material, power density requirement, degree of skin-effect required, and heating efficiency.

Heating Effects on Material

The characteristics of a material such as electrical and thermal conductivity, specific heat, emissivity, resistivity, and permeability play a large part in induction heating. A material must be a conductor or semi-conductor to be inductively heated with standard frequencies. The degree of skin-effect or current depth is a function of frequency, resistivity, and permeability. Thermal conductivity and resistivity play a large part in the establishment of temperature gradients. Thermal conductivity of the material also determines the power requirement.

Susceptor Technique

When the specimen cannot be heated directly by induction, a technique often is used in which a susceptor is employed to provide indirect heating to the specimen. The susceptor, which is heated inductively, heats the specimen by radiation, conduction, and convection. A susceptor is chosen which is compatible with the required environment and specimen. It usually is shaped around the specimen with thickness dependent upon the current depth penetration. The susceptor also must have a continuity path parallel to the induction coil. If a crack develops across this path, the susceptor is rendered useless.

Oxidation often becomes a severe problem when high temperatures are involved. Inert atmospheres can be introduced to some tests in order to avoid oxidation. Coatings are available for many materials which will inhibit oxidation for extended periods at temperatures as high as 3000°F. For example, graphite and molybdenum can be coated effectively with silicon carbide and molybdenumsilicide, respectively.

Coil Design

After the characteristics of the power source and susceptor have been determined, the induction coil can be designed. The coil must be matched to both the power source and load. The number of turns can be calculated or in many cases, since coil is very inexpensive, determined by trial and error. When the power source has a fixed frequency and power output, tuning capacitors and a matching transformer may be required.

The coil is usually made from water-cooled copper tubing which is shaped around the susceptor in a fashion which gives the desired heating effects. Factors to be considered are susceptor size, shape and material, power density, temperature gradients, coupling efficiency, voltage breakdown, and cooling requirements. Literature is readily available on the above named parameters for calculating the coil design.

CONCLUSION

It has been shown that the requirements of a power source for an induction furnace are that it have suitable frequency and power output. Most environmental laboratories are equipped with a variety of power amplifiers designed to drive electrodynamic vibration exciters. These same amplifiers also are suitable for powering induction furnaces. Temperatures as high as 5000°F are possible with much less cost than may be realized. For some tests, induction heating has many advantages over other heating methods. The coil, and even the susceptor in most cases, can be designed and fabricated by laboratory personnel. The coil is very inexpensive and can be made into a variety of shapes. The most expensive items will be the tuning capacitors and matching transformer. For many heating requirements, however, the amplifier may have such a surplus of power that little attention has to be given to the efficiency of the system. The furnace can be controlled by the existing amplifier console.

All tests performed in the LTV Testing Laboratories utilizing the methods outlined above have been very successful.

Mr. Bieniecki (McDonnell): What is the upper limit of this system in temperature?

Mr. Robbins: We feel that with this particular setup we can go up to five thousand degrees. At that temperature the particular susceptor which we have wouldn't last very long.

* * *

THE NEL EXPERIMENTAL VIBRATION TEST STAND FOR USE IN CHAMBERS*

A. A. Arnold
U. S. Navy Electronics Laboratory

INTRODUCTION

The NEL experimental vibration test stand for use in environmental chambers was designed to provide reliability engineers with a simple and relatively inexpensive test facility which will enable them to investigate the effects of combined environments on equipment failure-rates. It provides for the type of vibration designated for "AGREE" testing except that it goes beyond the nominal levels of the "AGREE" tests by allowing for variable accelerations up to 5.00 g (in the 20- to 33-cps range) combined with temperatures from minus 65° to plus 200°F at relative humidities ranging up to 95 percent.

The test stand described herein was intended to be used in the vibration testing of two or more small electronic equipments such as small radio transmitters, receivers, and the like, simultaneously, while the equipments are experiencing extremes of temperature and humidity. It can also be used in testing sub-assemblies and component parts as well as various mechanical devices; utilizing one or both tables of the test stand.

GENERAL DESCRIPTION

The test stand is a portable (reaction-type) vibration machine which can easily mount into most any environmental chamber that has a substantial inner floor which will support 600 pounds or more of dead weight (the need for a massive foundation is not required for mounting a small reaction-type vibration machine). The inside dimensions of the chamber should be approximately 36 × 36 × 36 inches. The vibration generator is driven with an external drive motor (1/2 hp, "THY-MO-TROL" controlled) by way of a flexible drive shaft and a sealed bearing assembly through the side wall of the chamber. This particular motor and control was readily available and was the method used for varying the frequency of vibration and accelerations. Almost any type of variable speed drive could be used.

The test stand has two 24- × 24-inch tables (stacked one above the other, see Fig. 1) and weighs approximately 150 pounds (including the vibration generator, but excluding the chamber adapter plate and suspension system). It can easily be removed from the chamber by unfastening four suspension bolts and uncoupling the drive shaft by means of two set screws.

The main table, Fig. 2, of the vibration machine is suspended on four, low frequency, all metal vibration isolation mounts. The vibration generator which is an integral part of the main table has two flywheels (one at each end of a common shaft). Eccentric weights are affixed to each flywheel and the amount of vibration amplitude, for any particular load, is controlled by varying the mass of eccentric weights. The correct amount of eccentric mass required for any desired amount of vibration amplitude can almost always be obtained by selecting the right combination of weights from the ten pairs of weights that are furnished with the machine. This process requires a few simple calculations; however, for most reliability testing, there is seldom any need to change the weights. One of the inherent features of the reaction-type vibration machine is that any preset amplitude of vibration remains practically constant throughout the useful frequency range. This may or may not be a desirable feature (depending on the type of testing to be done) but it does permit varying the acceleration level without changing the eccentric weights.

In order to restrain the movement of the vibration machine within the chamber, the chamber adapter plate is equipped with four

*This paper was not presented at the Symposium

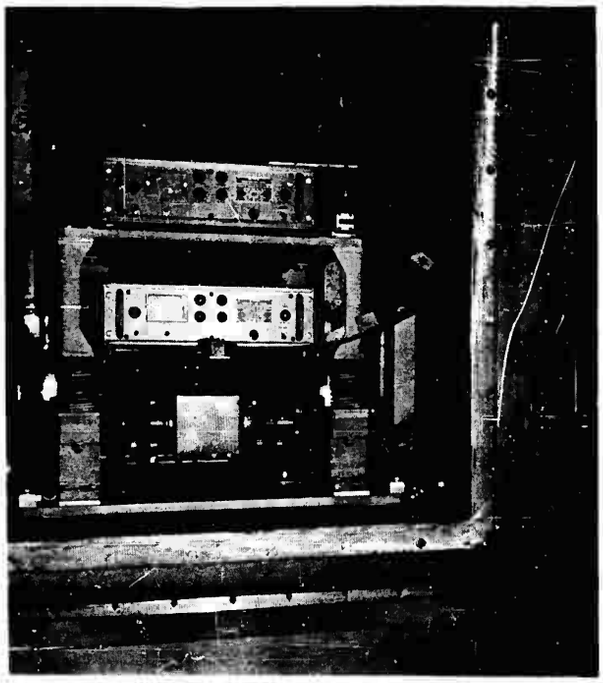

Fig. 1 - NEL experimental vibration machine in chamber with top table in use

hand-tightened spreader jacks (with silicone rubber pads) which bear against the inner walls of the chamber. In addition, the chamber adapter plate is mounted on silicone rubber pads.

PERFORMANCE

Because of the planned simplicity of this vibration test stand, the resultant forces are not linear and are not intended to meet the requirements of MIL-STD-167; however, the forces do produce the type of vibration recommended by the Advisory Group on the Reliability of Electronic Equipment (AGREE). The equipment has been tested with dummy loads, and preliminary results indicate that the test stand should be satisfactory for its intended use.

The functional characteristics of the test stand are as follows:

1. The machine is capable of vibrating a 350-pound test load at 1.00-g or, at a maximum of 5.00-g acceleration (in the 20- to 33-cps range), the machine will vibrate a 70-pound test load.

2. The direction of vibration is predominately in the vertical axis with a small horizontal component in the front-to-back axis, which is due to a slight rocking motion of the table.

3. The amplitude of vibration (vertical) is adjustable from 0 to 0.090 inch (double amplitude), measured at the center of the table.

4. The frequency of vibration can be varied from 8 to 33 cps (shipboard range).

5. Vibration of equipments at temperature extremes of from minus 65° to plus 200°F with relative humidities ranging up to 95 percent are within the capabilities of the test stand.

CONCLUSIONS

The test stand may be considered as a simple vibration machine which could be adapted to existing environmental chambers without too much expense.

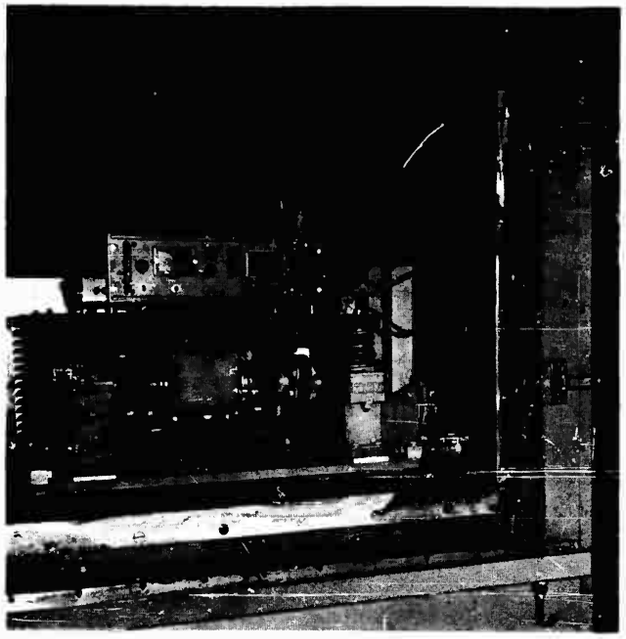

Fig. 2 - NEL experimental vibration machine in chamber with top table removed

As stated in the Introduction, the test stand was designed to provide reliability engineers with a simple test facility for use in investigating equipment failure rates. An eventual end-product of this investigation could be the reduction of reliability testing time, by accelerating equipment failure-rates utilizing relatively high g levels of vibration combined with extremes of temperature and humidity. Of course, there will have to be a definite correlation between the present long-term reliability testing and the reduced-time testing in order to prove the validity of a short-term reliability test.

* * *

A TECHNIQUE FOR PERFORMING VIBRATION TESTS AT HIGH TEMPERATURE IN EXCESS OF 3500°F

C. F. Hanes and R. W. Fodge
LTV Military Electronics

This paper presents the application of a propane fueled furnace as a heat source in conducting high temperature vibration tests. The methods of applying heat to a test article while conducting random vibration tests are discussed as well as instrumentation and cooling problems.

INTRODUCTION

Subjection of missile and aircraft components to controlled vibration at ambient temperatures has presented many problems to the testing industry. More advance designs and increased performance characteristics required of aircraft and missiles have increased the problems of testing these components. Our problem at LTV was to simulate the vibration and temperature environment that a missile nose cap would encounter during re-entry. The conditions to be applied were 3-g rms random vibration, in one direction only, while a specified test article temperature profile was maintained from ambient to a maximum of 3640°F.

TEST SPECIMEN

The test specimen provided was a center section of a re-entry nose cap consisting of a circular curved surface about 10 inches in diameter, and composed of individual tile made of Zirconia and reinforced with Iridium wire. The tile were held in place by pins made of Zirconia and at ambient temperature each tile was loose to allow for expansion at high temperature. Figure 1 shows the test article mounted on the vibration fixture prior to testing. The tile are held to a graphite base by pins, and the graphite base is then clamped securely to the test fixture.

Fig. 1 - Test article in place prior to test

VIBRATION FIXTURE

In order to conduct the required tests the vibration fixture, as shown in Figs. 2 and 3, was designed with the following features: (1) provides a sturdy mounting platform for the specimen; (2) withstands high temperature; (3) allows the underside of the specimen to be exposed for mounting and instrumentation; and (4) affords as much protection to the shaker as possible. The final design consisted of an all-welded chromium-molybdenum, water-cooled, steel structure, weighing 285 pounds. The design was such that the flow of water through the fixture was not picked up by the monitoring accelerometers. The base of the fixture was a plate 17 by 17 inches square and 2 inches thick. Supporting the specimen was a stanchion welded to the base plate providing mounting of the specimen such that vibration could be applied to the vertical axis, as defined by the customer. The fixture was designed with a 4-inch-diameter opening to the rear of the specimen. The cooling

Fig. 2 - Side view of test fixture and instrumentation setup for fixture evaluation

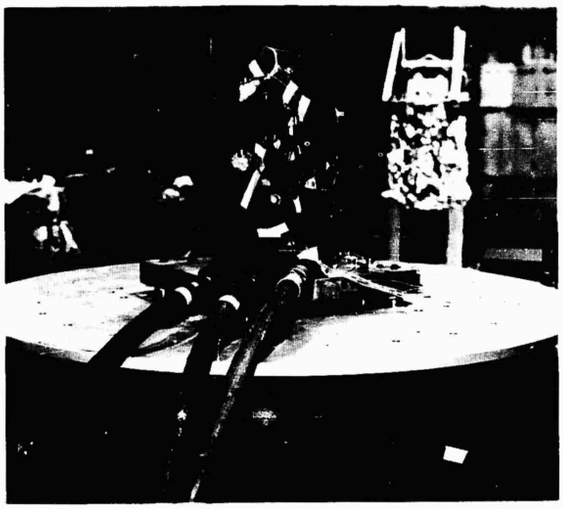

Fig. 3 - Rear view of test fixture showing cooling water parts and accelerometer installation for fixture evaluation

water flow was in at the bottom, up and around the center opening, out the top, and away from the fixture, providing cooling for the fixture, accelerometers, and shaker head. In addition, an air bleed petcock was provided in order that all air could be purged from the system. See Fig. 4.

HEATING SOURCE

To achieve the high temperature required, a heating source capable of intense heat and fine control was desired so that the temperature profile of Fig. 8 could be maintained. A platform was mounted on two slides and connected to a Hydraulic cylinder. As hydraulic pressure was applied, the slide containing the heating source was moved toward or away from the test article, as necessary to maintain the prescribed temperature. The heating elements consisted of seven (2-inch, heating-type) acetylene torches equipped to burn propane instead of acetylene with the oxygen. The heating torches were arranged in a circular pattern of six torches and one large center torch. The commercial designation of the torch tips are H4 for the six outside tips and H5 for the center tip. Each tip was modified by adding additional holes to increase the heating area. To keep the heat concentrated and also to cool the torches a 4-inch-wide, 10-inch-diameter, stainless steel, Zirconia-lined ring was placed around the torches. Air flow between the torches and the ring provided cooling for the torches. The number of torches which were turned on and the location of the torches in relation to the specimen were governed by the temperature required. A manifold was built to accommodate nine oxygen bottles per torch, and one propane bottle per torch except the H5 center torch which required two propane bottles. The fuel consumed by the torches in conducting these tests, including all calibration runs, was 8 25-gallon propane tanks and 63 oxygen bottles. Total cost of all fuel consumed was $165.

INSTRUMENTATION

Temperature

Fourteen high-temperature thermocouples were used to record the temperature at desired points; 4 tungsten thermocouples were placed behind the test article, and 10 chromel-alumel thermocouples were used to monitor other points. In addition a Shawmeter (optical temperature measuring device) was used to check temperature at different places on the specimen and to control the temperature profile above 2300°F. All thermocouples were continuously monitored on strip chart recorders. All testing was conducted at night so that the Shawmeter would not read sun reflected heat.

Vibration

For monitoring vibration inputs, Endevco 2216 accelerometers were used during the fixture evaluation to determine the proper location of the acceleration control monitor. It was determined that the most suitable location of the control accelerometer was inside the fixture about 4 inches behind the test article. Since this location was considered a high temperature area, an Endevco 2242 high temperature accelerometer (good to +500°F) was selected and a heat barrier was made to enclose the inside of

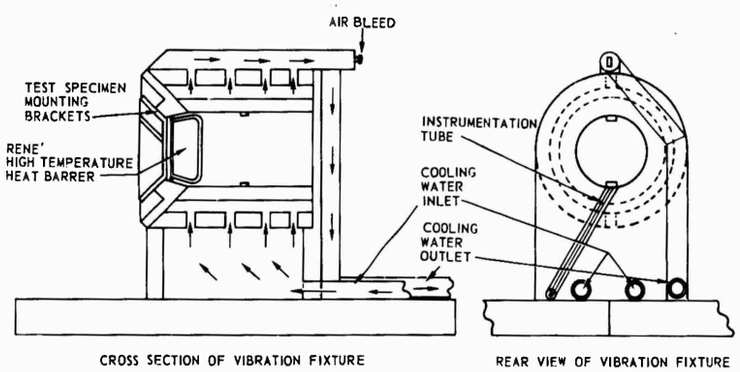

Fig. 4 - Cross sectional view of the vibration fixture showing direction of cooling water flow

the fixture near the test article. This barrier was made from a Rene' steel material, 0.004 inch in thickness and filled with micro-quartz. The remaining space inside the fixture was filled with micro-quartz wrapped in aluminum foil. For added protection all accelerometer cables were wrapped with Refrasil tape. Figure 5 shows the accelerometer leads coming from the fixture.

Fig. 5 - Rear view test fixture showing water table fitting, shaker protection, and Rene' heat barrier

A CEC data tape and Sanborn recording equipment using log audio preamplifiers were used to monitor the vibration response. For fixture evaluation a Ling L-200 exciter system with automatic equalization was used for excitation with no heating of the test article. For the actual test, an A-182 exciter was used with Ling PP175/240 power amplifier and 85 channel automatic equalization system. Figure 2 shows the overall setup for fixture evaluation and Fig. 6 shows the overall setup for the high temperature test. Sanborn recorders, CEC data tape, and control equipment were inside the building.

VIBRATION EXCITER PROTECTION

Heat deflected from the test article onto the exciter had to be removed to prevent severe damage to the shaker. A water table was constructed to fit over the test fixture and cover the entire A-182 shaker top. This heat barrier provided a continuous flow of cooling water carrying off excess heat. Figure 7 shows the water table in place. Half inch marinite board was placed over the water table and in front of the shaker for protection when the torch was first ignited. When the torch is at maximum heating position (approximately one half inch from the test article) the surface area around the fixture becomes a blast area and is subjected to extreme temperatures. To prevent damage to the fixture and the water table, additional pieces of marinite were placed around the fixture and painted with Zirconia paste. Refrasil cloth was placed in the cracks between the fixture and the water table.

TEST PROCEDURE

One high temperature thermocouple was placed on the center tile. All torches were ignited and the test article heated. The torch position was maintained to produce the desired test article stagnation temperature. The actual and desired temperature versus time curves are shown in Fig. 8. The thermocouple on the face of the tile was used to control the torch from ambient temperature until it melted away at approximately 2300°F after which the Shawmeter was used. At time 0 + 32.0 minutes from ignition of the torch the specimen was subjected to 0.61-g rms random vibration for 15 minutes. From time 0 + 47 minutes to time 0 + 65.5 minutes the vibration level was increased to 1.37-g rms. At time 0 + 63.5 minutes the propane torch was turned off. The test article was allowed to cool at ambient conditions. At time 0 + 65.5 minutes the vibration level was increased to 3.0-g rms. At time 0 + 78 minutes all vibration was turned off. Each accelerometer output was recorded continuously on the Sanborn recorders and the CEC data tape throughout the vibration test.

CONCLUSION

By the use of optical temperature measuring equipment and high temperature thermocouples accurate control of high temperature

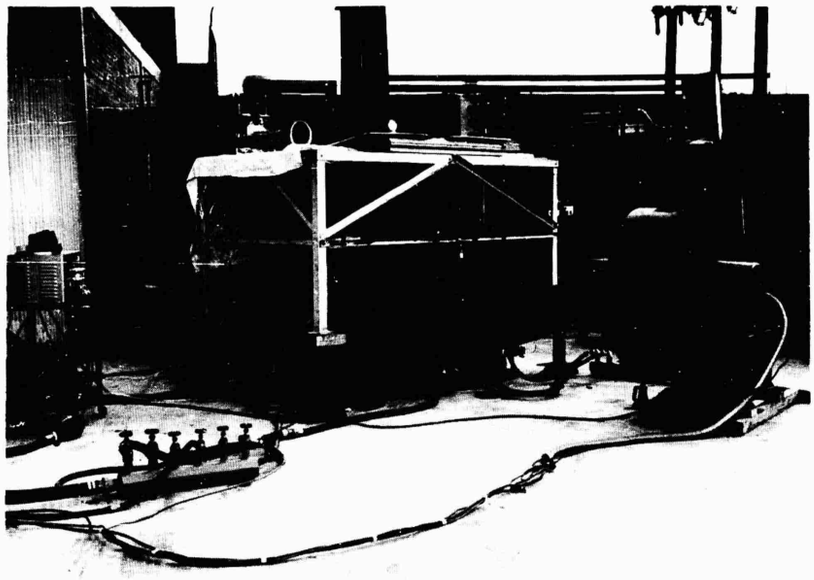

Fig. 6 - Test setup showing water table in place

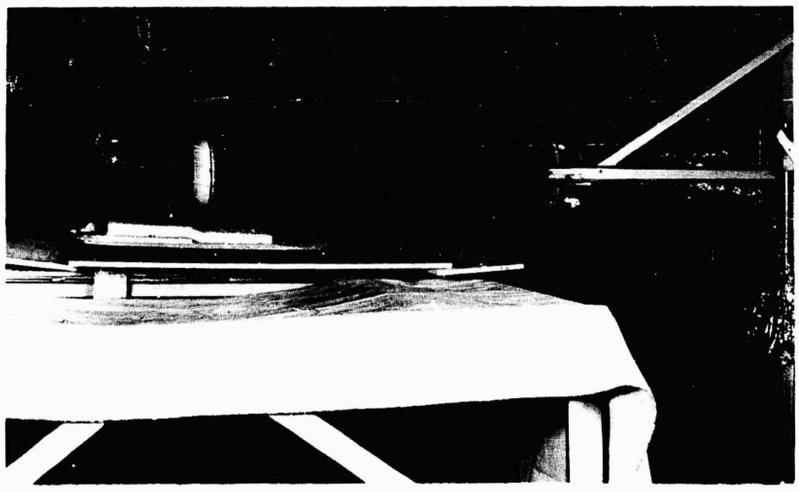

Fig. 7 - Shaker protection in place and torch assembly

heat sources can be maintained. The test article temperature maintained during this test varied no more than 6 percent from the desired profile. The use of the propane fueled furnace heating system is safe, economical, and easily controlled.

Accelerometers can be placed in close proximity to very high temperature sources and can be sufficiently well insulated that their operation will not be degraded. The maximum temperature recorded in the area with the accelerometers was 475°F with a test article

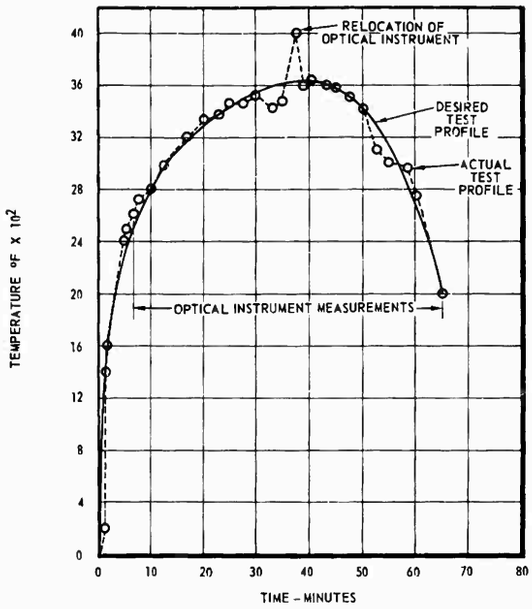

Fig. 8 - Temperature profile

temperature of 3570°F less than 6 inches away.

By using the water filled table as a heat barrier, vibration can be conducted while subjecting test articles to high temperature. The temperature on the exciter mounting surface did not exceed 80°F during the application of heat.

* * *

Section 5
VIBRATION TEST SPECIFICATION

A PROCEDURE FOR TRANSLATING MEASURED VIBRATION ENVIRONMENT INTO LABORATORY TESTS

K. W. Smith
White Sands Missile Range

A method is described that may be used to derive laboratory vibration tests when the measured environment induces failures of the type generally associated with fatigue. The method is derived from basic concepts by the use of a probabilistic model.

INTRODUCTION

The purpose of this document is to present a method for deriving laboratory vibration tests from the measured environment which occurs during transport of a missile system. This derivation is, of necessity, a qualitative one since many of the parameters associated with the dynamic testing of structures must be assumed, and further, approximations are necessary in order to derive a practical test procedure. These approximations tend to decrease the realism of the derived laboratory vibration test. Therefore, an attempt will be made to point out the probable effect on test realism associated with each approximation.

Most of the concepts explained in this document are developed elsewhere in the literature. The use of a probabilistic model to combine these concepts into a method for qualitatively specifying a vibration test, however, has not yet been accomplished It is hoped that this development will provide an interim method for qualitatively specifying laboratory vibration tests until more realistic tests (which circumvent some of the simplifying assumptions) can be formulated.

GENERAL CONCEPT OF THE PROBLEM

The life cycle of complex and sometimes fragile Army Missile Systems from factory to launch position is in many cases more severe than the environment associated with launch to target destruction. The method of devising a qualitative laboratory vibration test from measured environmental data is based on the following approach.

1. A simple, linear, lumped parameter system, similar to the shock spectrum model, is used to mathematically represent the system.

2. The response of this model to both the service and laboratory environment is given mathematically.

3. An assumption is made concerning the way damage accumulates in the simple model. The damage associated with the service environment is then equated with the damage input by the laboratory test environment. In effect this assumption fixes the mechanism of failure for the simple model.

4. The simple shock spectrum model is transformed into a type of probabilistic model by considering the statistical probability distribution of variables which affect the accumulation of damage under the service and laboratory environments.

5. A probability distribution representing the ratio of required laboratory test level to measured service environment, is generated. This statistical distribution can then be used to

select a discrete ratio such that a reasonable percentage of the idealized shock spectrum systems will be subjected to at least the same damage as induced by the service environment.

6. From the above procedure a vibration test is uniquely specified. In the event of a particular failure, however, the calculated equivalent service time is derived to determine if the failure will occur during service.

DYNAMIC RESPONSE OF THE SIMPLE MODEL

Equivalent Test Concepts

McCool[1] derived a method for computing the response of a simple model and established a digital computer program for efficiently computing the shock spectrum for arbitrary transient input pulses. In our analysis, here, the primary interest is the steady-state response of the simple model to both harmonic and stationary random inputs. To fix ideas, and to provide a basis for the discussion of the effect of damping, a discussion of the response of the simple model is accomplished in this document. The usual model used to construct the shock spectrum is shown in Fig. 1, with damping included. An arbitrary shock pulse, $f(t)$, is applied to the base of the model, and the corresponding relative displacement, $u(t)$ is calculated. The maximum value of $u(t)$, converted to acceleration for each of the spring-mass systems, defines the simple shock spectrum. The basic idea of using the shock spectrum concept to define laboratory tests is that the damage potential of an arbitrary pulse, $f(t)$, may be produced, at least qualitatively, by a laboratory pulse whose shock spectrum characteristics are approximately identical. Thus, the idea of comparing the shock spectrum of a transient which occurs during service with a shock spectrum of a pulse produced in the laboratory is an equivalent testing concept. The philosophy behind equivalent testing is to produce the same damage in the laboratory as that which occurs in service, through the use of a laboratory test that is different from the service environment. The principal advantage of the equivalent testing is that conventional laboratory test facilities may be utilized. A major disadvantage of the equivalent testing technique is that precision is many times sacrificed in the analytical development of the test procedure.

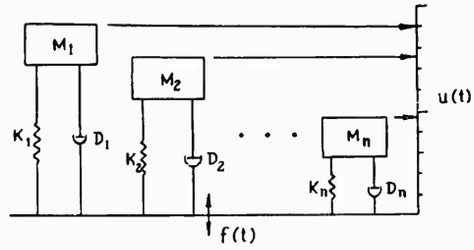

Fig. 1 - A shock spectrum model

Figure 2 is an illustration of one of the lumped parameter, linear, single-degree-of-freedom systems from Fig. 1.

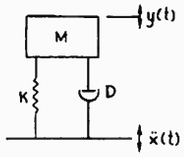

Fig. 2 - Model of the simple system

In Fig. 1,

M = mass (lb-sec^2/in.),

D = total damping (lb-sec/in.),

K = compliance of the spring (in./lb),

$\ddot{x}(t)$ = acceleration input to the system at its base (in./sec^2), and

$y(t)$ = displacement response of the mass (in.).

This system is not intended to represent actual structure in the missile. Rather, it represents a simple model in which it is proposed to calculate the damage that is likely to occur during a laboratory test. This damage will then be equated to that expected from the in-service vibration environment. It is doubtful that a more complex model can be justified at this time. In Ref. 2 the characteristics of damping, or energy dissipation, are outlined as being dependent on the condition of the material, state of internal stress, applied stress history,

[1] W. A. McCool, "A Digital Computer Program for the Analysis of Recorded Shock Motions," White Sands Missile Range, Nike Zeus Data Report No. 23 (May 1961).

[2] B. J. Lazan and L. E. Goodman, "Material and Interface Damping," Chap. 36, Vol. II, Shock and Vibration Handbook (McGraw-Hill Book Co., Inc., New York, 1961).

configuration of the structure, and many other factors. For this model it is assumed that the actual nonlinear system is approximated by a linear system with viscous damping. As explained in Ref. 2, this is probably satisfactory for approximations of systems with small damping, but is not, in general, a realistic approximation to the damping characteristics of structural materials. Whereas the viscous damping force is proportional to velocity, the actual damping of structural materials is often proportional to the amplitude of vibration. Further, the use of lumped, instead of distributed parameters, and the assumption of linear structure cannot be justified experimentally or analytically. However, more research is necessary before a more realistic model can be developed which will offset its increased complexity by a corresponding increase in realism. Until a better model can be formulated, the shock spectrum model will be employed for derivation of equivalent test parameters.

Response of System to a Harmonic Input

The differential equation describing the motion of the system of Fig. 2 is written as:

$$M\frac{d^2y}{dt^2} + D\left(\frac{dy}{dt} - \frac{dx}{dt}\right) + \frac{1}{K}(y-x) = 0. \qquad (1)$$

The following terms are now defined:

$u = y - x$ = relative displacement (in.),

$\omega_n = 1/\sqrt{KM}$ = natural angular frequency (rad/sec),

η = ratio of actual damping to critical damping of the system (D/Dc), and

Dc = critical damping $(2\sqrt{M/K})$.

Equation (1) becomes

$$\frac{d^2u}{dt^2} + 2\eta\,\omega_n\frac{du}{dt} + \omega_n^2 u = -\frac{d^2x}{dt^2}. \qquad (2)$$

By Laplace transforming Eq. (2) and collecting terms, the following is obtained

$$U(s) = \frac{u(0+)(s + 2\eta\omega_n) + \dot{u}(0+) - \mathcal{L}[\ddot{x}(t)]}{s^2 + 2\eta\,\omega_n s + \omega_n^2}, \qquad (3)$$

where

$U(s)$ = Laplace transform of $u(t)$,

$u(0+)$ = initial relative displacement at $t = 0+$,

$\dot{u}(0+)$ = initial relative velocity at $t = 0+$, and

$s = \phi + j\omega$, a complex number $j^2 = -1$.

By rearranging Eq. (3) into a form where a table of transform pairs[3] is useful and letting $\omega_d = \omega_n\sqrt{1-\eta^2}$, Eq. (4) is obtained for the inverse Laplace transformation, $\mathcal{L}^{-1}[U(s)] = u(t)$

$$\mathcal{L}^{-1}[U(s)] = \mathcal{L}^{-1}\left\{\left[\frac{u(0+)(s+\eta\omega_n)}{(s+\eta\omega_n)^2 + \omega_d^2}\right] + \left[\frac{u(0+)\,\eta\omega_n}{\omega_d}\,\frac{\omega_d}{(s+\eta\omega_n)^2 + \omega_d^2}\right] + \left[\frac{\dot{u}(0+)}{\omega_d}\,\frac{\omega_d}{(s+\eta\omega_n)^2 + \omega_d^2}\right] - \left[\frac{\mathcal{L}[\ddot{x}(t)]}{(s+\eta\omega_n)^2 + \omega_d^2}\right]\right\}. \qquad (4)$$

The inverse Laplace transformation yields,

$$u(t) = \epsilon^{-\eta\omega_n t}\left\{u(0+)\left[\cos\omega_d t + \frac{\eta}{\sqrt{1-\eta^2}}\sin\omega_d t\right] + \frac{\dot{u}(0+)\sin\omega_d t}{\omega_d}\right\} - \frac{1}{\omega_d}\int_0^t \ddot{x}(\tau) \times \epsilon^{-\eta\omega_n(t-\tau)}\sin\omega_d(t-\tau)\,d\tau, \qquad (5)$$

where the integral in Eq. (5) is the convolution integral giving the inverse transformation of the last bracketed expression in Eq. (4), and $\epsilon = 2.7183$. Notice that the nature of the acceleration forcing function $\ddot{x}(t)$ is unspecified and may be represented by any arbitrary signal. By writing difference equations from Eq. (5), this expression is readily adaptable to digital

[3] D. K. Cheng, "Analysis of Linear Systems" (Addison-Wesley Publishing Co., 1961).

computation.[1] Suppose the acceleration of the base, $\ddot{x}(t)$, is a complex harmonic function,

$$\ddot{x}(t) = \ddot{x}_o \epsilon^{j\omega t}, \quad (6)$$

where

$\ddot{x}_o$ = maximum amplitude of the signal (in./sec^2),

t = time (sec), and

ω = angular forcing frequency (rad/sec).

The steady-state value of $u(t)$ may easily be determined for the excitation function of Eq. (6). Notice that the terms multiplied by $\epsilon^{-\eta\omega_n t}$ can be neglected as t becomes large and, for the steady-state response to a harmonic excitation, Eq. (5) reduces to:

$$u(t)_{ss} = -\frac{1}{\omega_d}\int_0^t \ddot{x}_o \epsilon^{j\omega\tau}\epsilon^{-\eta\omega_n(t-\tau)} \sin \omega_d(t-\tau)d\tau. \quad (7)$$

By letting $\xi = t - \tau$ and noting that

$$\sin \omega_d\xi = \frac{\epsilon^{j\omega_d\xi} - \epsilon^{-j\omega_d\xi}}{2j}$$

Eq. (7) may be written as

$$u(t)_{ss} = -\frac{\ddot{x}_o e^{j\omega t}}{2j\omega_d}\left[\int_0^t \epsilon^{[-\eta\omega_n - j(\omega-\omega_d)]\xi} d\xi - \int_0^t \epsilon^{[-\eta\omega_n - j(\omega+\omega_d)]\xi} d\xi\right], \quad (8)$$

which is easily evaluated as

$$u(t)_{ss} = -\frac{\ddot{x}_o \epsilon^{j(\omega t - \theta_z)}}{\omega_n^2} \times \left\{1\Big/\left[1 - \left(\frac{\omega}{\omega_n}\right)^2\right]^2 + \left(2\eta\frac{\omega}{\omega_n}\right)^2\right\}^{1/2}, \quad (9)$$

where

$$\theta_z = \tan^{-1}\left[(2\eta\omega/\omega_n)/1 - (\omega/\omega_n)^2\right].$$

To find the ratio of maximum response to input we take the absolute value of both sides and note that the response is given by $u(t)_{ss} = u_o \epsilon^{j(\omega t - \theta_z)}$ so that,

$$\left|\frac{u_o}{\ddot{x}_o}\right|_{ss} = |H(j\omega)| = \frac{1}{\omega_n^2} T\left(\frac{\omega}{\omega_n}, \eta\right), \quad (10)$$

where

$$T\left(\frac{\omega}{\omega_n}, \eta\right) = 1\Big/\left\{\left[1 - \left(\frac{\omega}{\omega_n}\right)^2\right]^2 + \left(2\eta\frac{\omega}{\omega_n}\right)^2\right\}^{1/2},$$

and $|H(j\omega)|$ = absolute value of the transfer function for an acceleration input and relative displacement response of the system.

Equation (10) gives the maximum relative displacement response to an acceleration harmonic excitation of the base. It is important to note that this is a steady state response of the system (forcing angular frequency constant and excitation time large) because of the method used to apply the laboratory vibration environment.

Response of the System to a Random Acceleration Input

The dynamic forcing functions which occur during the operational life of a weapon system are generally represented by their statistical properties. Since the statistical definition of these forcing functions is important from the standpoint of determining the response of particular systems, a large amount of the current literature is devoted to the study and analysis of these phenomena (see Refs. 4 and 5 for example).

A restriction generally imposed is that the random process be stationary in nature. A stationary process is one having statistics which do not change with time. If the probability density of the random process and all its higher-order densities are independent of time, the process is strictly stationary. If the average of the product $x(t) \times (t+\tau)$ depends only on τ, the process is "wide sense" stationary. An ergodic process is a random process for which time and ensemble averages are equal. Thus, all ergodic processes are stationary, but not necessarily vice versa. The assumption that the process is stationary appears to be reasonable

[4] H. Press and J. W. Tukey, "Power Spectral Methods of Analysis and Application in Airplane Dynamics," Bell Telephone System Monograph 2606 (June 1956).

[5] J. W. Miles and W. T. Thomson, "Statistical Concepts in Vibration," Chapter 11, Vol. I, Shock and Vibration Handbook, 1961, McGraw-Hill.

for random processes resulting from rail, truck, or aircraft transport. Serious errors will generally result, however, if this property is assumed to hold for missile launch and flight. A complete discussion is beyond the scope of this paper. For details see Refs. 4 and 5. Since this document is concerned with developing an equivalent vibration test which simulates the damage associated with the transportation of missiles and missile components, the random process will be assumed to be stationary. In order to present an example of some of the physical reasoning involved in defining the random processes, a brief development is given in this document. In order to illustrate these concepts in a simple way, the assumption will be made that the process is ergodic (which in turn also implies a stationary process).

In Eq. (5), the form of the excitation function $\ddot{x}(t)$ is not specified. In general, if $\ddot{x}(t)$ is a random process, then the response, $u(t)$ is also a random process dependent on $\ddot{x}(t)$ and the transfer characteristics given by Eq. (5). The generation of a random process $u(t)$ in the time domain, however, is not generally useful unless laborious numerical methods are employed to define the response statistically. The assumption that the random process is stationary and ergodic becomes important for this example since these properties allow Fourier analyses to be utilized to transform the time domain into the frequency domain. In addition, notice that the system transfer function derived in Eq. (10) may then be used to characterize the relationship between input-output of the system. For a function $x(t)$, whether it is random or not, the time average is given as:

$$\bar{\ddot{x}} = \operatorname*{Limit}_{T \to \infty} \frac{1}{T} \int_{-T/2}^{T/2} \ddot{x}(t)\, dt , \qquad (11)$$

and the mean squared value is

$$\overline{\ddot{x}^2} = \operatorname*{Limit}_{T \to \infty} \frac{1}{T} \int_{-T/2}^{T/2} \ddot{x}^2(t)\, dt , \qquad (12)$$

where T = period of the analysis.

If a recording of $\ddot{x}(t)$ is accomplished and a finite interval is selected for analysis, the function $\ddot{x}(t)$ may be represented by a Fourier series. In the complex form this is:

$$\ddot{x}(t) = \sum_{k=-\infty}^{k=\infty} \alpha_k \epsilon^{jk\frac{2\pi}{T_o}t} , \qquad (13)$$

where ω_o = fundamental angular frequency for the repeating signal with period T_o,

$$\alpha_k = \frac{1}{2}(a_k - jb_k) ,$$

$$a_k = \frac{2}{T_o} \int_{-T_o/2}^{T_o/2} \ddot{x}(t) \sin \omega_o k t\, dt ,$$

and

$$b_k = \frac{2}{T_o} \int_{-T_o/2}^{T_o/2} \ddot{x}(t) \cos \omega_o k t\, dt .$$

By substituting Eq. (13) into (12) and noting the orthogonal relationships associated with Fourier series, the following is obtained:

$$\bar{\ddot{x}}^2 = \alpha_o^2 + 2 \sum_{k=1}^{\infty} |\alpha_k|^2 . \qquad (14)$$

Figure 3 represents a typical plot of $|\alpha_k|^2$ versus angular frequency, $\omega = 2\pi/T$. If the record length to be analyzed is increased by some factor, say m, the amplitude of the $|\alpha_k|^2$ coefficients becomes $|\alpha_k'|^2 = |\alpha_k|^2/m$ which are spaced ω_o/m units apart. Therefore, the sum of the $|\alpha_k|^2$ coefficients remains constant and the increment in $\ddot{x}^2$ divided by the increment in frequency, $\Delta\omega$, is approximately the same for all m.

Thus

$$\frac{\overline{\Delta\ddot{x}^2}}{\Delta\omega} = \left[2 \sum_{i=1}^{N+1} |\alpha_k|_i^2 - 2 \sum_{i=1}^{N} |\alpha_k|_i^2 \right] \Big/ \Delta\omega . \qquad (15)$$

As the length of the record to be analyzed is increased, more spectral lines appear so that in the limit,

$$\operatorname*{Limit}_{\Delta\omega \to 0} \frac{\overline{\Delta\ddot{x}^2}}{\Delta\omega} = \operatorname*{Limit}_{T_o \to \infty} \frac{|\alpha_k|^2 T_o}{\pi}$$

and

$$\frac{d\bar{\ddot{x}}^2}{d\omega} = \Phi(\omega) ,$$

where $\Phi(\omega)$ = input acceleration power spectrum corresponding to $\ddot{x}(t)$. The mean squared value is,

$$\bar{\ddot{x}}^2 = \int_0^{\infty} \Phi(\omega)\, d\omega . \qquad (16)$$

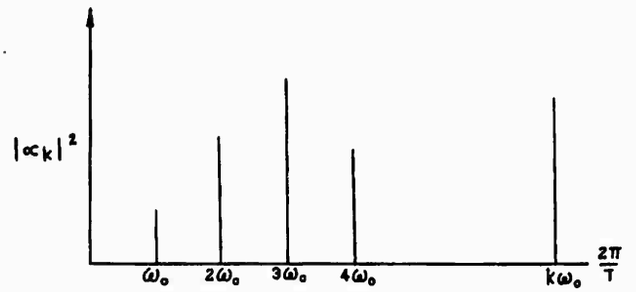

Fig. 3 - Typical plot of spectral lines

The power spectrum, $\Phi(\omega)$, has units of acceleration amplitude squared divided by frequency and may be evaluated by using either analog analysis facilities or by numerical means. Notice that $\Phi(\omega)$ as determined in this analysis assumes the random process $\ddot{x}(t)$ is ergodic. The length of the record and frequency bands of the analysis are important parameters to consider in the analysis of $\Phi(\omega)$. Details are found in Ref. 4. From these references, the statistical confidence band assuming a Gaussian variation and small variations in $\ddot{x}^2$ is approximately:

$$\overline{\Delta\ddot{x}^2} \pm d\,\overline{\Delta\ddot{x}^2} \Big/ \left[\frac{1}{2\pi} T_o (\omega_2 - \omega_1)\right]^{1/2}, \quad (17)$$

where

$$\overline{\Delta\ddot{x}^2} = \int_{\omega_1}^{\omega_2} \Phi(\omega)\, d\omega,$$

and d = normal curve value associated with a particular confidence band (Ref. 6).

Since the system is linear and the principle of superposition applies, the relative steady state displacement response is

$$u(t)_{ss} = \sum_{k=-\infty}^{k=\infty} \alpha_k \epsilon^{jk\frac{2\pi}{T_o}t} H(jk\omega_o), \quad (18)$$

where $H(jk\omega_o)$ is given in Eq. (10) with $\omega_o \to k\omega_o$ for the summation.

This is the superposition of the harmonic components from the Fourier analysis of the random signal of length, T_o, given in Eq. (15) multiplied by the system transfer function to yield the relative displacement response as a function of time. Since the input function is assumed to be an ergodic random process, the response $u(t)$ is also an ergodic random process. In this case the mean squared steady-state displacement response is given by

$$\overline{u^2_{ss}} = \underset{T\to\infty}{\text{Limit}} \frac{1}{T} \int_{-T/2}^{T/2} u^2(t)\, dt. \quad (19)$$

By substituting $u(t)_{ss}$ from Eq. (18) into (19) and again noting the orthogonal properties of Fourier series, the following is obtained:

$$\overline{u^2_{ss}} = H^2(0)\,\alpha_o^2 + 2\sum_{k=1}^{\infty} |\alpha_k|^2 |H(jk\omega_o)|^2. \quad (20)$$

By utilizing the same argument associated with Eq. (17), the following is obtained:

$$\frac{\overline{\Delta u^2_{ss}}}{\Delta\omega} = \frac{2|\alpha_k|^2}{2\pi/T_o} |H(jk\omega_o)|^2,$$

and in the limit as $T_o \to \infty$ and $\Delta\omega \to 0$ the spectral lines become continuous, so that

$$\frac{\overline{du^2_{ss}}}{d\omega} = \Phi(\omega)\,|H(j\omega)|^2. \quad (21)$$

The mean squared relative displacement response may be evaluated as

$$\overline{u^2_{ss}} = \int_0^{\infty} \Phi(\omega)\,|H(j\omega)|^2\, d\omega. \quad (22)$$

Consider the function $|H(j\omega)| \times \omega_n^4$ for the simple system of Fig. 2. For typical value of η, this is shown in Fig. 4.

[6] M. Schwartz, Information Transmission, Modulation, and Noise (McGraw-Hill Book Co., Inc., New York, 1959).

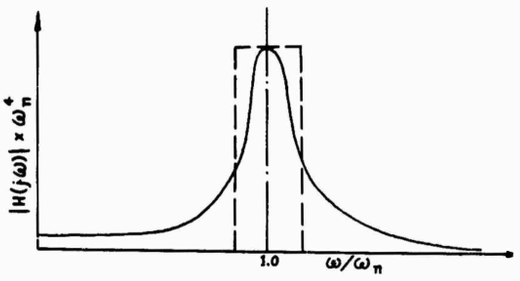

Fig. 4 - Typical frequency response curve for the simple system

Notice that the response is grouped about $\omega = \omega_n$ and acts as a mechanical filter to the base excitation function. The concept of a "Noise equivalent bandwidth," B, is now introduced. Observation of Fig. 4 reveals that the contributions of $\Phi(\omega)$ to the output of the system will be approximately limited to a certain frequency bandwidth. A rectangular frequency spectrum, which is equivalent to the $|H(j\omega)|^2$ frequency spectrum, is defined as B.

From Ref. 6 (pages 205-207) this is derived as:

$$A_m^2 B = \int_0^\infty |H(j\omega)|^2 d\omega , \qquad (23)$$

where

A_m = maximum value of $|H(j\omega)| = 1/\omega_n^2 2\eta$, and

B = noise equivalent bandwidth centered about ω_n (rad/sec).

In order to evaluate B, it is necessary to perform the indicated integration. The necessity of evaluating B will become apparent during the discussion of the equivalent laboratory test. The evaluation of Eq. (23) involves complex integration and is given in Appendix A.

From Appendix A, B is calculated as

$$B = \pi \omega_n \eta . \qquad (24)$$

The output mean squared, relative displacement response is a function of the contributions of the input power spectrum, $\Phi(\omega)$, in the bandwidth B. It is considered that values of $\Phi(\omega)$ outside B contribute nothing to the response of the system of Fig. 2. If $\Phi(\omega)$ is essentially constant within B, the mean squared relative displacement output is approximated by

$$\bar{u}^2 \approx \Phi(\omega)_B A_m^2 B = \Phi(\omega)_B \frac{\pi}{4\eta\omega_n^3} , \qquad (25)$$

where $\Phi(\omega)_B$ = average of $\Phi(\omega)$ within the frequency bandwidth B. If $\Phi(\omega)$ is not constant within B, Eq. (25) will be somewhat in error. In this case, numerical evaluation of Eq. (22) will yield accurate results; however, it is doubtful that the increase in accuracy justifies the use of (22) except for extreme variations of $\Phi(\omega)$ within the bandwidth B.

The assumption of ergodicity is not necessary for the derivation of the principal results of this section; i.e., those given by (16), (22), and (25). The assumption that the random process, $\ddot{x}(t)$, is stationary is required. In the subsequent development, the excitation function will be assumed to be a stationary random process. In addition, the statistics of the process will be restricted to the Gaussian probability distribution with zero mean in order to define the output of the system in a simple way.

Comparison of Damage Assiciated with Random and Harmonic Inputs

The assumption of the mechanisms of damage in the simple model is one of the most critical areas in the development of an equivalent test. In general there are two types of failure which occur during the application of vibration environment:

1. Intermittent Failures. There is no damage in a mechanical sense; the relative motion of component parts of vacuum tubes, relay contacts, and other parts, whose electrical

properties are sensitive to position, may cause maloperation of the equipment. When the vibratory oscillation ceases, the equipment returns to normal. To detect intermittent failures, the operating characteristics of the equipment must be monitored during application of the vibratory equipment.

2. Fatigue Failures. These failures are caused by exceeding the endurance strength of structural elements for a sufficient length of time such that mechanical failure does occur.

In the present analysis it is assumed that the components are undergoing tests which simulate the damage associated with the transportation environment and are therefore not operating. Fatigue failures are then the primary source of concern. If intermittent type failures are important, then the laboratory test should consist of the application of the maximum levels which occur in service with the equipment being operated. Intermittent type failures occur when the equipment will not operate within specifications, but the investigation of fatigue failures is not an objective for a test of this type.

Much fatigue data have been collected in the form of a conventional stress versus number of cycles to failure. These are plotted for different materials onto "σ-N" curves and exhibit wide scatter. Figure 5 is a hypothetical σ-N curve plotted on logarithmic paper for fully reversed loading.

If σ_u is exceeded, failure occurs almost immediately. For most structural materials failure before 10^4 cycles is indicative of the fact that σ_u has been exceeded. If the stress is below σ_e, fatigue failure will not occur no matter how many cycles are input to the test specimen. In general, if failure does not occur prior to the application of 10^6 to 10^7 cycles, the applied stress is less than σ_e. In a laboratory test for simulation of fatigue failures, it is necessary to obtain at least 10^4 cycles in order to consider the fatigue as primarily a fatigue phenomenon. Failure prior to 10^4 cycles represents a ruptive type damage associated with the application of shock transient and is outside the scope of this paper. The effect of stress application below σ_e will be discussed presently.

It is necessary now to specify a criteria for the way damage occurs in the fatigue environment. Several theories have been advanced concerning cumulative damage; however, none have proven to be particularly accurate from the experimental standpoint. Those interested may consult Refs. 7 through 10. The concept given by Miner[7] appears to be adequate to estimate the fatigue life of a single specimen, and because the mathematical form of the theory is particularly simple; it is adopted here.

First a tensile bar is assumed. If the work is taken as w, then

$$w/\text{cycle} = \frac{u_{max} P}{\text{cycle}} = \frac{P^2 \ell}{AE}, \qquad (26)$$

where

u_{max} = maximum relative displacement (in.),

P = force (lb),

ℓ = length of tensile specimen (in.),

E = modulus of elasticity (lb/in.^{2}), and

A = area (in.^{2}).

[7] M. A. Miner, "Cumulative Damage in Fatigue," J. Appl. Mech. (Sept. 1945).
[8] Shanley, "A Theory of Fatigue Based on Unbonding During Reversed Slip," Rand Report P-350-1.
[9] Dolan and Carter, "Cumulative Fatigue Damage," International Conference on Fatigue of Metals, Session 3, Paper 2 (Nov. 1956).
[10] J. C. Levy, "Prediction Fatigue Life," J. Roy. Aeronaut. Soc., Vol. 61 (July 1957).

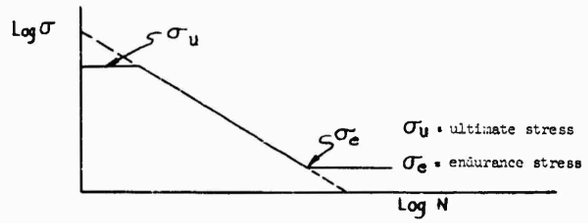

Fig. 5 - Hypothetical σ-N curve

The total energy per unit area for n cycles would be

$$e \approx \sigma^2 \frac{\ell}{E} n , \tag{27}$$

where

$e = (w/A)n$,

σ = stress (lb/in.^{2}), and

n = actual number of cycles at force P.

For failure

$$e_F = \sigma_1^2 \frac{\ell}{E} N_1 , \tag{28}$$

where

e_F = energy input at failure,

σ_1 = stress associated with a particular force (P_1), and

N_1 = the number of cycles to failure as determined from the S-N curve of Fig. 5.

For less than failure the damage is partial in nature and $N_1 \rightarrow n_1$. When dividing the partial damage by the total damage to failure,

$$\frac{e_1}{e_F} = \left(\sigma_1^2 \frac{\ell}{E} n_1\right) \Big/ \left(\sigma_1^2 \frac{\ell}{E} N_1\right) = \frac{n_1}{N_1} . \tag{29}$$

Miner theorizes that the damage accumulates linearily, or that:

$$e_1 + e_2 + \cdots + e_i = e_F . \tag{30}$$

By dividing both sides of the identity in (30) by e_F and combining with (29), the following is obtained:

$$\frac{n_1}{N_1} + \frac{n_2}{N_2} + \cdots + \frac{n_i}{N_i} = 1$$

or as is usually expressed:

$$D = \sum_i \frac{n_i}{N_i} = 1 , \tag{31}$$

where D = damage coefficient, assumed to be unity at failure.

Many experiments have been conducted in an attempt to verify Miner's theory, and it has been found that D is somewhat dependent on the sequence of loading with range of 1/3 to 3. Since the analysis here is concerned with equating the damage associated with the service environment with the damage that might be introduced during a laboratory test, a specific value of D is not required.

Since the statistical properties of the service environment are assumed to be stationary and gaussian in nature, the relative displacement output of the shock spectrum model will also be stationary and Gaussian. The frequency content of the output, however, will be limited to the bandwidth of B. An output signal of this type is called a "random sine wave" and is illustrated in Fig. 6.

In Ref. 11, it is shown that the distribution of the envelope of u(t), say u_p, is given by the Rayleigh probability provided that $\bar{u} = 0$. Since the mean value of the excitation function was assumed to be zero, the output $\bar{u} = 0$ and the probability density of the peak response may be written as

$$P\left(\frac{u_p}{u_r}\right) = \frac{u_p}{u_r} \epsilon^{-\frac{1}{2}\left(\frac{u_p}{u_r}\right)^2} , \tag{32}$$

where

$u_r^2 = \bar{u}^2 - (\bar{u})^2$, the variance, and

$P(u_p/u_r)$ = probability density of the normalized peak value of u(t).

In order to determine a harmonic input to the model which is equivalent to damage induced by the service environment, $\Phi(\omega)$, it is necessary to assume that Hooke's Law holds in the dynamic case, i.e.,

$$\sigma = \frac{u}{\ell} E . \tag{33}$$

Equation (33) is probably not valid for most materials for the dynamic case; however, a standard relationship relating dynamic stress and relative displacement is not available. Until more data are available, it will be assumed that stress in the model is directly proportional to the total strain (since E/ℓ is a constant for a particular model). If σ is replaced by u in Fig. 5 and the straight portion of the σ-N curve

[11] S. O. Rice, "Mathematical Analysis of Random Noise," Selected papers on Noise and Stochastic process (Dover Publications, 1954).

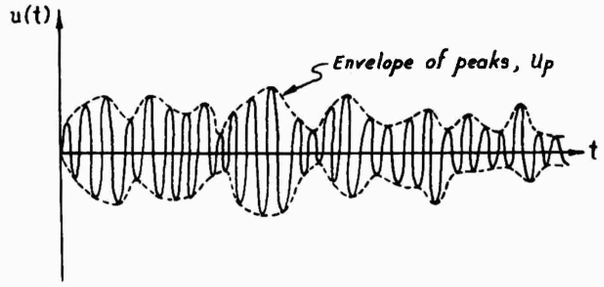

Fig. 6 - Random sine wave for response u(t)

extended for mathematical simplicity, the curve of Fig. 5 may be represented by

$$\log_e u = \log_e U_1 - \frac{1}{\alpha} \log_e N, \qquad (34)$$

where

U_1 = hypothetical relative displacement required to produce failure during 1 cycle, and

$-1/\alpha$ = slope of the straight line on the curve of Fig. 7, and

$N \geq 10^4$ cycles.

Equation (34) may be written as:

$$N = (U_1/u)^{\alpha}. \qquad (35)$$

The value of α may be determined from σ-N curves plotted for particular materials. These curves generally exhibit wide scatter, and the value of α varies from 3 to 25 depending on the fatigue characteristics of the material.

The problem now is to determine a single sinusoidal vibration amplitude, u_e, that will produce the same damage as the random sine wave whose probability density is characterized by Eq. (32). Both the single sinusoidal amplitude, u_e, and the random sine wave oscillate with frequency, ω_n. The determination of u_e is given by Miles[5,12] in terms of stress. The equation as derived by Miles, writing in terms of u, is

$$\frac{u_e}{[\bar{u}^2]^{1/2}} = (\pi\alpha)^{1/2\alpha} \left(\frac{\alpha}{\epsilon}\right)^{1/2}. \qquad (36)$$

Figure 7 is a plot of the u versus N curve with a typical value of u_e and distribution of u_p given. The cross hatched portion of the damage induced by the random sine wave represents displacements associated with stresses below the endurance limit, σ_e. Since there is no direct way to calculate the relative displacement

[12] J. W. Miles, "On Structural Fatigue Under Random Loading," J. Aeronaut. Sci., Vol. 21, No. 11 (Nov. 1954).

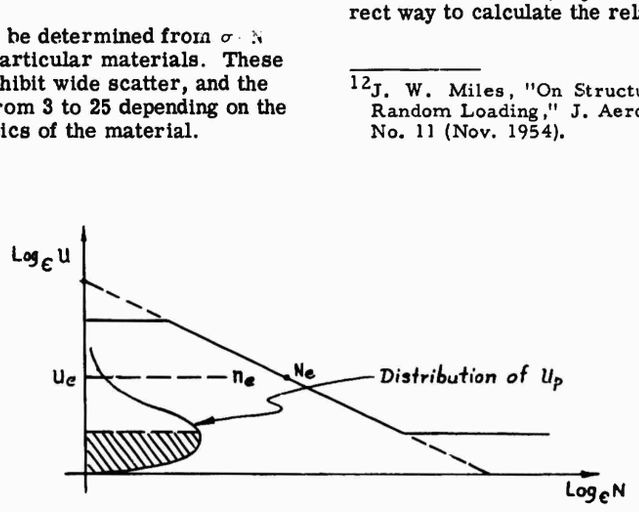

Fig. 7 - Damage induced by random sine wave and single sinusoid

corresponding to the stress endurance limit, it must be assumed that these levels of the random sine wave contribute to the damage. It is evident that the calculated value of u_e will be slightly higher than that actually required to induce an equivalent damage. This means that the laboratory test will be conservative in nature since damage is counted for all of the small displacements below the endurance limit. This conservation will be left as a "factor of safety" for the equivalent test.

ESTABLISHMENT OF LABORATORY TEST PROCEDURES

Laboratory Test Parameters

Equation (36) could be used to derive a laboratory vibration test for inducing equivalent damage in a particular model shown in Fig. 2. A laboratory test of this sort would consist of a sinusoidal input which induces a relative displacement of u_e and whose frequency of oscillation is ω_n. The duration of the laboratory test would correspond to the time the test specimen is subjected to the service environment. The disadvantages of such a test are obviously:

1. Only those components of the test specimen whose natural frequencies are in the vicinity of ω_n will receive damage.

2. The required test time will be impractical since conceivably several hundred hours might be required to produce a one to one correspondence between laboratory and service times. In order to circumvent these problems, a laboratory test is specified in which the vibration frequency sweep rate is logarithmic throughout the frequency range of interest. It is easily shown that for η a constant a logarithmic frequency sweep rate will result in equal time within B for each shock spectrum model; i.e., the time the excitation of the model is within B is independent of ω_n. Figure 8 is a curve illustrating a typical logarithmic frequency sweep vibration test schedule. In writing the equation for the curve in Fig. 8

$$t = t_f \left[\log_e \left(\frac{\omega}{\omega_L} \right) \Big/ \log_e \left(\frac{\omega_u}{\omega_L} \right) \right], \qquad (37a)$$

where

t = time (sec), and

ω_L, ω_u = lower and upper angular frequencies, respectively, of the test schedule.

The response of the simple model is essentially resonant, as shown in the development of the equivalent noise bandwidth given in Eq. (24). Since only the values of $\Phi(\omega)$ within the frequency bandwidth, B, contribute to the response of the system, it is reasonable to assume that significant system damage occurs during application of the laboratory test frequencies within B. Rearranging Eq. (37a) to determine the time the laboratory sweep frequencies are within B,

$$\Delta t = t_f \left[\log_e \left(\frac{\omega_2}{\omega_1} \right) \Big/ \log_e \left(\frac{\omega_u}{\omega_L} \right) \right], \qquad (37b)$$

where

Δt = time the sweep frequency is within B,

ω_2 = upper frequency limit of B, and

ω_1 = lower frequency limit of B.

From Eq. (24)

$$\frac{\omega_2}{\omega_1} = \left(1 + \frac{\pi}{2}\eta\right) \Big/ \left(1 - \frac{\pi}{2}\eta\right).$$

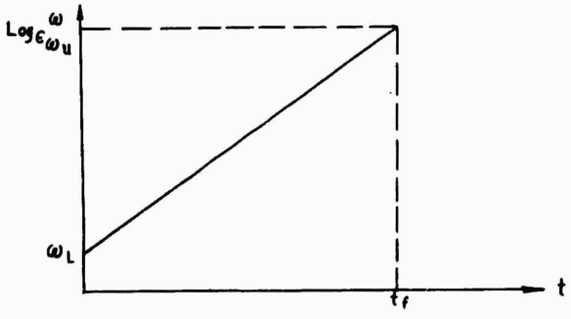

Fig. 8 - Vibration test schedule

and by substituting into (37b),

$$\Delta t = t_f \left[\log_\epsilon \left(\frac{2 + \pi\eta}{2 - \pi\eta} \right) \Big/ \log_\epsilon \left(\frac{\omega_u}{\omega_L} \right) \right]. \quad (38)$$

Thus, Δt is independent of ω_n; given that a logarithmic change in the frequency sweep rate is effected. Caution must be exercised, however, in the application of Eq. (38). The response of the model to a harmonic input, as given in Eq. (10), was determined by assuming steady state conditions, i.e., that the applied excitation frequency was constant. The excitation function selected for the laboratory test is fundamentally different from that given by Eq. (6). In fact,

$$\ddot{x}(t) = \ddot{x}_o \sin [\omega(t)\, t] , \quad (39)$$

where

$$\omega(t) = \omega_L \left(\frac{\omega_u}{\omega_L} \right)^{t/t_f} .$$

A rate of change of $\omega(t)$ which is too rapid will prevent the response of the item from building up to the steady-state value given by Eq. (10). This problem was first studied by Lewis[13] and adopted to the vibration problem in Ref. 14. From Ref. 14 an expression was developed to insure that the response level experienced by the simple model was greater than or equal to 95 percent of the response level given by the steady-state value for a particular damping. For large damping, the rate of change of frequency through B is not critical; however, for small damping, the sweep rate must be slow. To determine a logarithmic sweep rate which will insure that all of the models will respond to at least 95 percent of the value predicted by Eq. (10), it will be assumed that the minimum value of η to be considered in this analysis is 0.01.

Adapting the results of Refs. 1 and 14 to provide the required levels within the frequency bandwidth B, the following relationship is given:

$$\Delta t_{min} = \left[g_m (B/\omega_n) \right] / f_L , \quad (40)$$

where

Δt_{min} = minimum time required to sweep within B to insure a response 95 percent or greater of the steady state value,

g_m = (from Ref. 13), a measure of the rate the system is being accelerated is dependent on η and the required response level, and

f_L = lower frequency limit, $\omega_L/2\pi$ (cps).

From Ref. 13 the values of g_m for a response of 95 percent or greater than the value predicted for steady-state vibration are as shown in Table 1.

TABLE 1
Values of g_m for 95-Percent Response from Ref. 13

η	g_m
0.2	6.62
0.1	26.5
0.05	300
0.025	424

A value corresponding to g_m when $\eta = 0.01$ can safely be assumed as $g_m = 600$. By substituting $g_m = 600$ into (40) and combining this with (38),

$$t_f \geq \left[600 \log_\epsilon \left(\frac{f_u}{f_L} \right) \right] / f_L . \quad (41)$$

The application of Eq. (41) provides a method for selecting the total elapsed cycling time for one logarithmic sweep. Suppose now that an integral number of vibration sweep cycles, say p, are selected for the vibration laboratory test. A comparison between the time to failure at any two levels can be accomplished through the use of Eq. (35). Thus a mechanism for accelerating the damage in the simple model can be introduced. Let Ne be the number of cycles to failure associated with the stress level induced by relative displacement u_e, and similarly N_t be the number of cycles to failure for the relative displacement, u_t, associated with the laboratory test, then

$$\frac{Ne}{N_t} = \frac{(U_1/u_e)^{1/a}}{(U_1/u_t)^{1/a}} .$$

[13] F. N. Lewis, "Vibration During Acceleration Through a Critical Speed," APM 54-24, Transactions ASME (1932), pp. 253-261.

[14] C. E. Crede and E. J. Lunney, "Establishment of Vibration and Shock Tests for Missile Electronics as Derived from the Measured Environment," WADC Technical Report 56-503 (Dec. 1956).

Noting that

$$Ne = \frac{\omega_n}{2\pi} t_s$$

and

$$N_t = \frac{\omega_n}{2\pi} p\,\Delta t ,$$

where Δt is defined by Eq. (38) and t_s is the total time in service, this equation may be rewritten as

$$u_e = u_t \left(\frac{p\,\Delta t}{t_s}\right)^{1/\alpha} . \qquad (42)$$

It is now possible to combine the previous results to obtain a ratio of the required laboratory test level to the mean squared acceleration density measured in service. This ratio is derived on the basis that the total number of sweep cycles, p, and the total elapsed cycling time per logarithmic sweep cycle, t_f, is selected to conform to practical test considerations. From Eqs. (10), (25), and (42),

$$\frac{u_e}{[\bar{u}^2]^{1/2}} = g(\alpha)$$

$$= \left[\frac{\ddot{x}_t(max)}{2\eta\,\omega_n^2}\left(\frac{p\Delta t}{t_s}\right)^{1/\alpha}\right] \Bigg/ \left[\Phi(\omega)_B \frac{\pi}{4\eta\,\omega_n^3}\right]^{1/2} , \qquad (43)$$

where

$\ddot{x}_t(max)$ = required test acceleration level (in./sec^2), and

$$g(\alpha) = (\pi\alpha)^{1/2\alpha} \left(\frac{\alpha}{e}\right)^{1/2} .$$

Rearranging Eq. (43) and converting angular frequency to cycles per second, the following is obtained:

$$Re = \frac{a_t}{[f_n\,\psi(f_n)]^{1/2}} = \left[(\pi\eta)^{1/2} \Big/ \left(\frac{p\Delta t}{t_s}\right)^{1/\alpha}\right] g(\alpha), \qquad (44)$$

where

Re = equivalent test ration normalized to f_n,

$f_n = \omega_n/2\pi$ (cps),

$a_t = \ddot{x}_t/g$, required input test level in gravitational units (g),

$\psi(f_n)$ = measured service mean squared acceleration density, g^2/cps within B, and

g = acceleration due to gravity (386.4 in./sec^2).

Notice that $p\Delta t$ is given by Eq. (38) as the total significant time the applied laboratory acceleration is within the frequency bandwidth, B. Equation (44) is the central result of this analysis, since the equivalent test ratio,

$$\frac{a_t}{[\psi(f_n)]^{1/2}} ,$$

may be calculated throughout the frequency spectrum by varying f_n.

Calculation of Statistical Distribution of Re

The equivalent test ratio given by Eq. (44) for a particular frequency, f_n, and laboratory test sweep pattern is a function of two variables; i.e.,

$$Re = \phi(\alpha, \eta) . \qquad (45)$$

Unfortunately, the fatigue characteristics given by the parameter α and the damping values associated with η are impossible to determine on a practical basis in a complex structure. Data are available, however, to indicate the range of these parameters that might be expected in a complex test specimen. For example, the value of α is approximately 3 for magnesium, 10 for aluminum, and 25 for steel, assuming a straight tensile bar. It is also well known that the configuration of the structure affects the value of α. Further, for a particular material and structural configuration, the statistical variance of α determined by experiment is large. It would appear reasonable, then, to analyze the complex structure to be tested to estimate a statistical distribution of α. In addition, since the damping is dependent on stress level, material, structural configuration, and so on (see Ref. 2) in a complex way, the treatment of η on a probabilistic basis also appears to be warranted. In general, η may be expected to vary between 0.01 and 0.1 for the structure normally used in missile airframes and ground support equipment.

It is proposed to generate a statistical distribution of Re in a rather straightforward manner. An analysis of the physical properties of the test specimen will be accomplished to estimate the statistical distribution of α and η.

A digital computer program is then formulated to generate a large number of values of Re. An assessment of the values of Re generated by the digital computer program allows a particular equivalent test ratio to be selected by the test engineer. Since a statistical distribution of Re is generated, the probability that the test specimen will receive the same damage from the laboratory test as was received from service can be estimated. In order to provide a specific example of how an equivalent vibration test can be formulated, a hypothetical situation is assumed and a laboratory vibration test is derived in Appendix B. A digital computer program capable of generating Re is available from White Sands Missile Range, New Mexico.

Treatment of Laboratory Test Failures

It is evident that after a particular value of Re has been selected that the possibility of overtesting particular elements of the structure exists. As a matter of fact if a value of Re is selected such that a probability, P, is estimated that the laboratory test is as severe or more severe than the service environment, then it is clear that we must estimate P percentage of the structural elements as being overtested and (1-P) structural elements as being undertested. If a particular structural element fails during the course of the vibration test, it is important to calculate equivalent service time, t_s, associated with the failed specimen. This is accomplished by first estimating the fatigue and damping characteristics of the failed component based on the structural configuration and material involved. After these parameters have been estimated, the resonant frequency, f_n, must be determined by either calculation or measurement. (In most complex structure, measurement is the preferred method.) Equation (44) may then be transposed for a solution of the equivalent service time associated with the laboratory test as:

$$(t_s)_L = \left\{ [Re(f_n)]_s \Big/ (\pi\eta)^{1/2} g(\alpha) \right\}^{\alpha} \Delta t \, P_L, \quad (46)$$

where

$(t_s)_L$ = equivalent laboratory service time,

$[Re(f_n)]_s$ = selected value of Re at the measured or calculated value of f_n corresponding to the failed component,

α, η = estimated values of fatigue and damping characteristics of the failed component, and

P_L = actual number of logarithmic sweep cycles accomplished during the laboratory test prior to failure of the element.

If $[t_s]_L > t_s$, failure has not really occurred since the service life has been exceeded by the test life; however, if $[t_s]_L < t_s$, the obvious conclusion must be that the structural element has not passed the test.

It should also be mentioned here that the equivalent test concepts derived in this document assume that the response of the simple model is translational. Therefore, application of the vibration environment in the laboratory should be in three dimensions. Assuming that the required vibration test input parameters have been calculated for each of three mutually perpendicular axes, a practical laboratory vibration test procedure requires that the calculated parameters corresponding to each axes be input sequentially. Unfortunately, considerable response is induced in adjacent axes causing damage to accumulate for test in these axes. Thus, if the same test specimen is used for testing in each of the axes, overtesting will result for particular elements during tests in the second and third axes. Several alternatives are possible:

1. Use a new test specimen for tests during each axis.

2. Test only in the most significant axis. (This is possible if the service environment is essentially unidirectional in nature.)

3. Measure the response in the adjacent axes, calculate $[t_s]_L$ in each of these directions and adjust any subsequent failures by this calculated value.

Appendix A

EVALUATION OF EQUIVALENT BANDWIDTH INTEGRAL

The integral

$$\int_0^\infty |H(j\omega)|^2 \, d\omega = \frac{1}{\omega_n^4} \int_0^\infty \frac{d\omega}{\left[1 - \left(\frac{\omega}{\omega_n}\right)^2\right]^2 + \left(2\eta \frac{\omega}{\omega_n}\right)^2}$$

may be rearranged as shown in Eq. (A1) and since $f(\omega)$ is an even function:

$$\int_0^\infty |H(j\omega)|^2 \, d\omega = \frac{1}{2\omega_n^4} \int_{-\infty}^\infty \frac{d\omega}{\omega^4 - 2\omega_n^2(1-2\eta^2)\omega^2 + \omega_n^4} \, . \quad \text{(A1)}$$

Equation (A1) is most easily evaluated using complex variables. To accomplish this we let

$$f(s') = 1\Big/\left[s'^4 - 2\omega_n^2(1-2\eta^2)s'^2 + \omega_n^4\right] , \quad \text{(A2)}$$

where

$s' = \omega + j\gamma$,

ω = Real [s'], and

γ = Im [s'],

and integrate around the closed contour C as shown in Fig. A1.

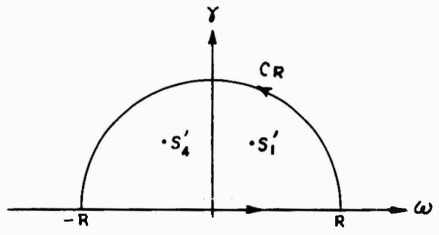

Fig. A1 - Path of complex integration

Equation (A1) is then written as:

$$\int_0^\infty |H(j\omega)|^2 \, d\omega = \frac{1}{2} \int_C \frac{ds'}{s'^4 - 2\omega_n^2(1-2\eta^2)s'^2 + \omega_n^4} \, . \quad \text{(A3)}$$

It may readily be determined that $f(s')$ is analytic throughout the s'-plane except for the simple poles corresponding to the roots of

$$s'^4 - 2\omega_n^2(1-2\eta^2)s'^2 + \omega_n^4 = 0 \, .$$

The four simple poles (order one) are most easily written in terms of polar coordinates

$$\left.\begin{aligned} s_1' &= \omega_n \epsilon^{j\theta/2} \\ s_2' &= -\omega_n \epsilon^{j\theta/2} \\ s_3' &= \omega_n \epsilon^{-j\theta/2} \\ s_4' &= -\omega_n \epsilon^{-j\theta/2} \end{aligned}\right\} , \quad \text{(A4)}$$

where

$$\theta = \tan^{-1}\left[2\eta\sqrt{1-\eta^2}\,/(1-2\eta^2)\right] ,$$

$$0 < \theta < \pi , \qquad 0 < \eta < 1 ,$$

as a result of the Cauchy-Goursat theorem, the following may be written:

$$\int_C f(s')\,ds' = 2\pi j(K_1 + K_2 + \cdots + K_i + \cdots + K_n) \quad \text{(A5)}$$

where $K_i = i_{th}$ residue at the singular point s' within the closed contour C.

Here the simple poles within C for $f(s')$ are s_1' and s_4'. The residues K_1 and K_4 are evaluated:

$$K_1 = \left[(s' - s_1')\, f(s')\right]_{s'=s_1'}$$

$$= 1/(j4\omega_n^3 \sin\theta)\, \epsilon^{j\theta/2} ,$$

and in a similar manner

$$K_4 = 1/(j4\omega_n^3 \sin\theta)\ \epsilon^{-j\theta/2},$$

so that

$$\int_C f(s')\,ds' = 2\pi j(K_1 + K_4) = \frac{\pi}{2\omega_n^3}\sin\frac{\theta}{2}. \quad (A6)$$

From Eq. (A4) $\cos\theta = 1 - 2\eta^2$. The simple identity,

$$\sin\frac{\theta}{2} = \sqrt{(1-\cos\theta)/2} = \eta$$

may be used to evaluate (A6) as:

$$\int_C f(s')\,ds' = \frac{\pi}{2\omega_n^3\eta}. \quad (A7)$$

From Fig. A1 it is evident that

$$\int_C f(s')\,ds' = \int_{-R}^{R} f(\omega)\,d\omega + \int_{C_R} f(s')\,ds' = \frac{\pi}{2\omega_n^3\eta}, \quad (A8)$$

where C_R = path of integration along the semicircle of radius R. Rearranging this equation, taking the absolute value of letting $R \to \infty$,

$$\underset{R\to\infty}{\text{Limit}}\left|\int_{-R}^{R} f(\omega)\,d\omega - \frac{\pi}{2\omega_n^3\eta}\right| = \underset{R\to\infty}{\text{Limit}}\left|\int_{C_R} f(s')\,ds'\right|, \quad (A9)$$

considering the integral on the right:

$$\underset{R\to\infty}{\text{Limit}}\left|\int_{C_R} f(s')\,ds'\right| = \underset{R\to\infty}{\text{Limit}}\left|\frac{\pi R}{R^4 - 2\omega_n^2(1-2\eta^2)R^2 + \omega_n^4}\right| \to 0. \quad (A10)$$

Since $|s'| \to R$ when C is on C_R. Taking the limit in (A9) and remembering the principal value theorem:

$$\int_{-\infty}^{\infty} f(\omega)\,d\omega = \frac{\pi}{2\omega_n^3\eta},$$

and from Eq. (A1):

$$\int_0^{\infty} |H(j\omega)|^2\,d\omega = \frac{\pi}{4\omega_n^3\eta}. \quad (A11)$$

Combining (23) and (A11), the noise equivalent bandwidth is given as:

$$B = \omega_2 - \omega_1 = \pi\omega_n\eta. \quad (A12)$$

Appendix B

SOLUTION OF AN EXAMPLE PROBLEM

It will be assumed that it is required to test a missile system's ability to withstand vibratory environments associated with transport from factory to the tactical position. The first items to be determined are:

1. A definition of the service environment consisting of a mean squared acceleration density plot, and

2. An analysis of the time the test specimen is exposed to the service environment, ts.

In order to present a definite example, suppose that Fig. B1 is a plot of $[\psi(f)]^{1/2}$. Also suppose ts = 1000 hours. The problem now is to decide how much we wish to accelerate the test. Suppose it is decided to accomplish the laboratory vibration tests in 20 hours. Assuming that the frequency range of interest is between 2 and 2000 cps, we may apply Eq. (41) to determine the minimum elapsed time per logarithmic cycle in the laboratory. Repeating Eq. (41),

$$t_f \geqq [600\ \log_\epsilon (f_u/f_L)]/f_L$$

or, substituting for f_u and f_L, $t_f \geqq 2050$ seconds. Therefore, we select t_f = 2400 seconds per sweep and p = 30 sweeps to obtain a laboratory test time of 20 hours.

A qualitative analysis of the complex structure must be accomplished to estimate the distributions of α and η. An example of the distribution of α for a number of different materials in a hypothetical situation is given by Table B1.

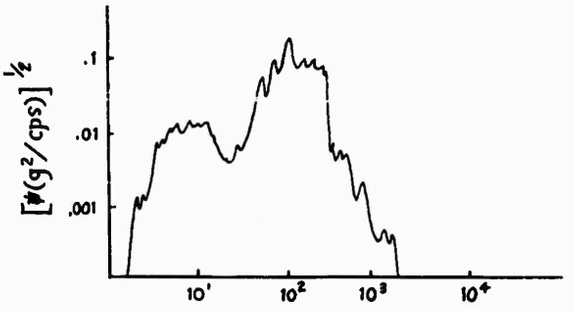

Fig. B1 - Plot of $[\psi(f)]^{1/2}$ for hypothetical problem

TABLE B1
Tabulation of Fatigue Characteristics

α_a	α_b	Percentage of Components between α_a and α_b
3.0	5.0	17
5.0	6.5	5
6.5	8.5	8
8.5	9.5	10
9.5	10.5	12
10.5	13.5	15
13.5	18.5	23
18.5	21.0	5
21.0	25.0	5

In order to utilize the digital computer program, the cumulative probability distribution of α must be given as input data. Assuming that the distribution is uniform between the given values of α_a and α_b, Table B2 gives the required input to the digital computer program. Notice that the tabulation is given in terms of equal increments of the cumulative probability.

It is recognized that a fair amount of engineering effort must be expended to determine the data given in Table B1. In order to utilize a cumulative damage concept, however, an estimate of the fatigue characteristics of the structural elements in the complex test specimen must be accomplished.

TABLE B2
Cumulative Probability of Fatigue Characteristics

Cumulative Probability	α
0.00	3.00
0.05	3.59
0.10	4.18
0.15	4.76
0.20	5.90
0.25	7.25
0.30	8.50
0.35	9.00
0.40	9.50
0.45	9.92
0.50	10.33
0.55	11.10
0.60	11.90
0.65	13.10
0.70	14.15
0.75	15.29
0.80	16.32
0.85	17.40
0.90	18.50
0.95	21.00
1.00	25.00

A similar method must be used to estimate the damping characteristics of the structural elements. To illustrate a slightly different approach, we suppose that the structure is of such a complex nature that it is impractical to obtain a reasonable estimate of the distribution of η.

Suppose, however, it is known from preliminary tests that the resonant amplification factors ($f = f_n$) vary between 5 and 50. Then, using the damped shock spectrum model, the limits of η would be expected as 0.01 to 0.1. If we assume a "quasi-gaussian" distribution of η between these limits with mean = 0.055, a table for the distribution of η may be generated. We define the "quasi-gaussian" distribution as a truncated gaussian distribution determined by letting η = 0.01 and η = 0.1 correspond to cumulative probabilities P = 0 and P = 1.0, respectively. The probability intervals between these levels are then adjusted to obtain a distribution very close to gaussian. Table B3 is a tabulation of the "quasi-gaussian" distribution. It is possible to obtain the exact normal distribution by calculation; however, the increased accuracy is not warranted.

TABLE B3
Cumulative Probability of
Damping Characteristics

Cumulative Probability	η
0.00	0.0100
0.05	0.0303
0.10	0.0348
0.15	0.0395
0.20	0.0424
0.25	0.0449
0.30	0.0471
0.35	0.0492
0.40	0.0511
0.45	0.0531
0.50	0.0550
0.55	0.0552
0.60	0.0589
0.65	0.0601
0.70	0.0629
0.75	0.0651
0.80	0.0676
0.85	0.0705
0.90	0.0752
0.95	0.0797
1.00	0.1000

We are now in position to generate the distribution of Re as given by Eq. (44). A total of 1000 values of Re were calculated utilizing the distribution of α and η given in Tables B2 and B3. As mentioned previously, the test parameters include t_f = 2400 seconds, $t_s = 3.6 \times 10^6$ seconds, P = 30, f_L = 2 cps, and f_u = 2000 cps. The distribution of Re is shown in Table B4.

TABLE B4
Statistical Distribution of Re
(1000 Points)

Interval No.	Limits of Re on Interval	Percentage of Re within Limits
1	.851 to 1.574	7.3
2	1.574 to 2.298	61.2
3	2.298 to 3.021	11.9
4	3.021 to 3.745	4.5
5	3.745 to 4.468	4.7
6	4.468 to 5.191	3.0
7	5.191 to 5.915	2.6
8	5.915 to 6.638	2.0
9	6.638 to 7.361	1.3
10	7.361 to 8.085	1.5

The test engineer must select a value of Re from the distribution of Table B4 to conform to the level of risk that can be tolerated. For example, assuming that the parameters used to generate Table B4 are fairly reliable, a value of Re = 5.915 would encompass approximately 95 percent of the distribution of Re. If Re = 5.915 is chosen to establish the laboratory test, we would expect that approximately 95 percent of the elements would receive at least the same damage from the laboratory test as from the service environment. Actually only those values of α and η which yield Re = 5.915 are tested in an equivalent way. Approximately 95 percent of the structural elements are overtested by the laboratory test and 5 percent are undertested. Selecting Re = 5.915 and noting from Eq. (44) that

$$Re = a_t / [f_n \psi(f_n)]^{1/2} = 5.915 , \qquad (B1)$$

it is evident that Re is dependent on the frequency range used during the laboratory test. This has been specified as f_n (lower) = 2 cps and f_n (upper) = 2000 cps. Rearranging Eq. (B1) as

$$\frac{a_t}{[\psi(f_n)]^{1/2}} = (f_n)^{1/2} (5.915) , \qquad (B2)$$

a point by point calculation may be used to generate a laboratory vibration test level. Using Fig. B1 to derive values of $[\psi(f_n)]^{1/2}$ and Eq. (B2) to calculate a_t a laboratory test level is shown in Fig. B2.

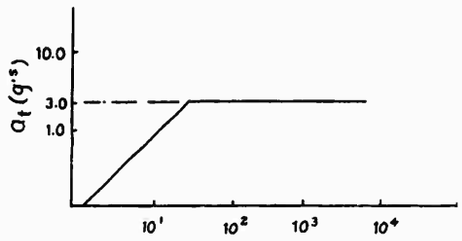

Fig. B2 - Vibration test level

Here the a_t has been drawn as a constant from 50 to 2000 cps to yield a more practical test input.

The vibration level given by Fig. B2 combined with the logarithmic frequency sweep schedule time of 2400 seconds between 2 and 2000 cps repeated 30 times defines the laboratory vibration test in one of the three orientations of the missile system. A similar procedure is necessary for the derivation of laboratory test inputs to the adjacent missile axes. In the event a failure occurs, the section entitled "Treatment of Laboratory Test Failures" is applicable.

DISCUSSION

Dr. Mains (General Electric): You refer to a logarithmic sweep; which logarithmic sweep? Any exponential sweep rate that you plot is linear on log-log paper. You can also put any slope on it that you wish. Which slope did you use?

Mr. Smith: I used a slope corresponding to my time, T_f. I used semi-log paper, not log-log. The ordinate was frequency, which is logarithmic, and the base was time which, of course, was linear. T_f started from zero and went to 2400 seconds, the frequency limit being 2 to 2000 cycles per second. This automatically fixes the slope and adjusts the sweep. This is very important because if the slope is too great, the model elements will not respond to the predicted steady-state calculations.

Dr. Mains: You use a straight line on semi-log paper?

Mr. Smith: Yes.

Mr. Winans (University of Pittsburgh): It is my understanding that this work is based upon Miner's cumulative damage law. Were any of the other more sophisticated rules of cumulative damage looked into, such as Freudenthal's work?

Mr. Smith: I did look into the other theories concerning cumulative damage on fatigue specimens. I felt that since we had all these other approximations involved, Miner's work was as good as any.

Mr. Bowman (Jet Propulsion Laboratory): What was the significance of the shock spectrum analysis?

Mr. Smith: We used the shock spectrum here as our mathematical model in deriving an equivalent test. We calculate the response of this model to some pulse, and compare this with the shock spectrum associated with some sort of transient that we observe in service. It's essentially the same thing that I did here. I used the shock spectrum model and compared it with the damage associated with the laboratory test and service environment.

Mr. Bowman: Is this for transient data?

Mr. Smith: The formula that I gave is good for an arbitrary input. It may be transient, steady-state, or any input you wish as long as it's mathematically well behaved.

* * *

MEASUREMENT OF EQUIPMENT VIBRATIONS IN THE FIELD AS A HELP FOR DETERMINING VIBRATION SPECIFICATIONS

I. Vigness
U.S. Naval Research Laboratory

The limitations of current methods of translating field vibration data into specifications are discussed. It is shown that in many cases an overtest may result. Several practical solutions to the problem are suggested, one of which is to make measurements of the response of structures in the field.

INTRODUCTION

It is customary to base shock and vibration specifications on measurements of field environments. The measurements are made on structural members and represent inputs to equipment mounting points. The environments are expected to represent conditions similar to those that an equipment might encounter during its eventual life. To obtain information about the environment, large numbers of measurements are made, enough to be statistically significant. These measurements are usually analyzed in terms of Fourier or shock spectra. Envelopes are drawn which include most of these spectral values, and specifications are based on the envelope values. The equipment will then be tested to the specification, which represents the worst of actual measured field conditions at locations similar to those where the item will be used. At first glance nothing could appear more reasonable than to require that an item be able to withstand shock and vibration levels at least as great as those known to exist at locations where the item will be used. Unfortunately life is neither simple nor reasonable, and oftentimes neither is this requirement.

This approach takes no account of the reaction of the item on its foundation. It requires that the foundation motion be maintained at specified levels regardless of this reaction. This does not happen in the field. When the item reaction is large the foundation motion is small. This causes those components of the motion, which are most likely to cause damage, to be consistently at lower amplitudes than the average level. If the tests are performed at fixed levels, regardless of equipment reaction, they may result in the unnecessary destruction of the equipment or of the test machine.

HYPOTHETICAL EXAMPLE OF OVERTEST CAUSED BY "ENVELOPE" SPECIFICATION TESTING

Consider an item, m, shown in Fig. 1, mounted on a foundation M. The foundation contains a source of vibration, say an unbalanced rotating mass, that generates a force in a certain direction which is equal to

$$F = F_o \frac{\omega^2}{\omega_o^2} \sin \omega t .$$

The force is made to vary as the square of the frequency to account for the variation of centrifugal force with frequency.

If the item, m, were not attached, the foundation (a rigid mass subjected to no other forces) would vibrate at a constant displacement amplitude at all frequencies. Assume that under this condition the amplitude is normalized equal to unity. This is represented by the straight line of unity value in Fig. 1. Let the item, m, now be attached to M by means of a linear flexible system that includes a known amount of viscous type damping. For a mass m equal to M, and for 5 percent of critical damping, the foundation motion will be as shown by curve B. The usual amplification curve for a single-degree-of-freedom system with this amount of damping is shown on curve R. The amplitude of vibration of m can be obtained by

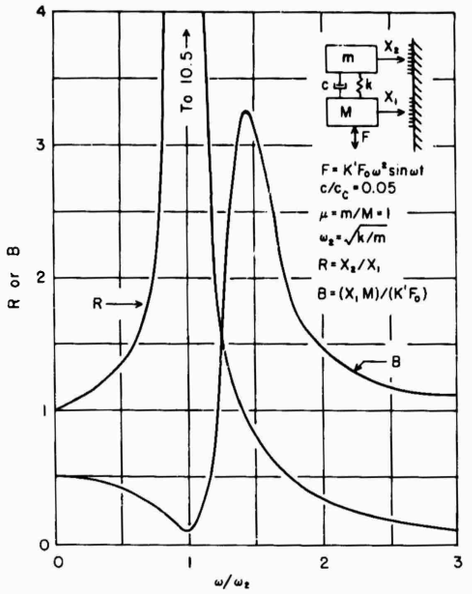

Figure 1

multiplying the ordinate values of curves R and B for any particular frequency.

If a large number of field measurements were made involving many such systems such as are shown in Fig. 1, and if the frequencies of the systems could be any value over a relatively wide range, then we would have a scatter diagram of vibration amplitudes such as is shown in Fig. 2. The maximum amplitude would be 3.25 which is the peak of curve B in Fig. 1, and the minimum value would be 0.1, which is the smallest value of curve B. Specifications would then require an amplitude of vibration at least as great as 3.25 (the envelope value) over the frequency range covered.

Now the actual amplitudes of vibration that item m experiences in the field, for our example are shown as curve D on Fig. 3. This is the product of the ordinates of curves R and B of Fig. 1 for corresponding abscissae. The actual vibration amplitudes of the item vibrated according to the envelope specification are shown on curve E of the same figure. This specification merely requires that the test amplitude be as great as the maximum amplitudes observed in the field. But for the hypothetical case illustrated this results in the item vibrating at an amplitude almost 30 times greater under the test condition than under the field condition.

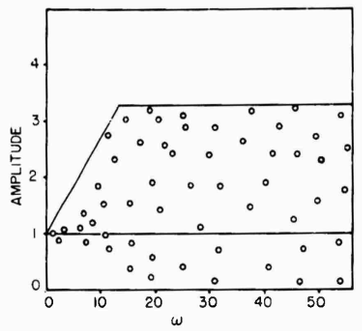

Figure 2

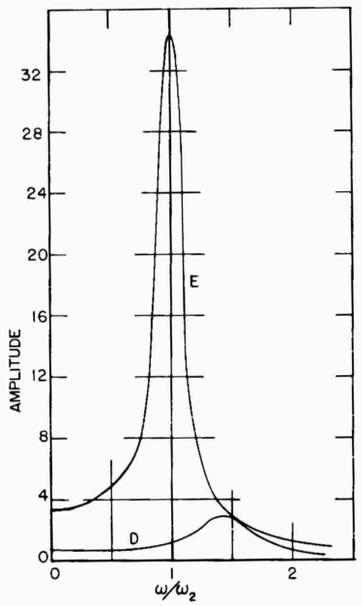

Figure 3

Obviously an extreme situation has been used in order to illustrate a principle. It is not implied that what has been said should permit any general relaxation of specifications. There may be tests, however, for a few items where study may be warranted to determine if the specifications are reasonable. Specifications should not be relaxed until it has been shown that they are unreasonable, and that it is impractical to comply with them. Not enough is known about the behavior of an equipment in its true eventual environment to permit acceptance

of an equipment if it can be made better without great penalties in weight or cost.

The illustration has been given for sinusoidal excitations. The problem exists as well for random vibration and for shock.

PRACTICAL SOLUTION OF PROBLEM

One practical solution to this problem is to equalize the vibration machine with a dead-weight load and to merely require for the live weight equipment load that the amplitude value, averaged over a fairly wide frequency range, be maintained at a specified level. This would still be a conservative test (assuming the mechanical impedance, or effective mass, of the vibration machine armature to be at least as great as the foundation) as we are basing our average value on the resonant-peak field value.

Another solution based on mechanical impedance measurements is possible. This would require that the vibration amplitudes of the foundation be determined together with the mechanical impedance of the foundation and of the mounted item as viewed by the foundation. This procedure could be followed for specific cases, but appears to be impractical for general field vibration studies.

A third approach is suggested as an additional possible solution. Instead of relying only on a statistical array of foundation motions for the derivation of specifications, a statistical assembly of equipment responses should additionally be obtained. In general, subject to many qualifications, specifications would permit the input to be decreased in certain frequency regions where equipment responses are considerably in excess of the envelop of such responses determined from field measurements.

Specifically the method would require:

1. Measurements of the amplitudes of vibrations of equipment as well as the amplitudes of the foundations on which they are mounted. Generally a point on an equipment would be selected which had the greatest amplitude, and measurements would be taken in the direction of greatest amplitude. Enough measurements must be taken of a sufficient number of different items so as to obtain a statistically significant sample.

2. Categorize the equipment as to mounting method (flexible or solid mounts), weight, and foundation structure. The latter would be very general, but should distinguish at least between a ship and a missile.

3. From this statistical study of equipment vibrations set an upper limit (envelope curve) of equipment vibration amplitudes for vibration tests. If resonances occur which cause the equipment to vibrate at amplitudes in excess of those observed in the field, for its category, the excitation amplitude would be reduced until this is no longer the case.

The test engineer must be permitted to exercise his judgement as to the category of the equipment. He must pass judgement as to whether the vibration characteristics of the equipment, as mounted, are so unusual that the field data are inapplicable.

* * *

DETERMINATION OF AN OPTIMUM VIBRATION ACCEPTANCE TEST

G. J. Hasslacher, III and H. L. Murray
General Electric Company
Utica, New York

A method of determining an optimum vibration acceptance test specification for aerospace electronic equipment is described. Electronic equipments are subjected to repeated test sequences at given levels until failure occurs. Data thus produced will yield an acceptance level which will not fatigue the equipment. A discussion of the related statistical and reliability problem is presented.

The acceptance test plays an increasingly important part in the military and space electronics industry. In many instances the acceptance test may be the key to success or failure of a mission. For the purposes of this paper the acceptance test is defined as a test or series of tests to which all deliverable equipments are subjected to insure they are representative of the design, free of defects, and meet certain acceptance standards. The concern of this paper is with the vibration portion of these tests. The performance of the acceptance test can, of itself, reduce, or even increase, the probable life of the equipment. If the vibration acceptance test is run at a level above the endurance limit of the equipment, the resultant fatigue damage reduces the useful life of the unit. On the other hand if the acceptance test rejects a defective unit the overall reliability of the equipment is increased. This paper is concerned with one approach to the problem of determining an acceptance test which minimizes or eliminates fatigue damage and maximizes the detection of defects.

For our purposes we shall define the ideal acceptance test as having the following characteristics:

1. The test should not reduce the life or reliability of the equipment;

2. The test should detect all defects or design deviations; and

3. The test should be representative of the typical mission environment.

This ideal acceptance test is probably an unattainable goal. Any operation of the equipment expends some of its useful life. At the same time it is certain that no test can detect all defects or design deviations. These first two characteristics, however, are approachable goals and certainly form the basis of the ideal test. The third characteristic, simulation of mission environment, is not necessary but is desirable. If the acceptance test is representative of a typical mission and if the acceptance test level has been determined by the method described herein there is added confidence (both psychological and statistical) that the equipment has the desired reliability.

Any study involving determination of reliability must concern itself with failures. For the present study, failure is defined in terms of equipment operation. Any deviation from acceptable performance standards is defined as a failure. All failures were further divided into two classifications — noncritical and critical failures. A critical failure is one which would jeopardize mission success; and a noncritical failure would not endanger mission success. For the purposes of acceptance test criteria all failures were classified according to cause of failure as follows:

1. Manufacturing or component defects;

2. Fatigue failures or equipment wear out; and

3. All other failures (random failures).

Manufacturing or component defects are the result of the manufacturing process and not the design. Typical defects in this category are unsoldered or poorly soldered wires, wires nicked

during stripping, machining chips, components which short or open during vibration, and similar defects that are not part of the design. It is these defects that the acceptance test is designed to detect. Fatigue failures should not occur in normal use with well-designed equipment. Continual use of equipment beyond its normal life will result in failure due primarily to time. Such failures include mechanical fatigue of wires and leads, wear-out of moving parts, filament failure due to repeated use, and similar failures. An improper acceptance test can cause fatigue damage even in well-designed equipment. For example, missile equipment with a flight time measured in seconds or minutes spends more time in acceptance test than in flight. Even the best designed equipment will have failures that cannot be attributed to fatigue or to production defects. Such failures are generally random and actually constitute the ultimate reliability of the equipment. If the acceptance test can detect all failures of the first kind – production defects – and does not introduce failures due to fatigue, the maximum reliability of the equipment can be achieved.

The curves of Fig. 1 illustrate the problem we are trying to resolve. As the acceptance test level is increased the number of defects detected increases. This will result in improved reliability. The fatigue curve, however, shows that as the acceptance level increases the fatigue life decreases, and there is a consequent loss in reliability. The optimum vibration acceptance level which is being sought is one which maximizes defect detection and minimizes fatigue damage. The reliability curve shows what is believed to be the overall effect. The reliability increases with acceptance test level and reaches a maximum at some point. The problem is to define that optimum level.

It should be noted here that an added factor in the problem is that the procedure in acceptance testing is to repair or replace defective elements and repeat the acceptance. Also, if the unit requires repair or modification before actual use it must be subjected again to an acceptance test. The number of acceptance tests to which an equipment may be subjected during its life may result in vibration exposure many times as long as its actual flight life.

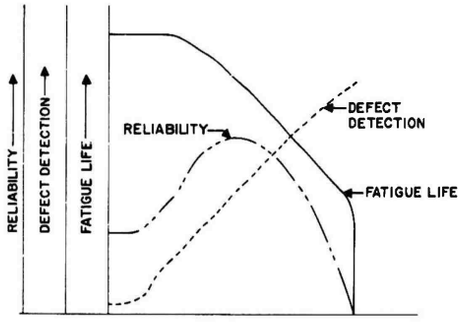

Fig. 1 - Acceptance level

In the course of this discussion a number of assumptions have been expressed or implied. At this point many of these are worth listing and discussing.

1. Defect detection improves with increased acceptance test level.

2. Repeated tests of one unit equals single tests of many units.

3. Failures may be identified and classified.

4. Repair of units does not shorten or lengthen life.

5. Electronic equipment under vibration does exhibit "fatigue" failure.

6. Failures are a function of level only.

The most important of these is the assumption that increasing acceptance test level will increase the detection of defects. In order to investigate this assumption the results of two evaluation programs have been analyzed. In these programs electronic systems have been subjected to repeated "flights" or missions. Failures were defined as any deviation from required operating specification. Some failures occurred only during actual vibration. During this evaluation testing which consisted of hundreds of simulated missions, eleven failures occurred. Of these eleven failures, seven could be detected only under high level vibration. These seven failures or defects could not be detected at the previously used acceptance test levels. A new higher level would have found these defects and improved the MTBF of the equipment by a factor of 2.75. During this and subsequent evaluation programs, many hundreds of simulated missions with the same type system have shown that the majority of the failures cannot be detected except at higher vibration levels. During a recent evaluation program four systems were acceptance tested at the new higher acceptance level. The systems were then subjected to another acceptance test at twice this level and two manufacturing defects were uncovered. A more vivid, but less scientific, illustration was uncovered by accident. One of the evaluation systems which had been

subjected to hundreds of "flights" at the old low acceptance level was used for an engineering evaluation at higher levels. At the first application of the high level vibration the equipment failed. The source of failure was an unsoldered joint.

Another assumption that is somewhat more difficult to justify is that repeated flights of one equipment are equivalent to single flights of many equipments. If there are no fatigue failures — any failure due to repeated stresses — this assumption is valid. In determining reliability from repeated flights any fatigue failures are censored out. It might be noted here that for the purpose of determining fatigue levels all non-fatigue or random failures must be censored from the data.

All of this discussion leads to the question of whether it is possible to separate failures into such categories as random, fatigue, or design failures. Here we must rely on engineering judgment and extensive analysis. Some failures are rather obvious, such as, unsoldered joints, failures at first excitation, and shorts between elements with no mechanical damage (all random failures or manufacturing defects). Broken wires after extensive vibration, any element with mechanical damage after repeated excitation, and similar failures are due to fatigue. In summary it is only after careful analysis by several experts that we can assign a classification to a failure. Even after this classification, additional thought must be given to the problem before a failure is censored from data.

Since the units used in these evaluation programs were repaired whenever a failure occurred there is some question of whether the repair affected the life of the equipment. The justification for assuming that repairs do not affect equipment life is simply that these repairs are the same as one encounters on the production line when a unit electrical test shows a defect. The repairs during the program are no different from those made on new equipments during production.

The question of whether electronic equipment exhibits "fatigue" failure is partly a problem of definition. If "fatigue" behavior is defined as a time dependent failure that follows the pattern of classical fatigue failure when level vs time are plotted on log-log coordinates then the results of this evaluation will speak for themselves. Some mechanical failures during this program have been isolated and examined microscopically. These failures show the classical fatigue failure pattern. These add further weight to the assumption of "fatigue" failure in electronic equipment.

That failures are a function of level only is not basically correct. The response of a single-degree-of-freedom-system to random vibration, however, can be shown to be relatively independent of spectral shape variation as long as the general frequency range is the same. The shapes used in these studies were generally the same and the slight variations should not affect the results greatly.

In determining a vibration acceptance test one of the first decisions is the choice between random, sine, or random plus sine vibration. It is not the purpose of this paper to discuss the relative merits of the various types of vibration testing. Random vibration has been used for these acceptance tests since the vibration in missiles is typically random. In addition, a random vibration test, for equivalent excitation of all elements, takes less time than a sine test. The random vibration spectral shapes were derived from flight data. In Fig. 2 the three basic frequency spectra are shown. The first is a sinusoidal test, the second the Phase I low-level random spectrum, and the third the Phase II high-level random spectrum. The difference between Phase I and Phase II vibration spectra is the result of additional flight data obtained during the time between Phase I and Phase II. Recent flight data indicate that the second shape is most typical of current missile vibration.

The evaluation program from which the data on fatigue were obtained was conducted in the following manner. Identical units of missile equipment were selected for the program. Seven samples of three different packages were used but data for only two of the packages are presented here. The results for the third package

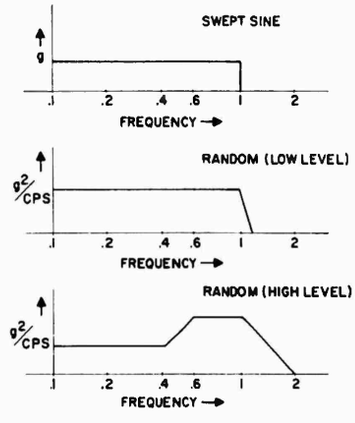

Fig. 2 - Vibration spectra

have not been presented for the simple reason that there were no significant failures of this unit. Each sample was subjected to repeated simulated "flights" or acceptance tests. A "flight" consists of pre-vibration electrical test, application of vibration with electrical exercise of the package and post vibration electrical test. Failures were defined in the following manner:

1. Critical failures — failures or deviation in performance that would affect mission performance.

2. Noncritical failure — deviation in performance or measured parameters that would not affect mission performance.

All failures were investigated and the component or other defect found and repaired before proceeding.

The program was actually accomplished in two phases. After the completion of the first phase, which was basically a reliability program, the need for further work on fatigue was recognized.

The results of the Phase I program that pertain to the fatigue and acceptance test problem are shown in Figs. 3 and 4. In determining reliability from repeated tests of the same equipment the fatigue failures should be censored from the reliability data. The plotting of these censored data, the fatigue-failures, revealed an interesting pattern. At the 0.308 vibration level there were no fatigue failures. This same system was run at the 2.20 level and the first fatigue failure was noted at 0.22 time units for unit A and 0.51 time units for unit B. A second system was run at the 2.20 level and fatigue occurred in both units at 0.23 time units. The third system was subjected to the 0.923 acceleration level and the first fatigue failure of unit A occurred at 6.50 time units and of unit B at 4.35 time units.

A time unit of 1 represents an arbitrary safety limit on equipment life. The acceleration unit of 1 represents an acceptance test level goal. The results shown in Figs. 3 and 4 show no fatigue failures in the region bounded by these limits. Assuming that the acceleration-level-versus-fatigue-life curve follows a straight line in a 10-g log plot, we see that a reasonable level without fatigue for acceptance tests is somewhere in the region of 1.5 to 1.7 acceleration units.

These results indicated that increased acceptance test levels would be both profitable and possible. The evaluation program was continued with the objective of gaining further data in the region between levels 1.0 and 2.0. Four additional samples were added to the program. Two samples were run at the 2.05 level, one at the 1.88 level and one at 1.72 level. The results of this second phase are shown in Figs. 5 and 6 along with the first phase results. The first fatigue failures occur at 0.44 and 0.59 time units for the 2.05 level on unit A, and 0.44 for unit B. One sample of unit B has gone 0.60 time units without failure. The first fatigue failure at the 1.88 level occurred at 1.8 for A and 2.6 for B.

From the curves of Figs. 5 and 6, the best acceptance test level can be determined. The data do not automatically set a level without

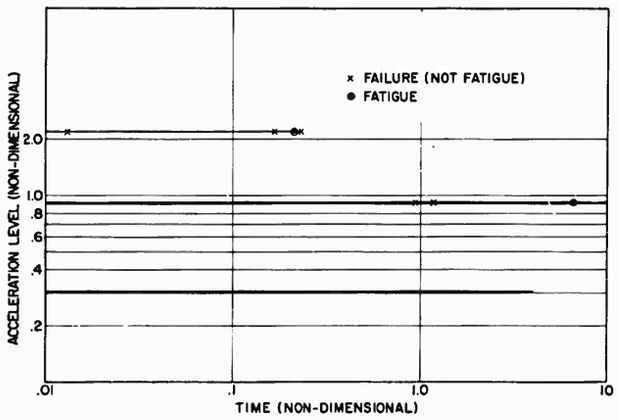

Fig. 3 - Phase I, Unit A; failures in repeated tests

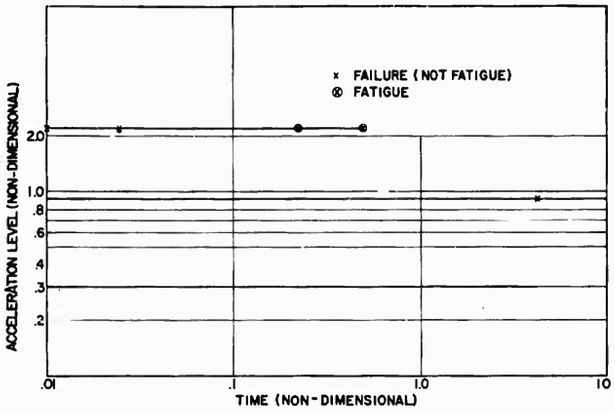

Fig. 4 - Phase I, Unit B; failures in repeated tests

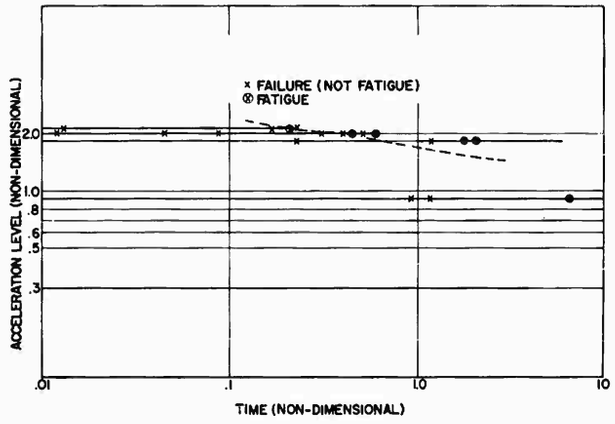

Fig. 5 - Unit A; failures in repeated tests

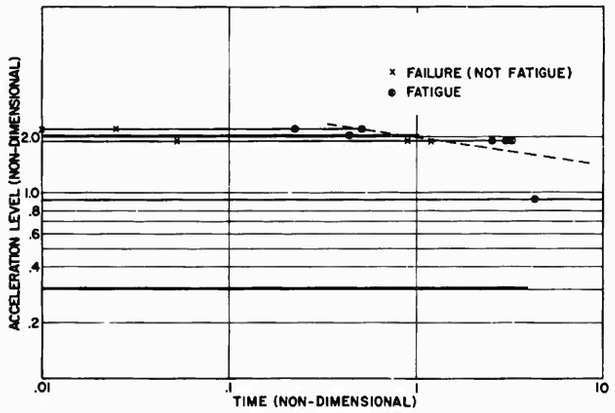

Fig. 6 - Unit B; failures in repeated tests

some information on the expected equipment life. If the equipment is single mission equipment (missile or spacecraft) the expected life includes the mission time plus all acceptance test vibration. For multi-mission equipment the acceptance test vibration is usually negligible. To this expected life must be added some factor of safety. With this established, in our case 1 time unit, the allowable acceptance test level is easily determined. The level selected here is 1.8 acceleration units.

The results of this study have led to several important conclusions. There is definite evidence that manufacturing defects are missed by low level acceptance tests. If these defects are not uncovered the reliability of the equipment is reduced. On the other hand it has been shown that these defects are uncovered by higher acceptance test levels. It has also been shown that fatigue does occur, as one would expect, but the fatigue is not haphazard. It follows a definite pattern consistent with fatigue theory and is reasonably predictable. A vibration acceptance test level can be determined that will not reduce the life of the equipment and will increase reliability by detecting manufacturing defects.

Perhaps the most important point to be made here is that the acceptance does affect equipment reliability. Arbitrary establishment of vibration acceptance tests without regard to fatigue or the effectiveness of the tests can do more harm than good.

There is still much work to be done in this general area of acceptance test and fatigue. The most important task is the verification, both analytically and experimentally, of the fatigue curve for real equipments subjected to random vibration.

Failure analysis is, at the moment, primarily a matter of opinion. In this area more careful investigations of failures and causes of failures can aid both the present problem and the general problem of reliability. One question to be answered is whether random failures do exist. Until more work is done in this and similar areas the question of what is the optimum acceptance test must remain open.

DISCUSSION

Mr. Callahan (McDonnell Aircraft Corp.): You used the term "typical mission environment." Are you suggesting that the acceptance tests on new units be the actual expected environment in each of the three axes for the time duration on the flight?

Dr. Hasslacher: The units I am talking about are subjected to many, many environments on many different vehicles under many different conditions. What I suggest by typical is that it have the spectrum shape. I would be delighted if it could be at the level of the mission. If the actual level were 10 g rms with hay stack shape, I would like the acceptance test to be at that level because it would give me added confidence.

Mr. Callahan: Have you done this on any other systems? Do you have any additional background? We build some spacecraft where the whole production run is 12 units. You set seven or nine units to determine the acceptance test. Naturally we can't do that.

Dr. Hasslacher: Right, if I knew the fatigue behavior, I could extrapolate with more intelligence from the qualification test levels and come up with an acceptance test level that was high enough, but still low enough to avoid fatigue. There is a lot of work to be done in this area, and I hope it will be possible to do this eventually without all this testing. Right now, we are fortunate. I can get the equipment.

Mr. Callahan: If you are suggesting a full typical mission in each of the three planes, what do you do in case of retest? Do you say that you can repeat this time after time until you get the thing to pass the test in each of three planes without any trouble? What is your criterion for acceptance in the acceptance test?

Mr. Hasslacher: The criterion for acceptance would have to be set up by agreement. My own feeling would be that you should get the equipment to pass completely your acceptance test in the three directions. If you have a good acceptance test setup, the level is high enough so that you get the defects but low enough so that you will not fatigue the item even though the test is repeated 18 or 20 times to get it through. It can be done.

* * *

VIBRATION TESTS, AN ESTIMATE OF RELIABILITY

J. L. Rogers
Martin Company
Denver, Colorado

This paper discusses the use of vibration tests as a tool in the evaluation of component reliability. Test data will be presented to show how raw data are tabulated, reduced, and illustrated. Examples of correlation between flight-test-measured reliability and estimates from vibration tests will be shown.

SCOPE

Most Flight Certification and Qualification Test Programs have certain deficiencies which can be overcome in a well integrated test program. These deficiencies are:

1. The tests yield no margin of safety (reliability) data.

2. The tests yield insufficient life data.

3. The overall test program on a given component is not integrated, resulting in redundant testing and increased costs.

4. The tests provide no real basis for establishing the reliability of each critical component.

5. A non-integrated test program besides being costly, yields information too late in the program and divorces the designer from direct responsibility for his component.

TEST PROGRAM PHILOSOPHY

This testing is the systematic analysis of hardware reliability potential. Since component reliability of 1.00 cannot be achieved, it is necessary to determine the relative reliabilities of the components to be used. This knowledge then establishes a priority for concentration of efforts on the least reliable components. The program is characterized by the use of a sequential series of tests designed to promote the maximum reliability growth rate through time-induced failures, parametrically induced failures, some attribute tests, the use of statistical analysis of test results, and extensive use of failure analysis.

Component unreliability occurs primarily as the result of an insufficient margin of safety existing between the mean failure-producing stress, and the mean true-operating stress. Since unreliability represents a probability of failure, every effort is undertaken to minimize it.

These tests are primarily "Test-to-Failure" with subsequent failure analysis, repair, and retest. This technique permits accumulation of a maximum of data with a minimum quantity of test hardware. This testing is sequential inasmuch as the extent of testing on each component is dependent upon initial results from previous tests. It makes use of testing-to-failure in the time domain, separation of variables, induced failures in the stress domain, attribute test, failure analysis, and determination of system tolerances as analyzed by transfer functions. Statistical analysis is employed to evaluate susceptibility to each dominant stress in terms of standard deviations from the design criteria.

Part I, Survey and Analysis Tests

In the absence of sufficient test data to evaluate properly the reliability or the potential reliability of a component, it is necessary to subject the components to survey-type testing in order to determine critical weaknesses and dominant failure modes. Survey testing will assume the form of abbreviated life testing, or testing in the time domain under both bench and

simulated minimum acceptable environmental conditions. Aside from determining problem areas and establishing priority for further testing, results from survey testing will be used to expedite corrective action on critical usage components. Additionally, a foundation of basic data is obtained which is a reference point throughout the remainder of the program for measuring reliability growth.

Part I Testing will be divided into two types — bench operating and minimum acceptable environmental operating. All of the pertinent environments at the minimum acceptable levels for the minimum acceptable time, as well as a minimum number of cycles or minimum operating time, are accomplished during Part I. The primary advantages of Part I testing over development, design confirmation, and flight certification testing are the substantial savings in time and money because duplication of testing is avoided. All failures produced during this part are time-induced inasmuch as all applied stresses will be maintained at minimum acceptable levels. Both types of testing are described in the following.

Bench Operating Tests — Bench operating tests consist of operating the component at ambient environments and within design performance specifications, for sufficient time to demonstrate accomplishment of minimum acceptable life, the test sample will then be exposed to a sequence of the applicable environments (humidity, salt-fog, and so on). These tests will be singularly applied followed by a functional cycle. After completion of this series of tests, the test samples will be returned to the bench and the life test continued until failure, or the accumulation of sufficient time to yield increased confidence in the "life" capability of the equipment.

Environmental Operating Tests — Environmental operating tests will consist of operating the equipment under selected minimum acceptable environments, such as the design level of vibration, for sufficient time to demonstrate accomplishment of minimum operating time or cycles. The unit will then continue to be cycled at this level of vibration until failure or until a designated time is reached. This time would be sufficient to demonstrate a practical margin of safety in the time domain. The purpose of these tests will be to collect failure data on those failures induced by the design level of vibration.

Part II, Marginability Tests

To promote the maximum system reliability growth rate, it is essential that those components exhibiting the least reliability receive the maximum improvement effort. Since this effort can be most expediently applied by basing the corrective action on actual failures, it follows that a program designed to accelerate the accumulation of failure data is needed. Critical stresses, including those introduced by flight environments will be manipulated to induce failures independent of time.

The purpose of Part II tests will be to establish the margins of safety associated with each operating stress and to isolate, through failure analysis, the element or subcomponent assemblies responsible for the failures. Margins of safety will be determined in terms of the standard deviation of the failure producing stress distributions. Part II tests will be divided into two types as described in the following.

Environmental Marginability — During this phase of testing, the vibration level will be varied to the point of equipment malfunction, while holding the input parameters, such as, voltage or pressure, constant at the designed operating level. The following technique will be used in obtaining the data:

1. Determine the magnitude of the increments in which the vibration level will be varied (such as 2 db).

2. Determine the input stresses to be applied (voltage, pressure, load, and the like) to the component; these stresses will be held within the design tolerance.

3. Determine which outputs are to be monitored and what value or values of the outputs will be considered a failure condition.

4. In performing the actual test it is essential that the selected output be monitored constantly to record the precise point of failure. It should be determined if the failure is of a permanent or temporary nature. To be permanent, the failure condition must persist after the vibration level has been returned to the design level. Failures found to be temporary or transient in nature must be repeated to determine if there is a distribution associated with the failure-producing level.

5. The number of temporary and permanent failures which must be induced by each environment will be specified for each type of equipment.

Performance Marginability — Input parameters will be varied one at a time to the point

of equipment malfunction, while holding the environmental conditions constant at minimum acceptable flight levels. The following techniques will be used in obtaining the data.

1. Select the input stresses to be applied and the input stress (voltage, load, pressure, and so on) to be varied.

2. Determine the direction and magnitude of the increments in which the selected input stress will be varied.

3. Determine which environments will be applied. These environments must be held constant or within specification (temperature, vibration, and so forth).

4. Determine which outputs should be monitored to detect failure, and the values of these outputs which constitute a failure condition.

5. In performing the actual test, it is essential that the selected output be monitored constantly and the input stress varied to record the precise point of failure. It should be determined if the failure is of a permanent or temporary nature. To be permanent, the failure condition must persist after the failure producing stress has been returned to specification levels. Failures found to be temporary or transient in nature must be repeated to determine if there is a distribution associated with the failure-producing level.

6. The number of temporary and permanent failures which must be induced by each input stress will be specified for each type of equipment.

FAILURE ANALYSIS

Failure analysis shall be performed on all components that fail in both stress and time. The failure analysis shall be accomplished in the following steps.

Isolation of Weak Link

The cause of failure shall be determined by isolation of the failed elements or piece parts through inspection and checkout techniques.

Determination of Cause

After it is determined that the failure is repetitive in nature, the cause of failure shall be determined by analysis of stress or operating conditions on the failed element. The environmental or operating stress that produced the failure under either Part I or Part II shall be duplicated to reproduce the failure. A group of these elements shall be subjected to marginability type tests of Part II to establish the failure distribution of the element under the failure producing stress. The results of these tests shall be utilized in establishing corrective action or redesign.

Verification

After an improvement has been incorporated, a retest is necessary. This will be in the form of a repeat of the test that proved the need for an improvement.

TEST DATA PRESENTATION

The examples of test data presentation included herein are intended to show how raw test data are tabulated, reduced, and illustrated.

Figure 1 illustrates how the raw data from a typical induced-failure test would be tabulated and reduced. The first column headed Test Number, indicates the testing sequence. Each failure analysis report shall reference one of these numbers. If more than one unit was utilized in this sequence, the serial number of the units will be included with these numbers. The second column, headed Failure-Stress (X), indicates the value of the stress which produced the failure. This could be an input voltage in the case of a performance marginability test, or a "g" level in the case of vibration marginability test. Other column headings are self explanatory. As indicated, the mean failure producing stress is determined to be 95, the standard deviation — 6.98, and the standard deviation corrected for sample size — 8.46.

Figure 2 illustrates graphically the data tabulated in Fig. 1. The reference level shown in the figure represents the design level for the particular stress under study. The safety margin shown is determined by dividing the corrected standard deviation of the distribution into the difference between the mean failure producing stress (x) and the reference level.

Figure 3 illustrates graphically the results of a design improvement action on a component which reduced the magnitude of the standard deviation of the frequency distribution of the failure producing stresses. The solid curve represents the distribution of the failure

Test Number	Failure Stress (X)	Deviation from Mean (x)	$(x)^2$
1	99	4	16
2	82	13	169
3	96	1	1
4	90	5	25
5	102	7	49
6	98	3	9
7	94	1	1
8	103	8	64
9	90	5	25
10	88	7	49
11	106	11	121
12	92	3	9

$\Sigma X = 1140$ $\Sigma x^2 = 538$

Mean Failure Producing Stress $\bar{X} = \frac{\Sigma X}{N} = 95$

Standard Deviation $s = \sqrt{\frac{\Sigma x^2}{N-1}} = 6.98$

Standard Deviation Correction = $s_e = 1.213s = 8.46$

Correction Factor for small samples = $1 + \frac{1}{\sqrt{2(N-1)}} = 1.213$

Fig. 1 - Tabulation and reduction of raw data from a typical induced-failure test

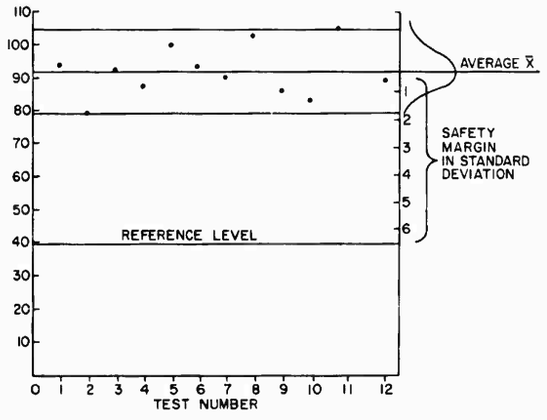

Fig. 2 - Graphical reduction of data

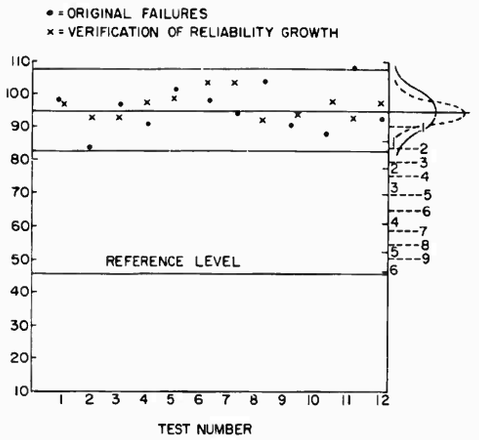

Fig. 3 - Example of reliability growth by reducing scatterband

producing stresses before the design improvement, and the broken curve represents the frequency distribution of the failure-producing stresses after the design improvement. Note that while the mean is unchanged, the margin of safety has increased from 6 standard deviations to almost 10.

Figure 4 illustrates the results of a design improvement which produced an increase in the average strength or in the mean failure-producing stress. In this example, the frequency distribution curves are identical, but the margin of safety has been increased from 6 standard deviations to approximately 9 by increasing the average strength from 95 to approximately 120.

Figure 5 illustrates the most common condition of unreliability. These curves represent a condition in which either the design criteria for the component was improperly specified, or the component was improperly designed. The condition depicted is one in which a "negative" safety margin exists. Since the data graphically presented in the bottom curve would not become available until a considerable amount of missile testing has been accomplished, the approach to component development should be to minimize the magnitude of the standard deviation of the frequency distribution of the failure-producing stresses as determined by induced-failure testing, and to maximize the mean failure-producing stress as determined by testing.

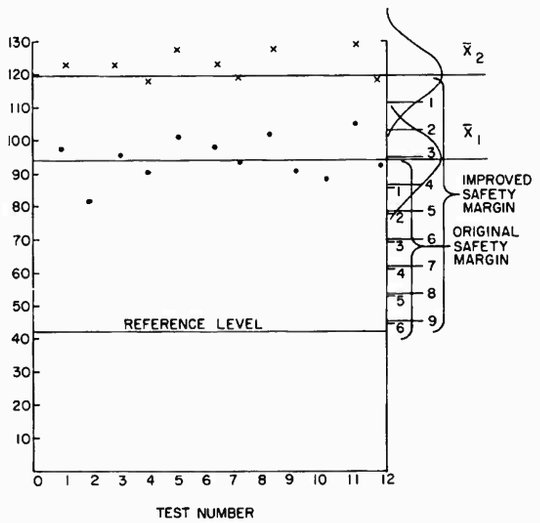

Fig. 4 - Example of reliability growth by increasing average strength

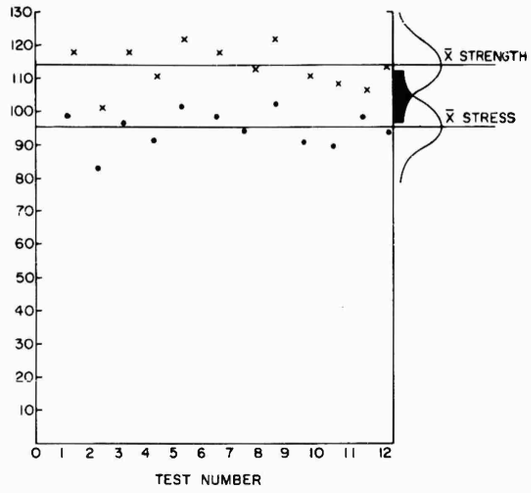

Fig. 5 - Example of negative margin of safety

* * *

Section 6
STANDARDIZATION OF VIBRATION TESTS

SINUSOIDAL VIBRATION TESTING OF NONLINEAR SPACECRAFT STRUCTURES

W. F. Bangs
Goddard Space Flight Center, NASA
Greenbelt, Maryland

The vibration testing of large spacecraft structures in accordance with procedures similar to those developed for military equipment during the 1940's has numerous shortcomings, particularly if the testing process is considered to be a duplication of an equipment's in-service vibration. The purpose of this paper is to discuss some of the shortcomings associated with the familiar sinusoidal sweep test.

Waveform distortion, being one of the more obvious problems, is discussed. An analytical model of a simplified structure undergoing vibration testing was studied with the aid of an analog computer. Solutions for a nonlinear model demonstrate distortion of the armature acceleration even though the applied force is sinusoidal. Filtering the control signal to eliminate distortion may unduly penalize the specimen, although this technique is acceptable where the distortion is the random type caused by the banging of parts.

The current trend toward larger spacecraft structures will undoubtedly continue, and the problems we now face will be small in comparison to those of the future unless some revisions are made in today's philosophy.

INTRODUCTION

The sinusoidal sweep vibration test is required by Goddard Space Flight Center (GSFC) for the qualification of spacecraft structures and subassemblies. Although it is generally agreed that random vibration testing more closely simulates the actual flight environment, sinusoidal tests will continue to be specified either as a supplement to the random test or, in some cases, as the sole vibration requirement. The reason for this policy is that the sinusoidal test offers certain advantages over the random test:

1. The sinusoidal test is superior as a diagnostic tool. Since excitation is applied at a single frequency, resonant frequencies and modes can be accurately described. Because random excitation produces the simultaneous response of many modes, the behavior of each mode is obscured. Performed in the development stage, the sinusoidal test invariably points out design deficiencies that can be corrected early in the test program.

2. Sinusoidal vibration can be applied in the frequency ranges not included in typical random tests. Most important is the frequency range of 5 to 20 cps, in which stress levels are likely to be high and interaction of a spacecraft and a vehicle, in its low frequency modes, is likely to occur. Many of the larger spacecraft now being developed have resonances below 20 cps.

3. Sinusoidal testing is relatively inexpensive, and equipment is readily available. For this reason, testing at the subassembly level is often accomplished by using only sinusoidal excitation. Sine wave tests are usually specified

in terms of motion (acceleration, velocity, or displacement) at the normal mounting point of the equipment under test.[1] One of the major problems occurring in sinusoidal vibration testing of structures that are heavy compared with the shaker armature is waveform distortion in the motion of the mounting point.

Since the input, or specification level, is normally monitored at the mounting point, waveform distortion here raises questions about the adequacy of the test. Figures 1 and 2 show examples of distorted waveforms that were observed during the vibration testing of the Orbiting Solar Observatory I satellite (1962 ζ 1) structural model.[2]

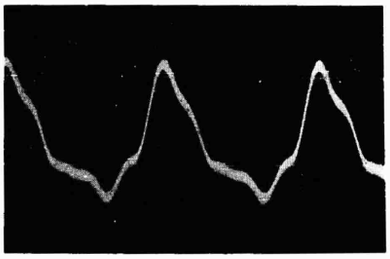

Fig. 1 - Harmonic distortion of input

The purpose of this report is to review some possible sources of waveform distortion, present the results of an analog study of a nonlinear system that exhibited distortion, and discuss the effects of distortion on vibration testing.

SOURCES OF DISTORTION

The problem of distortion in sinusoidal vibration testing is not a new one. Its magnitude, however, has increased in recent years until it can no longer be ignored as it has in most cases in the past. In some recent tests,[3]

[1] One exception is the specification for the NASA Scout and Delta payloads, in which there is an option allowing simulation of the solid rocket motor vibration by controlling the force imparted to the payloads.

[2] E. J. Kirchman and R. Hartenstein, "Evaluation of Vibration Test Data from the S-16 Structural Model Tests," NASA/GSFC Report 321-1 (RH) S-16-09 (May 1961).

[3] E. F. Shockey, "S-51 Dutchman-Separation Mechanism Vibration Tests," NASA/GSFC Memorandum Report 621-7 (Dec. 1961).

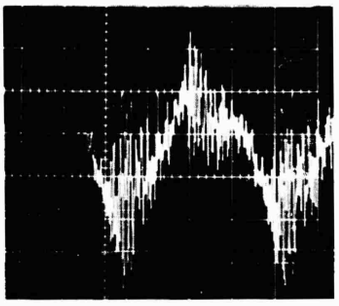

Fig. 2 - Aperiodic distortion of input

the harmonic components have exceeded the fundamental, so that determination of the source of the distortion has became imperative.

Wrisley[4] suggests that in some cases the equipment can be at fault. If a small amount of harmonic distortion is present in the output of the vibrator's power supply, we can expect a condition in which the frequency of a harmonic is coincident with that of a lightly damped resonance in either the structure being tested or the armature. The resonant structure could then be excited at a level great enough to produce a significant amount of harmonic motion at the input transducer location.

Although waveform distortion in the electrical input can certainly be a cause of input motion distortion, the type of distortion plaguing the engineer in spacecraft testing is that resulting from structural nonlinearities. The following symptoms support this theory:

1. The frequency of the harmonic usually does not correspond to a resonant frequency of the structure.

2. The apparent resonant frequency varies with the amplitude of excitation. This is a well-known characteristic of nonlinear structures.

3. The random distortion (as shown in Fig. 2) couldn't very well be attributed to electrical wave distortion.

Structures exhibiting nonlinear stiffness properties can be broadly classified as either

[4] D. L. Wrisley, "Some Effects of Acceleration Waveform Distortion in Sinusoidal Vibration Testing," Test Engineering 5(2):16-18 (Feb. 1961).

continuous or discontinuous. An example of a discontinuous structure is one in which there is small clearance or looseness between parts. If, during the vibration excitation, parts collide, many modes of the parts will be excited at high accelerations. Figure 2 shows the effect of this phenomenon on the input acceleration.

Structures that are continuously nonlinear influence the shaker motion by adding harmonics to the waveform. Figure 1 is an example of this. To further understand the effects of nonlinear structures undergoing vibration, a simplified shaker and a single-degree-of-freedom specimen with a cubic hardening spring were studied by means of an analog simulation.

ANALOG SIMULATION

The mathematical model is based on the following assumptions:

1. The vibrator's armature, the test fixture, and the part of the test specimen not resonating act as a rigid mass.

2. The part of the specimen in resonance can be represented as a mass with a nonlinear connecting spring.

3. The force acting on the vibrator's armature coil is sinusoidal regardless of the motion of the armature.

The system is shown in Fig. 3. Summing the forces on each mass yields the equations of motion:

$$M\ddot{x} + C\dot{x} + D(\dot{x} - \dot{y}) + Kx + f[x - y] = F \sin \omega t , \quad (1)$$

$$m\ddot{y} + D(\dot{y} - \dot{x}) + f[y - x] = 0 , \quad (2)$$

where $f[\ ]$ is the nonlinear spring force, a function of the spring extension $(y - x)$ or compression $(x - y)$, and the notation for masses, spring constant, damping coefficients, and coordinates is indicated in Fig. 3.

Structures often have a tendency to become stiffer or to "harden" with deflection. Thin panels are known to behave in this manner.[5] A hardening spring, represented by a linear plus a cubic term in the force deflection expression, has been used to represent the

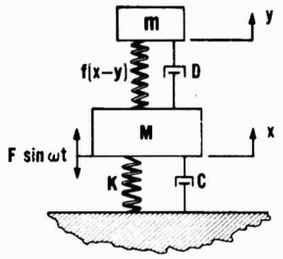

Fig. 3 - Mathematical model of vibrator and nonlinear load

structural stiffness. Thus, $f[x - y]$ in Eq. (1) has been taken as

$$f[x - y] = k(x - y) + \beta(x - y)^3 , \qquad f[y - x] = - f[x - y] . \quad (3)$$

Equations (1) and (2) can be expressed in dimensionless form by making use of Eq. (3) and the following identities:

$$\tau = \omega_0 t, \quad \omega_0^2 = \frac{k}{m}, \quad \Omega^2 = \frac{K}{M}, \quad \frac{C}{C_c} = \frac{C}{2\Omega M}, \quad \frac{D}{D_c} = \frac{D}{2\omega_0 m} ;$$

$$x = \left(\frac{g}{\omega_0^2}\right)\phi , \qquad y = \left(\frac{g}{\omega_0^2}\right)\psi ,$$

$$\dot{x} = \left(\frac{g}{\omega_0}\right)\frac{d\phi}{d\tau} , \qquad \dot{y} = \left(\frac{g}{\omega_0}\right)\frac{d\psi}{d\tau} ,$$

$$\ddot{x} = g\frac{d^2\phi}{d\tau^2} , \qquad \ddot{y} = g\frac{d^2\psi}{d\tau^2} ;$$

where g is the acceleration of gravity.

By substitution, Eqs. (1) and (2) become

$$\frac{d^2\phi}{d\tau^2} + 2\frac{\Omega}{\omega_0}\frac{C}{C_c}\frac{d\phi}{d\tau} + 2\frac{m}{M}\frac{D}{D_c}\frac{d}{d\tau}(\phi - \psi) + \frac{\Omega^2}{\omega_0^2}\phi + \frac{m}{M}(\phi - \psi) + \frac{m}{M}\frac{\beta g^2}{k\omega_0^4}(\phi - \psi)^3 = \frac{F}{Mg}\sin\frac{\omega}{\omega_0}\tau , \quad (4)$$

$$\frac{d^2\psi}{d\tau^2} + 2\frac{D}{D_c}\frac{d}{d\tau}(\psi - \phi) + (\psi - \phi) + \frac{\beta g^2}{k\omega_0^4}(\psi - \phi)^3 = 0 . \quad (5)$$

Most of the dimensionless coefficients in Eqs. (4) and (5) are simple ratios that need no

[5] E. J. Kirchman and J. E. Greenspon, "Nonlinear Response of Aircraft Panels in Acoustic Noise," J. Acoust. Soc. Amer., 29(7):854-857 (July 1957).

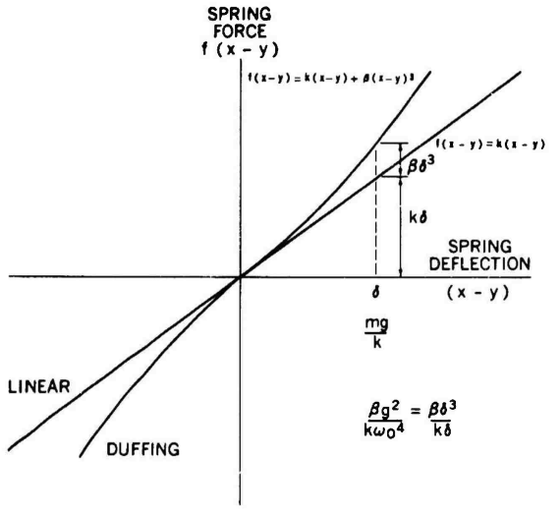

Fig. 4 - Force deflection curves for the linear and the cubic springs

explanation. The significance of the term $\beta g^2/k\omega_0^4$, however, isn't immediately obvious. If the substitution for the static deflection δ of a mass resting on a linear spring (of rate k) is made,

$$\frac{\beta g^2}{k\omega_0^4} = \frac{\beta}{k}\delta^2 = \frac{\beta\delta^3}{k\delta} .$$

Thus, $\beta g^2/k\omega_0^4$ is the ratio of the nonlinear force component to the linear force at the deflection δ. Figure 4, which shows the force deflection curves for the linear and the Duffing springs, better illustrates the significance of the parameter. It should be emphasized that the deflection δ is the static deflection for a linear spring (i.e., mg/k) and not the actual deflection for the Duffing spring.

An analog computer was used to obtain some solutions to Eqs. (4) and (5). The Duffing spring characteristic was obtained with a diode function generator. Seven connected straight line segments approximated the force deflection curve for the spring. Thus the accuracy of the solutions, for very low amplitudes, leaves something to be desired. Where $\phi - \psi$ is not small, several line segments are being utilized and the approximation is adequate.

To obtain a solution to Eqs. (4) and (5), specific numerical values had to be selected for the coefficients. The following values were selected as possibly representing an actual system:

$$\frac{C}{C_c} = 0.05 , \qquad \frac{m}{M} = 0.50 ,$$

$$\frac{D}{D_c} = 0.05 , \qquad \frac{\beta g^2}{k\omega_0^4} = 0.10 ,$$

$$\frac{\Omega}{\omega_0} = 0.20 .$$

With these parameters set into the computer, a sinusoidal input

$$\frac{F(\omega)}{Mg} \sin \frac{\omega}{\omega_0}\tau$$

was applied such that the peak nondimensional acceleration $d^2\phi/d\tau^2$ was approximately constant for the forcing frequency range of ω/ω_0, varying from 0.7 to 1.45. Some resulting waveforms are shown in Fig. 5 for the three values of zero to peak acceleration: 0.25, 0.50, and 0.75.

It is also interesting to note how the characteristics of the model vibrator change when the usually assumed linear load is replaced with a nonlinear load. Here, the sinusoidal force amplitude was held constant as frequency was varied. The armature acceleration $d^2\phi/d\tau^2$ was monitored, and the response curves for four forcing amplitudes are presented in Fig. 6. The zero to peak values of $d^2\phi/d\tau^2$ were plotted after dividing by F/Mg to normalize the curves.

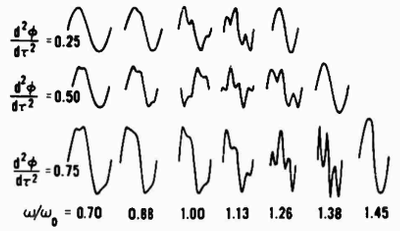

Fig. 5 - Vibrator's acceleration wave shapes

The curve for the near-zero force corresponds to the well-known linear solution in which the resonant specimen influences the vibrator's characteristics by the insertion of a notch and peak in the response curve. The distortion of the frequency response curve for the nonlinear case is clearly shown in Fig. 6. The waveform of $d^2\phi/d\tau^2$ is a distorted sine wave for all of the nonlinear curves. As the driving frequency is increased, a point is reached where the system response abruptly changes. The deflections of the nonlinear spring become small, and the system behaves very nearly as a linear system.

DISCUSSION

The analysis has explained one of the causes of distortion that occurs during a sinusoidal test. Experience with large spacecraft structures has shown that the nonlinear structural phenomenon is the most important one, namely because it appears at the major structural resonances where large excursions and high stress levels are likely to cause structural failure. On smaller packages the effect of nonlinear stiffness of the package isn't too important because the major resonances occur at higher frequencies with lower stress levels and also because the harmonic forces generated within the small structure are not capable of driving the relatively large mass of the shaker armature and fixture at significant amplitudes.

The usefulness of the analysis ends here since, by the nature of nonlinear problems, a solution for a given set of parameters cannot readily be extended to another problem. Also, the nonlinear parameters for a real structure are extremely difficult to define.

The question that naturally follows an explanation of the source of a problem is what to do about it. Suggestions from literature on the subject are summarized below:

1. Wrisley[4] attributes most distortion to harmonics in the amplifier output that may be multiplied when one of the harmonics corresponds to the armature or some other structural resonant frequency. He points out the errors in trying to measure and control peak

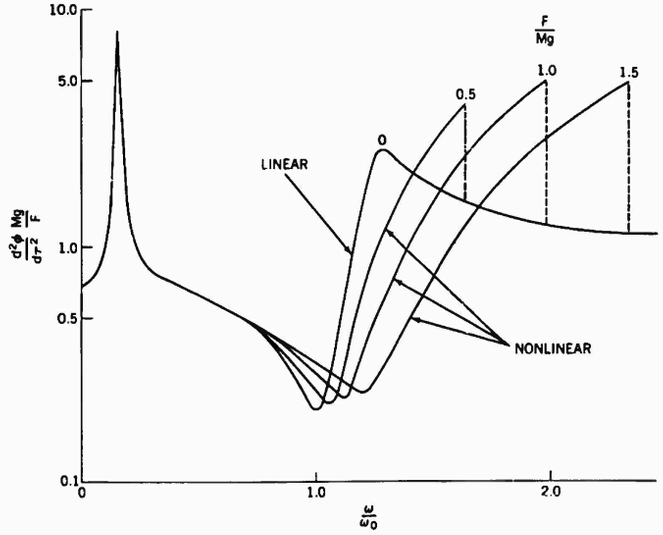

Fig. 6 - Vibrator acceleration for constant peak force

acceleration by using an averaging meter for varying percentages and phase of third harmonic distortion. Wrisley concludes that vibration facilities should be equipped to use feedback proportional to the peak acceleration and a true peak reading meter to monitor acceleration.

2. Schafer[6] points out that vibration amplitudes may be in error by ± 90 percent because of distorted acceleration waves. He feels that the insertion of a filter on the output of the control accelerometer, to eliminate all but the driving frequency component of acceleration waveform, would result in a test that comes closer to carrying out the intent of the specification.

Apparently these authors disagree, since Wrisley proposes that the instrumentation be such that the actual peak is sensed and used for control, regardless of the frequency components contributing to the peak, whereas Schafer feels that everything but the fundamental should be disregarded.

When a specification requires a given acceleration in the sinusoidal test schedule, it seems reasonable to assume that this level applies to the fundamental forcing frequency even if the motion cannot be maintained sinusoidal. Schafer's approach, then, is the obvious choice if the test is to be carried out in strict accordance with the specification.

In the case of spacecraft evaluation, where design margins are narrow, we can't afford the rigid interpretation of a specification. While testing the S-51 spacecraft[3] and its adaptor, the level of the second harmonic was about four times greater than that of the forcing frequency at the first mode resonance. In this case, filtering and driving the fundamental to the specified level would almost certainly have destroyed the structure. Increasing the input could cause the percentage of distortion to increase since the structure is nonlinear.

There are cases, especially when testing large structures, where presently available vibration equipment is being driven at maximum force output and still not meeting the specified acceleration levels, even including harmonics.

These problems point out deficiencies in test specifications which cannot be corrected by the use of filtering. At Goddard, the practice has been to perform the spacecraft test without filtering, thus allowing harmonics to contribute to the average of the control signal.

Experience with many spacecraft programs has demonstrated that the technique has produced a reliable product; however, it is not recommended that this method be applied to all sinusoidal test programs.

The problem of waveform distortion presents a dilemma that has to be resolved by the originator of the specification rather than the vibration equipment manufacturer. It is he who has failed to recognize the fact that, in testing real structures, nonlinearities exist and deviations from the required test are natural occurrences. This problem, which is one of many associated with vibration simulation, can be resolved only through a revision of present requirements. It is hoped that research now underway for improving test techniques by considering force as well as motion (e.g., impedance methods) will ultimately lead to a technically sound solution to the problem.

A few procedures that are recommended by GSFC for the testing of large spacecraft structures might be useful to those presently facing the problem with similar structures:

1. Waveform should be closely monitored so that we can at least know what happened during the test, right or wrong. This, by necessity, requires that data be stored on magnetic tape and spectrum-analyzed at critical frequencies.

2. The signal from the control transducer should not be filtered unless it has been established that the distortion is that resulting from looseness or banging of parts. On a satellite structure recently tested at GSFC, the second harmonic of the table acceleration was 3.8 times that of the forcing frequency.[3] In this case, filtering and driving the fundamental to the specified level would surely have destroyed the structure.

3. Since motion control can result in unreasonably high loads, fixtures should be equipped with force transducers to monitor bending moment and axial load. These loads should not be allowed to exceed the design limit during the vibration test.

ACKNOWLEDGMENTS

The author wishes to thank Dr. J. E. Greenspon, J. G. Engineering Research Associates; Messrs. E. J. Kirchman, W. R. Forlifer, and R. C. Hartenstein, GSFC, for their assistance in this study.

[6] C. T. Schafer, "Uniform Input Control—A Must for Accurate, Repeatable Tests," Vibration Notebook, published by MB Electronics, 7(4) (Oct. 1961).

Dr. Vigness: I thought that our mechanical shakers were the only ones that gave poor waveforms, but now I see that an electrodynamic shaker can also give a poor waveform under certain conditions and we shouldn't blame the shaker. I think that this paper has pointed out very strongly some of the problems that might be involved in standardization of vibration specifications, vibration tests, and vibration machines. The fact that the apparent input from the vibration machine is not really a function only of the machine, but also a function of what is on the machine, kind of messes things up.

Dr. Mains (General Electric): The implication, in at least part of what was said here, is that there is something sort of holy about a pure sinusoid. Now the only thing holy about it that I know is that it is one of the easier things to generate electrically; it is pretty doggone hard to measure it physically. If our testing is supposed to be somehow related to the field environment, we couldn't care less if we do not get a pure sinusoid, because this would be more realistic anyway. I think what is needed is an examination of what we should be measuring and why, rather than so much emphasis on how a pure sinusoid may be generated.

Mr. Bangs: I agree with everything that has been said and I did not mean to imply that there was anything holy about the sine wave. I think a real solution to the problem lies in how the equipment being tested would behave in its field environment. You pointed out that it would not be seeing sinusoidal input, which is correct. What it would be seeing is a function of the force that is acting on it, its own mechanical impedance and the mechanical impedance of the structure on which it is mounted. I think this is what we really should be trying to duplicate, but it is now impossible.

Dr. Vigness: Contractors frequently bring equipment into a test laboratory for tests which call for a sinusoidal waveform. If the waveform is not sinusoidal and the equipment fails, the contractor may say that it is not a proper test. What can you do about that?

Mr. Bangs: I am afraid I cannot answer that one. I would like to make one more point, though, concerning the first question. If a sine wave is desirable and we should be using it, we could get it by using a shaker armature that weighs a few thousand pounds and providing enough force to drive it.

Dr. Vigness: So it would be possible to have a remedy but it may not be desirable.

Voice: You make it sound as though we test these equipments in the laboratory for the primary purpose of having them pass the specification, rather than survive in service. Let's not forget what specification testing is supposed to accomplish.

Mr. Bangs: What the test is supposed to accomplish is, in our case at least, to give the project design people confidence that what they have built will survive the launch environment. The sinusoidal test as it is now run does give some of this confidence, but certainly there is a lot of room for improvement, and this is what I was trying to point out.

* * *

SOME PROBLEM AREAS IN THE INTERPRETATION OF VIBRATION QUALIFICATION TESTS

J. E. Wignot and M. D. Lamoree
Lockheed-California Company

This paper discusses problems concerned with the interpretation of vibration test specifications which arise in conducting qualification tests and those involved in the interpretation of test failures as they relate to the probability of failure in service. It is shown that more quidelines should be established for performing tests since test results can be influenced considerably by the way the test is conducted.

INTRODUCTION

Two types of problems are discussed in this paper, those concerned with the interpretation of vibration test specifications which arise in conducting the qualification tests, and those involved in the interpretation of qualification tests failures as they relate to the probability of failure due to vibration in the airplane. The role of standardization of test procedures as a means of alleviating these problems is emphasized. Although the discussion that follows is concerned exclusively with the sinusoidal qualification tests of electronic equipment for aircraft, many of the statements are applicable to vibration qualification tests in general.

Standardization of vibration qualification test procedures should perform three important functions: (1) eliminate discrepancies in test results due to the manner in which tests are conducted; (2) minimize vibration failures which are not service related; and (3) generate the maximum amount of information possible to aid the vibration engineer in assessing the probability of test failures occurring in service. Unfortunately, the latter two objectives are often overlooked. This omission is undoubtedly due, in part, to the general lack of criteria to apply in the evaluation of the relative severity of the response of equipment mounted in a rigid test jig undergoing sinusoidal oscillations and the response of the same equipment mounted in a more flexible aircraft being subjected to vibrations which are more or less random in nature. The purpose of this paper is to discuss several problem areas in regard to the first objective and to emphasize the importance of gaining the insight necessary to accomplish the remaining objectives.

TEST PROCEDURES

Most of the problems which arise in conducting vibration qualification tests center around defining the input to equipment and the determination of the dwell frequencies. In general, the seriousness of these problems is proportional to the weight and complexity of the equipment.

One of the major problems is that of jig resonances. Ideally, the jig should be of sufficient mass and rigidity so that its motion will not be significantly altered by the equipment response. In many instances, however, the weight of the equipment to be tested and the capability of the shaker available to perform the test, preclude the possibility of achieving ideal conditions. Under such circumstances the motion of the jig may be amplified at certain frequencies in such a way that the input levels may differ at the various equipment attach points. This difficulty was encountered in the vibration qualification test of an integrated electronics rack shown (with dummy equipment) in Fig. 1. The combined weight of the rack and equipment is 450 pounds. An illustration of the rack mounted in the vibration test fixture is shown in Fig. 2. With the complex structure required for the fixture, numerous resonances exist in the upper test frequency spectrum rendering impossible vibration inputs of equal amplitudes and in phase at all the support points for the shock mounts. On the basis of preliminary

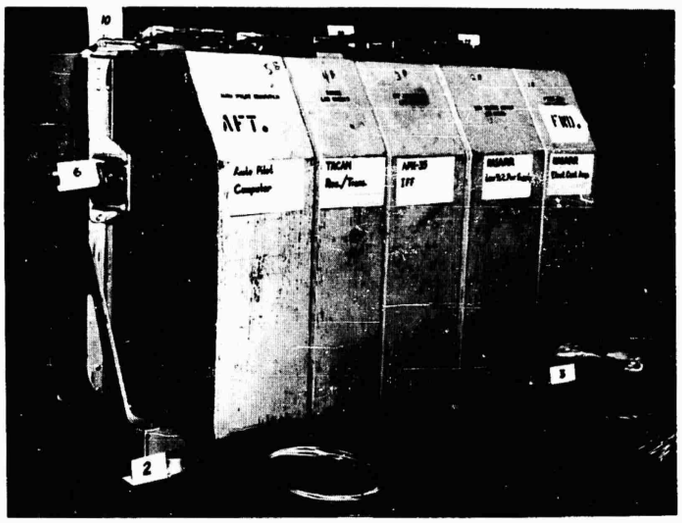

Fig. 1 - Integrated electronics rack with dummy equipment

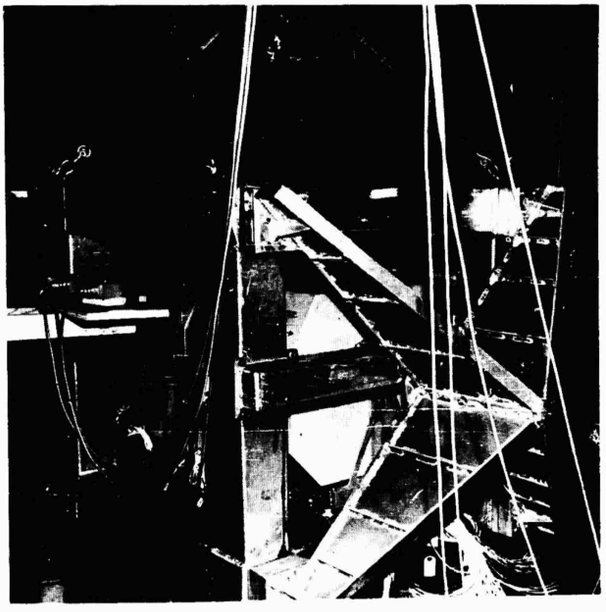

Fig. 2 - Electronics rack mounted in test fixture

tests, the number 3 accelerometer position appeared to provide a representative input to the isolation system. Therefore this accelerometer was selected as the control point for the input vibration levels. In the lateral direction of excitation, however, the dynamic behavior of the test system resulted in the presence of very high input vibration levels in the number 6 accelerometer position in the 300- to 500-cps frequency range as shown in Fig. 3. In this

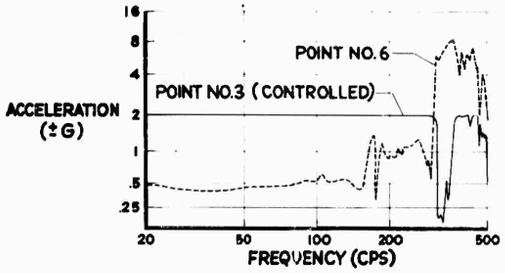

Fig. 3 - Vibration test input levels for the electronics rack

frequency range the input was monitored at position number 6. A standard procedure for specifying the input levels when this situation occurs should be defined.

Another problem which often exists under similar circumstances is that of maintaining a pure sinusoidal input at the equipment attach points. This phenomenon is illustrated in Figs. 4 and 5 for a 100-pound piece of equipment

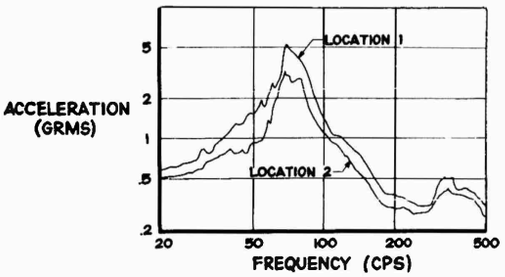

Fig. 4 - Unfiltered equipment response data for filtered input control signal

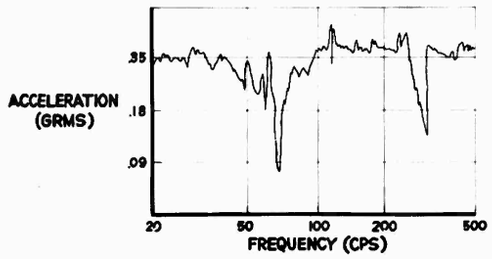

Fig. 5 - Filtered value of input for constant unfiltered input control signal

bolted to a 2-inch aluminum plate excited by a 5000-pound shaker. Figure 4 shows the unfiltered response at two equipment locations. The output from an accelerometer at the test fixture was filtered through a 20-cps bandwidth filter and used to maintain a constant 0.35 grms input level. Figure 5 shows the filtered grms level of the test fixture (20-cps bandwidth filter) when the unfiltered level is maintained at 0.35 grms. As can be seen by this example the severity of the test can differ drastically depending upon whether or not a filtered signal is used to control the input level. Determination of standardized procedures to resolve this problem is especially important in view of the fact that this phenomenon often occurs at a resonant condition for which the dwell test is required.

The treatment of nonlinearities must also be considered in standardization of test procedures. The philosophy of accelerated testing is based on the assumption that response levels are proportional to input levels. Nonlinearities in equipment response may negate the relation of test time and levels to those occurring in the aircraft. For example, a friction damped vibration isolater may not significantly attenuate the equipment response at low vibration levels which may exist in the aircraft over the major portion of its mission profile, but may provide a high degree of isolation at the qualification test levels. In such a case, the qualification test may not be sufficiently severe to disclose potential equipment failures which may occur in service. When this situation occurs the transmissibility of the shock mounts at levels representative of the aircraft vibration environment should be compared with that of the qualification test levels. The input levels should then be adjusted to take into account these differences so that the proper time and vibration level relationships between aircraft and test environments are maintained.

The opposite situation may also occur as illustrated by the following example. A black box is mounted in the pilot's console by means of spring loaded Zeus fasteners. Available flight vibration data on nearby equipment mounted in a similar fashion are in the ± 2-g acceleration level. When the black box was mounted to a test jig and vibrated at a ± 10-g acceleration level, response levels up to ± 70-g were obtained over a wide frequency range. The high levels were due to the "bottoming out" of the fasteners. Since flight vibration data indicated that this did not occur in service, a more realistic test was performed by clamping the equipment securely to the test fixture.

In conducting the vibration qualification test, a distinction should be made between the

test input levels for performance requirements and for structural integrity. Since the vibration test is an accelerated test, it is, generally speaking, unrealistic to specify that the performance requirements be met during the test for structural integrity. For this reason a sweep test with input levels representative of the aircraft vibration levels should be conducted after the completion of the structural integrity test to check equipment performance. For shock mounted equipment this test should also be conducted with a preload on the shock mounts, simulating aircraft maneuver loads, to insure proper functioning of the mounts and equipment during all flight conditions. Since an accurate determination of time to failure is important in vibration qualification testing, it may, of course, be necessary to monitor equipment performance during the qualification test to establish times to failure.

Perhaps the most controversial and difficult aspect of sinusoidal qualification testing is the selection of the dwell frequencies. For the heavier and more structurally complex equipment many resonances will be detected during the qualification test. The frequencies and amplitudes of these resonances will depend upon the location of the response measurement. This is illustrated in Fig. 6 where the response of the electronic rack and equipment (Fig. 1) is given at two different locations. The selection of frequencies for dwell cannot be realistically based on a simple criterion such as maximum response levels since the modes of vibration for which the maximum stresses are experienced are not necessarily the same as those for which the amplitudes at any given location on the equipment are a maximum.

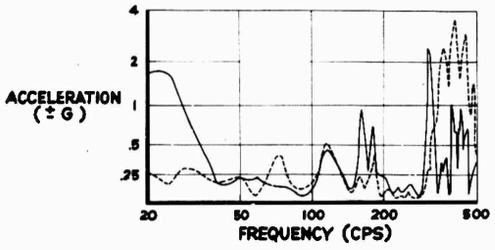

Fig. 6 - Vibration test response levels for the electronics rack

Before standard procedures are established for selecting dwell frequencies, the philosophy of the dwell test should be critically examined. Resonance dwell testing is based on the premise that the most probable types of vibration damage that will occur in service are those which will result from excitation of the equipment resonant modes observed in the qualification test. This reasoning follows from the fact that the highest stresses in a structure subjected to a force field having a wide-band frequency spectrum normally occur in the resonant modes of the structure.

Several considerations appear to cast considerable doubt on the validity of the dwell test, especially in the case of the heavier and more structurally complex equipment. From the standpoint of the basic structure, the greatest fatigue damage sustained during the qualification test will undoubtedly occur during the structural resonances. Equipment malfunction, performance degradation, or fatigue damage due to the existence of high stresses in the electronic components mounted to the structure can, however, occur in the qualification test either as a result of amplification of the structural displacements where the components are mounted or as a result of an excitation of a resonance in the component itself. The latter condition will not generally result in a significant increase in response at the points being monitored.

The situation is further complicated by the fact that the resonant modes of the equipment mounted in the rigid test fixture may differ significantly from those which will be experienced when the equipment is mounted in the aircraft. This is illustrated in Fig. 7 for a 180-pound shock-mounted piece of equipment. The solid curves are the transmissabilities of the shock mounts obtained in the qualification test. The dashed curves are the transmissabilities of the shock mounts obtained from measurements made during a ground shake test of the airplane. It is to be noted that the response of the equipment in the aircraft differs significantly from that in the qualification test. Transmissabilities computed from flight data, indicated by the circles on the graph, are in good agreement with the ground shake test results. It should be emphasized that this illustration is cited only to show the differences which may exist between responses of equipment in the test fixture and the aircraft, and does not, in itself, provide any indication of the relative severity of the qualification test and service environment with respect to the shock mounts. It does demonstrate, however, the fallacy of equating qualification test input amplitudes to aircraft structural amplitudes, even though the latter may have been measured at the mounting point of the equipment.

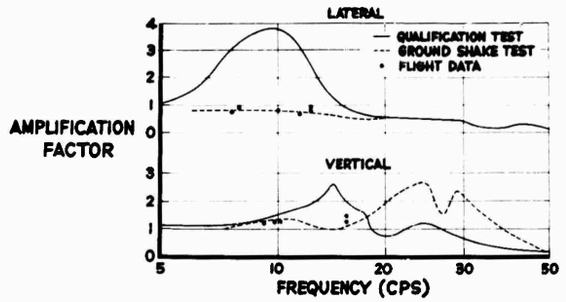

Fig. 7 - Shock mount transmissability curves

The philosophy of the resonant dwell test fails to take into proper consideration possible attenuation effects of aircraft structure which may be significant for even relatively light pieces of equipment. Consider, for example, a piece of equipment weighing 2-1/2 pounds whose structure is roughly that of a box 7 inches long with a 2-1/2- by 4-inch cross section which is mounted to a relatively flexible panel in the aircraft by four screws at one end of the equipment. Regardless of the rigidity of the equipment structure, it will exhibit clamped-beam type resonances when mounted in the test fixture with resultant high stresses in the structural members near the attach points. In the aircraft mounting, however, the mode of highest amplification may be a rigid-body mode whose resonant frequency is governed by the stiffness properties of the panel. If the panel is relatively flexible as compared to the equipment structure, the stresses in the structure will be much lower at resonance than those occurring during the qualification test.

One cannot make generalizations from the above simple examples as to the relative severity of stresses experienced in the test fixture and in the aircraft. However, the mere fact that the resonances in the aircraft may occur at frequencies different from those in the test jig indicates that the distribution of stresses within the equipment at resonances in the aircraft will differ from that which exists during the corresponding resonant modes in the test jig. For this reason, fatigue damage sustained in the dwell test may not be indicative of that which may occur in service. In the above example, dwelling at resonance may induce structural fatigue at the attach points whereas in the airplane the resonant frequency could coincide with a local resonance of a circuit board or some other electronic component with resultant wire breakage or component failure.

An additional unrealistic aspect of dwell testing is the possibility that some subassemblies of the structure may experience high stresses in several of the modes selected for dwell. This may be particularly true when a given structural mode responds in each of the axes of excitation. The probability that, in any given aircraft, all of these modes will be strongly excited is indeed remote. In such cases the qualification test may be overly conservative for these particular subassemblies.

The philosophy of dwell testing is best suited to the case where the equipment will be subjected to broadband, random, white excitation. Under this condition, the equipment resonances represent more closely the modes in which fatigue damage is most likely to occur. Equipment in aircraft is not usually subjected to this type of vibration excitation. Some excitations due to mechanical sources, such as engines, auxiliary power supplies, and cooling fans; or aerodynamic sources, such as, propeller inbalance, are sinusoidal in nature. Moreover, the broadband acoustic excitation to the aircraft is attenuated by the structure of the airplane so that certain frequencies are generally predominant at the attachment points of the equipment. Of course, there is always the possibility that one of the predominant frequencies may excite a resonant mode in the equipment which is similar to a resonance detected during qualification testing. Such occurrance would justify dwelling at this resonance in the qualification test. We must, however, weigh the odds of this event against the probability that the predominant frequencies of excitation will not result in high equipment stresses representative of those obtained in resonance dwell tests, before we arbitrarily elect to subtract time from the remaining frequencies in order to concentrate on a few in the qualification test.

A greater effort should be extended to determine under what conditions, if any, the dwell test is justifiable. If further investigation indicates that the dwell test is a valid one, then it should also indicate what procedures are required in the qualification test to select those resonant modes which are most apt to be critical in the aircraft environment. Moreover, it should also provide a better indication of what test levels and times should be used for those dwells which are deemed necessary.

Vibration requirements, like all other equipment requirements, are included in the contract with the vendor to assure delivery of an article which, in the contractor's best judgement, will provide satisfactory performance in the aircraft. One important advantage of standardizing test procedures is the elimination of ambiguities in test results due to possible choice of test procedures thereby resolving legal questions as to whether the contractual requirements have been met. If this were the only objective of standardization of test procedures, any arbitrary set of standards would serve the purpose equally well. The primary function of qualification testing is to detect and eliminate those failures which may occur in service. Since there is not a one-to-one correspondence between qualification test failures and probable service failures, standardization of testing techniques should also attempt to minimize the probability of occurrence of non-service related failures and provide the maximum amount of information needed to evaluate the probability of test failures occurring in service.

The problem of relating qualification test failures to the probability of similar failures occurring in service is a formidable one. The sole approach to this problem to date seems to be reliance on engineering judgement. Since considerable expeditures of both time and money often hinge on the decision of whether to accept equipment which has experienced failure in vibration testing on a calculated-risk basis, it is of utmost importance that fundamental principles be established to form a rational basis for such decisions.

The scope of this problem extends beyond the standardization of test procedures, it encompasses the specification of test levels and times and the manner in which test results are reported.

TEST SPECIFICATIONS

Equipment requirements are often established in the design phase of an aircraft prior to the availability of any environmental data. Even in the case of new equipment for an existing aircraft, practical considerations limit the amount of flight vibration data available to serve as a guide in establishing test levels. For these reasons the vibration requirements are often patterned after those of military specifications even though it is not the intent of the contractor to install equipment which meets the military specifications, per se.

A review of available flight data, as a basis for establishing qualification test levels for electronic equipment installed in aircraft was performed by Lunney and Crede.[1] Although this work provides a significant contribution to our understanding of the philosophy of the sinusoidal qualification test, it also points out the need for standardization of flight vibration measurements and data reduction techniques. Since much of the reviewed data was published before the concept of random vibrations to describe structural vibrations was widely accepted in the aircraft industry, one would tend to have reservations concerning the accuracy of the reported acceleration levels and frequencies. Moreover, the percentage of flight time the reported levels were experienced is unknown. The time factor is very important in the evaluation of test input levels and time duration. Finally, there is no way to relate the reported structural response levels to equipment test input levels as a function of equipment weight, relative stiffness properties, or any other factor which may influence the equipment response to aircraft vibration.

During recent years, a great deal of work has been done on the application of statistical procedures to the problem of characterizing vibration environments in aerospace vehicles (for example, see Refs. 2 and 3). The use of the concept of mechanical impedance as a means of achieving a more realistic simulation of the

---

[1] E. J. Lunney, and C. E. Crede, "The Establishment of Vibration and Shock Tests for Airborne Electronics," WADC Technical Report 57-75, ASTIA Document No. AD 142349 (Jan. 1958).

[2] J. S. Bendat, L. D. Enochson, G. H. Klein, and A. G. Piersol, "The Application of Statistics to the Flight Vehicle Vibration Problem," ASD Technical Report 61-123 (Dec. 1961).

[3] J. S. Bendat, L. D. Enochson, G. H. Klein, and A. G. Piersol, "Advanced Concepts of Stochastic Processes and Statistics for Flight Vehicle Vibration Estimation and Measurement," ASD-TDR-62-973 (Dec. 1962).

vibration environment in the test laboratory[4] is also receiving more attention. With additional knowledge, gained through experience in working with these approaches, it should be possible to develop a unified program of flight vibration measurement and analysis which will provide a better basis for the establishment of vibration test specifications than is currently available.

Meanwhile, available data on equipment vibration levels in aircraft should be utilized to the fullest possible extent as a guide in determining test specifications. Possible discrepancies in the use of vibration levels on the structure as a basis for test specifications is illustrated in the following example. Vibration levels up to ± 17-g at discrete frequencies were measured during gun firing on aircraft structure of the electronics compartment floor. Accordingly, the performance requirement of a piece of equipment which is mounted on a shelf attached to the floor structure and which must operate satisfactorily during gun firing was based on a ± 17-g input during the vibration qualification test. Inability of the vendor to meet this requirement resulted in a decision to measure vibration levels on the base of the equipment during inflight gun fire. These measurements showed a maximum level of ± 5-g. In this particular case, the equipment weight (45 pounds) and the support structure, each probably played a significant role in the attenuation of the vibration levels of the equipment.

Flight vibration data on equipment available to the engineers of any single company are too limited in their scope to form a reliable basis for judging relative vibration levels of equipment and aircraft structures. For this reason it is recommended that some central coordinating agency compile and correlate such data with the various parameters which may influence the levels of the equipment response.

TEST REPORTS

The importance of the role played by the qualification test report in the problem of interpretating test results cannot be over-emphasized. Since in many instances, the contractor's decision as to the course of action to be pursued as a result of qualification test failures must be based entirely upon the information contained in the test report, it is of vital importance that the report include all the pertinent facts needed to evaluate test failures. To insure that such information is included, it would be highly desirable to establish a standard format to be followed throughout the industry in the preparation of qualification test reports. In addition to insuring the inclusion of desired information, standardization of test reports would represent a cost savings to both the vendor and the contractor by reducing the time required to prepare, review, and revise the report.

In the authors' experience, test reports are often lacking in clear photographs or sketches showing test setups including the method of mounting the equipment in the test fixture and location of accelerometers for measuring equipment response and monitoring the shaker input. Information on how resonances were detected, descriptions of the resonant modes, and factors influencing the selection of dwell frequencies is, in general, meager or entirely missing. Attempts to obtain additional information needed to assist in evaluating qualification test results often prove futile because the necessary observations were not made during the test. For this reason, it is essential that the scope of the test procedure standards be sufficiently extensive to prescribe what records should be kept during the qualification test with particular emphasis on those required to evaluate equipment failures.

CONCLUSIONS AND RECOMMENDATIONS

In order to maximize the effectiveness of the vibration qualification test as a means of insuring that equipment will successfully withstand its vibration environment without undue penalties in cost, weight, and time, the following objectives must be accomplished:

Standardization of Flight Vibration Data

An accurate evaluation of qualification test specifications and procedures is possible only if the statistical properties of the aircraft vibration environment are determined. In order to pool data from many sources, standardization of vibration measurements and data reduction methods is required. Prior to establishing a standard for flight vibration data, however, it will be necessary to determine the type of data (i.e., equipment response, force measurements, or structural acceleration) which provides the best basis for specifying the vibration qualification test.

[4] F. J. On, and R. O. Belsheim, "A Theoretical Basis for Mechanical Impedance Simulation in Shock and Vibration Testing of One-Dimensional Systems," NASA Technical Note D-1854, (Aug. 1963).

Standardization of Test Procedures

Ambiguities in vibration qualification test results, due to the manner in which the test is conducted, can be eliminated by standardization of test procedures. Principal problems to be resolved in this area are: treatment of jig resonances, maintaining a sinusoidal input, treatment of nonlinear effects, and selection of frequencies for dwell.

Standardization of Test Reports

Standardization of the qualification test report would insure proper documentation of the test results.

Follow-Up Program on Equipment Failures Due to Vibration

The inclusion of mean-time-between-failures requirements in contracts for vendor supplied equipment will require that accurate records of equipment performance in service be maintained. Correlation of this field data with vibration qualification test results would provide a basis for evaluating the realism of the vibration qualification tests. To be noted in particular are (1) the types of failures attributed to vibration in the field but not observed during the qualification test, and (2) the types of failures occurring in the vibration qualification tests of equipment accepted for service without redesign and which did not subsequently occur in service. It is recommended that some central coordinating agency be assigned the responsibility of compiling and analyzing data on equipment for which service failures due to vibration is inconsistent with vibration qualification test results. The information brought to light by this means would provide a more rational basis for the evaluation of qualification test specifications and test failures than is currently available.

DISCUSSION

Mr. Todaro (University of California, LRL): It appears to me that there was a long coupling rod from a welded structure going back to the shaker. If that was the case, what was the natural frequency of that structure, and did it happen to coincide with a dip on one of your response curves?

Mr. Lamoree: I cannot answer this question because I am not aware of the details. This design was completed before I was involved and I am merely reporting on it.

Mr. Unholtz (Unholtz-Dickie Corp.): You stated that there are two military specifications, one of which is almost opposite to the other: namely MIL-E-5272 which states that the maximum vibration level of several accelerometers should not exceed the specification level;—while in another specification the minimum vibration level had to be at least the specification level. I believe I am correct in stating that MIL-E-5272 has now been amended so that it calls for the average of several accelerometer readings to be equal to or greater than the specification levels. It seems to me that this is a recognition on the part of the specification writers of the problems that have been discussed here, and while it may be an arbitrary solution, it may at least take the sharpness off the peaks and valleys of some of the responses.

Mr. Wilson (Emerson Elec.): I notice on most of your graphs that the frequency started at 20 cps and went on up. We have had a lot of trouble in the 5- to 20-cycle region. Do you also have trouble in this area?

Mr. Lamoree: No, our tests were made from 5 to 750 cps. The range in the slides was arbitrarily decreased. We sometimes, however, have had troubles at low frequency in getting a pure sine-wave.

Dr. Vigness: I think the problem of getting a uniform type of vibration test is one of the things which is going to bother us most in the future.

* * *

TAMING THE GENERAL-PURPOSE VIBRATION TEST*†

J. P. Salter
War Office, Royal Armaments Research and
Development Establishment
Fort Halstead, England

There is little doubt that the acceleration levels quoted in many of the general-purpose vibration test specifications issued by official agencies are based upon measurements made at vibration antinodes. Where this is so, there is no justification for permitting the acceleration level at any of the attachment points to exceed the level quoted, or for permitting the applied force to exceed a computable value. An extension of the control system results in a more rational test.

THE GENERAL-PURPOSE TEST

Considerable publicity has been given in the course of recent symposia to the difficult task facing the writer of a test specification dealing with vibration environments.[1-6, 8-11] (See References, 216-217.)

The test he evolves will form the basis of a contract (formal or implied) between a supplier and a user, and will result in the acceptance or rejection of a proffered article. Both parties to the contract would like the test to result in the acceptance of only what is service-worthy and the rejection of only what is not, but it is now becoming more widely appreciated that it is beyond our present ability to devise a vibration test which will give a verdict with a confidence level even moderately acceptable to supplier and user alike. In fact, such is the interaction between the dynamic characteristics of an article and those of the hardware with which it will be associated in real life that even a test carefully tailored to relate to a single specific article whose survival in a single environmental circumstance is at issue is likely to be seriously invalid in one or more respects.

Despite this, the specification writer finds himself called upon to tackle the problem of devising a general-purpose vibration test which can be applied by unsophisticated, minimally-equipped, test personnel to broad groupings of widely-diverse articles whose future environmental circumstances can only be guessed at. His protests are unavailing; he has to do the best he can; and in due course the outcome of his labours becomes yet another of the many generalized vibration test specifications issued over the past 15 years by the various official agencies.

We may not like this situation, and we may be further disturbed to note from this year's batch of symposium papers that it is those very writers whose practical experience is most broadly based who have most sympathy with disgruntled suppliers and users when they complain of service-worthy equipment being rejected and inferior equipment being accepted by the application of these tests.[7] But whether we like it or not, the situation will be with us for many years to come, and we would do well to accept and publicise the fact that such tests can be no more than arbitrary barriers to poor design or faulty production, and to do what we can to improve them as such.

TWO POSSIBLE IMPROVEMENTS

The most widely used general-purpose test calls for the article to be attached to a vibrator by its normal points of attachment and subjected to sinusoidal vibration whose frequency is swept backwards and forwards between stated limits.

*This paper has been reproduced from 'Environmental Engineering' by courtesy of the Society of Environmental Engineers, 167 Victoria Street, London, S.W. 1.
†This paper was not presented at the Symposium.

The intensity of the vibration is specified in quite simple terms: e.g., 10 g from 20 cps to 2 kc, and the accepted convention is that some form of control system (automatic, or manual) should be employed to maintain this intensity at a single point of the structure (normally one of the points of attachment) throughout the test.

Two aspects of such a test are considered here, each capable of modest improvement. The first is that in maintaining the specified acceleration level at the point of attachment which happens to carry the control accelerometer we may well be generating a much higher level of acceleration at one or other of the remaining points of attachment. This will occur whenever the excitation frequency is such that the control accelerometer finds itself at a local vibration node, as may repeatedly happen at the higher frequencies. The second is that in maintaining the specified acceleration level, regardless of the dynamic reactions of the article under test, we are treating the article as if, in service use, it will be attached to a structure of infinite mechanical impedance, rather than to a structure whose impedance, as the natural outcome of normal engineering practice, will seldom be vastly greater than that of the article itself, and may well be significantly less at certain critical frequencies.

As we shall see, neither practice is consistent with the line of reasoning which, consciously or otherwise, prompted the adoption of the particular acceleration level as being appropriate to the particular specification.

Bearing in mind that we have to be content to make the best of a notably bad job, it is suggested that the test can be improved in two ways: by employing multi-point rather than single-point acceleration control (i.e., insuring that at no point on the normal mounting surface of the article does the acceleration level exceed the specified value), and by setting an appropriate limit to the force we bring to bear on the test article.

THE DATA-REDUCTION PROCESS

To justify these suggestions we must examine, in some detail, the procedure adopted in the derivation of the stipulated test level, because inherent in this process is a factor which appears to have been generally overlooked.

In general, it can be said that these test levels are based upon a somewhat heterogeneous collection of acceleration measurements made over the years at a large number of selected points, on a large number of assorted articles of hardware, situated at a variety of locations, on a large number of vehicles,* and experiencing a variety of service environments.

Depending upon the sophistication of the trials instrumentation and upon the type of data-analysis equipment available to the investigator, each such exercise can be assumed to have yielded either a family of curves of intensity against frequency, or a number of traces of instantaneous acceleration against time, or a number of spot values related to the highest instantaneous value of acceleration encountered during the experience.

Stage by stage, over the years, this unwieldy mass of original data has been processed piecemeal by a variety of individuals employing a variety of data reduction techniques, probably the only commom factor being an understandable wish to err on the safe side.

It is this defensive approach which has lead each individual in his turn to adopt an intensity level high enough to embrace all the maximum values revealed by the data he has been processing, and it is here that the crux of the matter lies.

To take a very simple example let us consider the case of a vital article of navigational equipment which is to be installed in a particular type of jet aircraft. It is envisaged that the user may decide to mount the equipment in any one of three locations on the airframe, and tape records are made of the accelerations at each of the four points of attachment of the article during a particular phase of flight, with the article mounted at each location in turn.

On playback, the investigator may well have been encouraged to note that in terms of rms level of intensity there was little to choose between the dozen records; and had he investigated the spectral distribution of the vibrational energy by employing filters of unusually wide bandwidth (say two octaves wide) there may well have been little to choose between the dozen smooth curves that resulted.

But when he carries out the more normal frequency analysis using filter bandwidths appropriate to the work, and examines the resulting curves of spectral density against frequency,

*The term 'vehicle' is used here in its broadest sense to include a complete missile, a ship, an aircraft, and the like, as well as a land vehicle.

significant differences become apparent. Each curve displays a number of peaks and troughs, and the frequencies at which the major peaks occur differ significantly from curve to curve. If the dozen curves are plotted on a single sheet of paper it becomes clear that the peaks are distributed over quite wide sections of the frequency spectrum, despite the fact that he has so far investigated only three possible locations in a single version of one type of aircraft. In order to err on the safe side, and to cater for the possible use of his navigational equipment in a number of versions of the aircraft, he sees no alternative but to define a test level derived from a smooth curve enveloping not only the peaks whose existence and magnitude he has experimentally established, but also an adequacy of peaks at intermediate frequencies whose level he estimates by visual interpolation between the established peaks.

NODES AND ANTINODES

The implications of this action can best be appreciated by visualizing the behaviour of the complete aircraft structure if it were subjected to single-frequency sinusoidal excitation. For any spot frequency there would be a clearly defined standing-wave pattern distributed three dimensionally over the structure. Some points would be at vibration antinodes, others at vibration nodes. The transfer of a piece of equipment from one area to another would result in a change of pattern, localised or widespread.

If the excitation frequency were altered, a completely new standing-wave pattern would result, and if we confined our attention to a single point on the structure whilst the excitation frequency was being smoothly swept from a low frequency to a high frequency we should observe the acceleration level building up to a peak value as an antinode approached and coincided with our monitoring point, falling away subsequently to a trough as the antinode moved elsewhere and was replaced by a node, only to rise again with the approach of another antinode.

A plot of accleration level against frequency for this point would thus exhibit a number of peaks and troughs, much as did each of the spectral density curves relating to the navigational equipment, and in the main for the same reasons, the presence or absense of vibration antinodes at the measuring point.

Thus we see that in basing his test level upon a line enveloping all the peaks the investigator is in fact postulating the existence of all four points of attachment simultaneously, and their continuous existence over a wide range of frequency. He is in fact stating a level of acceleration that will not, in his opinion, be exceeded at any of the points of attachment in any service usage.

MULTIPOINT CONTROL

In the light of this, let us review the vibration test itself.

When the navigational equipment is mounted on a vibrator table for test purposes, the whole assembly (equipment, attachment jig, table, and suspension) becomes a single coherent structure which, when subjected to swept sinusoidal excitation, develops its own ever-changing pattern of nodes and antinodes. If the acceleration level is controlled at only one of the points of attachment, as is normal present-day practice, there will inevitably be frequencies at which this particular point is located at a node whilst one or other of the remaining points of attachment are in antinodal area. In such circumstances the article will suffer unjustified overtest since the excitation at the unmonitored points will greatly exceed the investigator's most pessimistic forecast. If this is to be avoided the control system must be such that the specified acceleration level is exceeded at no point on the attachment surface.

If such a system of control is accepted as necessary in the relatively straightforward example described above where the test level is based upon practical measurements relating to the actual article in a clearly defined usage, then it is suggested that it should be made mandatory where the test is to be a general-purpose one. In such a test the probability is that the test level is already unduly high for the majority of articles which will be subjected to it, since it will have been derived by enveloping a variety of envelopes, some of which will undoubtedly incorporate purely numerical (and unknown) factors of safety, others of which will result from isolated spot-measurements made upon lightly loaded, highly resonant, surfaces such as panels and brackets, and most of which have only marginal relevance to the nature and usage of the article under test.

For the acceleration level applied to articles having two or more points of attachment to be further increased by a factor of 2, or 3, or even 5, (even if this occurs only over parts of the frequency sweep) is quite unjustified and undoubtedly swells the volume of service-worthy stores rejected on test.

THE CRITICAL TROUGH

The second suggested improvement is most easily described in relation to an article constructed with a single clearly-defined point of attachment and liable at the discretion of the user to be mounted at any one of a number of locations in some structure. Again we imagine the input to the structure to consist of a sinusoidal force whose frequency is slowly varying, and we visualize the changing pattern of nodes and antinodes. Again we note that the transfer of the article from one location to another is accompanied by a further change of pattern, widespread or localised.

If, for each location, we prepared a plot of acceleration against frequency for the point of attachment of the article, each curve would have its quota of peaks and troughs and no two curves would be identical, particularly as regards the frequencies at which the peaks occurred. But it might well be noticeable that there was one particular frequency at which all the records revealed a trough, irrespective of the location of the article; and the more nearly the article approximated to a lumped mass supported on a lightly-damped spring the more pronounced would be the trough, and the more noticeably would it be a feature common to all the records.

In short, no matter where it was mounted, the article insured that there was a nodal trough at its point of attachment at this particular frequency. Investigation of the dynamic response of the article itself would show that this was the frequency at which some major internal element came to resonance and experienced an acceleration 5, 10, or 20 times as great as that existing at the point of attachment—clearly a frequency at which the article was very susceptible to damage.

PEAK-TO-TROUGH RATIO

We thus have the situation that the correct test level for this critical frequency would be that indicated by the nodal trough whereas, as we have seen, the test level demanded by the specification will be that decided by the height of the antinodal peaks on each side of the trough. The ratio of the one to the other, the peak-to-trough ratio, is clearly of some importance in that it establishes the degree of overtest which a resonant article will experience at a critical frequency as the result of just one of the many steps in the data reduction process.

Published literature contains little empirical data from which probable values for this peak-to-trough ratio can be evaluated.

Analogue studies based on the response of two single-degree-of-freedom systems mounted one upon the other, each having a Q of 10, with mass-to-mass ratios varying from 0.2 to 5 and resonant-frequency ratios varying from 0.3 to 3, suggest peak-to-trough ratios varying between 20 and 200. Such elementary systems, although they oversimplify the problem, provide useful pointers to the probable behaviour of resonant structures; they indicate the part played by the 'passenger' system (representing our article) in determining the magnitude and the frequency of the adjacent peaks as well as of the trough itself, and they suggest that the transmissibility of the 'passenger' system at the frequency of the adjacent peaks is unlikely to be greater than 1.5, an item of information which comes in handy in the derivation of a force-limited test.

More practical measurements, made on service structures carrying various sub-assemblies, and relating only to those peaks and troughs whose association with a basic resonance of the sub-assembly could be established, suggest peak-to-trough ratios ranging from 4 to 30 for sub-assemblies in which the weight of the resonant section varied between 20 and 80 percent of the total weight of the assembly.

THE IMPEDANCE MISMATCH

Is there any practical way in which a general-purpose test can be modified so as to moderate the degree of overtest which resonant articles experience at these critical frequencies?

It is informative to discuss the problem either in terms of mechanical impedance (the force required to produce unit velocity) or in terms of the closely related 'effective mass' (the force required to produce unit acceleration). Three such values are of interest: the effective mass of the article itself; the impedance of the point on the structure at which it will be mounted in service use; and the impedance of the vibrator table to which it will be attached for test. Each is a function of frequency.

As an example let us assume that half the mass of an article is virtually resonance-free below 200 cps whilst the remainder comes to resonance at 50 cps with a Q of 10. At very low

frequencies, below say 20 cps, the effective mass of the article will be constant, a force of say P pounds being required to produce an acceleration of 1 g at any frequency over this range. At 50 cps, however, whilst the non-resonant half is still moving with 1-g acceleration and requiring P/2 pounds of force, the resonant section will be moving with 10 g and requiring an input force of 10 times P/2 pounds to maintain this motion. The total force required to maintain 1-g acceleration at the point of attachment has thus risen from P pounds to around 5P pounds. Its effective mass has risen to around five times its low frequency value; its impedance is around five times as great as that of a non-resonant article of equal weight.

To what extent is this increased force brought to bear on the article, whilst it is undergoing a vibration test, and whilst it is mounted in a structure experiencing a typical service environment?

There is no doubt at all as to the situation whilst it is being tested to a typical general-purpose specification. A control system (manual or automatic) is employed to keep the acceleration at the point of attachment at the specified level, the installation developing whatever force is necessary to maintain this acceleration. No reactional force generated in the article, however great, results in the slightest change in the acceleration of the surface to which it is attached. To all intents and purposes, the article finds itself mounted on a surface of infinite mechanical impedance.

Quite a different state of affairs exists when, in service use, the article finds itself embodied in a practical structure. Practical structures are not of infinite impedance; they are the outcome of normal drawing office practice. Whether evolved by rule of thumb or by careful stress analysis they are no stronger than they need be, since extra strength or rigidity implies extra cost, or extra size, or extra weight. Furthermore, over the range of frequencies of interest, a mounting-point impedance is only marginally determined by the composition of the complete structure; it is predominantly a function of the dynamic characteristics of elements quite local to the mounting point—a section of panel, a bracket, another article closely comparable to the one in which we are interested.

In short, it is suggested that the impedance at a mounting-point on a supporting structure is likely to be of the same order of magnitude as that of the article to be mounted there, and at the critical frequencies with which we are concerned it may well be significantly less. So far from finding itself completely at the mercy of a vibrating structure of infinite impedance, as it does when on test, it experiences an impedance ratio which permits it materially to ameliorate its treatment at critical frequencies, as the existence of specific nodal troughs in acceleration-frequency curves confirms.

Inevitably, there are exceptional cases: small items mounted for convenience upon massive beams or girders designed to support major assemblies; but these are exceptions and must be treated as such: they must not influence the whole test pattern to the grave detriment of the generality of articles.

FORCE LIMITATION

Until such time, then, as we are in a position to define a general-purpose test in terms of a system of forces acting through an appropriate network of impedances, it is desirable to set an upper limit to the force we apply to the article whilst it is undergoing test, thus simulating a non-infinite impedance at the test table and permitting the development of a partial trough in the acceleration level at a frequency to be determined by the article itself.

At this stage it is important to remind ourselves of the many and varied processes of data reduction which led up to the adoption of the specified acceleration level, and to recollect the defensive approach of the successive data manipulators. In determining the maximum force to be applied to an article there is no need for the application of still further "factors of safety"; if anything, the requirement is to be merciful to the test victims. Equally inappropriate would be meticulous accuracy; the accuracy of our raw material does not justify it.

We do not know the magnitude of the force acting upon our article at the frequency of the critical trough when it is embodied in its service structure. We can, however, make an intelligent guess as to how it would compare with the force acting at the frequency of the adjacent peaks. If the twin single-degree-of-freedom analogue discussed above is any guide, the force acting at the trough is materially lower than that acting at the frequency of the adjacent peaks; certainly we shall run little risk of underestimating the former if we equate the two.

The analogue also suggested that the transmissibility of the 'passenger' system was unlikely to exceed 1.5 at the frequencies of the peaks, implying an effective mass at these

frequencies of not greater than 1.5 times the 'dead' mass. This figure, of course, relates to a passenger system in which 100-percent of the mass is resiliently mounted; for a more realistic article of which only a portion comes to resonance the figure could be anywhere between 1 and 1.5. We can therefore postulate with reasonable confidence that, in its service usage, the force acting on the article at its critical frequency will not exceed 1.5 times that required to produce the 'adjacent-peak' acceleration in an inert article of equal weight, and is likely to be significantly less.

This is a situation which we can reproduce during the test, by substituting the specified acceleration level for the 'adjacent-peak' acceleration, the former having been derived from the latter, as we have seen. Since we do not know the precise frequency at which the article will come to resonance, any force-limitation we apply must operate over much, if not all, of the specified frequency sweep; we must therefore apply a force at least 1.0 times that required to produce the specified acceleration in an equivalent dead weight. On the other hand, in view of manifold factors of safety inherent in the specified acceleration level and implied in the above argument, a factor of 1.5 appears excessive. An arbitrary figure of 1.2 is therefore suggested.

SUITING THE CIRCUMSTANCE

This factor of 1.2 can be adopted when the force to be controlled is that acting upon the article alone, via its single point of attachment. Where circumstances are such that the only controllable force is that acting upon an attachment-jig carrying the article (so that only a small percentage increase in the effective mass of the driven system is to be expected at the critical frequency) then it is suggested that the factor should be reduced to as near unity as is practicable. Where, again, the article has two, three, or four separate points of attachment and the specification calls for a constant level of acceleration over a frequency range extending down to frequencies at which the article can be relied upon to behave as an inert homogeneous mass, then the force limit appropriate to each point of attachment can be empirically adjusted at the low frequency end of the sweep to the minimum value which will allow the development of the specified acceleration level.

AUTOMATIC TRANSFER OF CONTROL

As the acceleration level, or the force acting, at one or other of the points of attachment rises to and tends to exceed the required level during the frequency sweep, the control function must be passed smoothly backwards and forwards between accelerometer and accelerometer, and between accelerometer and force gauge. This can be achieved quite simply with the aid of biassed semiconductor diodes. The use of relays or other mechanical switching devices is to be deprecated as introducing switching transients and backlash instabilities.

TAILPIECE

Despite its manifold shortcomings, the general-purpose vibration test calling for the application of a specified acceleration level will be with us for many years to come, thanks largely to its deceptive facade of precision, repeatability, and simplicity. It must be recognised for what it is—a crude, but necessary, barrier to poor design and faulty workmanship—and it must be improved where possible.

In its present form the test is unduly prone to result in the rejection of serviceworthy equipment. This tendency can be moderated by an extension of available control techniques.

REFERENCES

From Shock, Vibration and Associated Environments Bulletin No. 31, (Apr. 1963):

1. V. J. Junker, "Environmental Testing Standization via MIL-STD-810. Environmental Test Methods for Aerospace and Ground Equipment," II:34.
2. M. Gertel, "Derivation of Shock and Vibration Tests Based on Measured Environments," II:25.
3. R. C. Kroeger and G. J. Hasslacher, III., "The Relationship of Measured Vibration Data to Specification Criteria," II:49.
4. R. E. Blake, "A Method for Selecting Optimum Shock and Vibration Tests," II:88.
5. L. J. Pulgrano, "Impedance Considerations in Vibration Testing," II:236.

6. R. D. Bailey and J. W. Apgar, "Preparation and Analysis of Munson Road-Test Tapes for Laboratory Vibration Tests," II:64.

7. I. Vigness, C. E. Crede, R. M. Mains, E. Lunney, J. Bendat, M. Gertel et al., Contributions to Panel Sessions, II:273-301.

From Proc. Institute of Environmental Sciences, 1963 Meeting.

8. M. R. Madsen, "Interpretation of Vibration Signals."

9. J. R. Sullivan, "The Navy's Shock and Vibration Requirements for Shipboard Equipment."

10. J. P. Salter, "Problem Areas in Dynamic Testing."

11. F. Condos and W. Butler, "A Critical Analysis of Vibration Prediction Techniques."

* * *

PANEL SESSION

STANDARDIZATION OF VIBRATION TESTS

Moderator: Dr. Irwin Vigness, U.S. Naval Research Laboratory

Panelists: Edward Kirchman, Goddard Space Flight Center, NASA
Milton Madsen, Sandia Corporation
Edward Meeder, Bendix Corporation
Roland Seely, U.S. Naval Research Laboratory
Wayne Tustin, Tustin Institute of Technology

The comments of all speakers have been edited for the sake of brevity and clarity. In some cases, certain remarks have been deleted or summarized because they did not seem to contribute to the subject. It should not be assumed that the following are exact quotations of the speakers.

Dr. Vigness opened the discussion by introducing the members of the Panel and asking them to make brief opening statements relating to the general subject matter. He explained that the session was intended to stimulate audience participation and encouraged the many experts present to give everyone the benefit of their experience.

OPENING STATEMENTS BY THE PANEL

Mr. Madsen: I would like to tell just a bit about what we have done at Sandia Corporation in the past few years in regard to standardization. About 3 years ago, we produced and published a "Standard Test Methods" document, specifically to breed similarity, repeatability, and uniformity of testing within our own lab, which is fairly large, and within the whole AEC complex. This standard has been revised a couple of times and a recent addition was approved by all the AEC integrated contractors and they in turn will inflict this standard on their suppliers. This document contains some data that are a little controversial, some that are a little arbitrary, and some that even we are not too proud of. But there are several points that we feel very strongly about, and I will touch on the points I think are most significant in this document. I do feel, very strongly, that the average specification borders on being ridiculous. While discussing this subject with Dr. Mains in the lobby, he said, "Well, if we're going to play this crazy game, maybe we should just not worry about these things." I agree with him that we are playing a game with specification writers, but I do feel very strongly that as long as we have to play it, and until we do get more intelligent test specifications, we should perform tests in a standard, uniform way.

I think we can standardize, and should standardize, the characteristics of control circuitry. This does not mean that it is necessary to define each specific meter, but I think we can and should define the characteristics. I also think we can define the calibration requirements. This may be somewhat controversial, but there ought to be some measure of control on how accurate the circuits are. I think we can standardize on the location, or locations, of input control transducers and the methods of mounting them. I further think that this point of having multiple inputs should be in a standard. We at Sandia, although we do it intermittently, have not included this point in our standards as yet, but we hope to. I would like to say just a couple more words about the input control circuitries since they were discussed this morning and again this afternoon. We at Sandia categorically feel, without reservation, that in sinusoidal tests you should filter out all the distortion, regardless of the source, and control on the fundamental amplitude only. The unfiltered signal, however, should be displayed

on an oscilloscope so that the test technician may monitor it and make intelligent judgments as a result of any peculiarities, such as nonlinear response, which he might observe.

Mr. Tustin: I would like to express my rather low opinion of panel discussions. I like to define them as a group sweeping under the rug. We pick up the rug and look at lots of problems left over from previous panel discussions and then we put the rug back down again. We do not solve very many problems. Nevertheless, it might make some of the people happier to know that the other people are also confused and have similar problems. This is about all we can accomplish in this large a meeting.

I agree wholeheartedly with Mr. Madsen on a number of points. I recommend that workers in this field get this Sandia document on "Standard Test Methods" and read it. A great deal of work has gone into it, and it is a fine job.

Mr. Kirchman: I have looked at specifications for many years and I find that it is fairly general practice to make them as simple as possible to meet the legal and technical considerations of each project. It is common to avoid complex procedures and practices that might involve long-winded discussions. To give greater guidance, it is usually necessary to write a document, such as the excellent job that Sandia has done. This document constitutes what the issuing agency has in mind and gives what is thought to be good engineering judgment, or good engineering practice, to serve as a basis to interpret the specifications.

When I was asked to serve on this panel, I looked at several attempts in the past by some of our scientific societies to write specifications or standards and I found that most of these groups were never able to come to grips with the problem. The problem I feel is one of philosophy, or approach. Even standardizing the top of vibration tables so that you can build one fixture and shift it from one place to another has not yet been done. Maybe this lack of standardization is good in some cases because if this has not occurred, it is because there is something wrong somewhere. Maybe we understand these problems a little bit better today and maybe we will be able to resolve them in a better fashion now than we could 5 years ago. I think that the characteristics of our high-force, infinite-impedance test equipments are fairly well understood and fairly uniform if we test a small mass or a small box, but when we get up to large structures, we have a problem. I believe that maybe it is time for a change in our outlook to some impedance or force concepts which would lead us out of this problem.

I would like to say that I have no real firm convictions on an acceptable level of crosstalk. I think it is a matter between the tester and his conscience as long as he meets the specification. I have no real feeling regarding the control points or how many control accelerometers should be used. I believe each case determines what its own procedures should be. Of course, there are fixed types of tests which you can specify in detail, but in most cases it is a matter of engineering judgment.

Dr. Vigness: I would like to point out that there are really two types of specifications: the general specification that is supposed to apply practically everywhere, and that must necessarily not be in detail; and a specification which is specifically written for the component or piece of equipment involved. It may go into considerable detail as to how tests shall be performed. At a meeting at Wright Field some few months ago concerning MIL-STD-810, it was pointed out that these general specifications are intended to be used as guides. Unfortunately, many times they do not turn out to be that, but that is what the technical people would like them to be. The project engineers and those working on particular items should use these general specifications primarily as guides in writing individual specifications for the testing of their respective equipment.

Mr. Seely: Like most of the people I have talked with recently, I also have some strong feelings on standardization and what should be done about it. To list all my feelings would certainly take more time than has been allotted to me, so I will content myself with merely identifying my point of view with respect to a few of the problems.

I feel that many vibration test procedures should be, and can be standardized. I understand that there is an active ASA committee in this area, and that in due course they will probably give us a standard which will tend to eliminate many of our problems. I feel that such subjects as transducer calibration accuracy, mounting procedures for transducers, crosstalk, and the like, are relatively simple problems which result in many differences of opinion, but I do not think the problems which they present are insurmountable. The one area which does seem to be receiving more attention at present than others is the question of input control and the location of transducers. Now I believe that vibration tests should be approached first by conducting a resonance survey in which

recordings are made at various transducer locations. Then the proper input locations are selected on the basis of these recordings. I feel that filters should be used, and control should be based exclusively on the fundamental frequency. I am in favor of multiple input points and the use of an average signal as a basis for control. Furthermore, I feel that where filters are used with averaging techniques, the signals should be averaged on an instantaneous basis. Where filters are not used, averaging should be done on an rms basis.

Mr. Meeder: The purpose of environmental testing is to establish assurances that the test article will operate satisfactorily during its designed life in its intended environment. The success of this test effort depends upon three factors: (1) the normality of the test article, (2) the actuality of the specified test environment, and (3) the fidelity of the laboratory test. It is generally agreed that control of all of these factors needs improvement. Yet, although some embarrassing or disastrous evidence confirms this opinion, a fair degree of success in producing operational hardware has been achieved. This success is directly related to the design safety practices that have been evolved to compensate for this lack of control. At present these factors are, in my opinion, excessive. I do not believe that the factors associated with vibration should be arbitrarily increased in an attempt to improve the success record. Yet the trend over the past few years, as indicated by specification changes, and proposed vibration test standards, appears to be toward more severe tests. As examples, filtered input control and the averaging of multi-control points could result in more severe tests. Their use increases rather than decreases the uncertainties. This trend, if unchecked, will burden designs with added cost, weight, and volume. As an alternate, a test standard should be adopted which will not arbitrarily increase the test severity, but will reduce the uncertainties that are now plaguing us. I do not believe, however, that this can be realistically achieved through standardization. To do this, all test equipment, methods, procedures, personnel, and so forth, throughout the industry would have to be identical. I prefer to look upon standardization as a means of reducing uncertainties by improving the comparability of test results. This can be accomplished by a standard that establishes a few basic ground rules, a test philosophy, and a minimum of engineering data that must be included as part of the test results. The ground rules should include vibration terminology, transducer calibration, transducer mounting, transducer control circuits, selection of control, and the number of transducers required for a test. Engineering data should include a complete description and wiring schematics of all test equipment, a photograph of each test setup which shows shaker fixture, test specimen transducer orientations, plots of filtered and nonfiltered transducer data, a detailed explanation of how resonances were identified, and random vibration equalization at the beginning and during tests. The test philosophy should simply state that cross motion, harmonic distortion, and control distribution ratios should be minimized. Typical state-of-the-art goals should be included. Random vibration equalization accuracies and control could be handled in the same way.

Dr. Vigness: I do not think there is much question but that a lot of standardization is appropriate and proper in the area of measurement, or of items which are used for measuring-transducers, and the like. Specifications give a number, a spectrum, or something of that sort, when they define test parameters. Naturally, there must be some tolerance in those numbers because it is impossible to meet an exact value. So, probably, there should be some tolerances in our standards, even though they are difficult to determine. I would like to mention, just as a general comment, that specification standards should be deprecated, if the conformity they require causes great expense and effort for the tests, and also causes the tests to be unrealistic with respect to field conditions. I feel that good standards do not make legal conformity their prime consideration, that is, so as to override considerations of field environment and the problems of the test engineer.

The first question that we will consider is: What are reasonable standards of transducer calibration accuracy?

TRANSDUCER CALIBRATION ACCURACY

Dr. Bouche: In talking about transducer calibration accuracy I mentioned this morning in my talk that accuracies under ideal conditions of 1-1/2 percent to about 1000 cps and 3 percen to 10,000 cps are possible to obtain under laboratory calibration conditions. Seymour Edelman from NBS obtains 2 percent up to 10,000 cps by using the absolute interferometer technique. The 3-percent figure is acquired by comparison calibration methods, but both of these methods are designed for use in the calibration laboratory.

Dr. Vigness: I think we would wish to know what would be a reasonable standard to establish

for a vibration pickup that is used in a test laboratory. Not a primary standard nor a secondary standard, but one that is to be used. In what range should that accuracy be?

Dr. Bouche: I think about 2 to 3 percent, over the entire frequency range. I expect that most people will be working at the lower frequencies not exceeding 4 to 5000 cps, and then 2 percent could be achieved without much difficulty. There has been considerable improvement in recent years in shakers designed for calibration purposes. In the past, shakers have been the limitation in attaining this accuracy. At certain frequencies there were transverse motions introduced in such a way that the standard and test accelerometers did not see the same acceleration. With our new shakers designed for calibration purposes, this is not so much a problem anymore. If one has simple sinusoidal motion in the calibrator, this order of accuracy may be achieved. There is still a need in the calibration area for small calibrators that can be used for all types of transducers, including triaxial accelerometers at relatively high frequencies, that is 2, 3, and 4000 cps. That is the area where we could have some improvement.

Dr. Vigness: I think that it has been established that we can, without too much trouble, get an accuracy of about 2 or 3 percent to about 10,000 cps. Is that necessary? Let's have some answers from someone on the panel. Do you have any ideas on this?

Mr. Seely: I would like to quibble a little bit with Dr. Bouche because I do not think this order of accuracy is in any sense required in a regular testing laboratory which is performing routine tests. I feel that accuracies of 5 to 7 percent are entirely adequate. There are so many other inaccuracies in the testing procedure of much greater magnitude, that concern over 2 or 3 percent in calibration accuracy seems incongruous.

Mr. Kirchman: I think we are currently calibrating within 1-1/2 percent. The reason we do this is that the transducer is one thing that you can put your finger on and calibrate to a definite figure. Many other measurements have a probability of error of something like plus or minus 10 percent, which I think most of us agree is somewhat reasonable. But transducer calibration is the one thing that we can really put our finger on, so we do attempt to control it.

Mr. Edelman (Bureau of Standards): I would like to say that I think there is no single answer to this question. The calibration accuracy depends on the conditions of the test, and this 2 or 3 percent can be reached only under special conditions that do not apply to most tests. The 5 or 7 percent figure is a far more realistic one at the point where the pickup is being used. Not only does transverse motion raise this 2-percent to 5 percent or more, but also, the signal becomes distorted. It has been brought out already that sinusoidal excitation is not necessarily the ideal test condition, and if there is any amount of harmonic motion, this too spoils our fine accuracy. In setting the calibration accuracy, the kind of signal, the kind of structure, and the kind of motion must all be considered.

Mr. Scroepfer (Ryan Aeronautical Co.): Very recently we have had a case where crosstalk was more than twice the linear vibration in the normal direction. If you calibrate accelerometers for linear vibration only, you have quite a problem with crosstalk during tests with large and complicated fixtures when you use this accelerometer for control, even with a tracking bandpass filter. I would like to ask the question: Where do you draw the line on crosstalk for sine and random testing?

Dr. Vigness: I would like comment on this subject of the crosstalk, or cross-motion as some persons prefer, and to remind you that there is a very good standard on the calibration of shock and vibration pickups which is in existence and which takes into account some of the problems relating to crosstalk. It describes standard methods for the calibration of vibration and shock pickups and gives the accuracy that can be obtained by the different techniques. This is published by the ASA and was put together by a committee, first under Walter Ramberg of the Bureau of Standards, and later by Ray Bouche who completed the work. So, there is a very good standard on the vibration and shock pickups at the moment. It is identified by the American Standards Association as S2.2 1959 "Methods of Calibration of Shock and Vibration Pickups."

Mr. Todaro (University of California - LRL): I would like to break the calibration problem down into two areas. One is the transducer area and the other is the associated electronics. Now, I think that calibration of the transducer should be consistent with the economics of the particular organization. If it is expedient to calibrate to something like 2 percent, I think that is fine. It would also be okay to calibrate to 3 or 4 percent, or whatever they decide is justifiable, based exclusively on economics, providing it doesn't get too high. What

I would really like to bring out here is that it is utterly stupid to have an accelerometer that is good to 2 percent and then use an electronic system of unknown accuracy. During calibration, one should also calibrate the electronic system that goes with it as part of the calibration technique.

Dr. Vigness: I do not think anyone will disagree with you.

Mr. Mangolds (RCA): The figures which have been mentioned here of 1 or 2 percent may be good to show the limits of calibration accuracy that may be obtained under ideal conditions. I want to emphasize, however, that these accelerometers eventually have to be used in a test, and there are other factors which overshadow this accuracy completely. As an example, we recently had a sub-miniature accelerometer which was accurately calibrated, and then we found that during our test we had a condition which distorted its face. We found that this caused a 250-percent deviation from the actual calibration curve. I think that is quite an extreme case, but we should emphasize overall accuracy rather than by splitting hairs on 1 or 1-1/2 percent.

Mr. Lane (Lockheed, Sunnyvale): One small addition to Mr. Todaro's comment is that the calibration ought to extend all the way through the whole system, including the data reduction process. This has become standard procedure at Lockheed, Sunnyvale, where off-line processing is used for calibration, as well as other testing. On our missile and satellite vibration channels, the entire measurement systems is calibrated dynamically. We take this as a matter of course.

Dr. Vigness: The American Standards Association has standards which apply to associated equipment, although I do not know their numbers at the moment. I think most of us will be satisfied if we have a confidence of plus or minus 5 percent in the actual test instruments. I am afraid that sometimes our confidence is somewhat destroyed by the persons that use the instruments rather than the instruments themselves.

Our next subject is random-test equalization accuracy. I am not exactly sure what is meant by that, but someone who works with vibration machines can explain it.

RANDOM-TEST EQUALIZATION ACCURACY

Mr. Unholtz (Unholtz-Dickie Co.): I believe that what is meant by the random test equalization accuracy is how closely should the power spectral density of acceleration conform to the test requirement? I feel that there is a great deal of instrumentation and setup applied to this particular area of testing that cannot be justified from the point of view of economics by the improvement in the test item after the test has been run. This is related to the fact that the test environment is never known too well, and the variation from test item to test item is quite great. Also there are the questions of how to measure the power spectral density, and where accelerometers should be located. How does one account for the fact that moving the accelerometer to another location, or averaging over several accelerometers, gives quite widely different indicated values of power spectral density as a function of frequency, all for the same input? Therefore, I would be inclined to take the stand that many people are attempting to make things quite precise on the assumption that vibration tests are run with good precision, and I do not believe that is the case. I think that random-test equalization precision is of a completely different order of magnitude compared to that which you might be able to discuss with regard to the calibration of transducers.

Mr. Tustin: I quite agree with everything that Mr. Unholtz has said, but that does not answer the question exactly. Suppose a specification calls for a constant power spectral density from say 20 cps to 2 kc, how flat can we get it with equalizers that are commercially available? I think many people can obtain plus or minus 3 db. Other people have great difficulty achieving plus or minus 6 db. I think that the audience would like to hear some numbers.

Dr. Mains (GE): It is a grave error to talk about flattening the power spectral density curve of a test. You have seen magnification factor curves that had nice dips in them. At those points you overtest severely if you have, in fact, flattened the spectrum. The proper thing to do is simply to know what the transfer function is up to the point of attachment of the specimen. Then it does not matter whether you put in one or another kind of power spectral density curve so long as what comes out of the interface between the test fixture and the final article is the right value. Any other procedure is going to give the wrong value there. It does no good at all to equalize to 3 db or 6 db if the final article is to be mounted in a place where this can't happen. The final article is bound to sit on an impedance that is not flat.

Mr. Tustin: Then you are suggesting that a specification that says "Thou shalt equalize

flat" is a wrong specification? It should not be followed by test engineers?

Mr. Price (Hazeltine Corp.): We do quite a bit of both random and sine vibration testing on the electronic equipment which we produce. I have had occasion to witness many of these random tests and I have found many inadequacies. One of the problems is that peak-and-notch filters cover only the frequency range up to about 2000 cps. But practically many fixtures that have been designed for this type of test have harmonics above 2000 cps. The outcome of what I am saying is that if filters are not inserted before their readout, the test level can frequently be misconstrued. The harmonics that appear from 2000 cps to infinity do contribute to this nonflatness and it does appear in the readout. Our specifications do not now tell us how we should handle this type of problem. I would like to hear anybody who has a solution for this problem.

Mr. Booth (MB Electronics): I would like to state that the multiple-band equalization equipment which is the common equipment now being sold by all of the manufacturers, does have filtering in the output so that you just read the energy in each band. Therefore, of course, what is above 2000 cps is eliminated. With regard to equalization accuracy, my paper which was presented to the 31st Shock and Vibration Symposium discussed this point. Equipment now being supplied, having many bandwidths, averages equalization over the width of each band. For example, if we have a bandwidth of 25 cycles, we get an average equalization for that bandwidth. If the device you are trying to equalize has a resonance with a Q of 50 at 500 cps the bandwidth is only about 10 cycles. This resonance bandwidth is well within the bandwidth of the filter which cannot correct for the situation and it is possible to get very large errors. All equipment currently being used has these errors and they can very readily be of the order of magnitude of 5 to 1 (not 5 percent). These are the errors that are currently being lived with daily by all of the people who are doing testing. Now, the readout equipment has bandwidths which coincide with the bandwidths in the equalization equipment so that the readout, of course, is reasonably flat. But this is actually not the case because the power spectral density is not flat and varies tremendously within each bandwidth. This must be recognized when specifications are established.

Dr. Vigness: I would like to hear about the Sandia reaction on the importance of uniformity of random tests. Companies which have a lot of different contractors must require them to perform tests in a uniform way.

Mr. Madsen: First, I will have to agree with Dr. Mains that a flat random test should not be specified. We do not put an absolute tolerance on equalization in our standards document because of some of the problems just mentioned. You get into the problem of continuous filter analysis versus the discrete point analysis that the manufacturer supplies with this equipment, the problem of how narrow the bandwidth should be, and the acceptable accuracy of the electronics. We do, however, recommend to the test specification writer and to the test technician that plus or minus 3 db seems reasonable. I will confess that we are simply following previously published work which commonly uses these tolerances.

Dr. Vigness: I think most of us here probably realize what the present state-of-the-art is regarding this particular subject.

CROSS-MOTION

Mr. Madsen: With regard to cross-motion accuracy I want to comment that this has been real rough to put in a specification. We have put in 100 percent allowed knowing that it is questionable. It is obvious that the indicated cross-motion, at least on occasion, can be a function of the impedance of the driving mechanism. All electrodynamic shakers have armature characteristics which modify the input motion in some cases. I have, frankly, an open mind on this subject.

Dr. Vigness: I would like to point out the fact that cross-motion of 100 percent does not necessarily mean that the test is more severe. If you eliminate this cross-motion, you would most likely have some more severe test condition than if you allowed the test equipment to generate the cross-motion. Inasmuch as we have those conditions in the field, and if it is reasonable to have it in, and it is hard to get out, why, as far as I am concerned, I would just as soon live with it.

Mr. Houston (Northrop Norair): I think we have a roomful of professionals here. I wonder if a few of the questions that are considered here might be answered by a show of hands. Ask how many people have random equalization standards within their lab, how many have crosstalk standards?

Dr. Vigness then asked for a show of hands to indicate how many people worked directly with vibration tests. It appeared that about one-quarter of the audience was in that category. He then asked how many laboratories have

cross-motion standards. The result showed that there were three to four times as many laboratories in the latter category as in the first.

Mr. Held (Vapor Corp.): The acceptable level of cross-talk in our laboratory is determined by the unit being tested. The engineer in charge determines whether the unit can withstand the crosstalk to which it will be subjected. If not, he will do something about it.

Mr. Anderson (MB Electronics): The census just taken seems to be diametrically opposed to what people are currently asking for when they buy equipment. Everybody purchasing this equipment mentions figures like 1 db on equalization or crosstalk. They sometimes forget the plus or minus. We keep extending the specifications on the exciters beyond the axial resonance, and so on. We expect to get decent numbers on crosstalk, then our customers object when the tolerances start to increase. Our customers blame us for quoting specifications which they say we do not meet, but, generally speaking, there are many misunderstandings between them and us as to what a specification is in the way of equalization and over what conditions it is for. We are trying to provide a source or control point equalization for the whole system when we come up with a specification of plus or minus 1-1/2 db for a 40-db dynamic range. We also should set the spec requirement within the resolution of the set of filters.

Mr. Schnell (GE): I was one of the people who raised my hand to indicate that we do not use cross-motion standards in our lab. We had them but I am happy to say that we spent about 2 years getting rid of such standards. I think one of the things that a panel like this seems to somehow skip over is a consideration for the person that we are doing this testing for. We are doing this testing for some engineer, and if we spend a few minutes with him ahead of the test, explaining exactly what it is that we are going to do and another few minutes afterward going over what we did and what we saw, I think we might be a lot further ahead than we are by nit-picking at some of the details that go into standards. Now, I think some standards are necessary, and I think all of us have probably been exposed at times to the inspector who measures an inch to plus or minus 0.0001, and he wants you to measure the g unit with equivalent precision. I do not think it matters whether you use filters or not, except in very specific cases. I do not think it matters whether you have cross-talk or not, whether you equalize within 3 or 1 db, as long as the engineer that has the product responsibility has some understanding of what it is that you are doing. I think we tend to become so involved in our own little subject that we forget him, and are carried away with the science of our approach rather than the practicality of it.

Dr. Vigness: It would be very nice if we could do things that way. Perhaps if all new work was being done within one organization it could be done that way. But when you are working with different organizations and there are legal commitments and money involved, then you just cannot make agreements offhand between internal groups. Such agreements must be formalized, particularly if it is going to cost a lot more to do it one way than some other way. What you have said is very nice, and we would like to do it that way, except that we run into financial problems.

Mr. Gorton (Pratt & Whitney Aircraft): One gentleman just proposed that since he had a cross-motion about equal to the wanted motion, it might be eliminated by stiffening the fixture. That would raise the question that when the test components are placed in a vehicle, is somebody going to stiffen the vehicle to eliminate the cross-motion? I somehow doubt it.

I have the impression that many people get a bit specification-happy and forget to use common sense about what it is they are trying to do. For example, an accessory manufacturer is being required to design his unit to withstand a certain g limit. This accessory is proposed to go on an aircraft engine, and it seems fairly obvious that the weight of this accessory is such that when he bolts it down to the engine it is going to make that part of the engine sit still. We have certain vibration limits on the engine which may apply to a little accelerometer, but when someone takes that g limit and requires that a several-hundred-pound hunk of steel is going to have to withstand it, there has been something lost in the translation of information. As another horrible example, we have a clock on our laboratory wall, a plain ordinary clock, which is used to put time on the data sheets. Some specification-happy character has now insisted that periodically it has to be calibrated and have a little green sticker put on it saying that this is referable to the Bureau of Standards.

Dr. Morrow (Aerospace Corp.): The subject of equalization keeps coming up again and again, and I feel compelled to add a brief comment on this. It is a very reasonable thing to have plus and minus tolerances to describe the required capability of an equalizer which can be accurately measured and which you are about to buy.

But, I object in principle to having plus and minus tolerances on vibration test specifications, either written in them or applied subsequently by way of a standard. It seems to me that the task of the specification writer is to specify a minimum condition. Perhaps one way of doing this indirectly is to require certain equalization bands, which are not too narrow, to come up to the required level. If there is a narrow-band dip in the middle which would not normally be observed in the test process, we would be lenient. On the upper side, any deviation is certainly not the concern of the specification writer. The person that really should be bothered is the engineer who designed the equipment under test. The question is, just how much do you want to complicate the test effort in order to save effort in design. A little negotiation should go on there, but the specification writer should not put in plus or minus tolerances at the beginning.

FILTERING THE INPUT CONTROL SIGNAL

Mr. Tustin: I feel that the use of the tracking filter between the accelerometer and the servo control is very desirable from the standpoint of standardizing a test. No detector is completely satisfactory in the presence of harmonic distortion or rattling kinds of distortion, they all have various amounts of error. If it is desirable to standardize tests, and I believe that it is, then we should all either use the same type of detector, or we should eliminate the influence of the detector by the use of a narrow-band tracking filter so that they all work on a sine wave and behave the same. I think the simplest procedure is the addition of a tracking filter to vibration control systems.

Mr. Kirchman: You have all heard Mr. Bangs previously state Goddard's contention that the use of a filter is a matter of judgment. We feel that it is possible to get yourself into a lot of trouble and a lot of grief by their use. I would like to say, however, that we do approve and insist on using a filter in cases of distortion due to banging of parts and the like. It may be more acceptable to use filters which do not track closely rather than the present tendency to use commercial filters having about 10-cps bandwidth. I think perhaps, if we used filters which excluded the third harmonic on the fundamental input, this might be an appropriate way of running a test.

Dr. Vigness: It seems to me that if we are going to be concerned with the amplitude at a particular frequency, then we should use a filter, because that would give us the amplitude at that frequency. If a complex wave is applied to a vibration test and we do not use a filter, then the amplitude is not of any particular frequency, but of a variety of frequencies. If we do not make any attempt to standardize, but tell what we are doing, that should be sufficient.

Mr. Coler (IBM Corp.): I think it is impractical to come up with a standard that is intended to apply to a number of varying situations. To say that we are always going to run all our vibration tests by the standard, using a particular tracking filter with a particular bandwidth over a particular frequency range is to take on a job that should be done by on-the-spot engineers. I do not believe that a vibration test of any type should be blindly put on the shaker, the instrumentation calibrated, a tracking filter setup, and away we go according to a standard. I think that each vibration test should be performed by making a survey run at which time the engineer may spend half a day fooling around to find out what goes on. It may be at reduced levels, so that we get an understanding without putting too much time on it, but the engineer then has to decide what technique is going to be used to give this equipment a valid test. If he has a heavy shaker in relation to his test item and a virtually resonant free fixture, the distortion may not be severe, and he can use a tracking filter to get a very accurate input. In some cases the distortion is extremely severe (in one of the papers given here there was a third harmonic that was equal to or greater than the basic input) and it is possible to overtest. I think that during the survey is when the decision should be made as to what type of instrumentation and control we should use. A standard cannot apply to everything, because each item we test is different. This same problem is going to exist with regard to the proper number of control points and how their output should be averaged.

Mr. Meeder (Bendix): As I indicated in my opening remarks engineering judgment should be used to establish the performance details of the vibration test. In my test laboratory, I have to rely on interpreting the intent of a specification, and I think this is justifiable.

There are an awful lot of seat-of-the-pants designers who are accustomed to designing in terms of a 10-g test or a 5-g test as it is presently performed. This means something to them from years of past experience. They have taken their design, given it to a test lab, had it subjected to a 10-g test. They know more or less by experience how they should design for a 5- or 10-g test. If we now, arbitrarily, change

our ground rules (this distortion, by the way, is nothing new that came about with spacecraft — it has been here for years) and use a tracking filter on the control accelerometer, the severity of the test will increase. Now, unless this information is fed back to the specification writers and the designers, I cannot see any good that would come out of a change such as this. I do not think any specification writer should write a specification with tolerances unless he knows the test standards which are going to be used. I do not see how we can separate the standard from the specification. They go hand in hand in changes such as this, and standards should not be established without making appropriate compensating changes in specifications.

Mr. Forkois (NRL): This seems to evolve into a philosophical discussion regarding whether standards are likely to result in better equipment. This may, or may not be the case. Personally, I am inclined to agree with some of the speakers who indicate that many of the test details should be based on engineering judgment and experience.

CONTROL POINT LOCATION AND CONDITIONING

Mr. Gertel (Mitron Corp.): The question of whether we should have multiple control points and how to use them would not be asked if the recognition did not exist that there are fixture resonances in the frequency range of today's vibration tests. These tests in general seem to go up to 2000 cps and in some instances beyond that, because these higher frequencies have been observed. If you put accelerometers at the base of a black box with four mounting points, the only reason you get different results from each of these accelerometers is because the fixture is somehow going into resonance at one of the test frequencies.

A related subject is how specifications are created. I do not condone this, but what usually happens is that specifications wind up as enveloping many data. This process of enveloping makes the specification generally more severe than any one single condition which has been observed. Now, recognizing this, and trying to bring some judgment back into the problem in the laboratory, I have a feeling that we should place an input accelerometer at each of the mounting points where the test object is attached to some aircraft or missile structure. This seems rather obvious. I would then suggest that if it is a four-point item, all four points should be monitored and the test controlled by whichever accelerometer reads the highest. My feeling is that even if one attachment point of equipment goes to zero, and another point is at the specification value, keeping in mind the true condition that exists in the actual field, this is not a bad representation of the proper test level.

Dr. Vigness: You believe that several points should be monitored and that the point which vibrates the most be used to control the vibration level. This sounds like a suggestion from one of the contractors who makes equipment rather than from a person that buys the equipment.

Mr. Price (Hazeltine): I have made some studies in this area and have plotted out the transmissibilities at various input points. I have come to the conclusion after some consideration that the only real way to give a fair test is to use the square root of the average of the g^2 of the accelerometers. In this way it is possible to get an arithmetic average which fairly well represents the energy that is required to satisfy the test. We know that the cost of redesigning fixtures over a period of time is quite excessive in a big job. We have used this technique successfully to obtain what we consider a suitable average g value which will meet the specification and not smash up expensive equipment.

Dr. Vigness: I understand that you use the rms average for your control. We have two techniques now. A minimum and an rms average.

Mr. Anderson (MB Electronics): It would seem to me that any electrical averaging system should operate on some type of a detector output because of the phase relationships that might exist at various points. For motions that are 180 degrees out-of-phase, accelerometers could give a zero signal into the control device if an instantaneous average is used. This would, in turn, result in a maximum signal into the shaker. If an average of the rms signals is used, I believe that it would result in a more representative signal level for control purposes.

Mr. Madsen: We have not done averaging as a universal practice, but find it difficult to see why anyone would not agree that a single input control transducer is not adequate to define the mean motion of some package unless you had made a thorough investigation. If a specification states there should be the same g level over the frequency range it is implicit that it have a uniform motion. The thing I have not really solved in my mind is whether it should be an instantaneous average or an average of the peaks. It would seem to me that this is a question of whether you want to recognize

simple rotational modes. If you want them to be a factor, you should average the peaks and if you do not, do instantaneous averaging.

Dr. Vigness: I feel kind of sorry for the specification writers; they write a specification and, of course, we can always find something wrong with it, but we cannot find any way to make it right. What kind of a specification would come as a result of the discussions that we have had here? Everybody seems to have their own ideas and nobody knows for sure what they want to do.

Dr. Mains: I would like to suggest how to do it right. If the test article has low impedance compared to the place where it is going to sit, then whatever the motion of that place is, the article has to go along with it. On the other hand, if the test article has a large impedance compared to the place where it is going to sit, it can rock around and modify the motion of its mounting point appreciably. Now, in the first case, where the test article is on a high impedance, you would like to provide a controlled motion and perhaps some averaging technique is the best way to do that. On the other hand, when the test article is to sit on a low impedance support, then you are going to have all kinds of rocking modes in its service position, so you should allow that to occur also in the test. In this latter case, you should just measure in one spot, perhaps at the center of the area of input, or something of that sort. I think it is entirely possible to be rational about these measurement requirements provided you have some concept of the nature of the beast on which the article is finally going to be mounted.

Mr. Forkois (NRL): That is an important point; but we do not know, in many cases, whether the impedance is high or whether the impedance is low. It becomes very difficult to write a specification for a future missile component because there is no source of information. The specification writer is certainly in a quandary and he can only base the tests on information which may or may not apply to the actual specification he is writing for future generation equipment.

Mr. Hieber (RCA): I believe that the question of standardization of tests should be considered with reference to the size of the equipment to be tested. If we arbitrarily choose a test object of, say, black box size, it is certainly not illogical to standardize vibration tests for this size object (and smaller) in order to obtain uniform results. Since many suppliers are involved, and since it is difficult to determine exactly what the mounting conditions of the object will be, we cannot take impedances into account. If we are concerned with larger sub-assemblies and assemblies, however, it makes sense to treat this size test object on an individual basis, where talent should be brought to bear on the interpretation of the requirements and the results in order to obtain a meaningful test. In the case of large test items, therefore, standardization is not desirable.

Dr. Vigness: It certainly is unfortunate that we cannot treat vibration in much the same way as the Navy does with some of its shock tests; i.e., just specify a shock test machine and a testing procedure and let it go at that, rather than detail all these motions which we cannot get anyway. This concludes the panel discussion.

CONCLUSIONS

The standardization of vibration tests continues to be a subject on which there is no general agreement, even on relatively simple aspects. Each autonomous vibration laboratory will, no doubt, continue to perform tests according to rules which are not uniform throughout the country. Many of these differences in rules (or standards) will result in large differences in the loads which are imposed on the test item. Thus, a test according to a given specification may be different in one place from one given in another. This is undesirable from the standpoint of government procurement agencies.

On the other hand, a number of speakers have expressed the opinion that standards for many tests are not desirable at all. The argument they present is that the present state-of-the-art is simply not sufficiently advanced to make uniformity possible. Rigid standards would be unnecessarily restrictive and would, in many cases, defeat the purposes of standardization. Examples of many such cases are easily found. They usually involve relatively large structures of greater than average complexity. Such items are not well adapted to standardized tests because of the difference in mechanical impedance between the test conditions and the intended service application. It is commonly contended, with much justification, that large and expensive structures of necessarily low factors of safety require intensive and individual engineering study. Test details cannot be established solely on the basis of a study of the expected environment. Such information must be combined with a knowledge of the elastic response characteristics of the item under test, and the complex influence of mechanical impedance. Vibration test details, therefor

are properly determined by an on-the-spot engineer rather than by predetermined standards. He would base his decisions on extensive resonance surveys, a knowledge of the field environmental conditions, economic considerations, and on intuitive feeling for whether certain practices are reasonable or not.

Both views of the same situation seem to be merited from a technical standpoint. A reasonable compromise would be to identify the characteristics of structures or situations which do permit standardization. It would then be possible to concentrate on the achievement of a degree of uniformity in those areas where there is something like unanimity of agreement. At the same time the types of information required by the engineer making on-the-spot decisions should be studied for completeness and applicability.

There remains much work to be done in this area and we believe that it is the duty of test engineers and their managements to study this problem in their own laboratories. They should identify the characteristics of equipment where standardization may be of benefit, and establish and use appropriate standards in their own laboratories. They should also identify the characteristics of test items which should not be subjected to standardized tests, and should formalize the procedures by which decisions are made regarding test details. The results of such studies should be reported in these or similar symposia for the benefit of others in the field.

Specifically, it would seem that more study should be given to the following questions.

1. What are the characteristics of test items and test equipment which permit standardization of vibration test methods?

2. What is the relationship of transducer accuracy to economics and to test results?

3. What is the effect, in terms of test results, of cross-motion, of filtered and unfiltered input motion, of multiple input control points, and the like?

4. What is the feasibility of new approaches to the conduct of vibration tests, e.g., constant force techniques, controlled mechanical impedance, and so forth?

Questions regarding the correctness of specification tests have frequently been raised during this and similar panel discussions. It seems that specification writers frequently tend to simplify vibration test requirements to the point that they are technically undesirable in many aspects. When this occurs, the test engineer is urged to seek a change in the legal requirements, or to request a waiver. This is a basic problem area, but it is only indirectly related to the standardization effort. More frequently the test engineer is required to perform tests according to a particular specification which must be assumed to be correct. Even if he believes the specification to be improper or incomplete, it is frequently more expeditious or economic to perform the test than to seek relief. In all cases where a definite specification is to be followed, standardized test methods can be of great value. Therefore, the problem of incorrect specifications and the problem of standardization are two subjects which should be discussed separately.

R.E.S.

* * *

COMPARISON OF PREDICTED AND MEASURED VIBRATION ENVIRONMENTS FOR SKYBOLT GUIDANCE EQUIPMENT

J. M. Brust and H. Himelblau
Nortronics, a Division of Northrop Corporation
Hawthorne, California

The Nortronics modification of the Mahaffey-Smith procedure was utilized to predict the vibration environment of guidance equipment for the Skybolt air launched ballistic missile during B-52F takeoff and missile postlaunch conditions, and to establish design and test criteria for the hardware. A comparison is made with actual vibration measurements during aircraft takeoff and missile flight. Improvement to the prediction procedure is indicated. Comparison is also made with the prediction techniques developed by Franken, Winter and Curtis. The establishment of realistic criteria for missile and spacecraft equipment still requires additional research in this area. It is speculated that the early application of preflight acoustic testing of vehicle sections, in conjunction with mechanical impedance methods, would do much to improve prediction techniques.

INTRODUCTION

The GAM-87A or Skybolt missile was designed to be carried aloft by a strategic bomber and, upon command, put into a ballistic trajectory to reach its intended target. Douglas Aircraft Company was prime contractor for the missile while Nortronics was guidance subcontractor. Figure 1 shows four Skybolt missiles carried by a B-52 aircraft, two under each wing and located between the fuselage and an inboard set of turbojet engines. The missiles appear to be in the acoustic-near-field of these engines. Figure 2 shows the missile at closer range. The guidance equipment was located in the guidance bay, which is just aft of the intersection of the conical section (re-entry vehicle) with the cylindrical section of the remainder of the vehicle. A diagram of the guidance bay and its equipment is shown in Fig. 3. The Astro-inertial Instrument (AI), appearing in the upper left portion of the figure, was comprised of an inertial platform with stellar correction, some electronic circuits and thermal conditioning equipment. The platform was resiliently mounted to the AI housing, which was hard-mounted to the secondary structure of the missile. The Ballistic Computer (BC) and the Platform Electronics (PE), shown in the lower right portion, were mated along one surface and this combined package was resiliently mounted to the secondary structure of the missile.

The mission profile for the vehicle could be nominally divided into two phases: prelaunch and postlaunch. The operational requirements and design considerations for each phase differed significantly. The prelaunch phase was a long time environment with only certain guidance functions operative. The guidance subsystem was designed for many takeoffs of the carrier vehicle, as well as thousands of hours of carrier flight at high and low altitudes. As expected, B-52 takeoff was the controlling prelaunch condition for the acoustically-induced vibration environment. The runway and lowered wing flaps served as additional reflecting surfaces and increased the acoustic loading from the turbojet engines on the missile structure. The postlaunch phase was a relatively short time environment requiring the operation of other guidance functions. Combined environments not seen in the prelaunch phase were expected, such as sustained acceleration and vibration. For the postlaunch phase, the highest vibration levels were expected at the time of maximum dynamic pressure on the vehicle due to boundary layer turbulence. In addition, high transients were expected due to missile drop from the carrier aircraft, rocket engine ignitions, and staging events.

Fig. 1 - B-52H strategic bomber with four prototype GAM-87A ballistic missiles

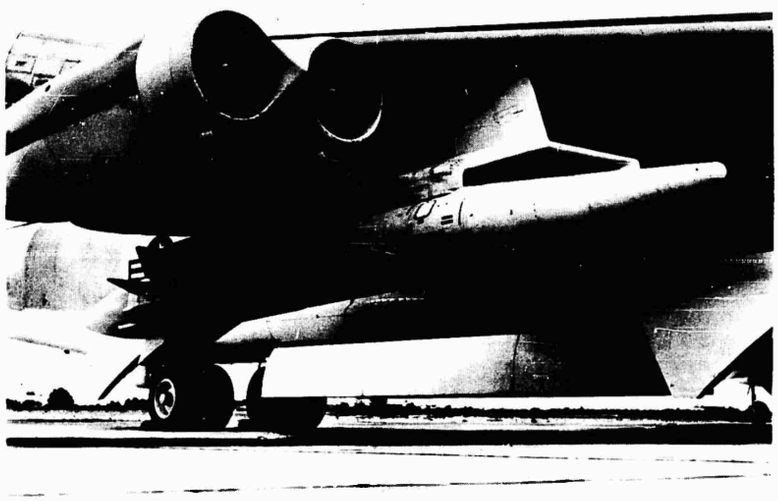

Fig. 2 - GAM-87A missile on B-52F aircraft prior to flight test. Guidance bay is located just aft of the intersection of the conical and cylindrical sections.

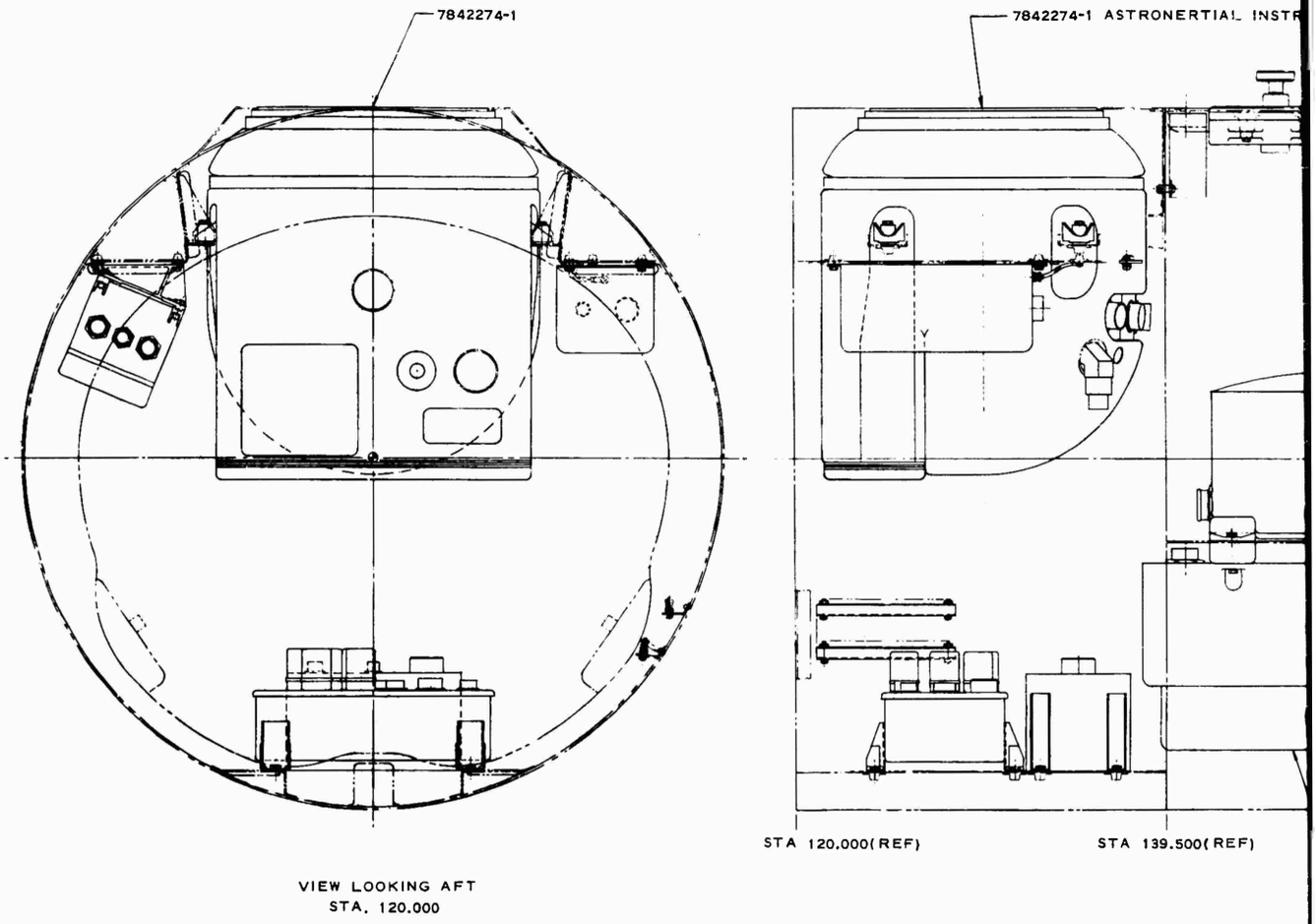

Fig. 3 - Layout of guidance equipment in guidance bay, showing Astroinertial Instrument a

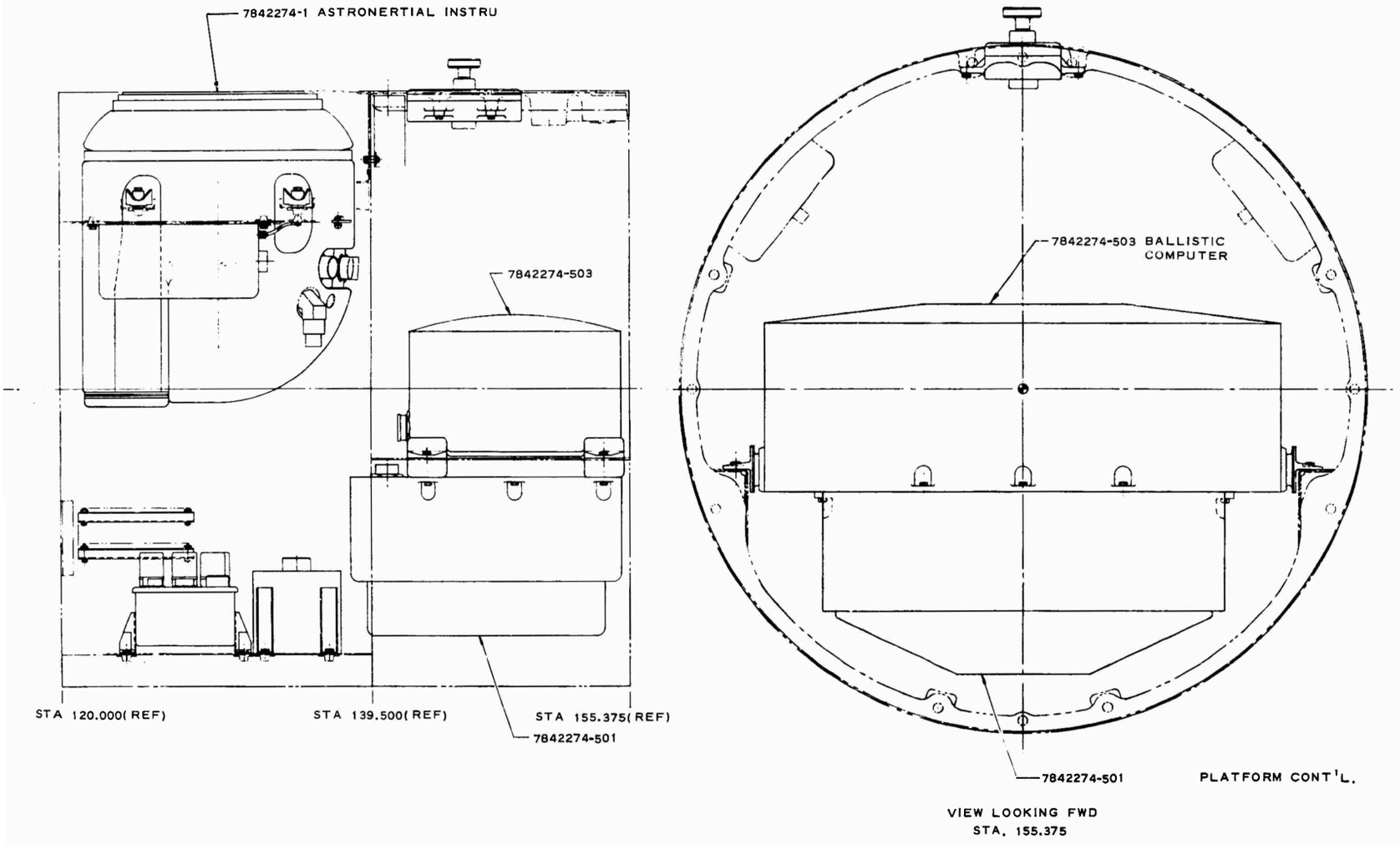

ɔment in guidance bay, showing Astroinertial Instrument and com'ned Ballistic Computer - Platform Electronics package

2

Early in 1960, when the design of the guidance equipment was initiated, acoustically-induced vibration was recognized as an important environment in the design of the guidance hardware. Work on two problem areas was initiated immediately. First, the vibration environment was predicted using the best information available at that time. Second, a laboratory development program was initiated to supplement preliminary analytical studies of the structural design. Since the basic structural configuration of the equipment had already been formulated in a general manner, it was decided to use prototype hardware in certain cases, and structural dummies in other cases, to investigate the vibratory response characteristics of the preliminary hardware. Both of these areas were upgraded continually throughout the design phase, and were considered essential to the delivery schedule of the equipment and to the intended reliability of the subsystem.

From measurements on similar vehicles, such as the GAM-77 (Hound Dog) missile, the environment during both prelaunch and post-launch phases was expected to be random vibration. Prior to the Skybolt program, laboratory testing performed on similar equipment indicated that sinusoidal vibration produced considerably different effects on guidance performance than did random vibration.[1,2] For this reason, it was decided to use random vibration for laboratory testing of Skybolt guidance and to predict the vibration environment in this form.

This paper will discuss the procedure for predicting the anticipated Skybolt environment and will compare this prediction with field measurements made later in the program during flight tests. It should be pointed out that the comparison of prediction with measurement will be made on the basis of the predicted field conditions, rather than an extrapolation of the prediction to laboratory test criteria, since the test criteria would logically include considerations of additional factors (test limitations, margins of safety, and the like) which will be described later. Before the Skybolt prediction is described, however, it would be appropriate to present the more general Nortronics prediction procedure.

In addition, other prediction procedures will be described which were developed subsequent to the initiation of Skybolt. Comparison of these predictions with Skybolt measurements will also be made.

[1]See References, page 278.

THE NORTRONICS VIBRATION PREDICTION PROCEDURE FOR DETERMINING DESIGN AND TEST CRITERIA

Equipment located in turbojet and rocket powered vehicles are often excited by random structural vibration caused by random acoustic noise generated externally to the vehicle. In general, the two primary noise sources are: (1) the turbulent jet of the engines, and (2) the turbulence in the aerodynamic boundary layer. Engine noise usually is most severe at takeoff or lift-off, while boundary layer turbulence is usually most severe at maximum dynamic pressure. Since flight and space vehicle structural vibration is caused principally by the external noise or turbulence field, it is generally possible to relate the severity of the vibration with the severity of the noise or turbulence. This relationship may be used to predict structural vibration levels and derive vibration design and test criteria for equipment inside the vehicle.

The acoustically-induced vibration environment may be predicted by utilizing the following steps: (1) the external acoustic or aerodynamic pressure levels are determined by measurement or prediction (preferably the former) on a wideband basis (octave or one-third octave is commonly used), (2) a relationship is used to find wideband vibration levels from the wideband acoustic or turbulence pressure levels (in this case the Nortronics modification of the Mahaffey-Smith procedure), and (3) a wideband-to-narrow band correction factor is applied so that the predicted vibration levels envelope the peaks of the spectrum, rather than average the peaks and valleys of the spectrum. After the narrow band vibration envelope is predicted, the design and test criteria are established. Each of the above steps will now be described.

Determination of External Acoustic Noise Levels from Turbojet and Rocket Engines

The noise environment of jet and rocket powered vehicles is usually most severe at takeoff or lift-off, due to the high engine thrust, the presence of noise reflecting surfaces, and the absence of significant forward motion effects. The noise levels are determined primarily by the number and sizes of the engines, and the location of the equipment relative to the engines. Actual field measurements are the best determination of this environment. Table 1 lists some approximate values of overall sound pressure levels (OA SPL) for present-day

aircraft and missiles. If acoustic data are not available, then measurements on a similar vehicle or configuration may be useful. (This includes properly scaled models, as pointed out in Refs. 3 and 4.) If an entirely new configuration is being proposed, then an acoustical prediction should be made. Several excellent sources of this information are available, namely Refs. 5-8. The near field OA SPL of a typical 1955-vintage turbojet engine at takeoff is shown in Fig. 4 with the octave band sound pressure level (OB SPL) obtainable from Fig. 5 (Ref. 9). The OA SPL and OB SPL for the surface of a large ballistic missile at lift-off is shown in Fig. 6 (Ref. 10).

In certain cases, it is possible to estimate grossly the OA SPL (such as those listed in Table 1), but not the shape of the spectrum. In these cases, it might be advisable to use as an interim measure the OB SPL shown in Fig. 7 (as the solid curve). This should be advantageous, for example, during the proposal stage or the preliminary design stage of a program.

The dashed curve of Fig. 7 is a typical spectrum for the internal acoustic noise inside a vehicle. Both the external and internal OB SPL are referenced to the external OA SPL. The internal OB SPL is assumed on the basis of typical values of octave band noise reduction for aerospace structure.

TABLE 1
External Acoustical Noise Levels for Rocket-Propelled Missiles at Lift-off or Jet-Propelled Aircraft at Takeoff

Vehicle	Location	OA SPL (db)
Titan I	Nose cone	139
	Interstage	143
	Engine compartment	155
Jupiter	Nose cone	148
	Engine compartment	153
B-52	Forward fuselage	137
	Mid fuselage	155
	Aft fuselage	157
B-58	Forward fuselage	128
	Mid fuselage	148
	Aft fuselage	156
	Forward pod	145
	Aft pod	157
RB-66	Forward fuselage	124
	Mid fuselage	133
	Aft fuselage	148

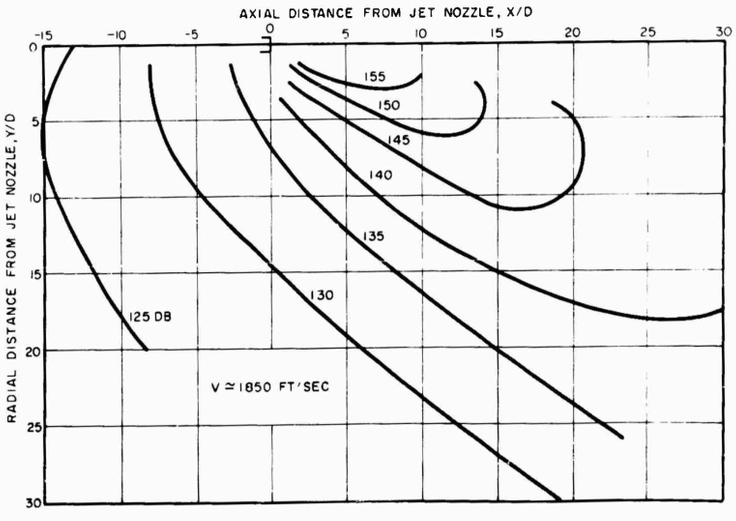

Fig. 4 - Contours of OA SPL in the near field of a typical 1955-vintage turbojet engine (Ref. 9)

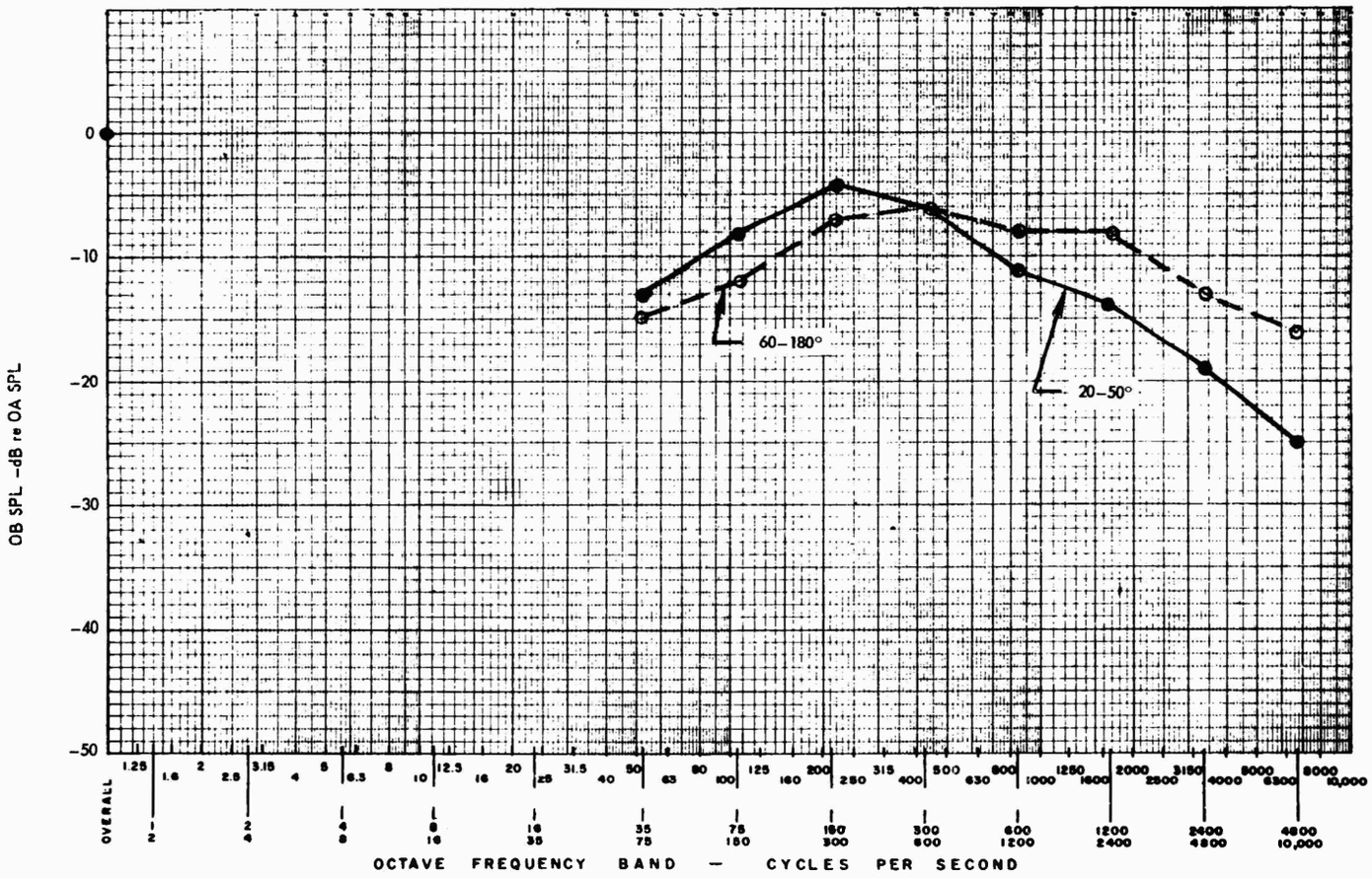

Fig. 5 - Typical acoustic noise spectra for a 1955-vintage turbojet engine (Ref. 9)

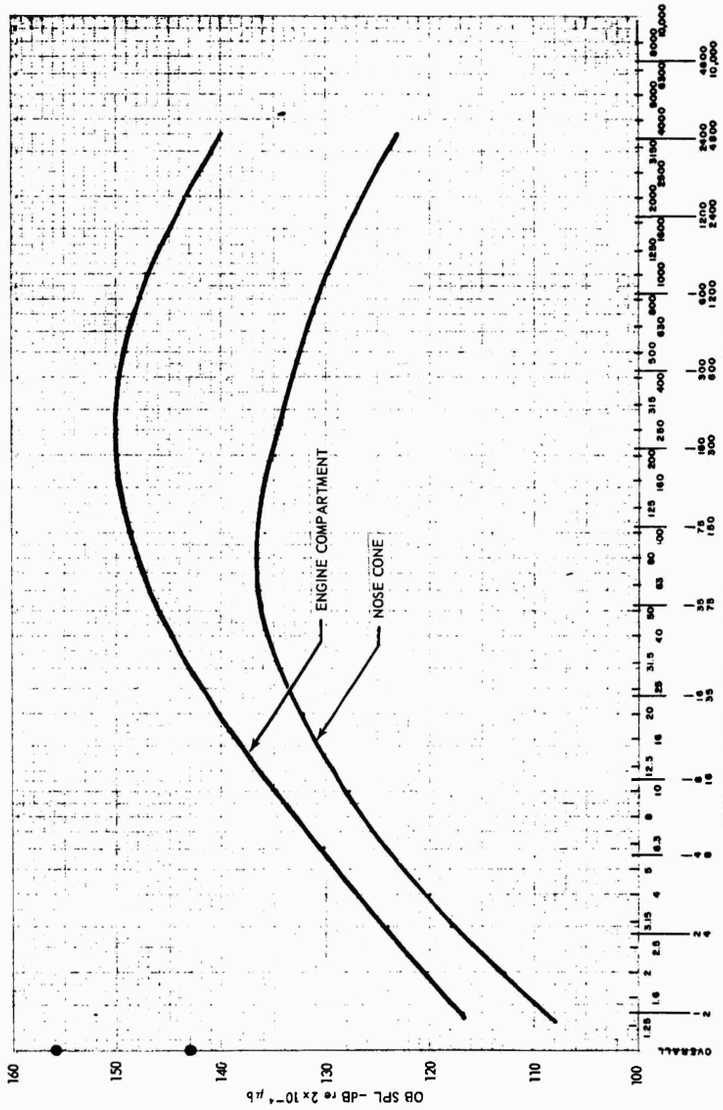

Fig. 6 - Typical acoustic noise spectra for the surface of a large liquid-propelled ballistic missile (Ref. 10)

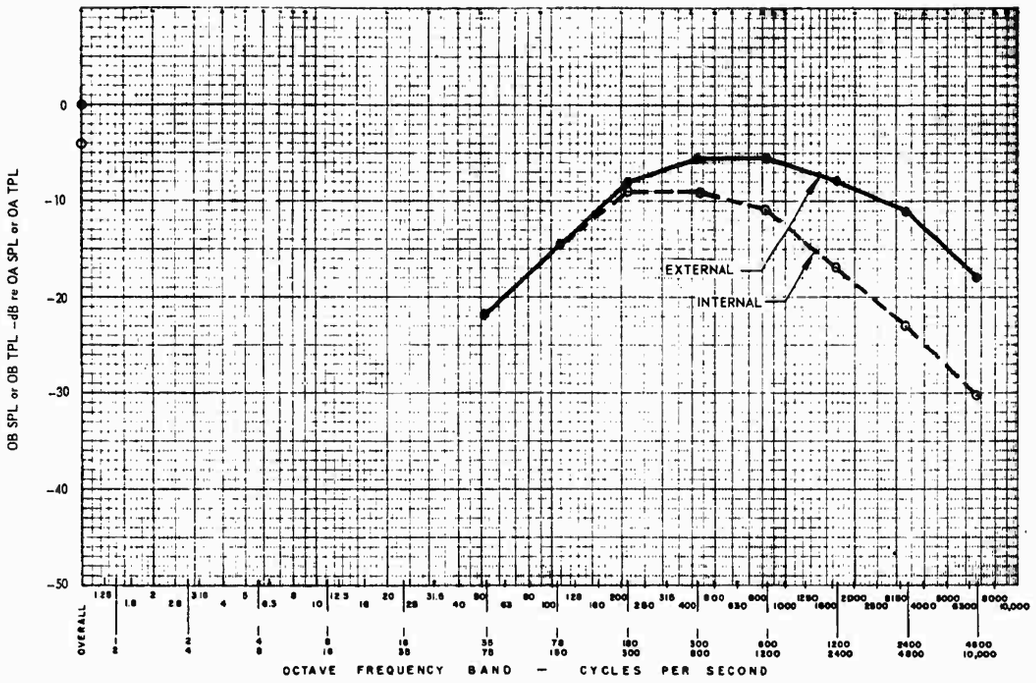

Fig. 7 - Typical acoustic noise or turbulence spectra for use during the preliminary design or proposal phase of a program

Determination of Boundary Layer Pressure Levels from Aerodynamic Turbulence

Boundary layer pressure fluctuations excite vehicle structure in a manner similar to that from acoustic noise fields. Actual field measurements are the best determination of this environment. If these are not available or if a new configuration is to be used, then a prediction is desired. References 5, 6, and 10 may again be used as source material. Based on empirical data from Refs. 5 and 11, a relationship between the rms boundary layer turbulence (p_r) and the free stream dynamic pressure (q_∞) has been found:

$$p_r = K_t q_\infty , \qquad (1)$$

where

$q_\infty = 0.7\, P M_\infty^2$,

P = atmospheric pressure at the altitude of operation, and

M_∞ = free stream Mach number of the vehicle.

Figure 8 shows that the value of K_t may vary over a wide range, depending upon the aerodynamic cleanliness of the vehicle. For vehicles that are relatively clean, a value of $K_t = 5 \times 10^{-3}$ is often utilized, particularly in a preliminary design stage. This value of K_t also coincides with data from turbulence over a flat plate.[5] It is often more convenient to express the turbulence pressure in terms of the overall turbulence pressure level (OA TPL). Using $K_t = 5 \times 10^{-3}$:

$$\text{OA TPL} = 20 \log p_r = 20 \log q_\infty + 82 \text{ db } (\text{re } 2 \times 10^{-4} \mu\text{b}). \qquad (2)$$

Table 2 shows the Mach number required to produce various dynamic pressures at several altitudes. (The corresponding values of OA TPL from Eq. (2) are shown, in parentheses, assuming $K_t = 5 \times 10^{-3}$.)

Once the OA TPL has been determined, the shape of the spectrum can be determined from Fig. 9, where TSL = turbulence spectrum level; c_∞ and c_o = speed of sound at the altitude of operation and at sea level, respectively; ν_∞ and ν_o = free stream kinematic viscosity at the

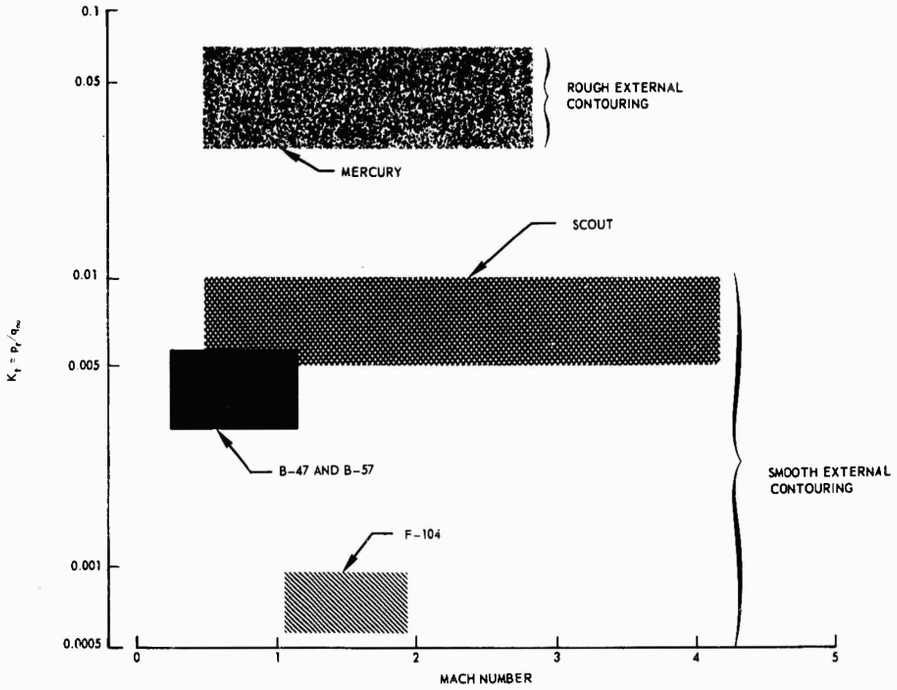

Fig. 8 - Ratio of boundary layer turbulence pressure to free stream dynamic pressure as a function of vehicle Mach number and aerodynamic cleanliness (Ref. 11)

TABLE 2
Mach Number Required to Produce Certain Free Stream Dynamic Pressures at Various Altitudes of a Vehicle (Overall Turbulent Pressure Levels Are Shown in Parenthesis for $K_t = 5 \times 10^{-3}$)

Pressure Altitude (ft)	Speed of Sound (ft/sec)	Kinematic Viscosity (ft^2/sec)	Free Stream Dynamic Pressure (and OA TPL)				
			450 psf (135 db)	800 psf (140 db)	1400 psf (145 db)	2500 psf (150 db)	4500 psf (155 db)
Sea Level	1120	1.57×10^{-4}	0.5	0.7	1.0	1.3	1.7
10,000	1080	2.01	0.7	0.9	1.2	1.6	2.1
20,000	1040	2.62	0.8	1.1	1.4	1.9	2.6
30,000	990	3.49	1.0	1.3	1.8	2.4	3.2
40,000	970	5.06	1.3	1.7	2.3	3.0	
50,000	970	8.16	1.6	2.2	2.9		
60,000	970	13.16	2.1	2.8	3.6		
70,000	970	21.22	2.6	3.5			
80,000	970	34.20	3.3				

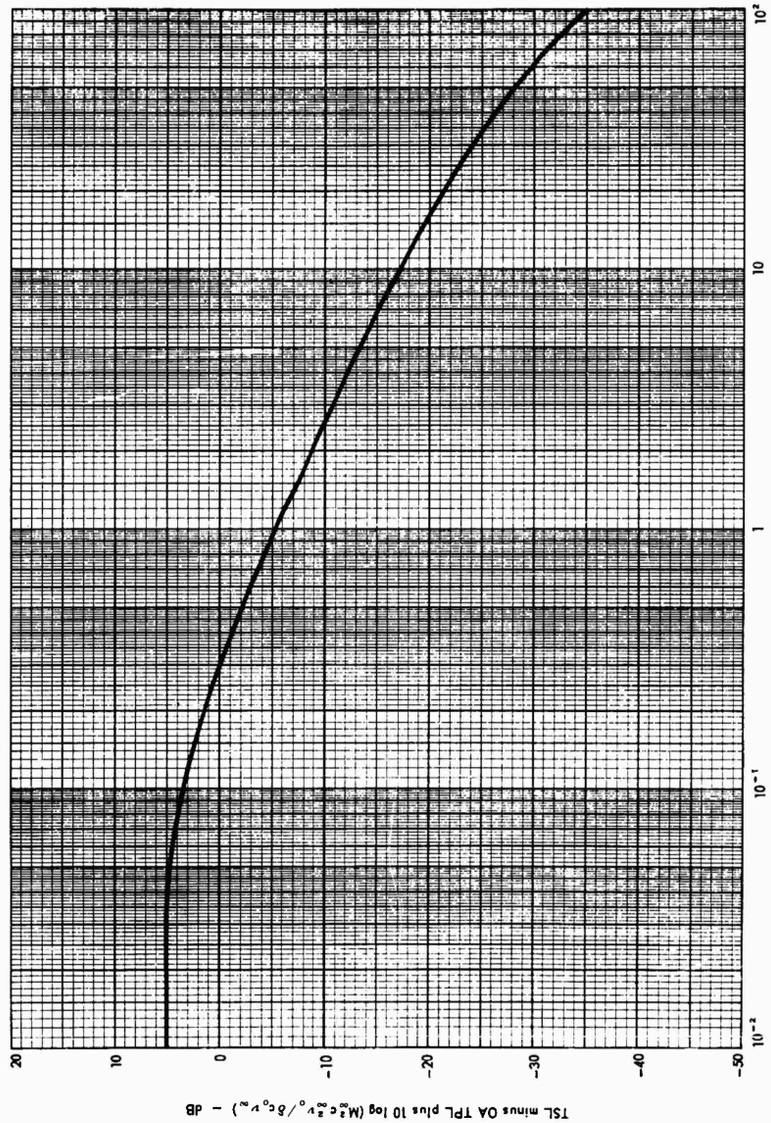

Fig. 9 - Normalized boundary layer pressure spectrum (Ref. 5)

altitude of operation and at sea level, respectively, and δ = boundary layer thickness. Table 2 presents the speed of sound and the kinematic viscosity at several altitudes. The boundary layer thickness may be obtained from

$$\delta = 0.37\, L\, (\nu_\infty c_\infty M_\infty L)^{1/5}. \qquad (3)$$

where L = the distance from the leading edge of the structure initiating the turbulence, and the dimensionless quantity (within the parentheses) is the inverse of the Reynolds number. It should be pointed out that Eq. (3) was obtained for a flat plate only (Refs. 5 and 12) and that other data are available which do not substantiate this equation.

The octave band turbulence pressure level (OB TPL) can be calculated from the turbulence spectrum level by

$$\text{OB TPL} = \text{TSL} + 10 \log \Delta f \qquad (4)$$

where the TSL is established at the geometric mean frequency

$$\left[f_m = (f_\ell f_h)^{1/2}\right]$$

of the octave band of interest, and $\Delta f = f_h - f_\ell$ is the bandwidth.

In certain cases, it is possible to estimate grossly the OA TPL (such as those listed in Table 2), but not the shape of the spectrum. In these cases, it might be advisable to use again the spectrum of Fig. 7 as an interim measure. This should again be advantageous during the proposal stage or the preliminary design stage of a program.

Determination of Wideband Vibration Levels (Nortronics Modification of the Mahaffey-Smith Procedure)

Several years ago, an investigation was carried out to determine a relationship between acoustic noise from turbojet engines and wideband random vibration of the structure on the basis of measured data. This investigation was made by Mahaffey and Smith at Convair-Fort Worth on B-52 and B-58 aircraft under takeoff conditions. The original random vibration data was later modified to relate acoustic noise and sinusoidal vibration (at the insistence of USAF) based upon a questionable conversion of random rms values to sinusoidal peak values. This information, published in Ref. 13, is considered to be of little value in the design and test of complex electronic and electromechanical equipment. If the original relationship of acoustic noise to random vibration is used, however, it is possible to predict wideband random vibration conditions on the basis of known or predicted external noise. Surprisingly, when the Convair-derived relationship was investigated for some other vehicles, the same general relationship was found to be applicable. Since the relationship holds for a variety of structures and noise sources, there is reason to assume it will be valid for many other vehicles.

The relationships between octave band random vibration and external OB SPL, as obtained from the Convair data (see the last paragraph of Ref. 13) are shown in Figs. 10 and 11. The upper 60-percent confidence lines of Ref. 13 envelope nearly all vibration measurements applicable to equipment locations. This is due primarily to the mass loading effects (mechanical impedance) of the equipment on the structure. The use of the 60-percent lines insure a small amount of conservatism for larger equipment. (This, of course, also means that the 60-percent lines are nonconservative estimates for the vibration response of unloaded structures.)

The random vibration levels are expressed in terms of the (mean square) acceleration spectral density averaged over the octave band. Only the frequency range below 2400 cps is considered, because it is assumed that higher frequency excitation produces no degradation to typical equipment.

In a preliminary design or proposal phase of a program, Figs. 10 and 11 can be used in conjunction with the solid curve of Fig. 7 to calculate octave band vibration levels from an external OA SPL or OA TPL. For example, if the OA SPL = 155 db, the OB SPL would be calculated from Fig. 7 for the six octave bands below 2400 cps. Then the predicted octave band vibration levels (average acceleration density) may be determined using Figs. 10 and 11. The resulting values are plotted as the dashed curve in Fig. 12.

Determination of Narrow Band Vibration Levels

Wideband analysis of structural vibration has the characteristic of averaging resonant and anti-resonant behavior within the band. If the analysis is to be used for determining design and test criteria, a correction must be made to account for the ratio of the spectral density for resonant response peaks to the average spectral density over octave bandwidths.

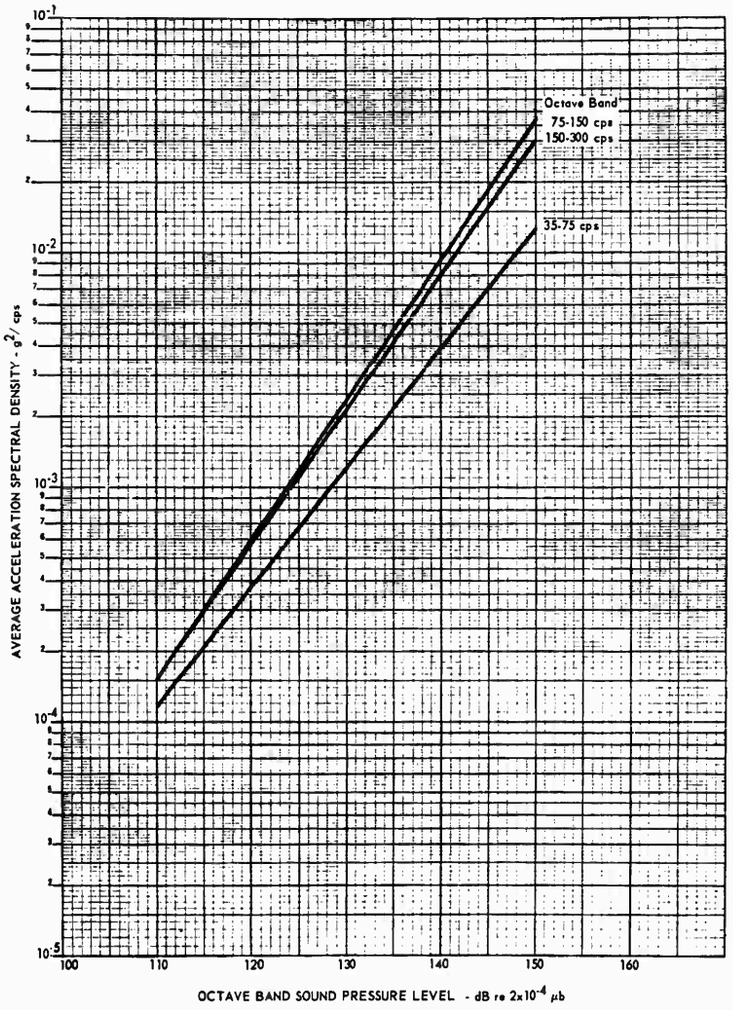

Fig. 10 - Relationship between wideband vibration and acoustic noise (35-300 cps) based on Mahaffey-Smith upper 60-percent confidence lines

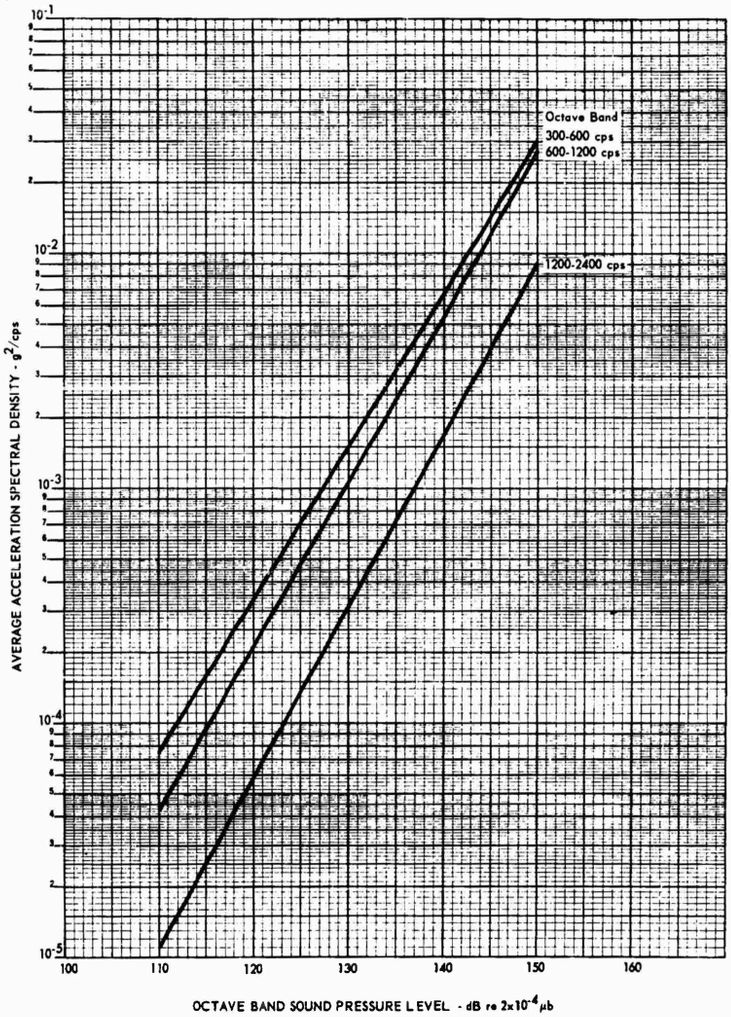

Fig. 11 - Relationship between wideband vibration and acoustic noise (300-2400 cps) based on Mahaffey-Smith upper 60-percent confidence lines

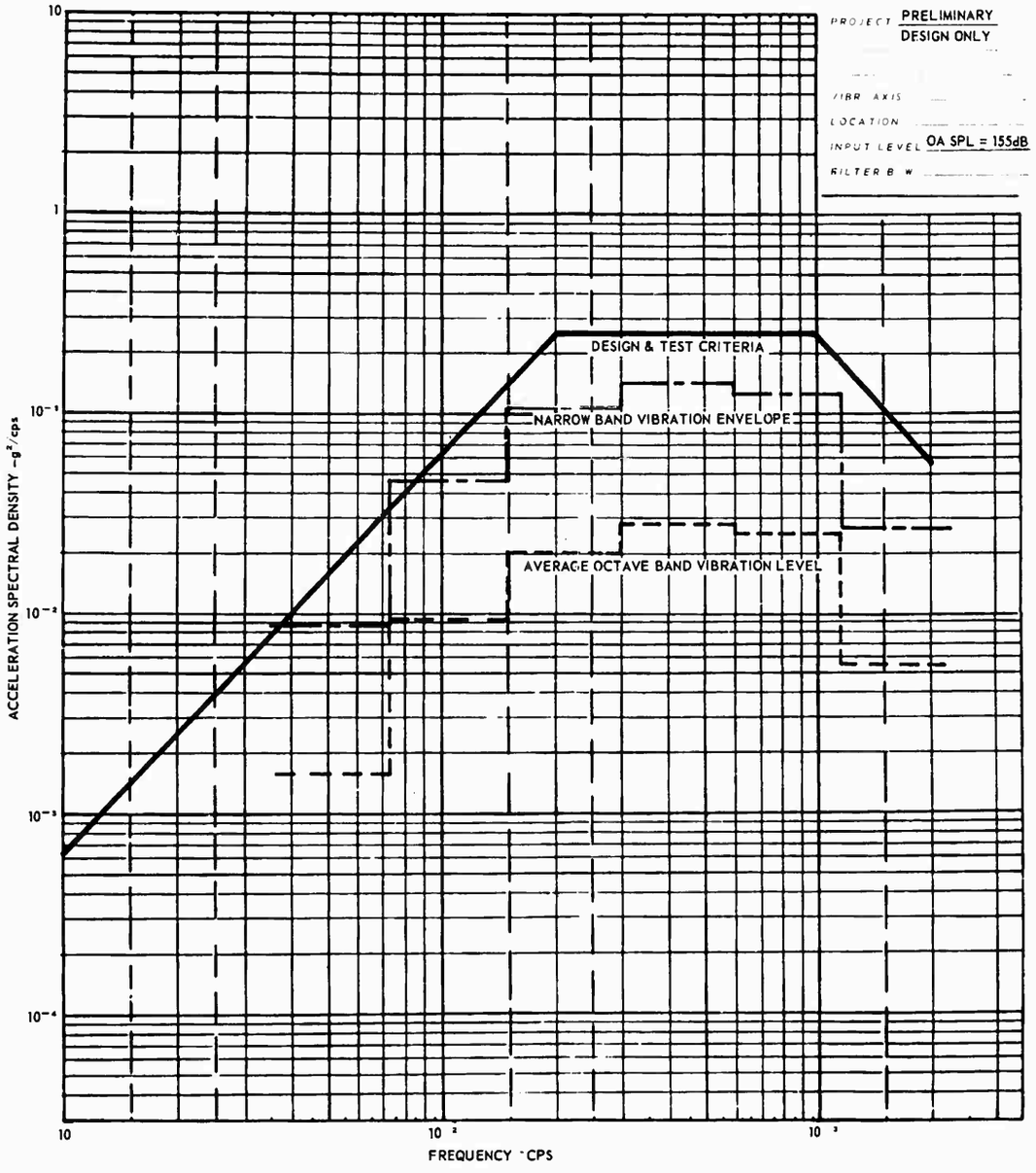

Fig. 12 - Determination of random vibration design and test criteria for OA SPL or OA TPL = 155 db for use during the preliminary design or proposal phase of a program (using Figs. 7, 10, and 11, and a correction factor of 5)

Referring to Ref. 14, a correction factor was established for Titan I applications by comparing a narrow band analysis (using a swept 5-cps bandwidth filter at Martin-Denver) with a wideband analysis (using a stepped 100-cps bandwidth filter at STL) of the same data. The ratio of resonant-to-average acceleration spectral density was approximately 3 in most cases, and always less than 5. A later comparison was made on a different set of Titan data, this time comparing a narrow band analysis (using a swept 6.4-cps bandwidth filter at Nortronics) with a wideband analysis (using a stepped one-third octave bandwidth filter at Bolt, Beranek, and Newman) of the same data. Plots of the one-third octave data (furnished by Bolt, Beranek, and Newman) are shown in Fig. 13, while narrow band data are shown in Figs. 14 and 15. Superimposed on the latter figures is the average acceleration spectral density calculated from the one-third octave rms acceleration, shown as dashed curves. By combining data from three adjacent one-third octaves, the average octave band value was calculated as well. These are shown in Figs. 14 and 15 as solid curves. For these data, the correction factor varied between 1.3 and 2.5 for one-third octave bands (with an average of 2.0) and between 2.3 and 4.7 for octave bands (with an average of 3.2).

On the basis of the above information, a correction factor of 5 was selected for converting octave band vibration levels to narrow band vibration levels. This correction was considered to be acceptably conservative for prediction purposes. Applying this correction to the wideband vibration data for an OA SPL = 155 db, the dashed curve of Fig. 12 is converted to the dot-and-dash curve of the same figure. (Note that the procedure of enveloping spectral peaks is not necessarily the best method for arriving at a test criteria. Mechanical impedance considerations may cause this procedure to be overly conservative.)

Determination of Design and Test Criteria

To determine test criteria, the narrow band vibration levels must be modified to reflect (1) laboratory test procedures and tolerances; (2) limitations of the laboratory test

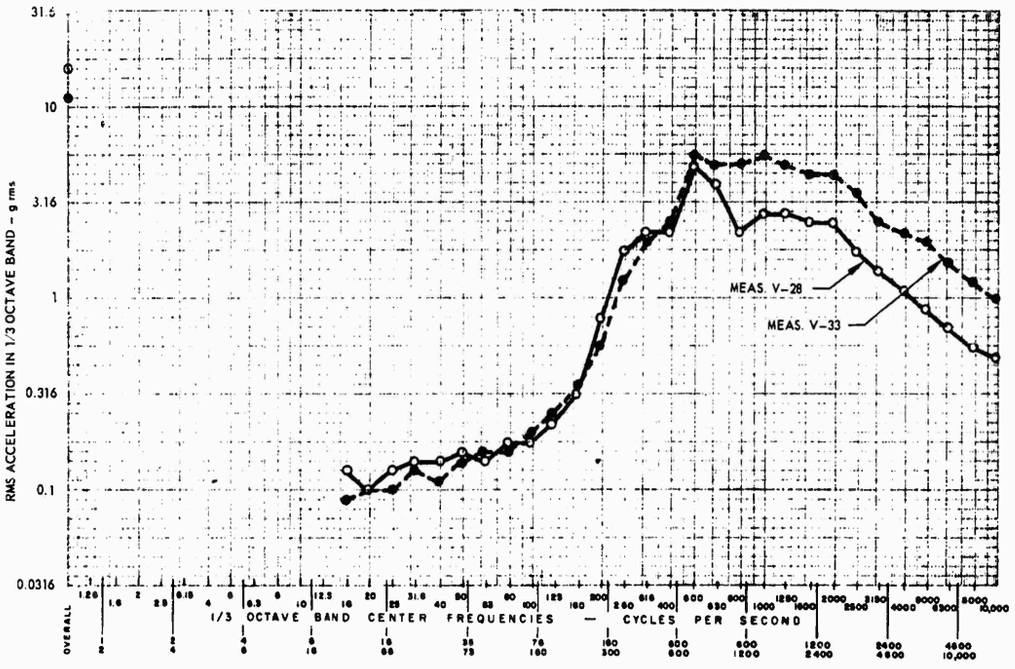

Fig. 13 - Measured one-third octave vibration spectra for Titan I ballistic missile during static firing

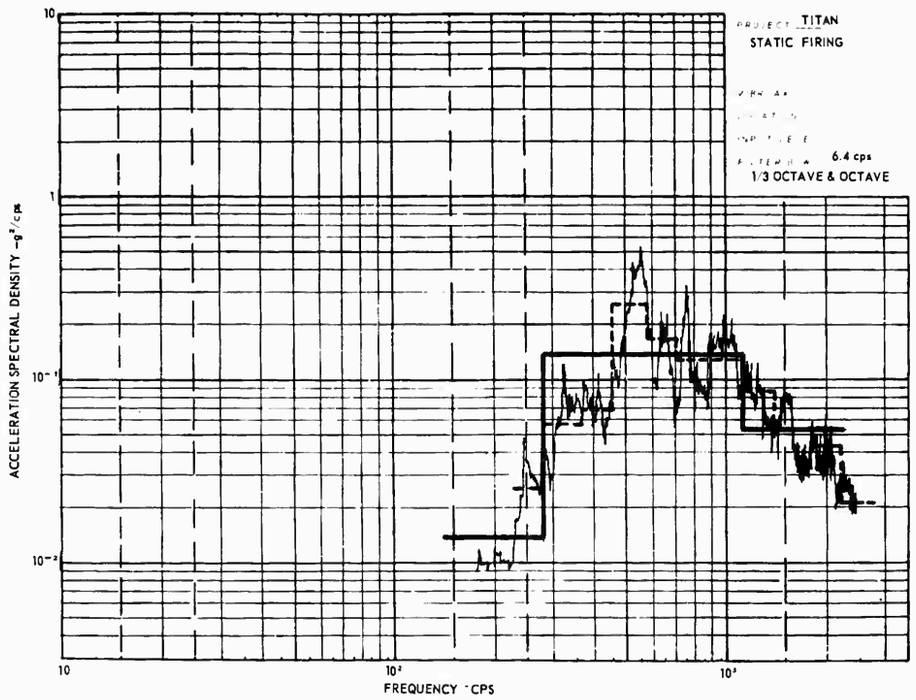

Fig. 14 - Comparison of narrow band, one-third octave and octave band random vibration spectra of same field data

(e.g., testing one direction at a time, not simulating combined environments simultaneously); and (3) the margin of safety desired. Most random vibration tests are performed to ± 3-db tolerances (when analyzed with a filter having an equivalent ideal bandwidth of 10 cps or less). Smaller tolerances usually produce difficulty in controlling the test unless wider bandwidths are used. In addition, a reasonably smooth spectrum is desired for use in monitoring the test. To account for these factors, the design and test criteria are drawn as comfortable envelopes above the narrow band vibration levels.

For example, in the proposal or preliminary design stage, this envelope is shown as the solid line in Fig. 12 for the vibration caused by an external OA SPL = 155 db. Using a similar procedure for the lower values of OA SPL or OA TPL, the family of curves shown in Fig. 16 is derived. By taking the square root of the area under each curve, the rms acceleration associated with each OA SPL or OA TPL is found. This value is listed on Fig. 16 next to the value of OA SPL or OA TPL.

The time duration of the test should be selected on the basis of the operational life of the equipment or structure of interest under conditions of (1) takeoff or lift-off, and (2) high dynamic pressure. Under each condition, if the total time is sufficiently short (say, less than 12 hours), then a real-time test should be employed. On the other hand, if the exposure time under a severe environment is much longer, then the time of test should be selected to reflect the number of vibration cycles applied to the equipment. The test duration need not be longer than that required to produce 5×10^6 cycles at the lowest resonant frequency of importance, since the endurance limit of nearly all materials used in aerospace vehicle equipment and structures will have been realized by this number of cycles. Vibration degradation would not be anticipated after this time duration.[15] For example, if the lowest structural resonant frequency is 120 cps or greater, 5×10^6 cycles can be realized in a 12-hour test.

Certain equipment may have resonant frequencies below 120 cps. This will be so, for

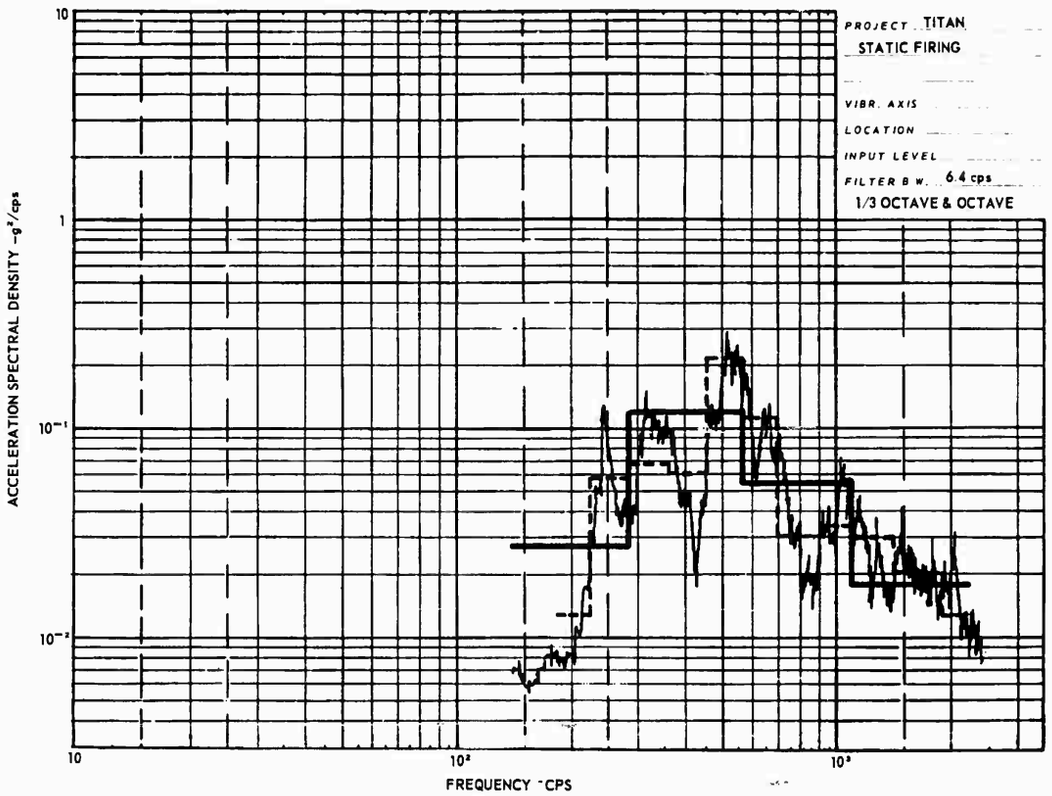

Fig. 15 - Comparison of narrow band, one-third octave and octave band random vibration spectra of same field data

example, if the equipment incorporates resilient mounts. For such cases, components with a low resonant frequency might be tested separately for the time duration required to accumulate 5×10^6 cycles, and thus avoid tying up the entire item of equipment for a long time on a large vibration shaker.

Consideration might also be given to performing a shorter test at higher levels.[15] Obviously, certain assumptions must be made for such a tradeoff, some or all of which may prove to be invalid. For example, equipment malfunction rather than structural fatigue may be of prime importance. This is true of most electronic and electromechanical equipment. When these conditions exist, accelerated testing may have to be ruled out, in spite of the extended times which may be involved.[1] If accelerated testing is considered, the manufacturer of the equipment should be given the option of choosing the longer, lower-level test or the shorter, higher-level one, on the basis of which is most economical on an overall basis (taking the costs of unnecessary redesign into consideration, as well as testing).

OTHER PREDICTION PROCEDURES

Other procedures are available for converting wideband (octave or one-third octave) acoustic noise to wideband vibration. The Franken procedure[16] and the Winter procedure[17] each relate the radial vibration of missile skin to external acoustic noise. Thus, they are not expected to predict vibration at equipment locations with reasonable accuracy. In fact, much higher vibration levels can be expected at the missile skin. The Franken procedure employs a frequency shift of the vibration spectrum inversely with the diameter of the missile, whereas the Winter prediction does not utilize the spectrum shift. As applied to the

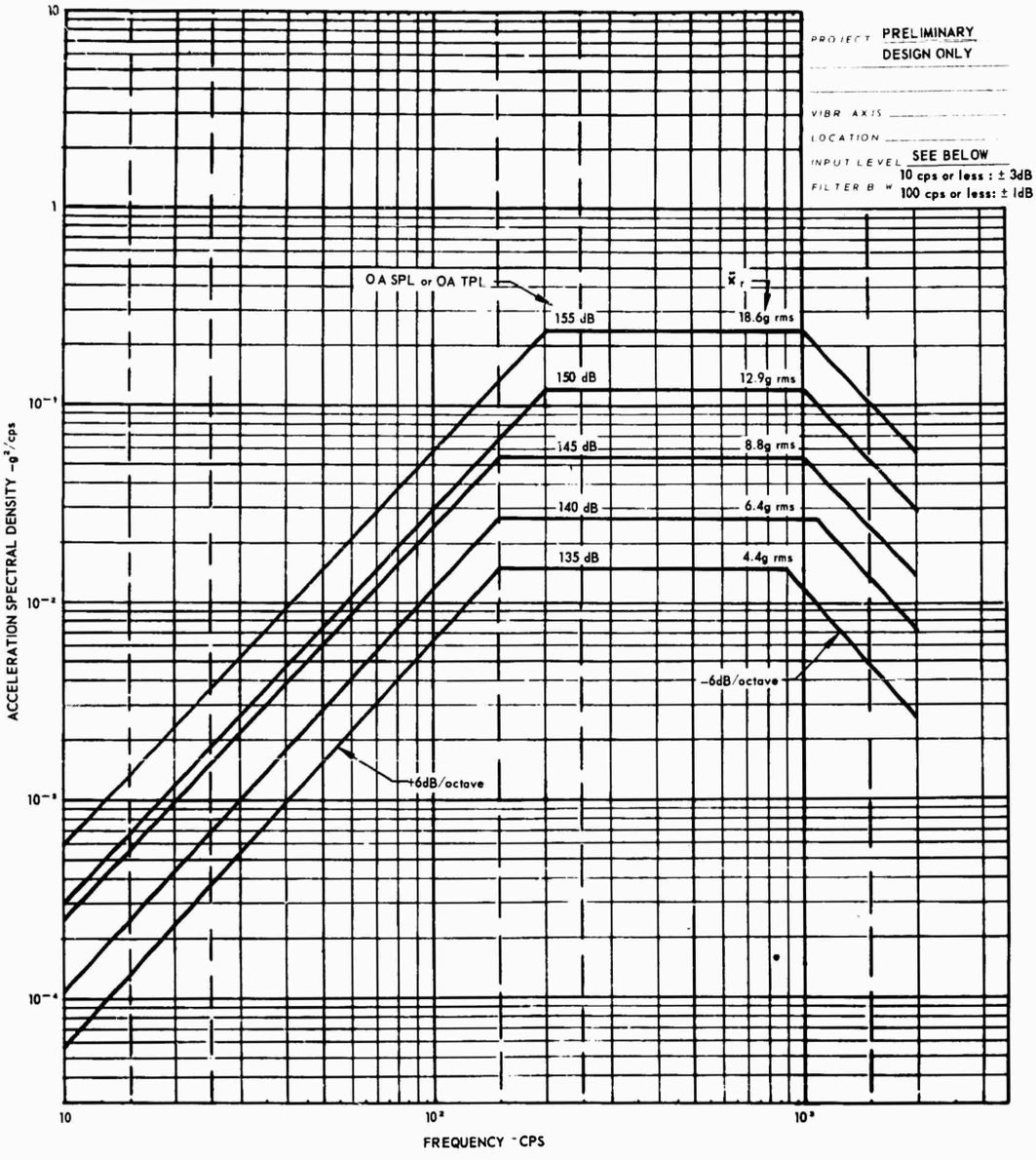

Fig. 16 - Random vibration design and test criteria for various OA SPL or OA TPL for use during the preliminary design or proposal phase of a program

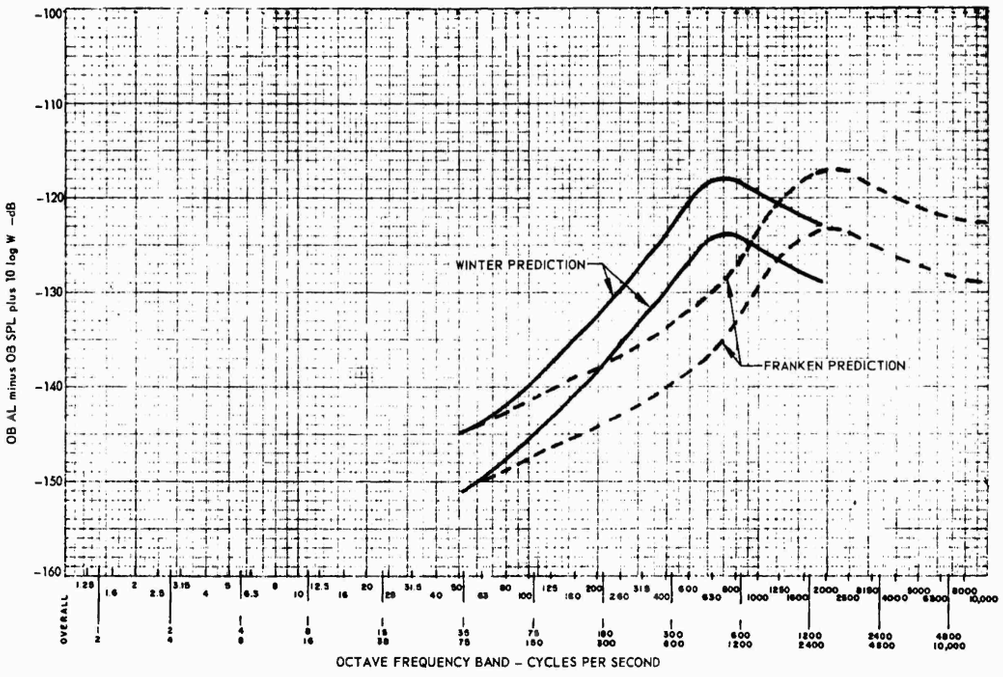

Fig. 17 - Predicted wideband structural response of missile skin to acoustic noise (Refs. 16 and 17)

Skybolt missile, with a diameter of 3 feet. Fig. 17 shows the Winter prediction as a region contained between two solid curves and the Franken prediction between two dashed curves. The ordinate contains a log term of the surface density (W), which for Skybolt was $W = (\rho g)(t) = (0.095\ \text{lb/in.}^3)(0.080\ \text{in.})(144\ \text{in.}^2/\text{ft}^2) = 1.10$ psf, or $20 \log W \approx 1$ db (re 1 psf). Thus octave band acceleration levels (OB AL) can be calculated from Fig. 17 for predicted or measured external OB SPL or OB TPL. The octave band average acceleration spectral density $[G(\Delta f)]$ can then be calculated from

$$G(\Delta f) = \Delta \ddot{x}_r^2 / \Delta f , \qquad (5)$$

where the mean square acceleration $(\Delta \ddot{x}_r^2)$ in the octave band can be obtained from

$$\text{OB AL} = 10 \log \Delta \ddot{x}_r^2 \ (\text{db re } 1\ g^2) . \qquad (6)$$

An octave band-to-narrow band correction factor of 5 can again be selected for enveloping the peaks of the spectrum.

Another prediction procedure has just been reported by Curtis,[18] relating the random vibration of equipment in several aircraft with the dynamic pressure of the vehicle during flight. Acoustic noise from engines during takeoff was not considered. For a typical aircraft with $q_\infty = 2130$ psf, Curtis finds that the broadband spectrum approaches (on the average) a constant $6 \times 10^{-3}\ g^2/\text{cps}$ in the frequency range from 10 to 2650 cps, and that 88 percent of the narrow band peaks (assuming a Rayleigh distribution) tends to reach a constant $3 \times 10^{-2}\ g^2/\text{cps}$. Using this value as enveloping the spectral peaks, the predicted narrow band acceleration spectral density $[G(f)]$ for any vehicle is

$$G(f) = 3 \times 10^{-2} \left[\frac{q_\infty}{2130\ \text{psf}} \right]^2 (g^2/\text{cps}) . \qquad (7)$$

Obviously, the Curtis procedure has the advantage of not requiring the prediction or measurement of OB TPL.

APPLICATION OF THE VARIOUS PREDICTION PROCEDURES TO SKYBOLT GUIDANCE EQUIPMENT

In all the above procedures (except the Curtis procedure), it is necessary to first establish the OB SPL or OB TPL. Early in the Skybolt program, acoustic measurements were made adjacent to the surface of a dummy Skybolt missile (at Boeing-Wichita) during simulated dry and wet takeoffs. Thus acoustical predictions for these conditions were not needed. Since later Skybolt vibration measurements were made only during dry takeoff, only dry takeoff acoustic noise need be considered for the comparison of vibration prediction with measurement. The measured acoustic spectrum at the guidance bay is shown in Fig. 18 (as the solid curve).

The external aerodynamic turbulence during the postlaunch flight of the missile was predicted using the procedure which incorporated Eqs. (2) - (4) and the spectrum of Fig. 9. Since Skybolt flight measurements (described later) showed that the vibration was actually higher before the maximum value of the free stream dynamic pressure was reached, the prediction will use the conditions of the missile at the time of highest vibration rather than at the time of q_{max}. During Skybolt flight tests, highest vibration occurred at a Mach number $M_\infty = 2.5$ and a pressure altitude of 45,000 ft. Using the ARDC model atmosphere[19]: $q_\infty = 1400$ psf, $c_\infty = 970$ ft/sec, and $\nu_\infty = 6.43 \times 10^{-4}$ ft^2/sec. Substituting q_∞ into Eq. (2), OA TPL = 145 db.

To utilize Fig. 9, the boundary layer thickness must be determined from Eq. (3). The value of L (the distance from the leading edge initiating the turbulence to the location of interest), however, must be selected. Now, from observing Fig. 2, two values of L seem logical: (1) the distance from the nose of the missile to the center of the guidance bay, i.e., L = 140 in.; and (2) the distance from the intersection of the conical and cylindrical sections to the center of the guidance bay, i.e., L = 20 in. The correct choice would be dependent upon the effects of the conical wedge on the aerodynamic flow. Selecting L = 140 in. assumes no suppression of the turbulent flow, while selecting L = 20 in. assumes complete suppression (i.e., laminar flow) until the cone-cylinder intersection. To avoid guessing which supposition is correct, both values of L will be used for predicting the

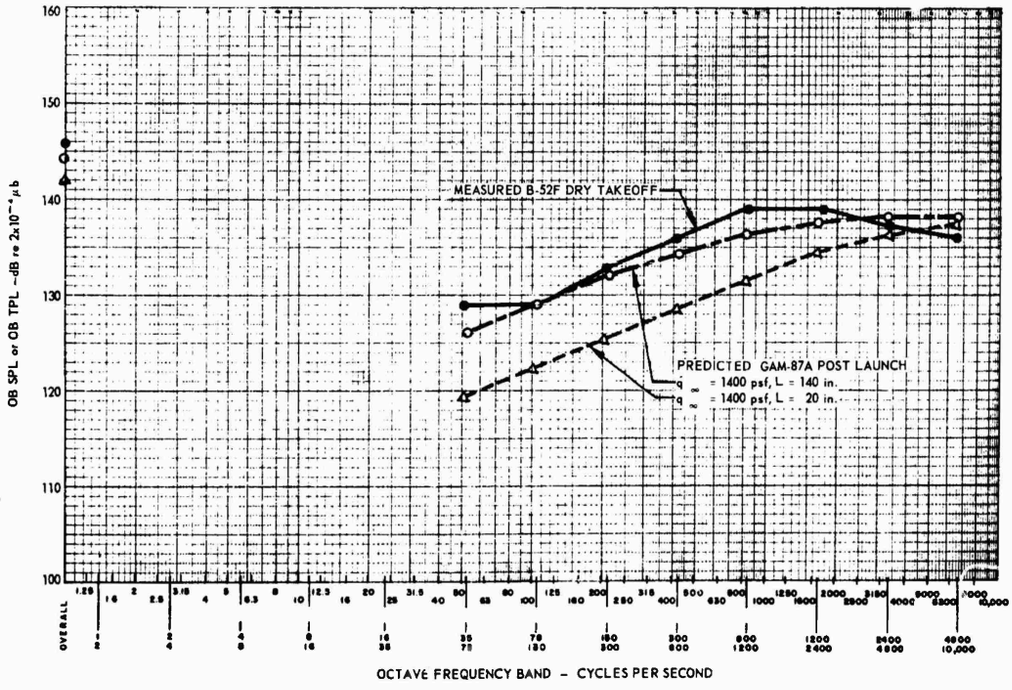

Fig. 18 - External turbojet noise and boundary layer pressure spectra for Skybolt missile

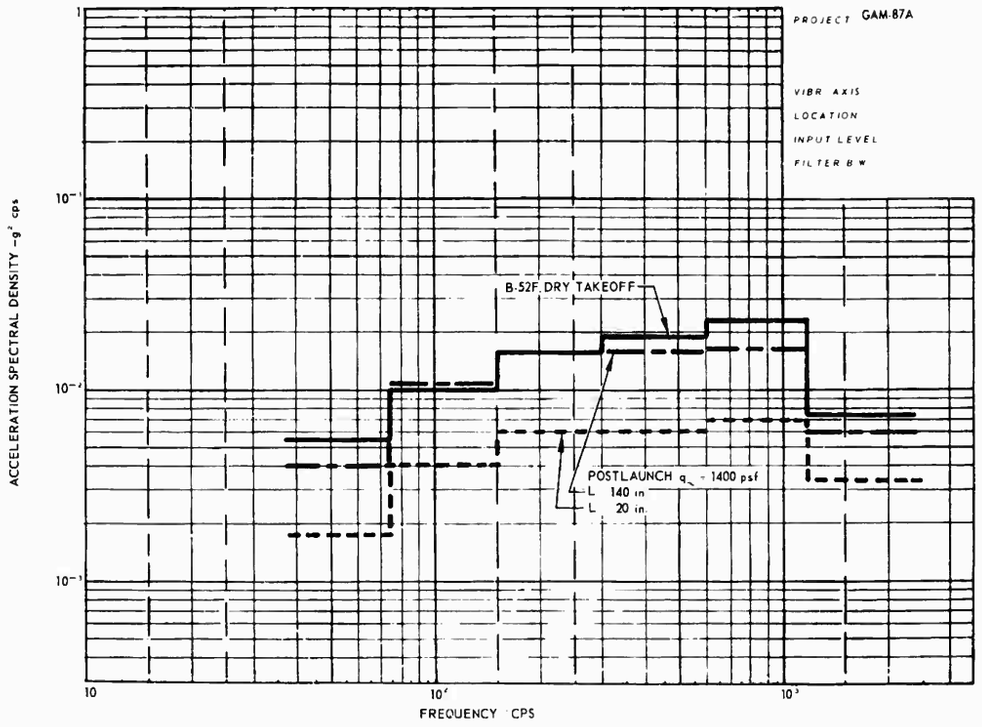

Fig. 19 - Predicted narrow band random vibration spectra using Nortronics modification of Mahaffey-Smith procedure

boundary layer spectrum. The two predicted spectra shown in Fig. 18 as the dashed and the dash-and-dot curves are derived by making the necessary substitutions into Eq. (3) and Fig. 9 to find the TSL (as a function of frequency), and then calculating the OB TPL from Eq. (4). With the three curves of Fig. 18, it is possible to predict vibration levels using three of the four available procedures. Each procedure will be covered separately.

Nortronics Procedure

The average acceleration spectral density $[G(\Delta f)]$ in each octave band is obtained from Figs. 10 and 11, by using values of OB SPL or OB TPL from Fig. 18. The vibration envelopes of Fig. 19 are obtained for the Nortronics procedure by applying the octave band-to-narrow band correction factor of 5.

Franken Procedure

The average acceleration spectral density in each octave band is obtained from the two dashed curves of Fig. 17, and then applying Eqs. (6) and (5). As mentioned previously, a value of 20 log W = 1 db should be used for Skybolt. Values of OB SPL or OB TPL are again selected from Fig. 18. Using a correction factor of 5, the vibration envelopes of Figs. 20 and 21 are obtained for the Franken procedure.

Winter Procedure

The vibration envelopes of Figs. 22 and 23 are obtained for the Winter procedure by using the two solid curves of Fig. 17.

Curtis Procedure

As stated previously, the Curtis procedure is used only for aerodynamic turbulence. The random vibration is predicted solely on the basis of the dynamic pressure. Substituting q_∞ = 1400 psf into Eq. (7), a white vibration envelope of 1.3×10^{-2} g^2/cps is obtained for the Curtis procedure.

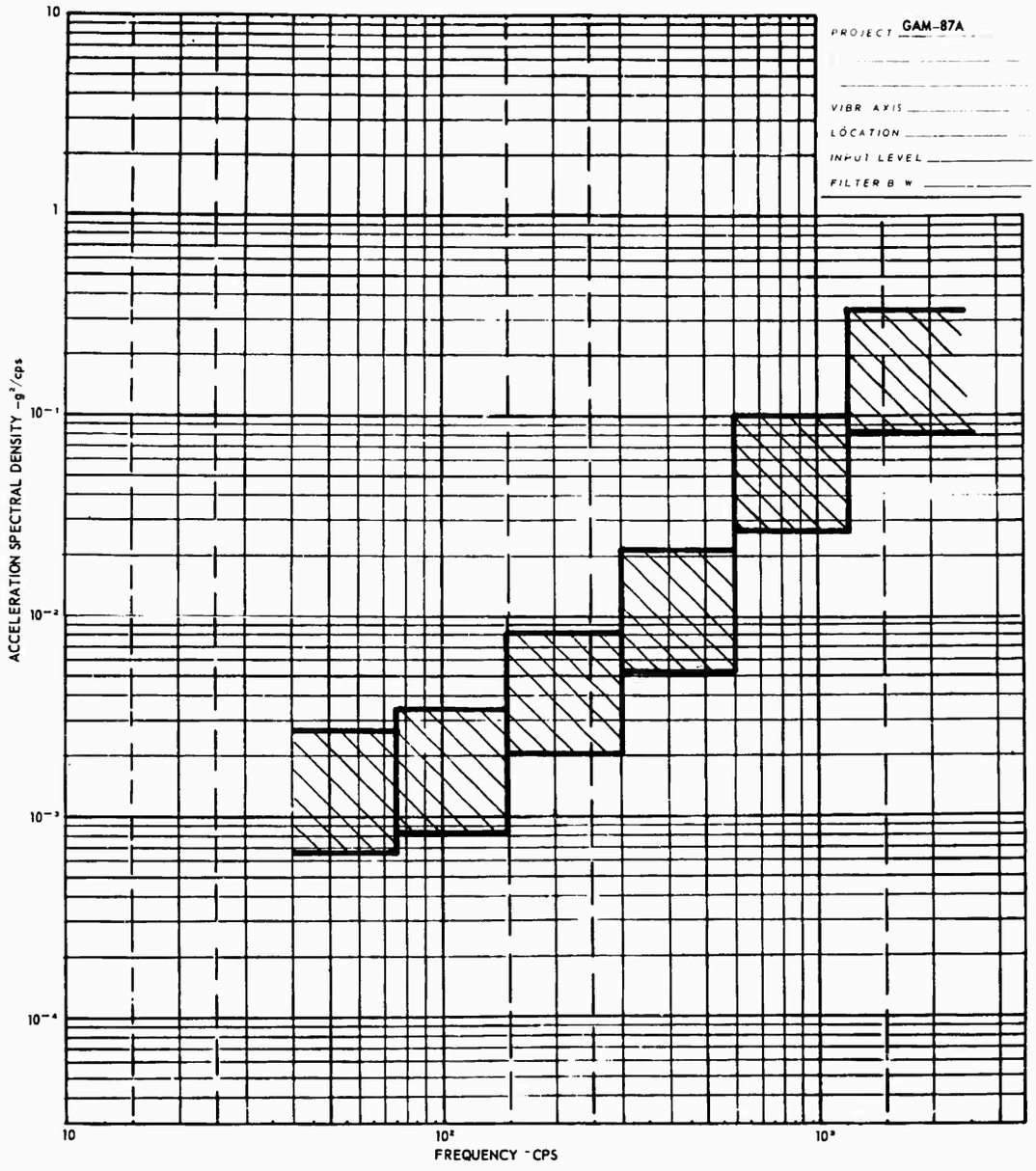

Fig. 20 - Predicted narrow band random vibration spectrum for B-52F dry takeoff using Franken procedure

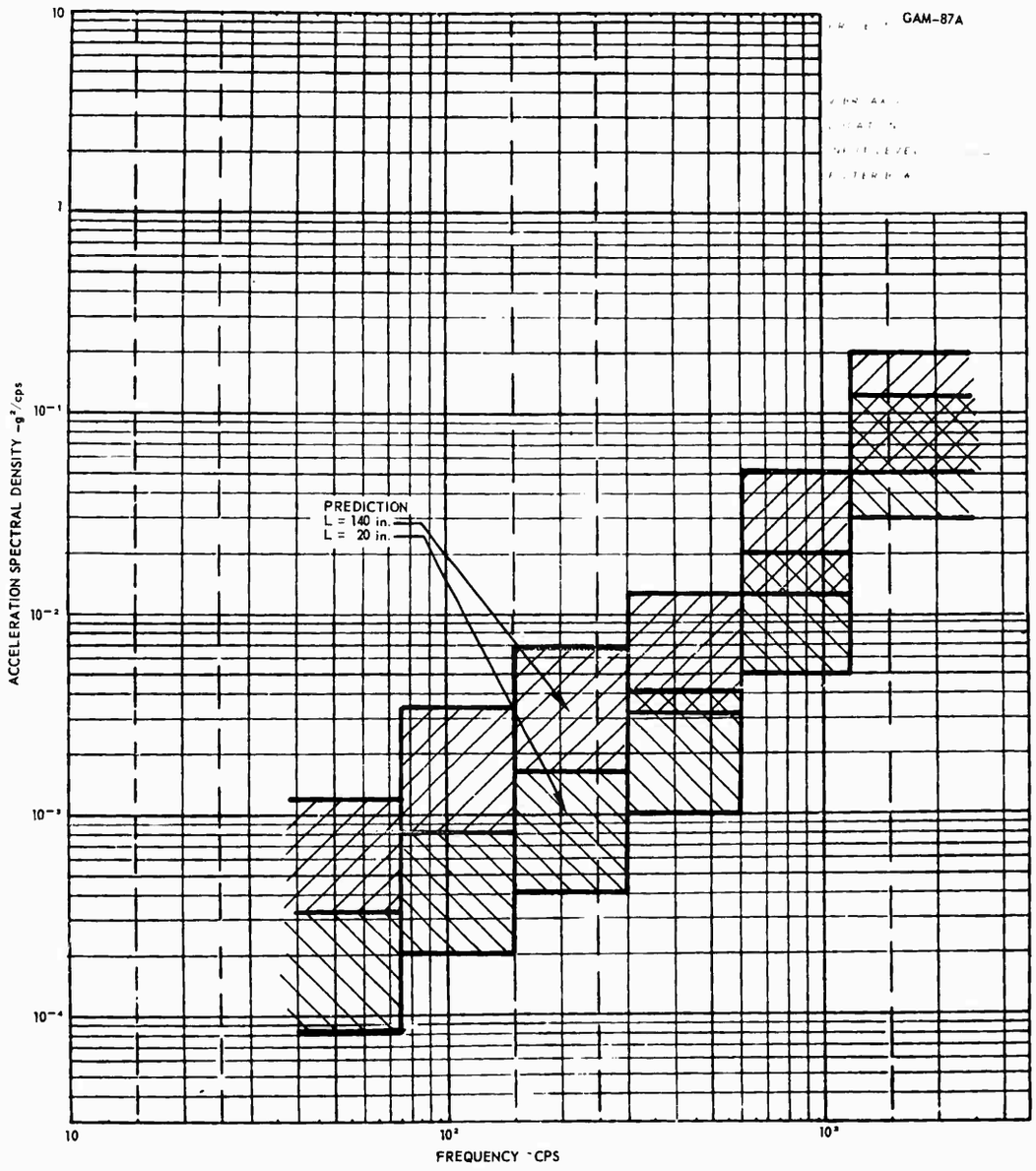

Fig. 21 - Predicted narrow band random vibration spectra for GAM-87A postlaunch (q_∞ = 1400 psf) using Franken procedure

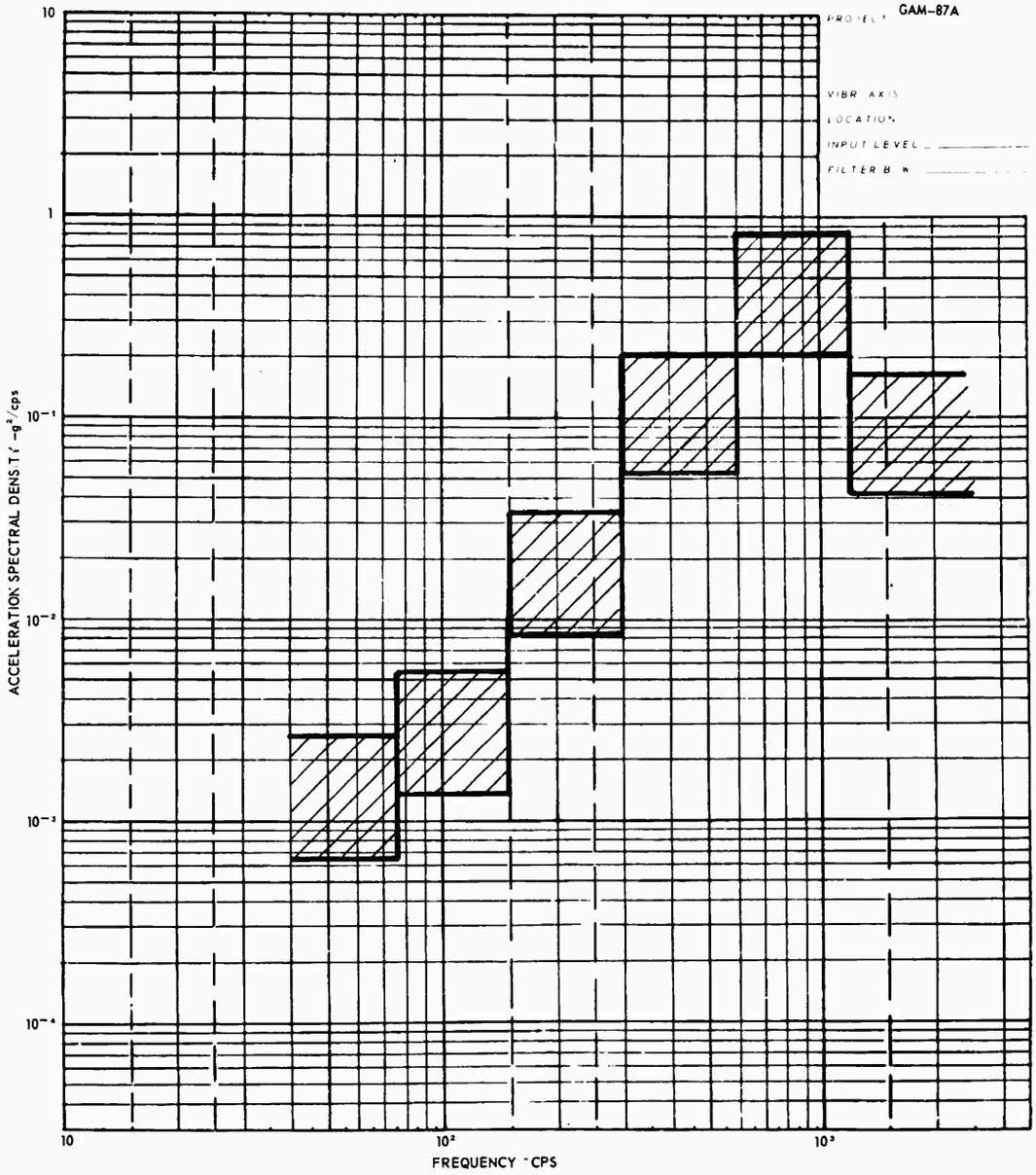

Fig. 22 - Predicted narrow band random vibration spectrum for B-52F dry takeoff using Winter procedure

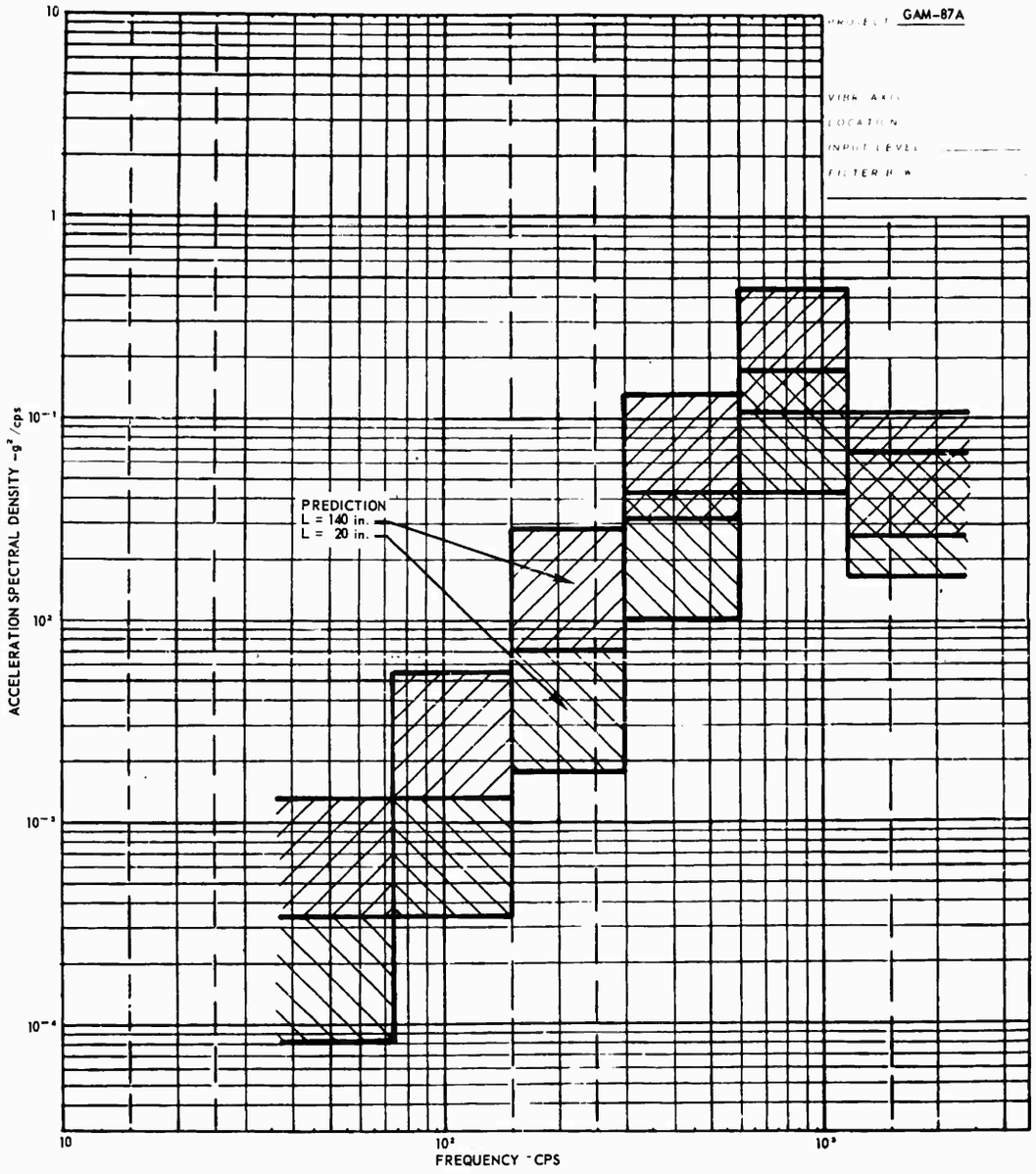

Fig. 23 - Predicted narrow band random vibration spectra for GAM-87A postlaunch (q_∞ = 1400 psf) using Winter procedure

SKYBOLT VIBRATION MEASUREMENTS

Vibration measurements were made at various times during GAM-87A flight tests. Three dry takeoffs and two missile flights were made with the Nortronics guidance equipment installed.[20,21] A failure developed on one of the flights, negating the use of that vibration data to a large extent. Most of the data were taken by accelerometers mounted on an aluminum block which was attached to secondary structure of the missile, as shown in Fig. 24. This structure held the combined Ballistic Computer-Platform Electronics (BC-PE) package through two of the four resilient mounts. In addition, some data were taken elsewhere in the guidance bay with interim equipment (not guidance equipment) installed.[22]

Data reduction was performed in several forms. Instantaneous acceleration vs time histories were recorded on an oscillograph. The rms acceleration vs time histories were recorded on a graphic level recorder, as shown in Fig. 25, for dry takeoff and low altitude climb and in Fig. 26 for high altitude cruise and postlaunch events. (The left side of each figure is devoted to instrumentation calibrations and the determination of the electrical noise floor of the analysis facility. All pertinent events and "bad data" (BD) intervals are clearly labeled.)

Narrow band frequency analysis was performed during the following events: B-52F takeoff, low altitude climb and high altitude cruise, GAM-87A free fall, pitch-up (after first stage ignition), high vibration preceding q_{max} (actually q_∞ = 1400 psf), second stage flight, and other intervals. These frequency analysis intervals are labeled FA in Figs. 25 and 26. The spectra are summarized in Figs. 27 - 32, each figure showing different events for the same missile number, location, and direction. Takeoff data for all flights are summarized separately in Figs. 33 - 35 for the three orthogonal directions. Postlaunch data for q_∞ = 1400 psf are summarized in Fig. 36. Figures 33 - 36 will be used for comparing the various predictions with measured vibration. In Figs. 27 - 36, spectra are seldom presented for frequencies less than 400 cps. The electrical noise floor usually equalled or exceeded the vibration

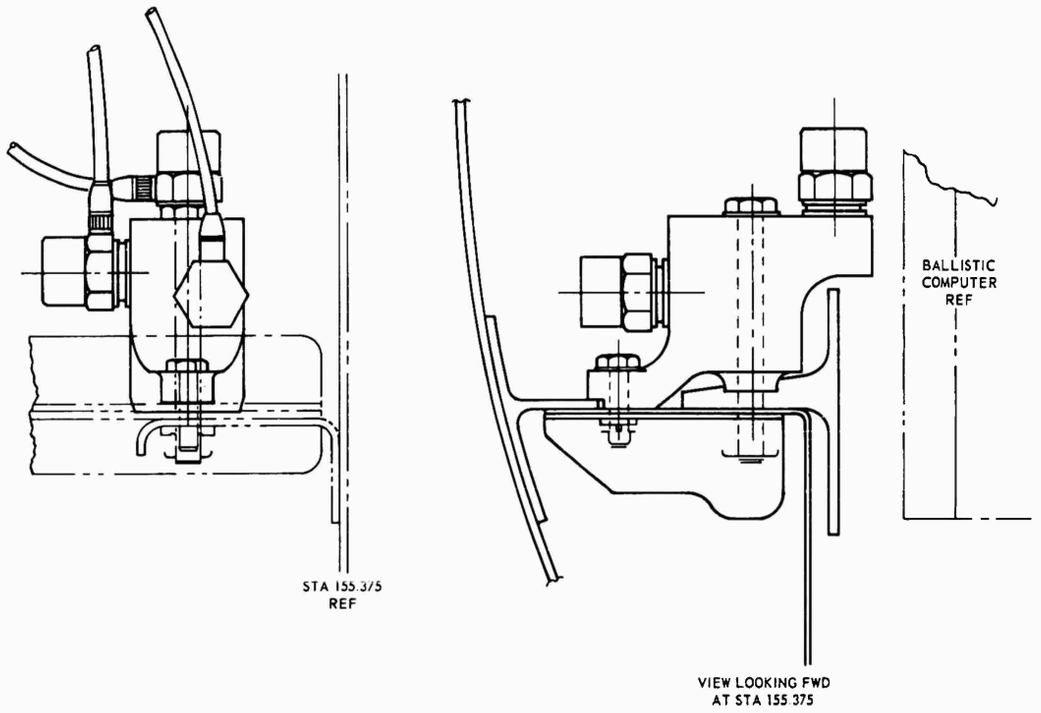

Fig. 24 - Accelerometer mounting location near BC-PE package

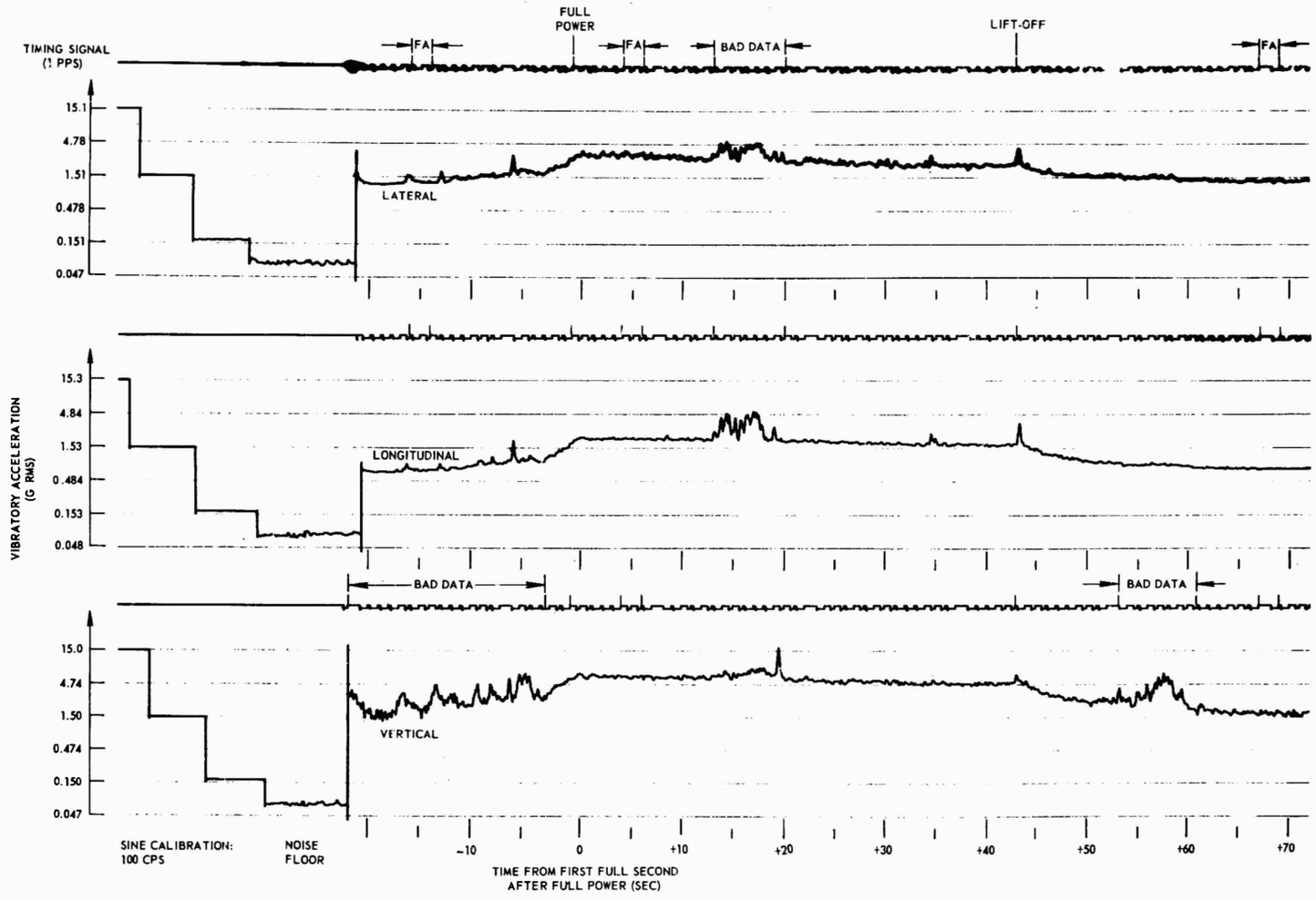

Fig. 25 - BC-PE during TM-108A takeoff

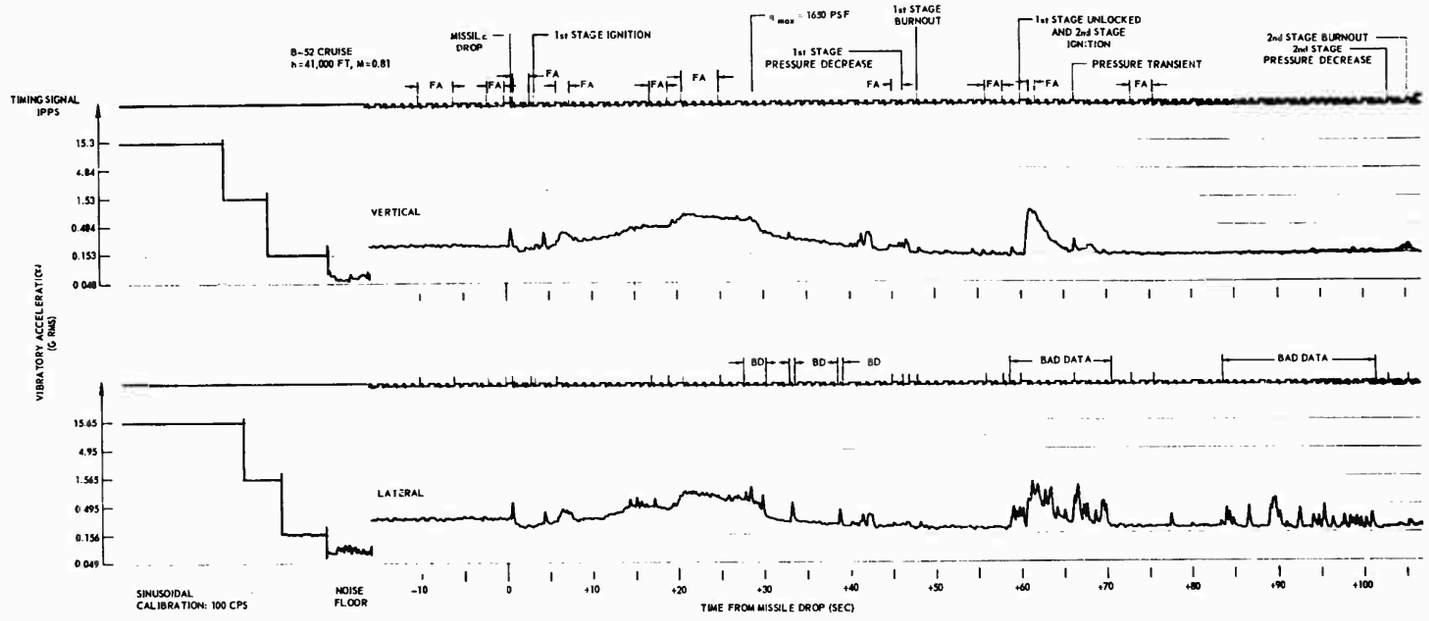

Fig. 26 - BC-PE during guided launch G-2

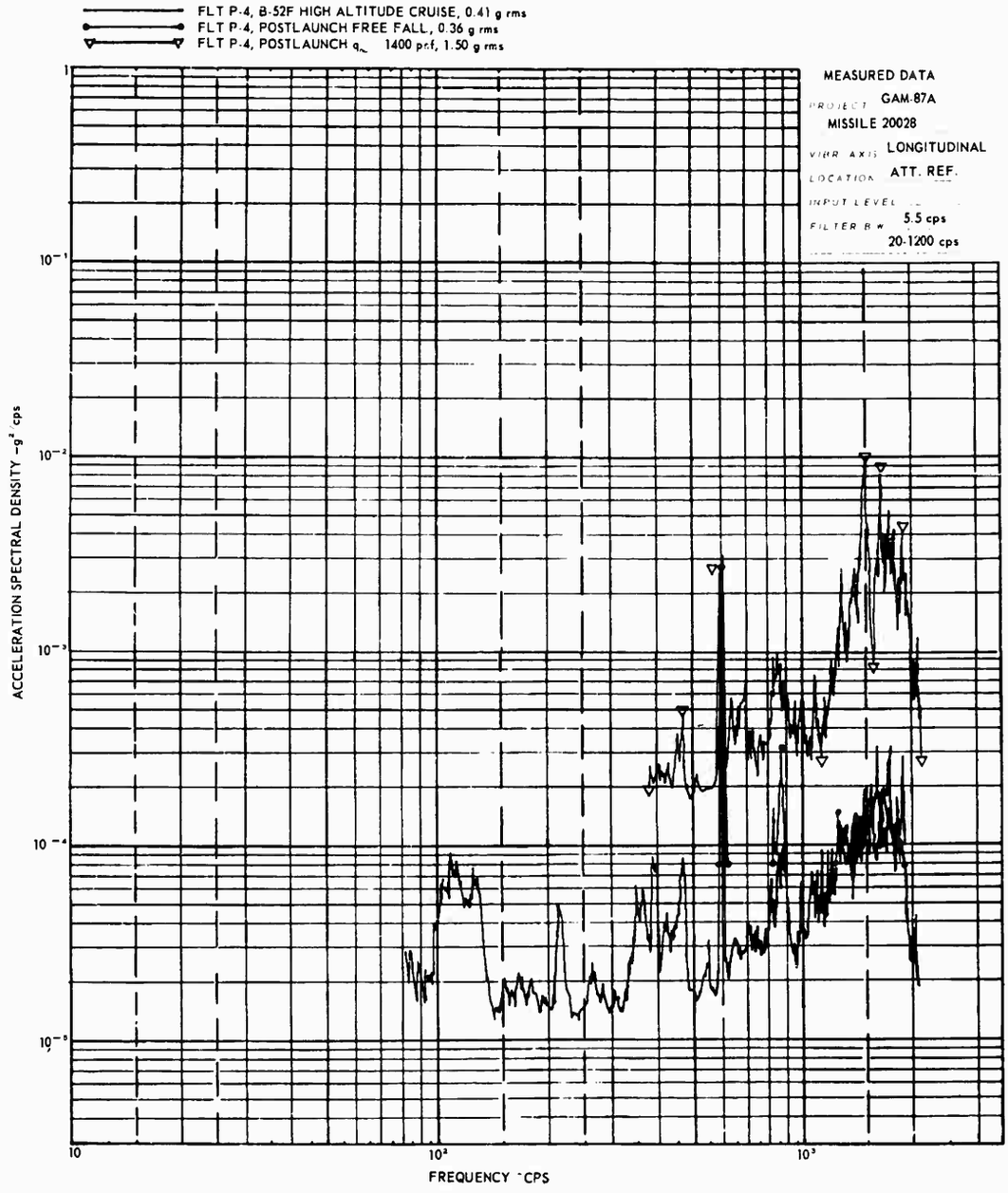

Fig. 27 - Measured narrow band random vibration spectra for attitude reference during programmed launch P-4

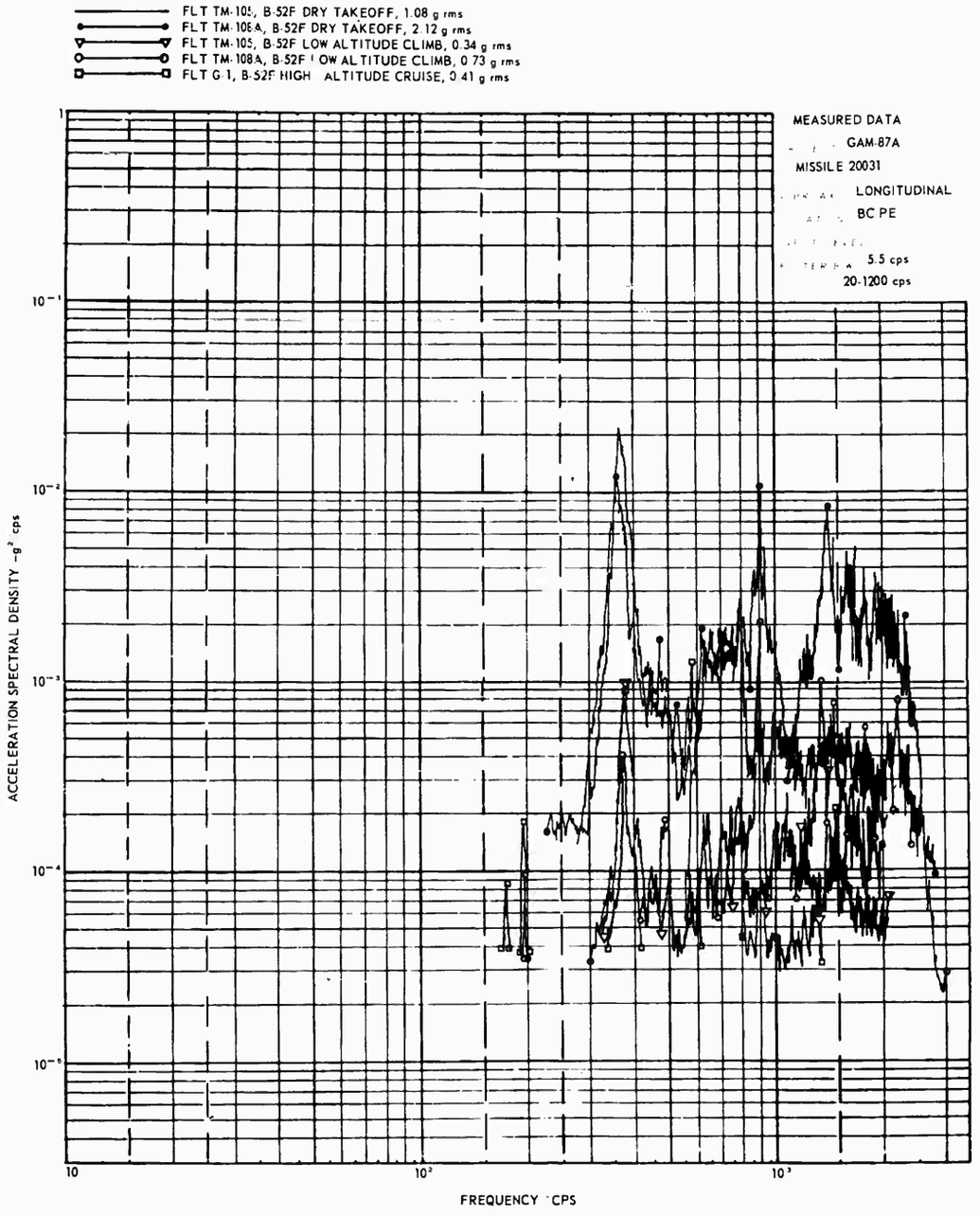

Fig. 28 - Measured narrow band random longitudinal vibration spectra for BC-PE during TM-105 and TM-108A takeoff and flight

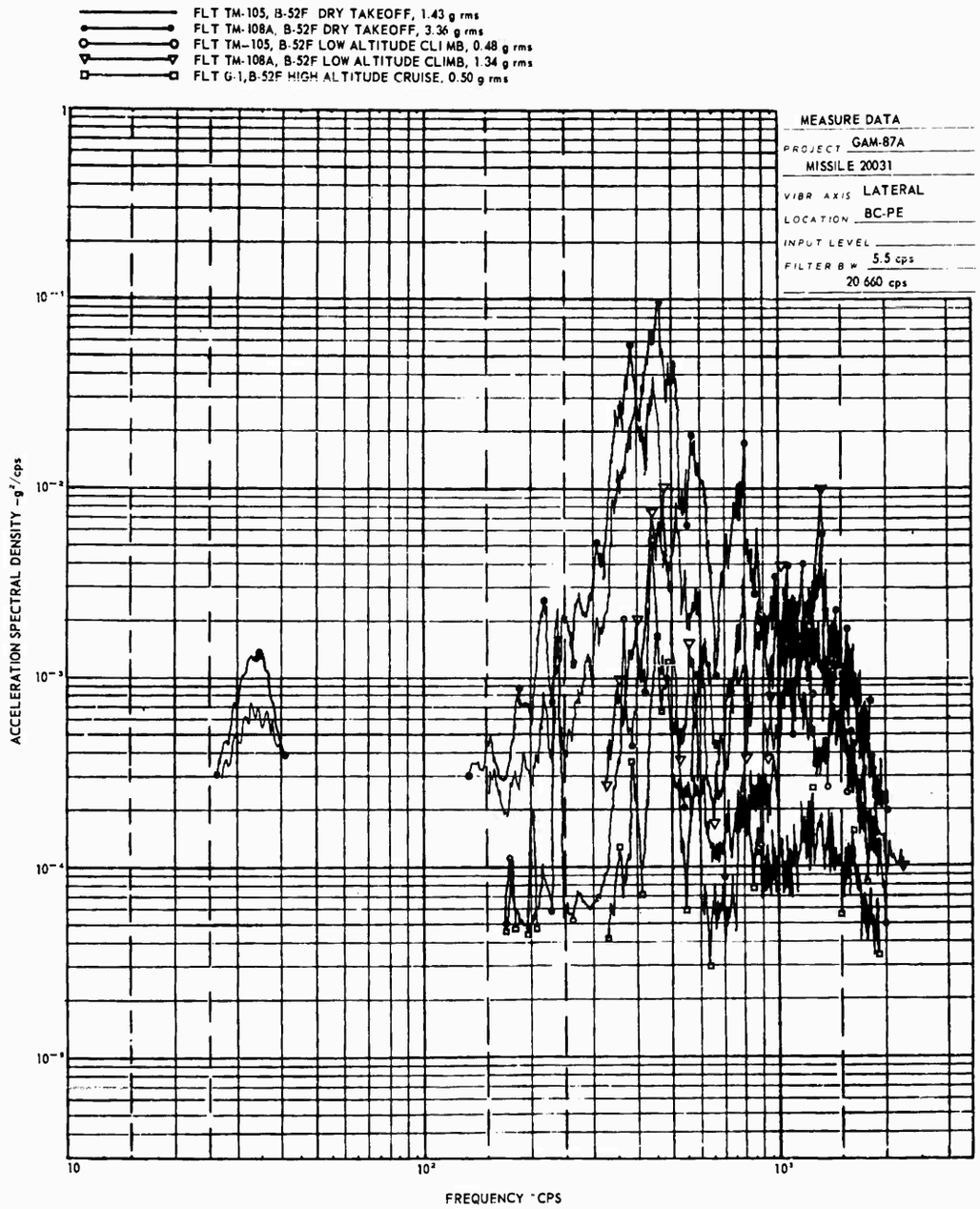

Fig. 29 - Measured narrow band random lateral vibration spectra for BC-PE during TM-105 and TM-108A takeoff and flight

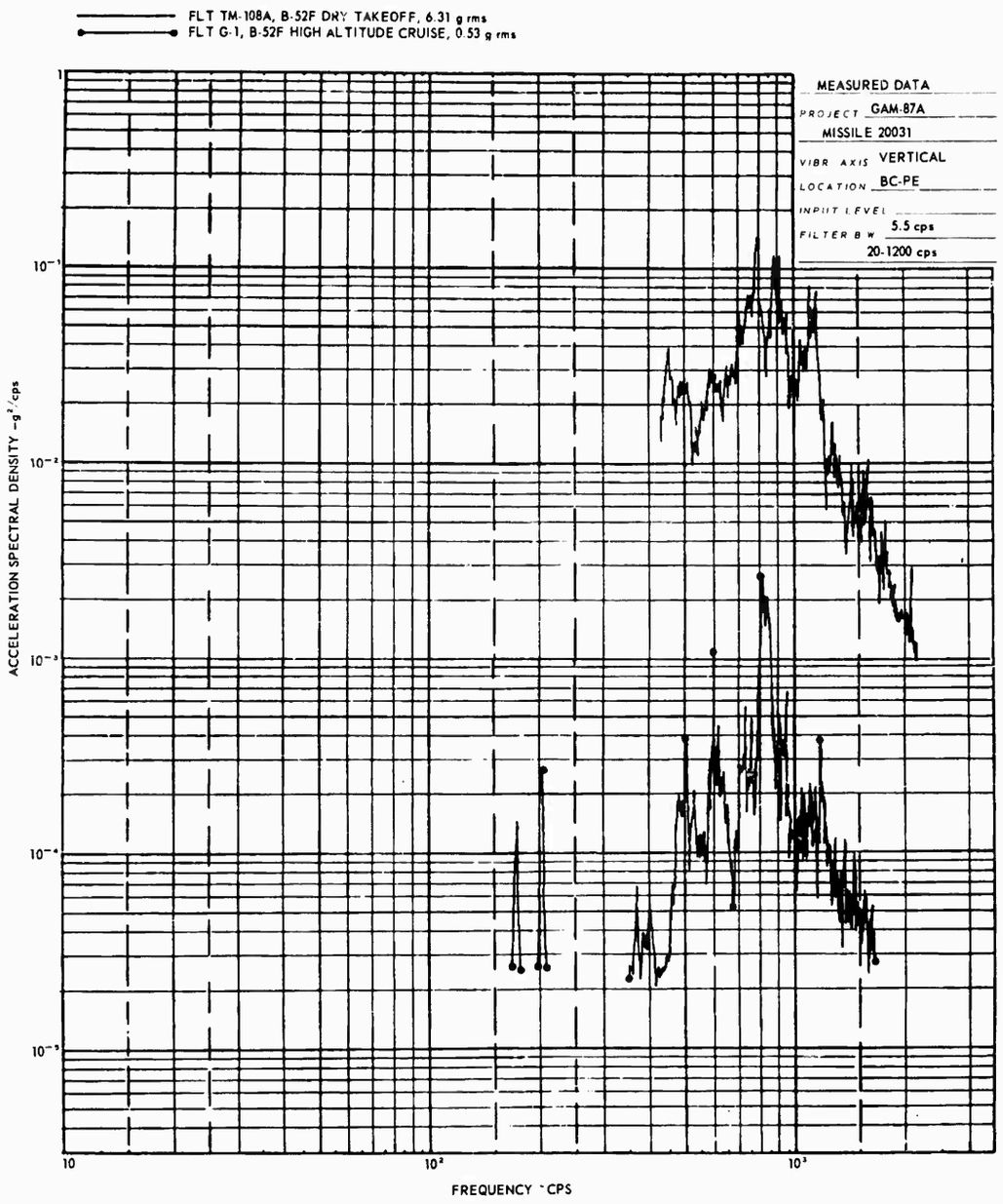

Fig. 30 - Measured narrow band random vertical vibration spectra for BC-PE during TM-105 and TM-108A takeoff and flight

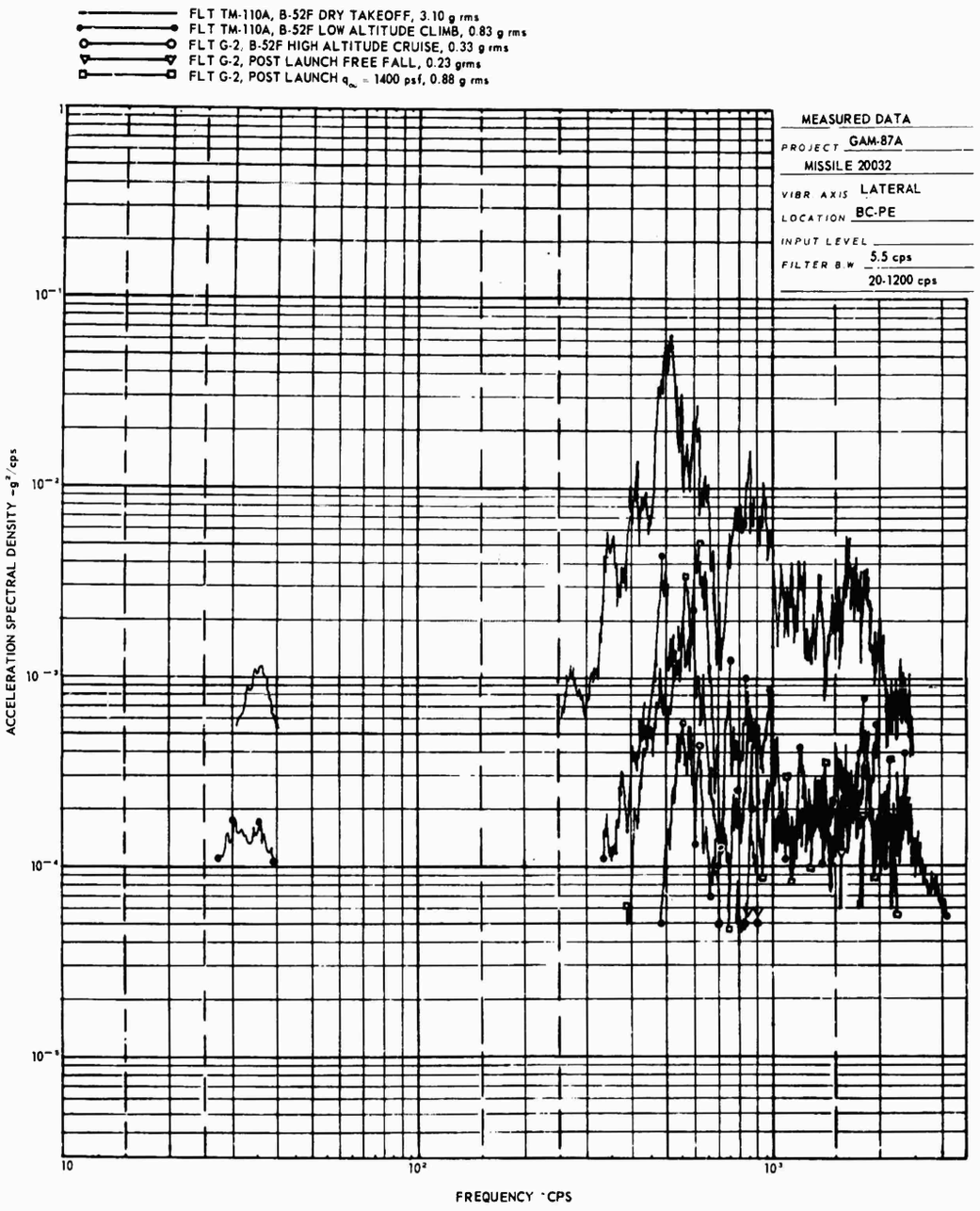

Fig. 31 - Measured narrow band random vibration spectra for BC-PE during TM-110A takeoff and flight and guided launch G-2

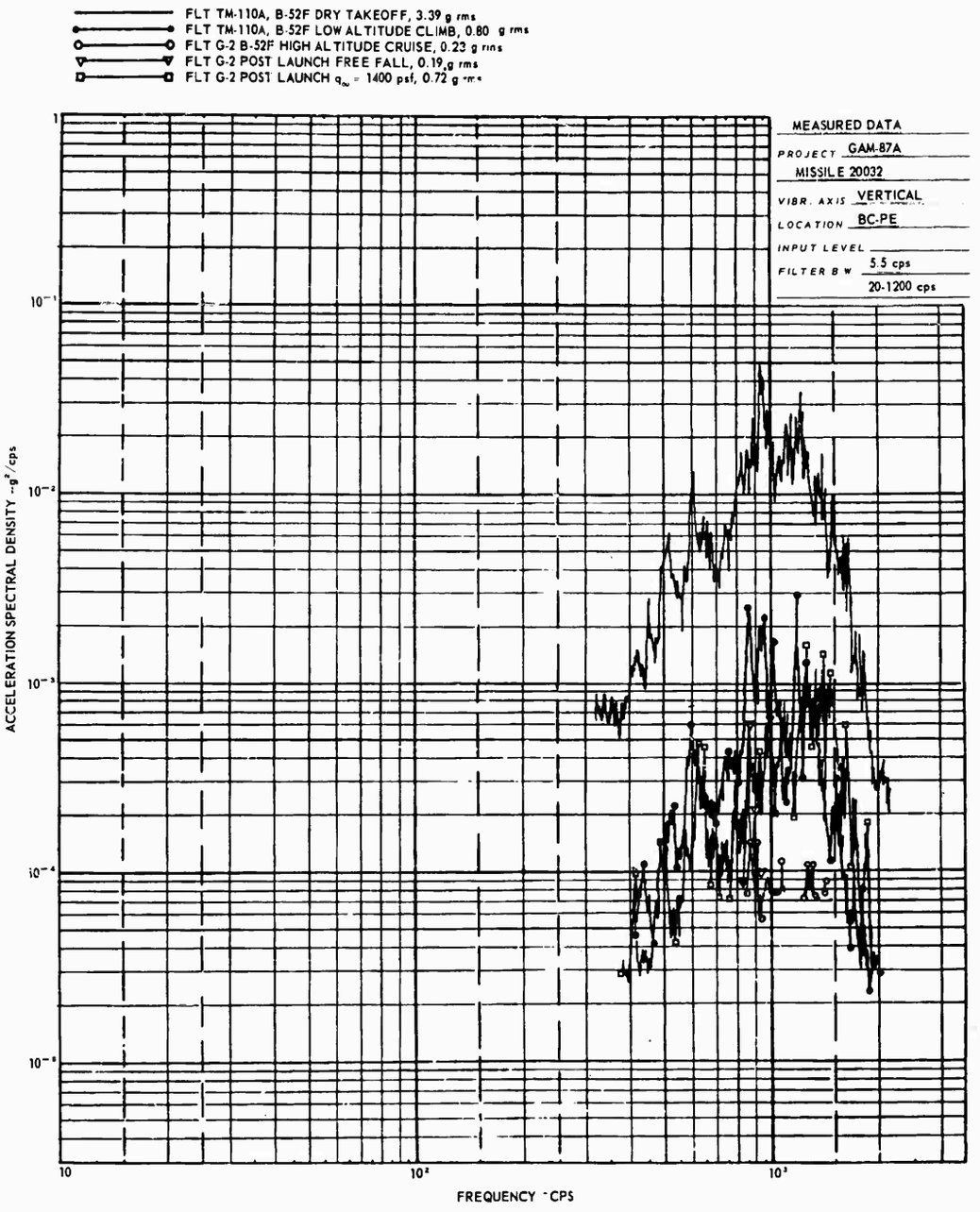

Fig. 32 - Measured narrow band random vibration spectra for BC-PE during TM-110A takeoff and flight and guided launch G-2

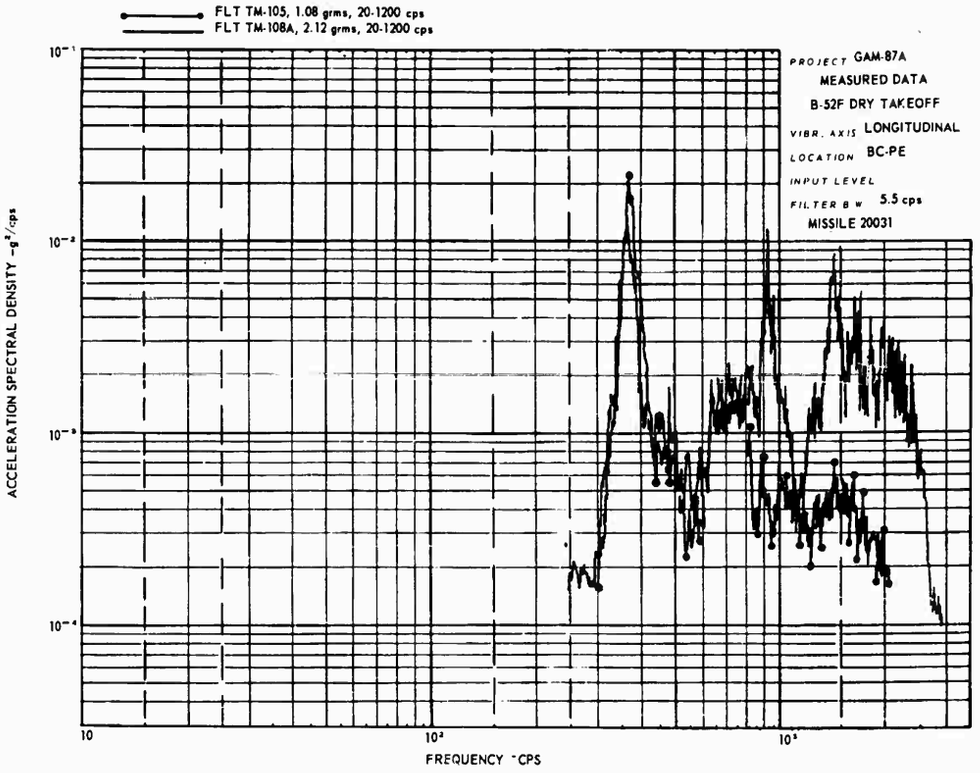

Fig. 33 - Summary of measured narrow band random vibration spectra for B-52F dry takeoff, longitudinal direction

signals at the lower frequencies, so that no reasonable estimation of the true spectra can be made. It is known, however, that the low frequency portion of each spectrum is less than the left end of the high frequency portion of the spectral line.

The vibration in the above intervals was examined for sinusoids, by inspecting the output of a narrow band filter which was tuned in sequence to significant spectral peaks. For example, Fig. 37 shows the output of three filters, each tuned to the same frequency, during the same analysis interval for B-52F high altitude cruise. Ignoring the effects of the magnetic tape splice blanker, the modulation of the envelope of the instantaneous signal indicates the presence or absence of any sinusoid within the band. If only random vibration were present the envelope would occasionally come to zero, while pure sinusoidal vibration would produce a constant envelope with no modulation.

Probability density analyses of wideband signals were also made. Figure 38 shows typical plots, indicating some deviation from the Gaussian.

Although not to be discussed here, significant shocks occurred at missile drop, engine ignitions, and burn-outs. Response spectra were obtained and reported by Douglas Aircraft Company.[20-22]

COMPARISON OF VARIOUS PREDICTION PROCEDURES WITH SKYBOLT VIBRATION MEASUREMENTS

The comparison between the above procedures and measured data will be made on the basis of the information in the two previous sections. Because most of the measurements did not extend below 400 cps (for reasons stated

earlier), an accurate comparison of prediction with measurements at lower frequencies is not possible. The left end of the higher frequency portion of each spectral line, however, can be used for a gross comparison.

The criterion selected for reasonable prediction is that the prediction envelopes the measured spectral peaks by a factor of 3 or less, but never underestimates the peaks (i.e., 0 to +5 db on a power basis). An occasional narrow band exceedance of the field data or an occasional overprediction (by a factor of 10) is considered acceptable, since minor changes in the resulting design and test criteria will probably not produce any changes in the final design of the equipment. Predictions which vary significantly from this criterion are considered to have serious deficiencies in its application to hardware design. This criterion will be used in judging the various procedures.

Nortronics Procedure

A comparison of the measured B-52F dry takeoff vibration data with the Nortronics-Mahaffey-Smith prediction is shown in Figs. 39-41, with the prediction shown as the dashed line on each figure. In Fig. 39, the prediction does a good job of estimating the spectral peaks above 300 cps, but is grossly overconservative below 300 cps. In Fig. 40, the prediction is satisfactory at high frequencies, but it seriously underestimates the measurements in the 300- to 600-cps range. At low frequencies, it grossly overestimates the measurements. In Fig. 41, a serious underestimation occurs above 400 cps, and an acceptable overestimation occurs below 400 cps. A comparison of the measured vibration data, for the missile postlaunch condition of q_∞ = 1400 psf, with the Nortronics-Mahaffey-Smith prediction is shown in Fig. 42. As mentioned previously two predictions were made,

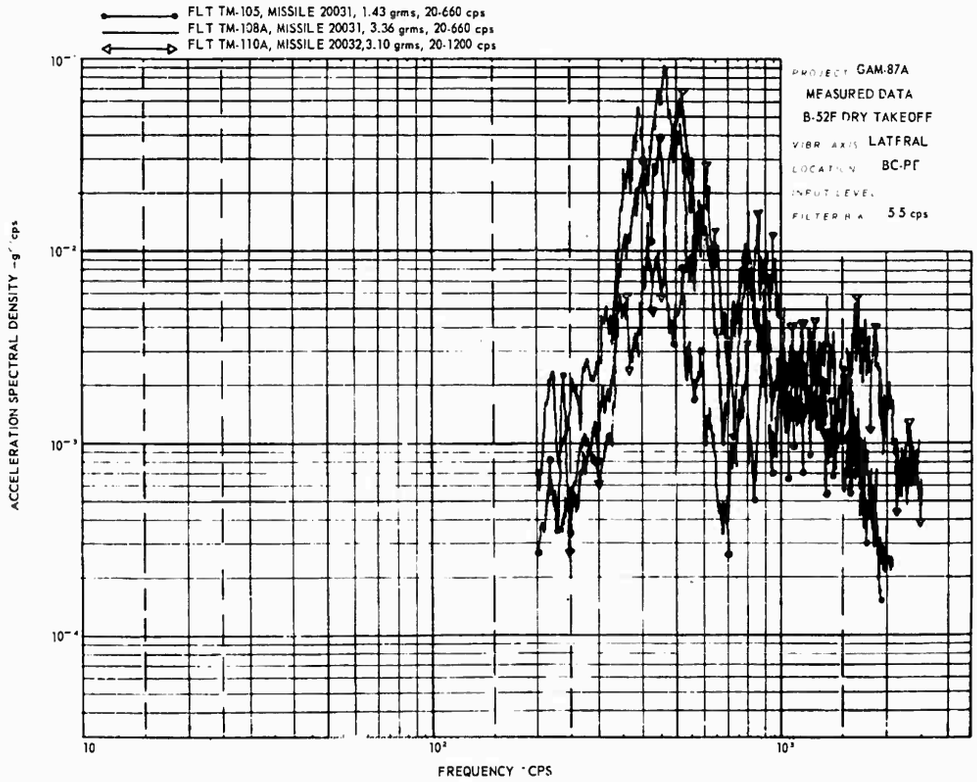

Fig. 34 - Summary of measured narrow band random vibration spectra for B-52F dry takeoff, lateral direction

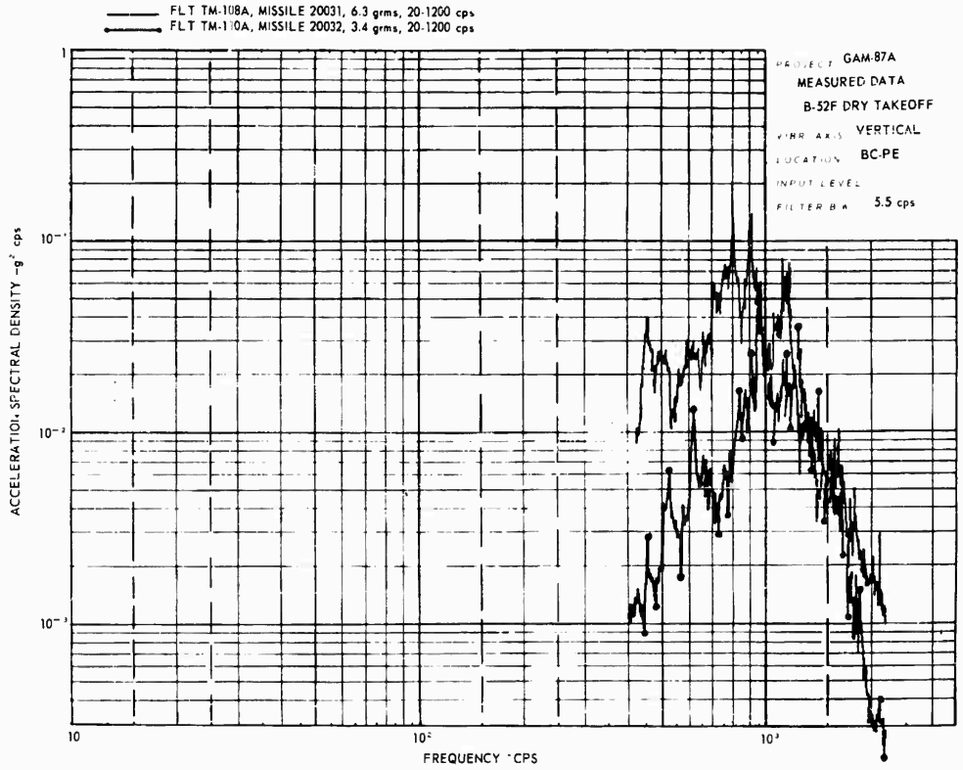

Fig. 35 - Summary of measured narrow band random vibration spectra for B-52F dry takeoff, vertical direction

one assuming L = 140 in. and the other assuming L = 20 in. As seen in Fig. 42, both predictions grossly overestimate the measurements in the range below 500 cps and are satisfactory from 500 to 1400 cps. Both predictions underestimate the field measurements from 1400 to 1900 cps, with the prediction for L = 20 in. considered an important underestimation.

Predicated on the above-mentioned criterion, the Nortronics procedure is not acceptable. The deficiencies of the procedure can most probably be laid to the differences between the structures of the B-58 and Skybolt. As pointed out by W. C. Smith of Boeing-Wichita (before Skybolt flight tests were made), the B-58 data should not be applied directly to vehicles of small diameter. As Smith pointed out, most of the B-58 low frequency resonances could be expected in the range of 100-300 cps, whereas vehicles of small diameter should have their low frequency resonances in the 300- to 1200-cps region. Figures 39-42 certainly verify this prophecy. These differences were not accounted for, however, in the Nortronics procedure. It was the intent of this comparison to judge the procedure without further modification.

Franken Procedure

A comparison of the measured B-52 takeoff vibration data with the Franken prediction is shown in Figs. 39-41, with the prediction shown as blocks having slanted lines from upper left to lower right. Because the Franken procedure predicts the highest spectral density at 1200-2400 cps, a gross overestimate of the measurements at high frequency is found. In Fig. 39, a satisfactory prediction is found at 400 cps and an acceptable overprediction occurs at lower frequencies. In Fig. 40, a serious underestimate occurs at 300-600 cps, and an acceptable overprediction below 200 cps. In Fig. 41, an acceptable prediction is found below 1200 cps, but a gross overestimation occurs above 1200 cps.

A comparison of measured vibration data, for the missile postlaunch condition of q_∞ = 1400 psf, with the Franken procedure is shown in Fig. 43. Again two predictions (L = 140 in. and L = 20 in.) are utilized. For L = 20 in., gross overestimate occurs above 600 cps, while a satisfactory prediction occurs below this frequency. The prediction for L = 140 in. appears grossly overconservative. Although the Franken procedure has some deficiencies when applied to Skybolt equipment, it should be remembered that the procedure was intended for predicting the vibration of missile skin. Since we have removed the procedure from its intended use, no criticism of the procedure should be leveled on the basis of these measurements.

Winter Procedure

A comparison of the measured B-52 dry takeoff vibration data with the Winter prediction is again shown on Figs. 39-41, with the prediction shown as blocks having the slanted lines from lower left to upper right. With the exception of the frequency range of 300-600 cps in Fig. 40, the procedure grossly overestimates the measurements. Compared to the Nortronics and Franken procedures, however, the Winter prediction does the best job of estimating the shape of the spectra.

A comparison of measured vibration data, for the missile postlaunch condition of q_∞ = 1400 psf, with the Winter procedure is shown in Fig. 44. Although the prediction grossly overestimates the measurements, the same general conclusions can be made regarding the spectral shape. For this reason, the Winter procedure appears to have more potential than the Nortronics and Franken procedures. Like the Franken procedure, the Winter procedure was intended for application to missile skin. By eliminating the octave band-to-narrow band correction factor of 5 that was appli[illegible] above to the Winter procedure, however, a reasonable

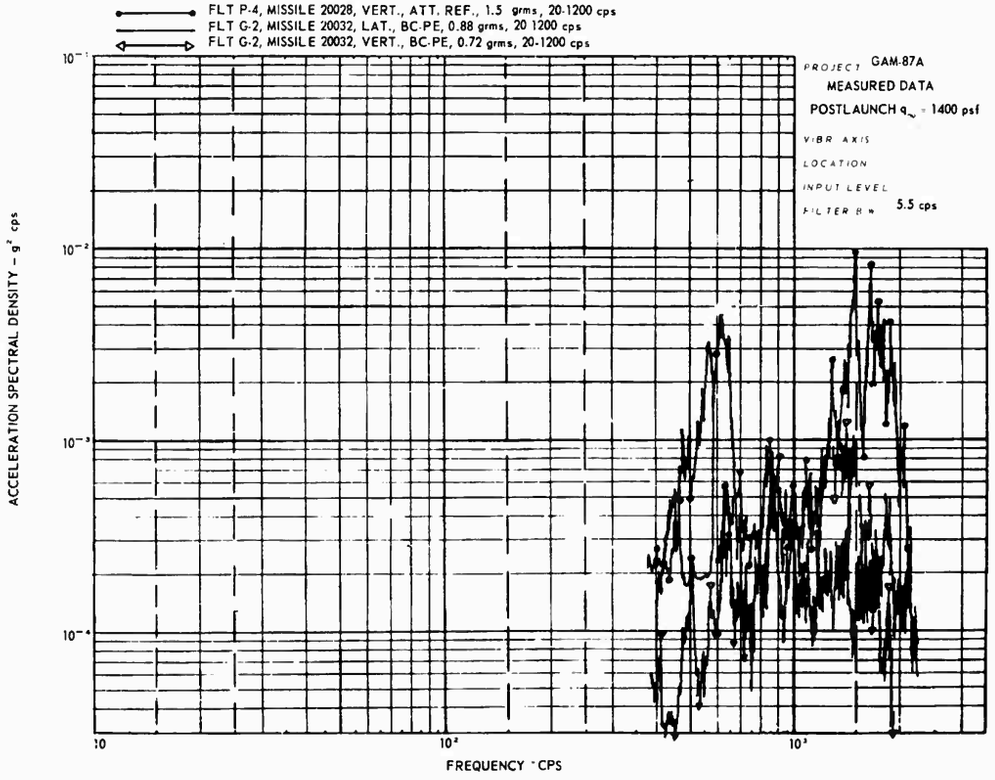

Fig. 36 - Summary of measured narrow band random vibration spectra for GAM-87A postlaunch (q_∞ = 1400 psf)

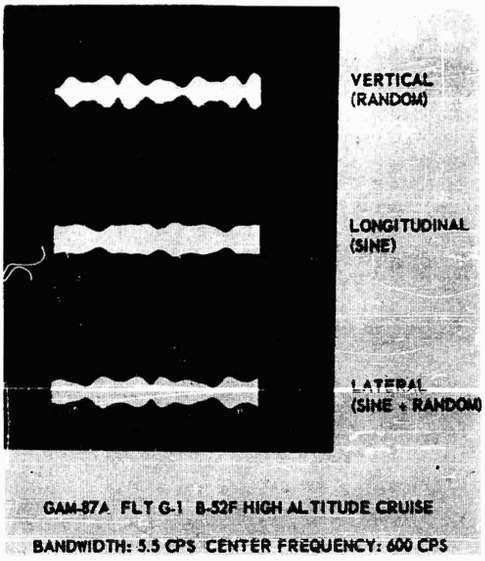

Fig. 37 - Output of narrow band filters

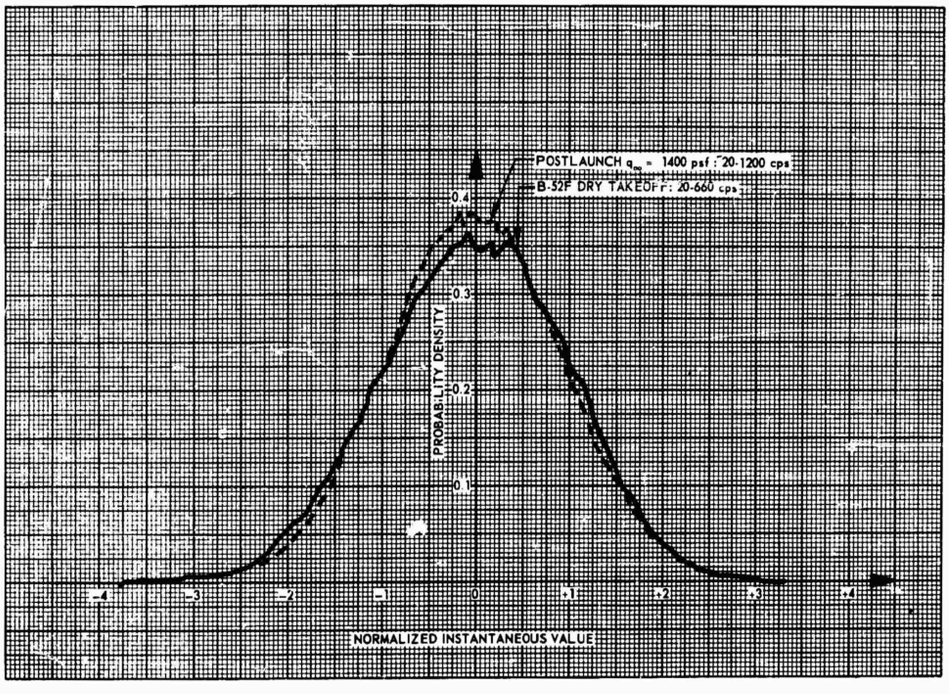

Fig. 38 - Normalized probability density function

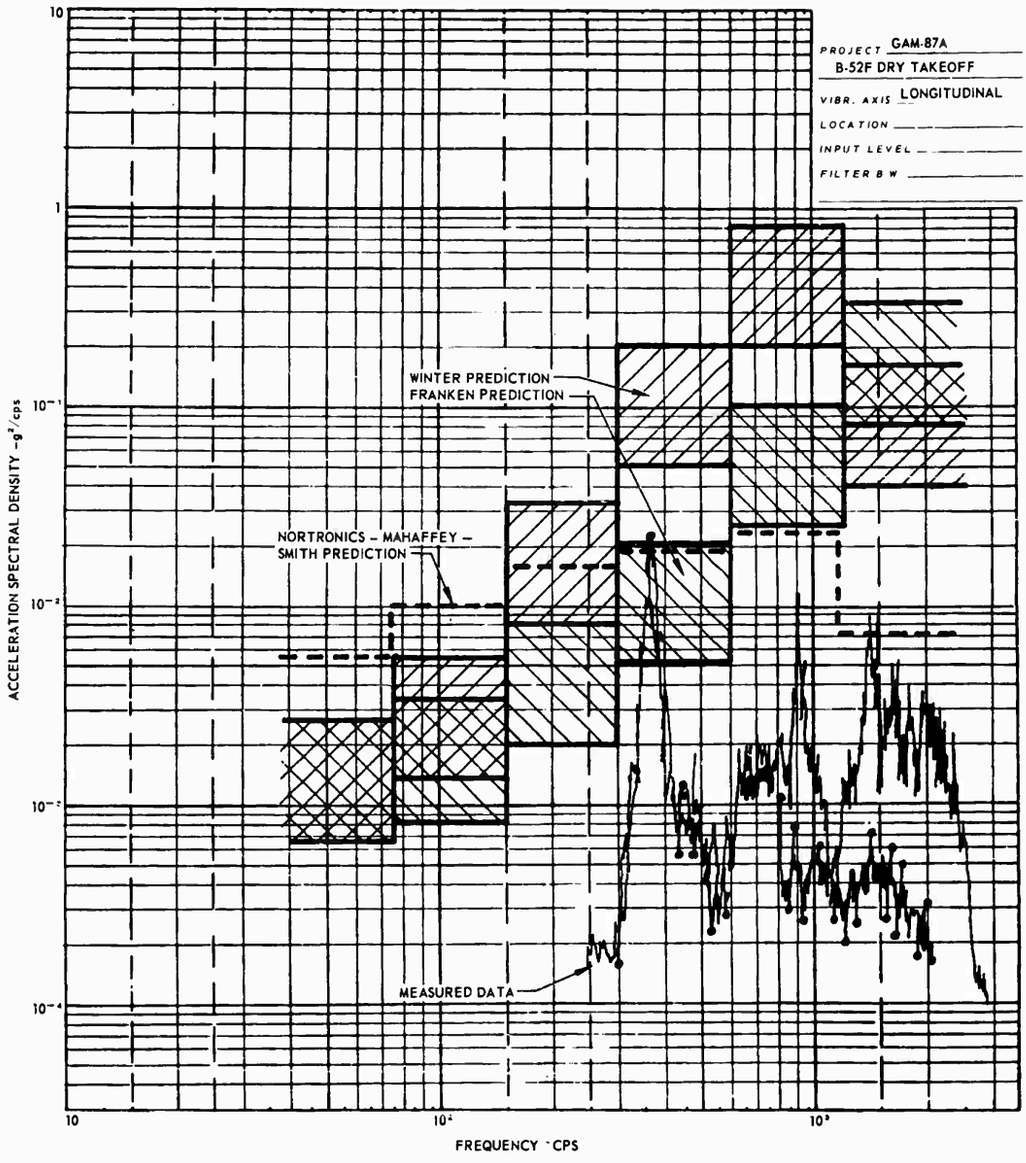

Fig. 39 - Comparison of measured takeoff data with three prediction procedures, longitudinal direction

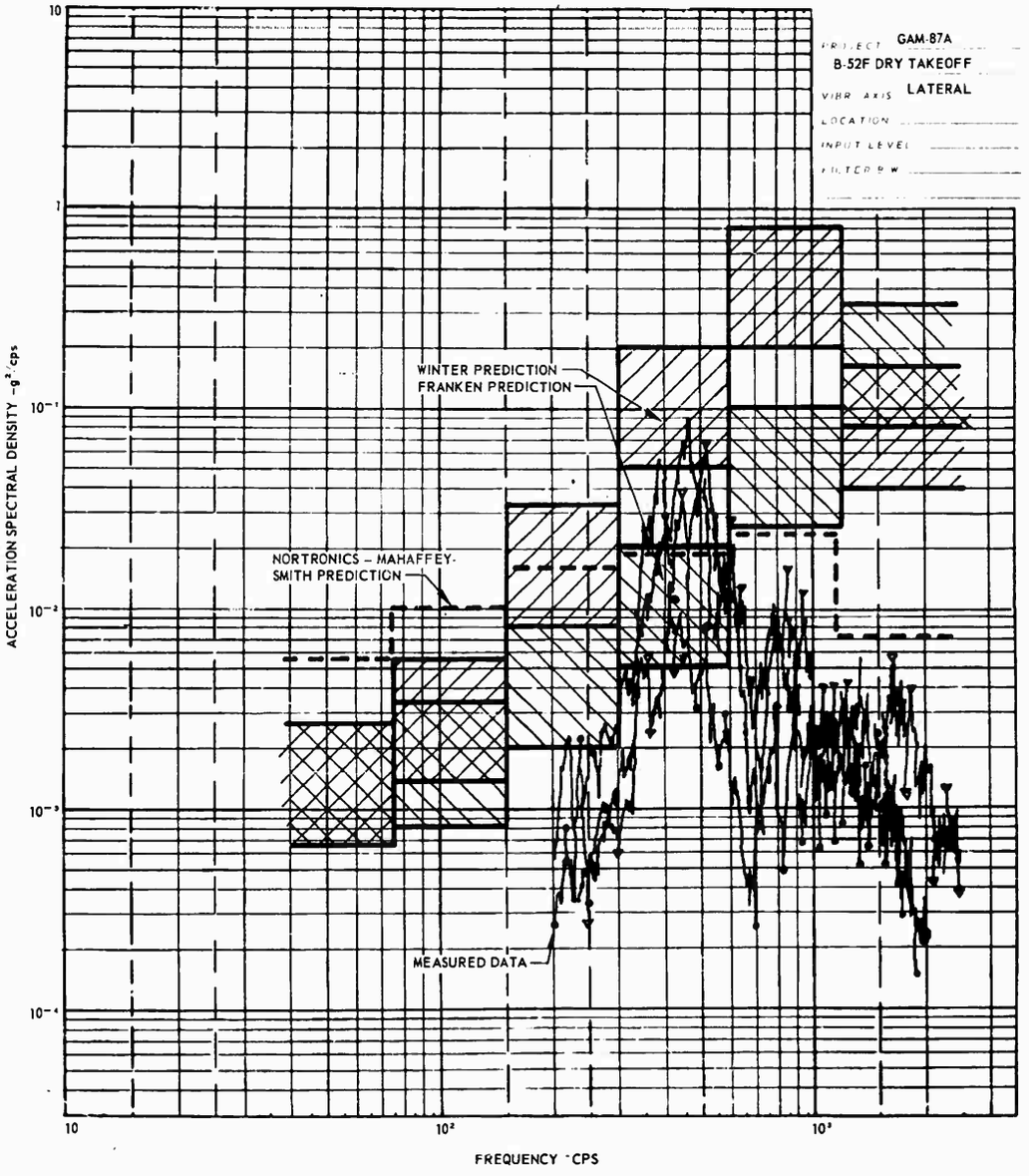

Fig. 40 - Comparison of measured takeoff data with three prediction procedures, lateral direction

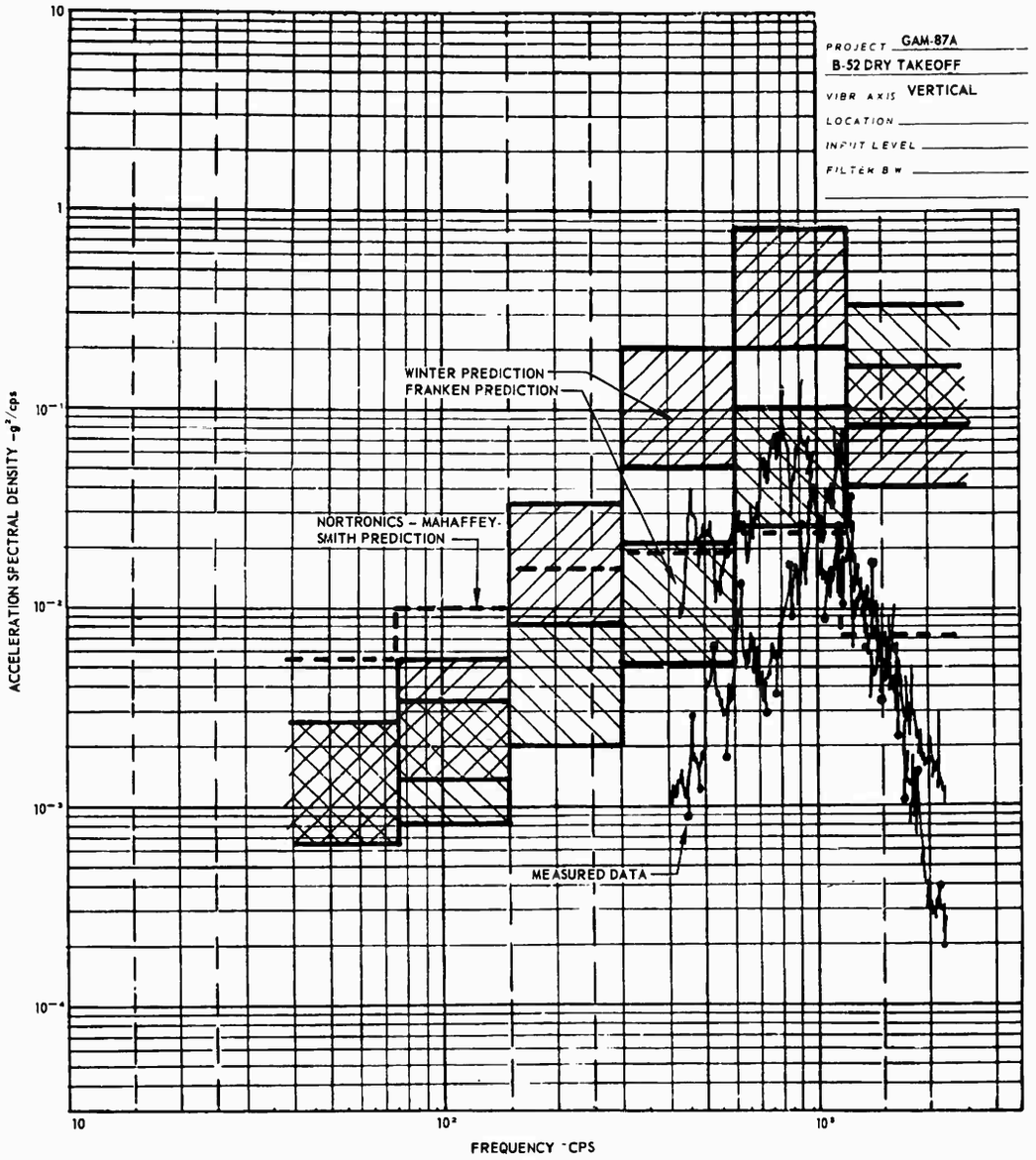

Fig. 41 - Comparison of measured takeoff data with three prediction procedures, vertical direction

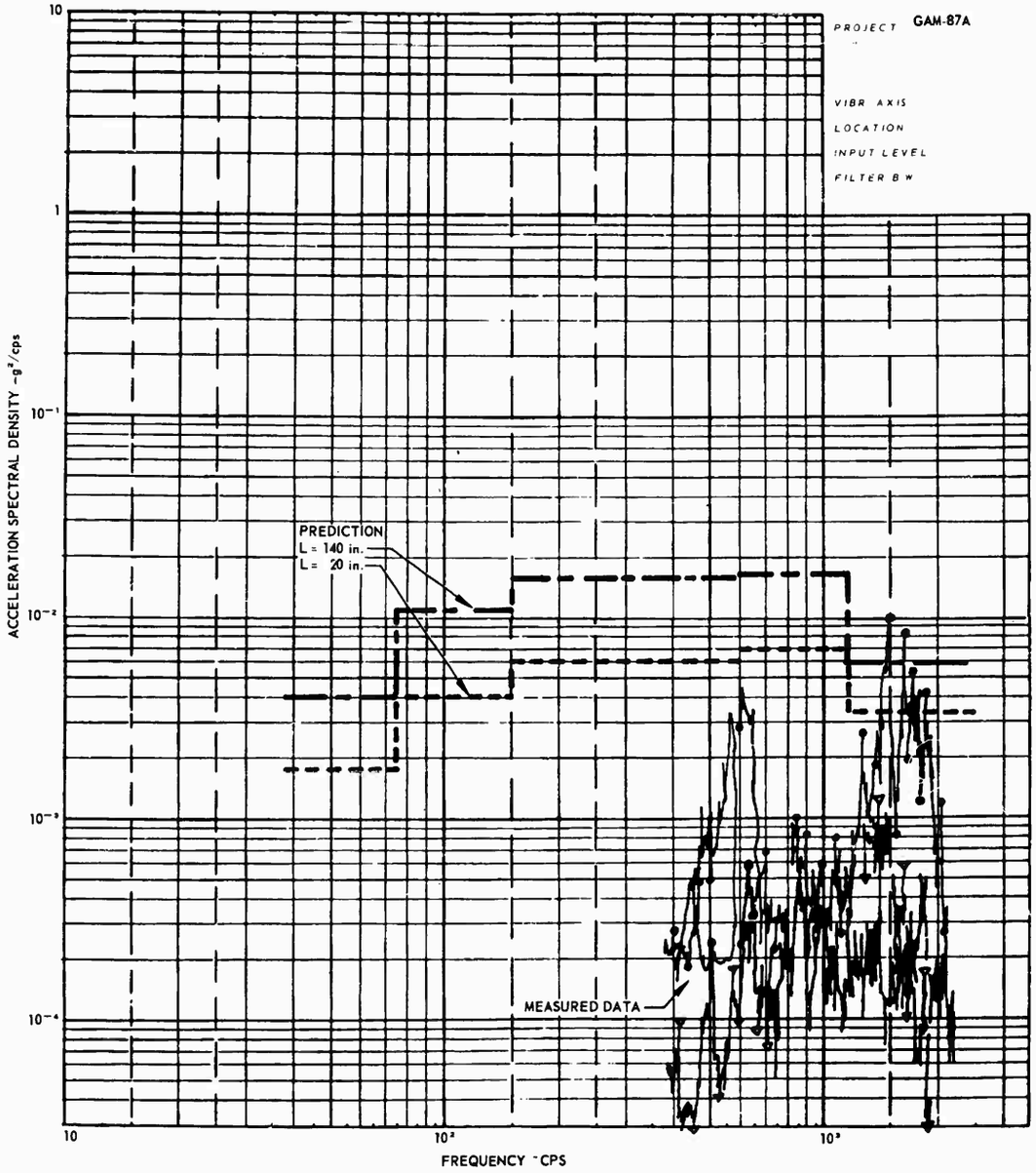

Fig. 42 - Comparison of measured postlaunch data (q_∞ = 1400 psf) with prediction using Nortronics-Mahaffey-Smith procedure

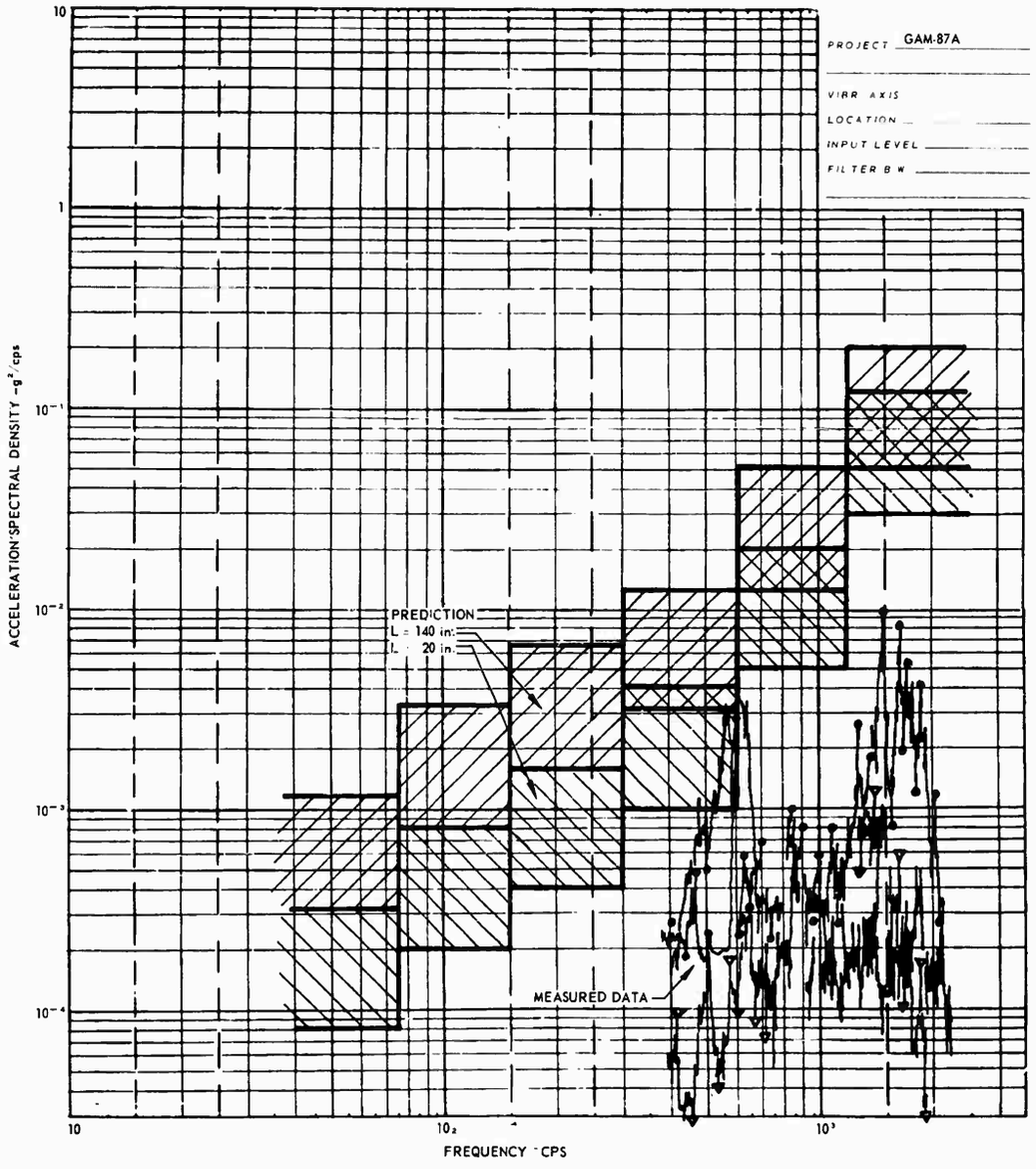

Fig. 43 - Comparison of measured postlaunch data (q_∞ = 1400 psf) with prediction using Franken procedure

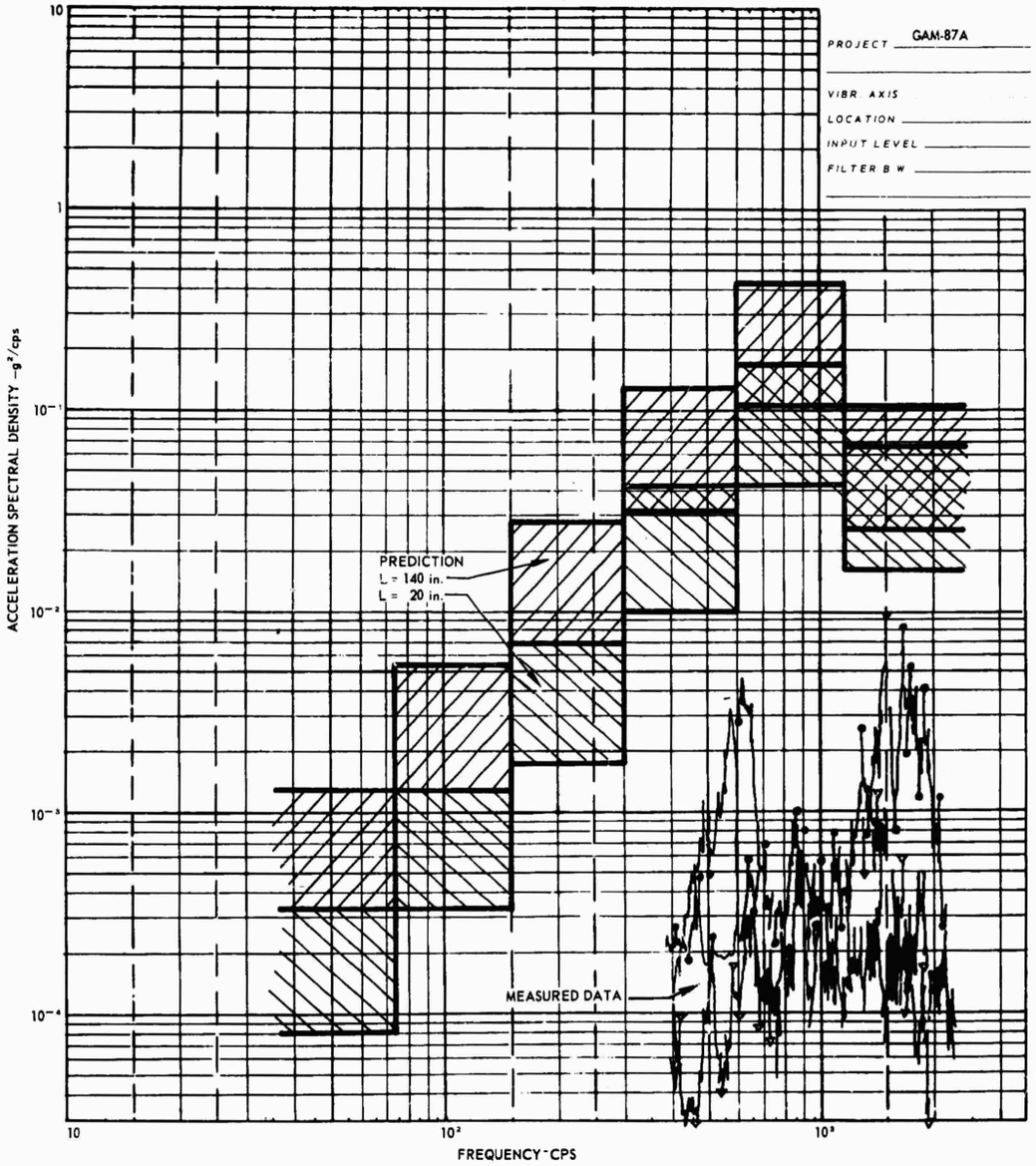

Fig. 44 - Comparison of measured postlaunch data (q_∞ = 1400 psf) with prediction using Winter procedure

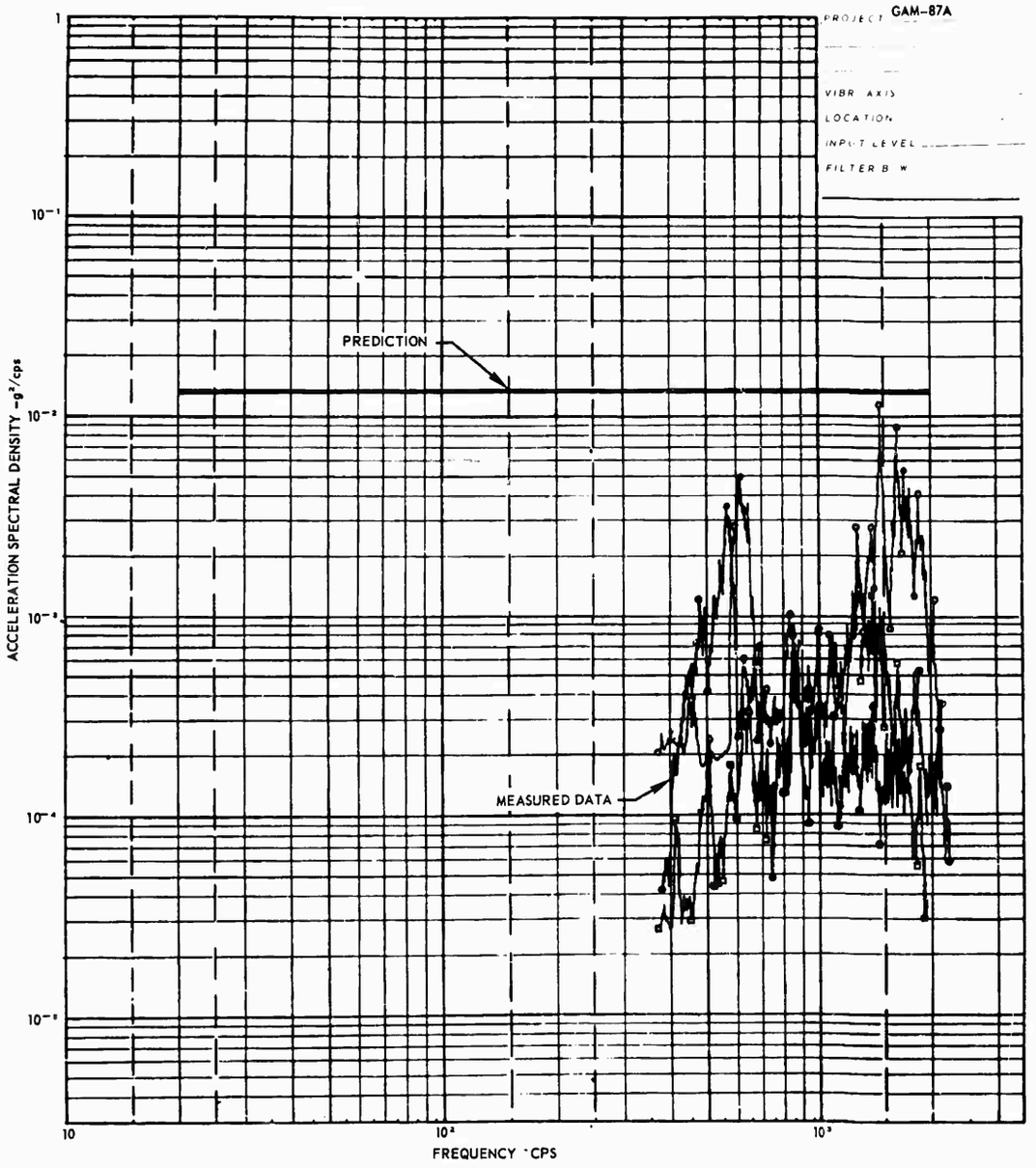

Fig. 45 - Comparison of measured postlaunch data[1] (q_∞ = 1400 psf) with prediction using Curtis procedure

prediction for equipment is obtained. (The authors feel that the cancellation of the correction factor is a fortunate coincidence.)

Curtis Procedure

A comparison of the measured vibration data, for the missile postlaunch condition of q_∞ = 1400 psf, with the Curtis procedure is shown in Fig. 45. (The Curtis procedure was not developed for jet engine noise.) Figure 45 shows that the prediction nominally overestimates the measurements above 500 cps, and grossly exceeds the measurements below this frequency. The cause of the overprediction at the lower frequencies is probably due to the same reason for the Nortronics procedure overprediction at lower frequencies, i.e., aircraft often have their low frequency resonance below 300 cps, while a small diameter vehicle would shift these resonances to the higher frequencies. Thus the Curtis procedure would probably do a better job on other aircraft, as Curtis had originally intended.

CONCLUSIONS AND RECOMMENDATIONS

The above comparisons clearly indicate that more work is required to develop a satisfactory generalized prediction procedure for equipment in aerospace vehicles. It is easy to see that installations other than Skybolt would show up deficiencies similar to those in Skybolt. For example, similar difficulties have already been reported on Titan[23] and will probably occur on other aerospace vehicles using present state-of-the-art techniques. As Condos and Butler have recommended, acoustic testing of large vehicle sections (with equipment installed) should be performed early in a vehicle program to refine the prediction. If flight equipment is not available for these tests, then structural dummies should be substituted. If dummies are utilized, mechanical impedance tests could be performed subsequently on (1) the dummy, (2) the flight item, and (3) the supporting vehicle structure, so that the vibration motion applied to the dummies could be altered to reflect the substitution of actual flight hardware. Obviously, these tests would have to be integrated into the overall vehicle program, just as hardware developmental tests are presently integrated.

Most aerospace engineers recognize the importance of accurate prediction to the proper design and optimization of aerospace equipment, in order to achieve the best tradeoff between reliability and weight. Considering present and future weight limitations of aerospace vehicles, and the demonstrated lack of reliability in the past, it is obvious that strong financial support is warranted for further development of prediction procedures. The authors seriously question, however, if this valuable work will be done in the near future. The present emphasis on cost effectiveness has already produced the result nearly every aerospace engineer had expected: the de-emphasis of true R&D and in its place substituting the idea of "getting along with what we have." This attitude will no doubt produce drastic changes to the progress of the aerospace industry. Using exactly the same philosophy of operation, the automotive industry has shown in the last 50 years that there is little progress beyond the internal combustion engine, four wheels, and marginal reliability.

ACKNOWLEDGMENTS

The authors would like to acknowledge the assistance of B. R. Vernier of Nortronics (who initiated the prediction procedure), G. E. Kahre and his associates at Douglas Aircraft Company (who were responsible for flight data acquisition), D. N. Keast of Bolt, Beranek, and Newman (who provided Titan vibration data for obtaining the wideband-to-narrow band correction factor), and W. L. Tribble of Norair and P. Gonzales and E. V. Gooselaw of Nortronics (who were responsible for flight data reduction and presentation).

REFERENCES

1. J. M. Brust, "Determination of Fragility to Meet Random and Sinusoidal Vibration Environments," SAE Paper 430A (Oct. 9, 1961).

2. J. E. Foster, "Random-Sinusoidal Vibration Correlation Study," J. Environ. Sci., 4:6-15 (Aug. 1961). (Also WADD TR 61-43, DDC No. AD 267509).

3. L. C. Sutherland and W. V. Morgan, "Use of Model Jets for Studying Acoustic Fields near Jet and Rocket Engines," Noise Control, 6:6-12 (May 1960).

4. D. A. Bies and P. A. Franken, "Notes on Scaling Jet and Rocket Noise," J. Acoust Soc. Am., 33:1171 (Sept. 1961).

5. K. V. Eldred, W. H. Roberts, and R. White, "Structural Vibrations in Space Vehicles," WADD TR 61-62 (DDC No. AD 273 304) (Dec. 1961).

6. P. A. Franken, E. M. Kerwin, et al., "Methods of Flight Vehicle Noise Prediction," WADC TR 58-343, Vol. I (No. ., 1958) and Vol. II (DDC No. AD 205776 and [illegible] (Sept. 1960).

7. I. Dyer, "Estimation of Sound-Induced Missile Vibration," Random Vibration, Ed. by S. H. Crandall (John Wiley and Sons, Inc., N. Y., 1958), Chap. 9.

8. J. E. Flowcs Williams, "The Noise of High-Speed Missiles," Random Vibration, Vol. 2, Ed. by S. H. Crandall (MIT Press, Cambridge, Mass., 1963), Chap. 6.

9. P. A. Franken, "Review of Information on Jet Noise," Noise Control, [illegible] (May 1958).

10. I. Dyer, P. A. Franken, and R. E. Fingar, "Noise Environments of Flight Vehicles," Noise Control, 6:31-49,5[illegible] (Jan. 1960).

11. D. A. Hilton, "Scout-Vehicle Aerodynamic Noise Measurements," 2:28-51 (Oct. 1963).

12. H. Schlichting, Boundary Layer Theory (Pergamon Press, N. Y., 1955), p. 35.

13. P. T. Manaffey and K. W. Smith, "Method for Predicting Environmental Vibration Levels of Jet Powered Vehicles," Noise Control, 6:20-26 (July 1960).

14. H. Himelblau, "Predicted Vibration Levels for Missile Equipment in a Titan ICBM Launched from [illegible] lined Silo," BBN Ltr [illegible] to STL, Apr. 1[illegible].

15. M. Gertel, "Spe[illegible] ation of Laboratory Tests," Shock [illegible] ibration Handbook, Ed. by C. M. Harris [illegible] d C. E. Crede (McGraw-Book Comp[illegible], Inc., N. Y., 1961), Chap. 24.

16. P. A. Franken, S[illegible] rd-Induced Vibrations of Cylindrical Ve[illegible] J. Acoust. Soc. Am. 34:153 ([illegible]).

17. R. W. Mustard, [illegible] tion of Random Environments," S[illegible] Paper 48B (Sept. 23, 1963).

18. A. A. Curtis, "A S[illegible] tistical Approach to Prediction of the [illegible] ircraft Flight Vibration Environment," Sh[illegible] ck, Vibration and Associated Environm[illegible] nts Bull. No. 33, Part I, pp. 1-[illegible].

19. C. W. Besser[illegible] t al., Missile Engineering Handbook, D. Van Nostrand Co., Princeton, N. J., 19[illegible]8), pp. 30-35, 45-[illegible]6.

20. "Final [illegible] t-Missile Flight Test No. 5, [illegible] nal No. 20031, Test Mission [illegible], SAC Rept. SM-42291 (Dec. 11, 1963).

21. "[illegible] Report—Missile Flight Test No. 6, [illegible] Serial No. 20032, Test Mission [illegible], SAC Rept. SM-43426 (Mar. 7, 1963).

22. "[illegible] al Report—Missile Flight Test No. 4, [illegible] ssile Serial No. 20028, Test Mission 27," [illegible] AC Rept. SM-42294 (Dec. 10, 19[illegible]).

23. E. M. Condos and W. Butler, "A Critical Analysis of Vibration Prediction Techniques," Proc. IES (1963), pp. 32[illegible]-336.

DISCUSSION

Mr. Clevenson (Langley Research Center): In the early slides, you did not show any flight data for frequencies lower than 400 cps because of electrical disturbances. You made quite a point of saying that various prediction methods were all very conservative in the low frequency range. How can you say that the predictions are conservative, and how do you know that electrical disturbances only affect frequencies below 400 cps?

Mr. Himelblau: The electrical noise floor in the low frequency range controls [illegible] of the frequency analyzer, and the data normally go below this. We determined the electrical noise floor by measurements at other times when only the electrical equipment was working—no substantial external field environment. So we know that the data go below—shall we say, where the data would if you drew a horizontal line—that is, where the noise floor would be. We had expected that the vibration levels would continue to go down, with an occasional exception. For example, we saw a couple of spikes around 30 cps which we feel probably represented the feedback response of the

equipment on the resilient mounts. I thought this problem would come up because we then no longer had a frame of reference for comparing the prediction with the environment. But, if you will notice, in the low frequency range, especially for the Mahaffey & Smith method, it was higher than where the data had stopped. So I think the conclusion is still the same.

Voice: You used three methods. Which one would you say is best? Or are they all pretty bad?

Mr. Himelblau: I guess a better question is: Which one would I use now? I think I would like to hold off on that answer until I try a couple more things. One, I would like to take the Winter prediction which seems to follow the spectrum shape a little bit better and perhaps reduce this by some fudge factor based on the transfer from the skin to the internal equipment. I would like to try that before answering your question. Also, I would like to try out the procedure that was presented earlier in this meeting by Allen Curtis of Hughes. As usual, the next door neighbors do not know what each other is doing; so I would like to see how well his method works with these data, and maybe make the decision at that time.

* * *